THE STRUCTURAL REQUIREMENTS OF HISTONE DEACETYLASE (HDAC) INHIBITORS: SUBEROLYANILIDE HYDROXAMIC ACID (SAHA) ANALOGUES MODIFIED AT C3, C6, AND C7 POSITIONS ENHANCE SELECTIVITY

by

SUN EA CHOI

DISSERTATION

Submitted to the Graduate School

of Wayne State University,

Detroit, Michigan

in partial fulfillment of the requirements

for the degree of

DOCTOR OF PHILOSOPHY

2012

MAJOR: CHEMISTRY (Organic)

Approved by:

_____

Advisor Date

_____

_____

_____

_____

DEDICATION

I would like to dedicate this dissertation to some people who have made me who I am today: my advisor Dr. Mary Kay H. Pflum, committee members (Dr. Jin K. Cha, Dr. David Crich, and Dr. Aloke Dutta), Dr. Zhongwu Guo, previous and current group members (Dr. Anton Bieliauskas, Dr. Sujith Weerashinghe, Geetha Padige, Satish Garre etc), room mates (Charlie Johnson, Derek Averill, and John Pompei), friends (Dr. Ivan Lysenka, Dr. Woo, Jun Hee Lee, Sung Jun Park, Yu Chen, Nitin Jabre etc), the oldest sister Moon Ea Choi and her family (Cheul Young Lee and Ha Jin), other sisters (Jung Ea Choi, Young Ea Choi, and Myong Ea Choi), brother Jin Young Choi, mother Hyang Joo Park, and specially, father Chang Soon Choi. I miss you so much, Dad.

TABLE OF CONTENTS

LIST OF TABLES

LIST OF FIGURES

LIST OF SCHEMES

CHAPTER 1 - INTRODUCTION

1.1 Gene expression by Histone Deacetylase (HDAC) proteins

The nucleosome is a unit of DNA packaged around a histone protein core (Figure 1.1).[1] The four core histone proteins (histone octomers, pink) are wrapped by the DNA double helix (gray), which form chromosomes (violet) through highly condensed nucleosomes. The nucleosomes carry epigenetically inherited information in the covalent modifications of the core histones. Covalent modifications of lysine residues located on histone N-terminal tails alter gene expression.

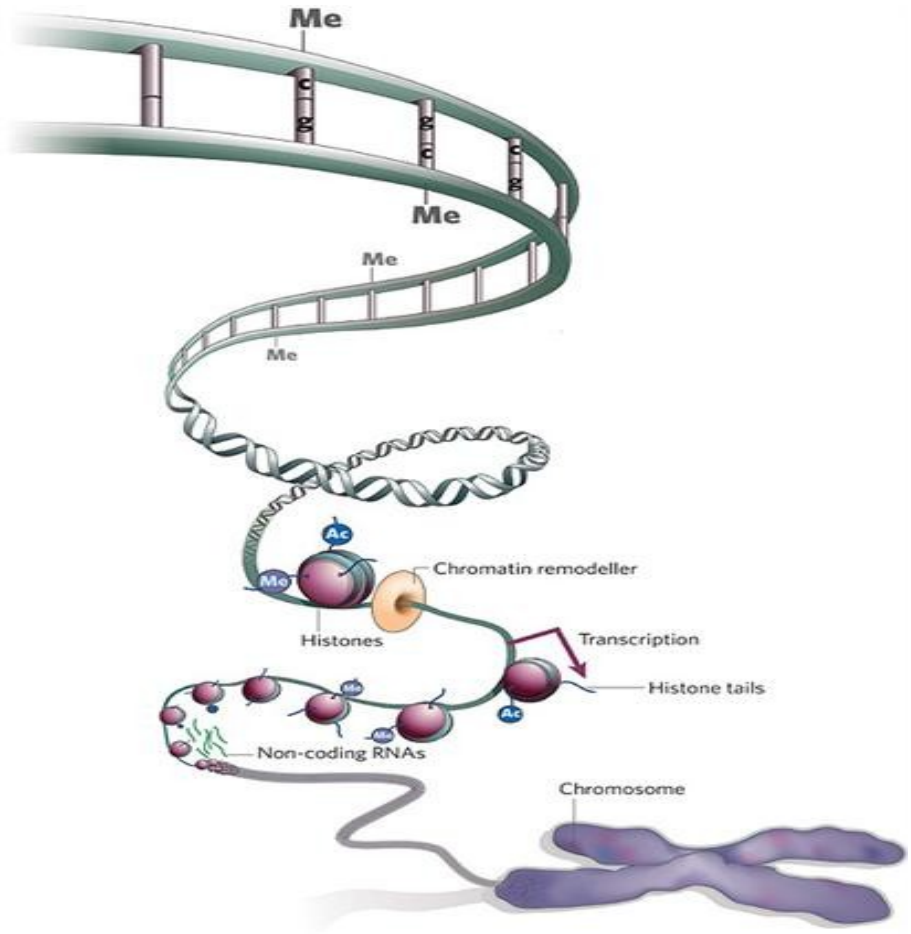

Figure 1.1 Epigenetic mechanisms.[1] Histone octomers (pink), DNA double stand (gray), and chromosomes (violet). *Reused with permission*

Among the covalent modifications, the acetylation status of histone lysines is governed by histone deacetylase (HDAC) proteins and histone acetyltransferase (HAT) proteins and is in equilibrium (Figure 1.2). HDAC and HAT proteins are two key enzymes that regulate gene transcription. The neutral, acetylated lysine allows DNA to interact with transcription factors to promote gene expression. Deacetylated positively charged lysine residues interact with the negatively charged phosphate backbone of DNA. The tight electrostatic interaction between the additional lysine residues and the negatively charged DNA backbone prevents activation with gene transcription. The overexpression of HDAC proteins shifts the equilibrium to the unmodified state and results in aberrant transcription in some cancer cells.[2] More specifically, overexpression of HDAC proteins induces repression of transcription and alteration in the accessibility of genes to transcriptional proteins causes reduced gene expression. Since decreasing gene expression can cause a variety of diseases, including cancers, the family of HDAC proteins has been studied.

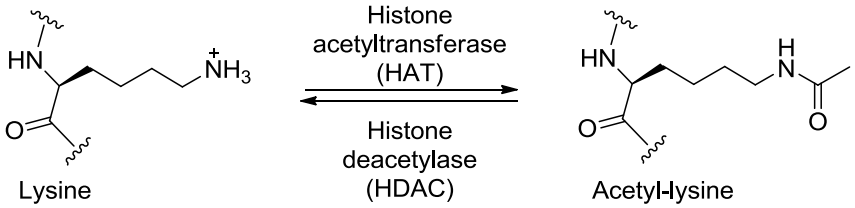

Figure 1.2 The equilibrium activities of histone acetyltransferase (HAT) and deacetylase (HDAC)

1.2 HDAC protein family

The HDAC protein family consists of 18 members and is divided into four classes based on size, cellular localization, number of catalytic active site, and homology to yeast HDAC protein (Table 1.1).[3] Class I includes HDAC1, HDAC2, HDAC3, and HDAC8. Class II includes HDAC4, HDAC5, HDAC6, HDAC7, HDAC9, and HDAC10. Class IV includes HDAC11 as the sole member because it displays similarities to both class I and II. Class III are NAD^+-dependent proteins, referred to as sirtuins (SIRT 1-7).[4] Class I, II, and IV are metal ion-dependant proteins and are sensitive to the inhibitors in this dissertation.

Table 1.1. HDAC family

Metal ion-dependent			NAD^+-dependent
Class I	Class II	Class IV	Class III
HDAC1	HDAC4	HDAC11	SIRT (1-7)
HDAC2	HDAC5		
HDAC3	HDAC6		
HDAC8	HDAC7		
	HDAC9		
	HDAC10		

Class I HDAC proteins (HDACs) are found in cancers, including ovarian (HDAC1, 2, and 3),[5] gastric (HDAC2),[6] and lung cancers (HDAC1 and HDAC3).[7] Class I HDACs are produced at higher levels in ovarian cancers compared to normal ovarian tissues, as assessed using small interfering RNA methodology.[5] Strong expression of HDAC2 was found in 44 out of a total of 71 gastric tumors.[6] HDAC3 is elevated in 92% of squamous cell lung carcinomas, as assessed using

immunoblot analysis.[7] HDAC8 is involved in acute myeloid leukemia (AML).[8] A common form of AML results from an abnormal fusion protein, Inv1, that binds HDAC 8. Overexpression of class II HDAC6 is observed in breast and ovarian cancer tissues.[9] Cell motility was increased by transfecting at HDAC6 expression plasmid into the breast cancer MCF-7 cells. Class II HDAC 10 protein is involved in the formation of tumors of skeletal muscle.[10] HDAC10 was detected at the highest level in the skeletal muscle tumor SJRH30 rhabdomyosarcoma cell line. The different activities that connect each HDAC isoform with cancer formation have been given significant attention on the pharmaceutical and carcinoma studies.[5, 9]

Even though each individual HDAC protein is involved in the formation of cancers, the role of each isoform in carcinogenesis is not clear yet. Therefore, elucidating the molecular mechanism connecting the HDAC activity of each isoform to cancer formation would facilitate studies that lead to treatment of diseases. To comprehensively understand the role of individual HDAC proteins in the growth and progression of cancer, development of selective HDAC inhibitors is required.

1.3 HDAC inhibitors

New approaches towards studying the causes and treatments of cancer have been rigorously studied since cancers are one of major causes of death in the United States. With a role in cancer, several HDAC inhibitor drugs are in clinical trials for treatment of cancer.[11] Specifically, suberoyl anilide hydroxamic acid (SAHA, Vorinostat) was the first HDAC inhibitor approved by the Food and

Drug Administration (FDA) for treatment of cutaneous T-cell lymphoma (CTCL).[12] Another recent FDA-approved HDAC inhibitor is depsipeptide (romidepsin, FK228), also for treatment for CTCL.[13] Currently, most HDAC inhibitors are pan-inhibitors, which similarly inhibit all HDAC proteins. Therefore, developing selective inhibitors would aid studies connecting HDAC activity to cancer formation.

Most metal ion-dependent HDAC inhibitors, including SAHA, have a similar structure construction consisting of a capping group that is solvent-exposed, a carbon linker that is surrounded by a hydrophobic tunnel, and a metal binding moiety that is buried in the protein active site (Figure 1.3).

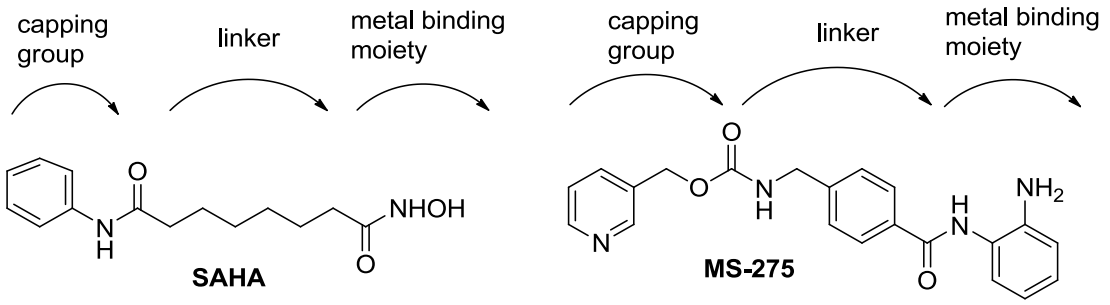

Figure 1.3. Structures of metal ion-dependent HDAC inhibitors

The crystal structure of SAHA bound in the active site of a bacterial homologue support that the SAHA anilide capping group is solvent-exposed near amino acids at the entrance of the active site, the linker positions in the hydrophobic channel, and the hydroxamic acid is located near the zinc atom at bottom of the active site (Figure 1.4). However, slight differences in the active sites of the human HDAC isoforms are not known in detail because limited crystallographic analysis is only available for HDAC2,[14] HDAC3,[15] HDAC4,[16]

HDAC7 and HDAC8.[17] Therefore, design of isoform-selective HDAC inhibitors that inhibit only related HDAC proteins is challenging.

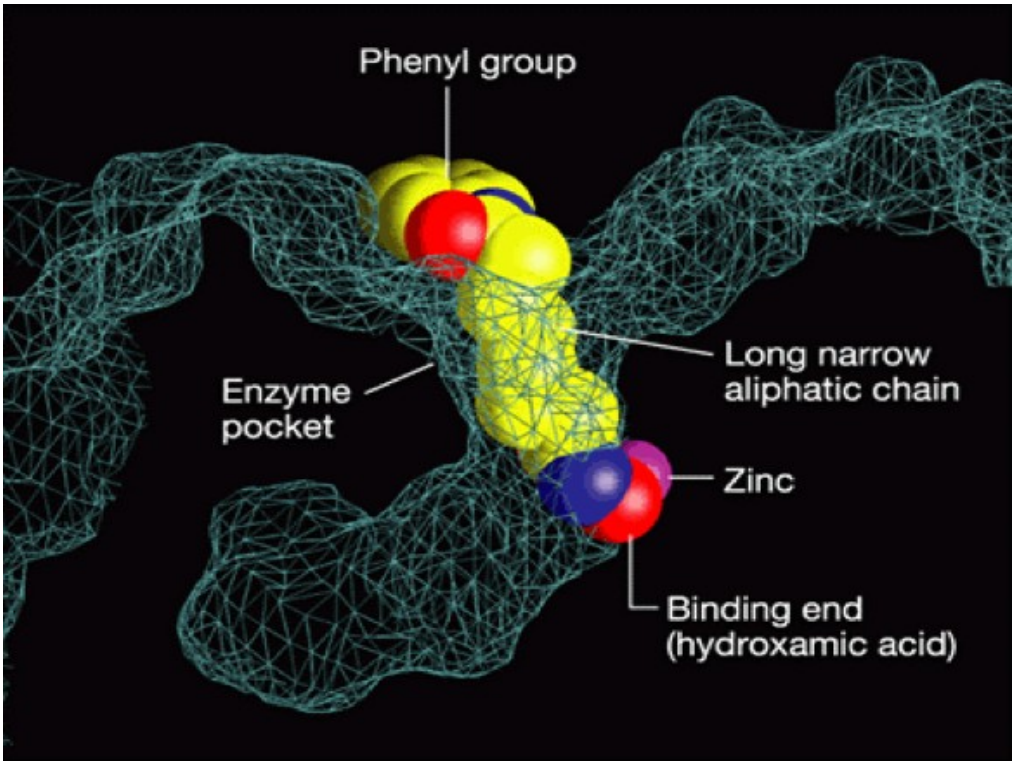

Figure 1.4. Structure of SAHA bound to an HDAC-like protein.[18] *Reused with permission*.

1.4 Inhibitor selectivity

Currently, most HDAC inhibitors, including SAHA, nonspecifically inhibit all eleven metal ion-dependent HDAC proteins. As a promising hypothesis, the non-selective HDAC inhibitors might cause cancer patients in the clinic to suffer from the side effects, such as fatigue, anorexia, diarrhea, and cardiac arrhythmia.[19] The clinical toxicity of selective inhibitors is unknown because there is no HDAC isoform selective inhibitor at present. In addition, the similarity in the active sites of the isoforms has challenged inhibitor design.[20] Elucidating the relationship between inhibitor selectivity and clinical toxicity might not only help understand

the role of the HDAC isoform function, but also contribute to the development of chemotherapies with fewer side effects for cancer patients.

1.5 Rationale for the synthesis of SAHA analogues containing substituents on the carbon linker

Towards creating isoform selective inhibitors, the structural regions of HDAC inhibitors have been studied. Particularly, the capping region and metal binding moiety have been extensively modified.[21] The influence of substituents on the linker region is relatively less studied, although the hydrocarbon linker has been investigated, such as varying chain length, producing points of unsaturated chain, and adding an aryl or cyclohexyl ring.[22] However, MS-275, which displays selectivity for class I[23], contains an aryl ring in the linker region (Figure 1.3). The intra-chain aryl group structure of MS-275 suggests that selectivity may be influenced by the structure of the linker region. We designed structure activity relationship (SAR) studies of SAHA to investigate the role of the linker on inhibitory activity and selectivity. Moreover, synthesis of a library of SAHA analogs would be simple through only several steps since SAHA can be synthesized in three steps.[21c] With these advantages, SAHA analogue libraries and SAR studies led us to explore the impact of substituents in the linker region.

1.6 Specific aims

Our goal is syntheses of SAHA analogues with substituents on the linker region. First of all, small molecule libraries of SAHA analogues would elucidate the structural requirements of potent HDAC inhibitors. Second, developing novel isoform or class selective inhibitors would be explored by testing the selectivity of

the SAHA analogues. Third, screening small molecule analogues by using Fluor de Lys™ activity assay (Enzo) would allow analyzing potency and selectivity, and exploiting veiled interaction between specific cancer formation and selectivity. The evaluation of these analogues will be helpful to improve chemotherapeutic drug design.

SAHA achieved the first FDA approval among HDAC inhibitors for cutaneous T-cell lymphoma (section 1.3). Cancer patients, however, are still suffering from side effects.[19] Because side effects may be caused by the fact that SAHA is a pan inhibitor, the development of isoform or class-selective inhibitors would be critical to understand the relationship between toxicity and individual HDAC activity associated with cancer formation. Therefore, the development of selective inhibitors has been a significant aim for biological and pharmacological studies. Likewise, structure activity relationship (SAR) studies of small molecule HDAC inhibitors are required because only limited numbers of the selective inhibitors are reported. Therefore, our SAHA analogue syntheses and biological activity studies are a fitting starting point to design selective HDAC inhibitor and develop better chemotherapy with fewer side effects compared to current pan inhibitors.

1.7 Development of isoform or class-selective inhibitors

Presently, a minority of examples of SAHA analogues containing modifications on the carbon linker are reported, in spite of the promising area. For example, a few studies of the impact of substituents on the linker have

explored hydrophobic substituents (Figure 1.5).[24] No potency improvement was observed in ω-Alkoxy analogues **A_a**-**A_d**.[24a] In contrast to the ω-Alkoxy analogues of SAHA, aminosuberoyl hydroxamic acid analogue **A_e** is slightly more potent than SAHA.[24b] Furthermore, studies modifying the chain, such as alternating chain length and creating an unsaturated chain, were performed as HDAC inhibitors.[22c, 25] None of the sulfonamides **B_{a-d}** (HDAC1 IC_{50} 0.1-1 μM) having different chain length and unsaturated chain displayed potency compared to highly potent HDAC inhibitors, such as trichostatin A (TSA, IC_{50} 0.005 μM) and SAHA (HDAC1 IC_{50} 0.096 μM).[25a] However, when polyaminohydroxamic acid derivatives **C_a**, **C_b** were altered in the polyamine chain and terminal group, these analogues promoted increased level of acetylated histones H3, H4 and acetylated α-tubulin.[25b] In case of **C_a**, the increased level of acetylated α-tubulin was significant while **C_b** had no effect on the acetylation status of α-tubulin. Despite the modest change in chain length, distinct differences compared to SAHA were observed. As examples of various aryl or cycloalkyl groups in the linker, *N*-hydroxycarboxamides possessing the 1,4-cylohexylene group **D_a** and 1.4-phenylene group **D_b** were synthesized and showed only modest activities (WST-1 IC_{50} 77.9, 38.8 μM).[20c] In summary, SAR series of SAHA with substituents have been modestly explored. As a result, in our exploratory studies of the impact of substituents on the linker, several libraries of SAHA analogues were synthesized on the 2, 3, 6, and 7 positions to explore potency and selectivity (Figure 1.6).

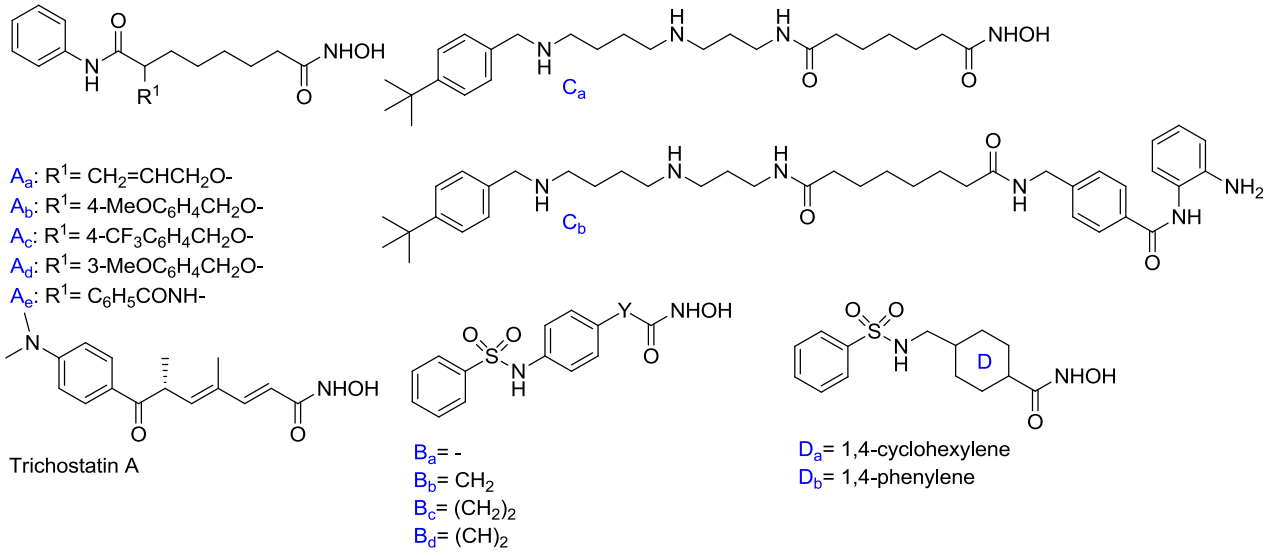

Figure 1.5. Structure Activity Relationship (SAR) Studies: HDAC inhibitors modified at the linker. The examples of substituents on the linker (left). The modification of chain length, creation of unsaturated chain, and alternation of aryl and cycloalkyl groups (right).

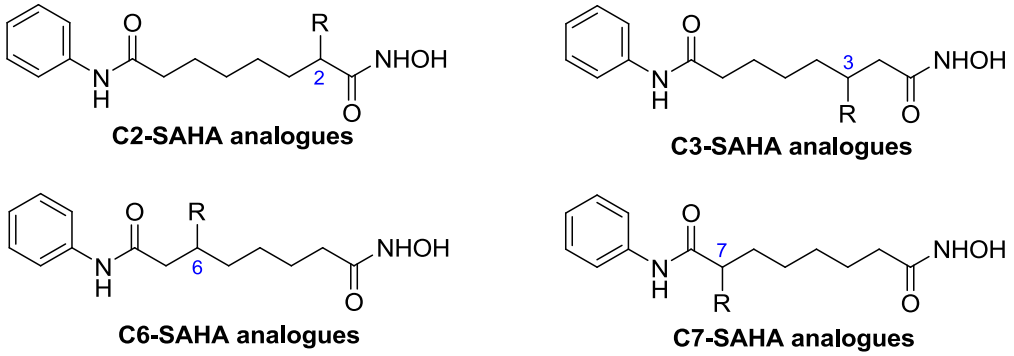

Figure 1.6. SAHA analogues containing substituents on the C2, C3, C6, and C7 positions

1.8 Preparation of SAHA analogues containing substituents on the linker near the hydroxamic acid

Since the metal binding site may be partially responsible for the potency of inhibitors, substituents on the SAHA linker area near hydroxamic acid were introduced. Our research group initially reported the synthesis and biological activity of C2-SAHA analogues to explore the impact of substituents near

hydroxamic acid.[26] HDAC inhibitory activities of C2-SAHA analogues were measured using in vitro fluorescence activity assay kit (Table 1.2).

Table 1.2. HDAC inhibition by SAHA, MS-275, and the C2-SAHA analogues using HeLa cell lysates

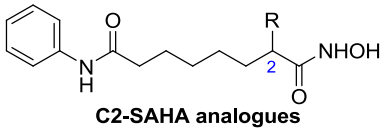

C2-SAHA analogues

Compounds	R	IC_{50}, μM[a]
SAHA		0.090 ± 0.004
MS-275		3.2 ± 0.1
	Methyl	134 ± 6
	Ethyl	449 ± 17
	n-Propyl	154 ± 7
	n-Butyl	72 ± 6
	n-Pentyl	40 ± 3
	n-Hexyl	60 ± 5
	Allyl	144 ± 9
	Propargyl	87 ± 5
	Benzyl	226 ± 11

[a]Values are the mean of three experiments with standard error given.

The smallest compound, the methyl variant (IC_{50} 134 μM), displayed 1500 and 50-fold decreased inhibition compared to SAHA (IC_{50} 0.09 μM) and MS-275 (IC_{50} 134 μM). Even the most potent pentyl variant showed 439 and 12-fold decreased activity compared to SAHA and MS-275. Regardless of the substituent size, SAHA analogues modified on the C2 position displayed inhibition in the μM range. The high IC_{50} values of the C2-SAHA analogues indicate that only limited steric size is tolerated in the HDAC active site near the

hydroxamic acid. In other words, bulky substituents near the solvent exposed capping group might be more tolerated in the HDAC active site.

The tendency for significantly decreased inhibition due to substituents near the hydroxamic acid proposed designing potent inhibitors. Specifically, the poor inhibition of C2-SAHA analogues suggests that analogues with substituents positioned closer to the capping group on the C3 position might be more tolerated in the HDAC active site. However, we hypothesized that the inhibitory activity could be unpredictable because substituents on each linker position would have different impact in the HDAC active site channel. Besides, the substituents on the C3 position could favorably interact with HDAC active site since the 14 Å internal channel near the hydroxamic acid is nearer to C3 carbon linker than C2 carbon (Figure 1.4). Therefore, a library of C3-SAHA analogues would explore the interaction of the inhibitor with the HDAC active site for potent and selective inhibition. The detailed synthesis and biological activity of the library of C3-SAHA analogues are described in Chapter 2.

1.9 Preparation of SAHA analogues containing substituents on the linker near the capping group

Small molecules with substituents on the capping group or on the linker region near the capping group have shown great potency (nM range) and moderate selectivity (class-selectivity) (Figure 1.7).[27] Specifically, FK-228 (depsipeptide), which gained FDA approval for cutaneous T-cell lymphoma in 2009,[28] displayed about 300-fold greater potency for HDAC1 and HDAC2 over HDAC6.[29] Apicidin also displayed 17-230-fold greater potency for HDAC2, 3, and

8 over HDAC1, 4, 6, 7, and 9.[30] Trapoxin B showed HDAC1 selectivity over HDAC6.[27c] The large capping groups in these HDAC inhibitors suggest that selectivity is influenced by the capping group substituents.

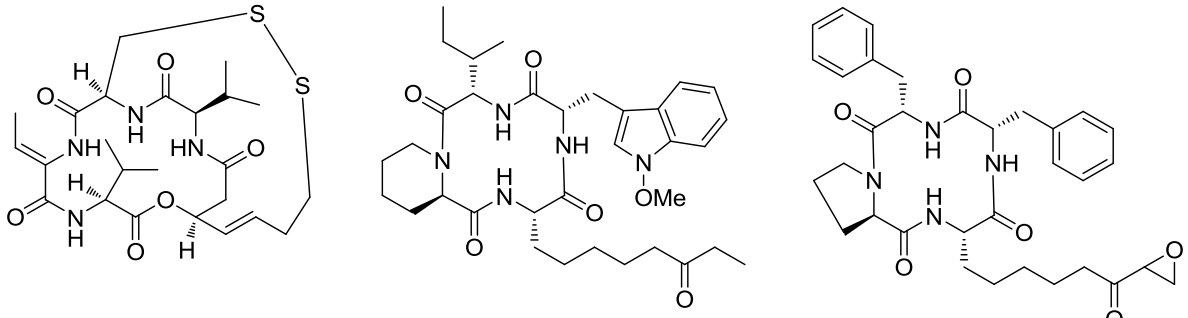

Figure 1.7. Known class-selective HDAC inhibitors with bulky groups

As an example of HDAC selective inhibitor SAR studies with bulky groups on the linker near the capping group, compound **E_a** (IC_{50} 730 nM) containing the unusual *L*-Aoda amino acid was selected and modified (Table 1.3).[31] The compounds contain a ketone motif, pentyl chain, and indole group instead of macrocycle. Although most of compounds lost 2-10 fold activity in the anti-proliferation assay, the 3-piperid-1-ylpropanamide variant **E_h** demonstrated improved enzyme and cellular activities. As a result, this SAR study altering the substituents near the capping group demonstrates the structural requirement between inhibitor structures and HDAC functions and directs the design of specific cancer drugs.

Table 1.3. HDAC1 and PRO (HeLa) inhibition by SAHA, MS-275, Apicidin, the compound **E_a**, and derivatives

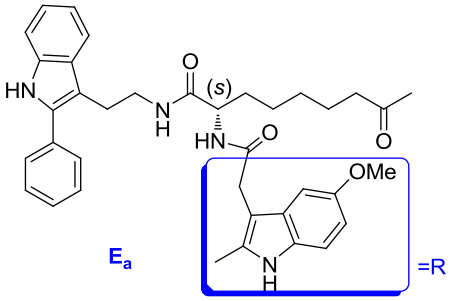

E_a

Compounds	R	HDAC1 IC_{50}, nM	PRO (HeLa)IC_{50}, nM
SAHA		27	460
MS-275		110	1800
Apicidin		44	290
E_a		590	730
E_b	Me	930	7600
E_c	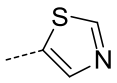	590	3000
E_d	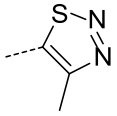	480	3400
E_e	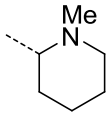	540	2500
E_f	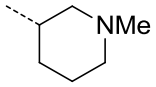	200	1200
E_g	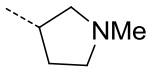	220	2000
E_h	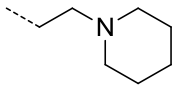	190	<390

Since selective inhibition could be influenced by bulky capping groups, SAHA analogues with large substituents on the capping group or on the linker

area near the capping group have been frequently designed, synthesized, and evaluated (Figure 1.8).[24a, 32 33] Based on a docking analysis in the crystal structures of HDAC7 and HDAC8[34] of the ω-alkoxy analogue **A_b**, a T-shape arrangement between substituents near the SAHA capping group and the lipophilic pockets surrounded by phenylalanine (Phe) residues was found. A π-π interaction between the p-methoxybenzyl moieties and Phe208 and Phe152 residues in the HDAC active site might influence isoform selectivity. Although selective inhibition of the ω-alkoxy analogue was not improved, it had superior antiproliferative activity. On the other hand, N^1-hydroxy-N^8-ferrocenlyoctanediamide, JAHA, displayed picomolar inhibition against class IIa HDAC6 (IC_{50} 8 pM) and anticancer action in intact cells (MCF7 cell line). Cytotoxicity against a breast cancer cell line indicated that SAHA is the most cytotoxic compound (IC_{50} 730nM in MCF7 breast cancer cell lines) compared to the JAHA series (IC_{50} 2-5μM in MCF7 breast cancer cell lines). The data suggest that the modification of SAHA with bulky groups improves selectivity with potency, but displays similar cytotoxicity against the cancer cell line to the parent compound *in vivo*.

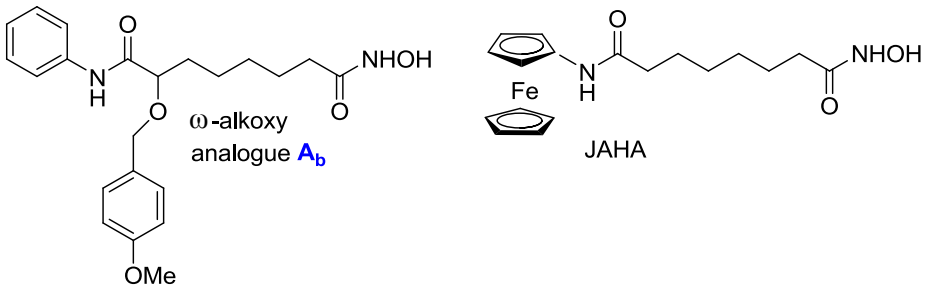

Figure 1.8. Examples of SAHA analogues containing substituents on the linker area near the capping group (left) and on the capping group (right)

1.10 Novel HDAC6-selective inhibitors

We have discussed potential isoform or class-selective inhibitors, and common efficacious compounds targeting class I-selectivity.[23a, 27c, 29-30] Fewer studies have focused on development of class II HDAC selective inhibitors. A recent cardiac study reported that stressed myocardium showed catalytic activity from the class IIb HDAC, HDAC6.[35] Also, overexpression of HDAC6 was detected in ovarian and breast cancer tissues.[9] Since HDAC6 contains two catalytic sites, development and design of HDAC6 selective inhibitor would elucidate the function and mechanism of HDAC6. Tubacin is a well-known HDAC6 selective inhibitor and displayed 4-fold greater potency for HDAC6 over HDAC1 (Figure 1.9).[36] Interestingly, the structure of tubacin has similarity with class I selective SAHA analogues with bulky substituents at the capping group. Slightly different modification on the capping group critically effects selectivity. The recent SAR studies of Tubastatin A showed improved selectivity (Figure 1.9).[37] Tubastatin A displayed greater than 1000-fold selectivity against HDAC6 (IC_{50} 15 nM) compared to HDAC1 (16 μM). An extensive library of tubastatin A indicated that tricyclic compounds displayed highly selective inhibition compared to other compounds. The structure of Tubastatin A motivates designing new isoform selective inhibitors. A detailed discussion of tricyclic compounds will be discussed in Chapter 4.

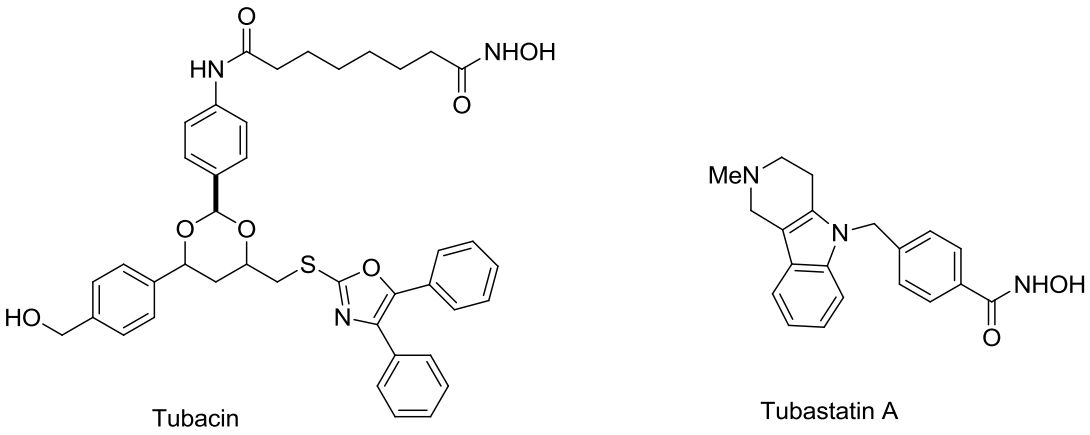

Figure 1.9. Structures of HDAC6-selective inhibitors

1.11 Evaluation of SAHA analogues containing substituents on the linker near the hydroxamic acid and capping group

Our initial syntheses of libraries of SAHA analogues on the C2 and C3 position was achieved with substituents containing hydrophobic groups since the carbon linker region of SAHA is surrounded by hydrophobic channel (Figure 1.4). The data showed that only limited tolerance exists in the HDAC active site near the metal binding moiety. In contrast, small molecules with large bulky groups have been synthesized near or on the capping group, leading to potent inhibitors.[21b, 37-38] The outcome suggests that the area near the capping group of HDAC inhibitors has great tolerance of steric bulky group in the HDAC active sites, confirming our hypothesis. Therefore, our syntheses of libraries of C6 and C7-SAHA analogues have introduced bulky substituents near the capping group (Chapter 3 and 4). Moreover, the substituents of the SAHA analogues on the C7 position, which is located closest to the capping group, might allow monitoring the interactions between hydrophilic substituents and the HDAC active sites

since the substituents would be placed on the entrance of the solvent exposed area.

1.12 Structure activity relationship (SAR) studies from matrix metalloproteinases (MMP), another hydroxamic acid binding protein

Several series of hydrophilic substituents were attached to small molecule inhibitors for improving anti-cancer drugs. Natural or medicinal compounds containing nitrogen have been designed and used in clinical studies or treatments of various diseases because of their outstanding chemical and biological activities. For instance, the matrix metalloproteinases (MMPs), like HDACs, are relevant enzymes involved in physiologically important processes.[39] Both MMP and HDAC protein are zinc-including metalloproteinases, which favorably interact with the hydroxamic acid moiety. Structural information on MMPs is related to HDACs because of their relationship as metal-dependent proteases. Since proteolysis of the extracellular matrix is found in numerous arthritis and cancers[40], several MMP inhibitors as therapeutics were discovered and modified. Even though HDAC and MMP proteins have similar proteases activities, SAR studies of MMP inhibitors with substituents containing nitrogen have been more explored than with HDAC inhibitors.

Table 1.4. Collagenase 1 (MMP1), gelatinase-A (MMP2), stromelysin 1 (MMP3), gelatinase-B (MMP9), collagenase 3 (MMP13) inhibition by *N*-aryl sulfonyl homocysteine hydroxamate analogues

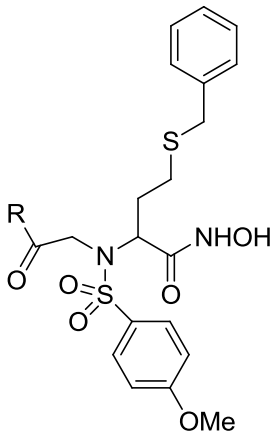

	IC_{50}, nM				
R	MMP1	MMP2	MMP3	MMP9	MMP13
F_a 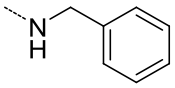	51	0.7	1.6	0.2	0.5
F_b 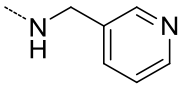	20	1.2	2.2	0.2	1.1
F_c 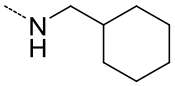	nt	0.30	nt	0.01	nt
F_d 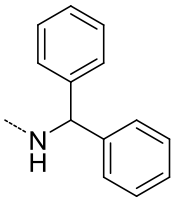	nt	2.3	3.7	0.5	4.5
F_e 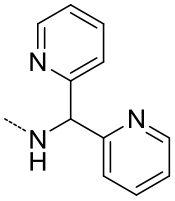	39	0.4	1.1	0.2	0.4
F_f 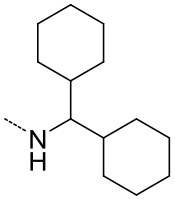	nt	8.82	nt	1.88	nt

As one fruitful example, the design, synthesis, and evaluation of MMP inhibitors were studied with *N*-aryl sulfonyl homocysteine hydroxamate inhibitors (Table 1.4).[41]The data showed that hydrophobic aryl groups significantly influenced potency. The dipyridyl methyl amide analogue **F_e** displayed similar potency to the monopyridyl analogue **F_b** while the additional cyclohexyl analogue **F_f** lost potent activity compared to the single cyclohexyl analogue **F_c**. On the other hand, both monopyridyl **F_b** and dipyridyl **F_e** analogues displayed greater than 20-fold selectivity against MMP2, MMP3, MMP9, and MMP13 compared to MMP1. The polarity of the pyridyl derivatives containing nitrogen might be a significant factor for MMP selectivity.

As another representative example, MMP pyridyl derivatives enhanced biological inhibitory activity (Table 1.5). Compounds **H_a**, **H_b**, and **J_b** displayed poor potency, while inactivity was observed in compounds **H_c**, **I**, and **J_a**. On the other hand, the pyridyl group on compound **J_b** lead to great potency with the selective inhibitory activity for MMP9 (IC_{50} 83 nM) against MMP1 (IC_{50} 15000 nM). The aliphatic substituents on compound **H_a** and **H_b** lead to greater inhibitory activity compared to analogues with the hydrophilic sustituents (**H_c**, **I**, and **J_a**). Despite the hydrophilicity of pyridyl group, the favorable interaction of the pyridyl derivative with MM9 specified that the nitrogen atom may impart selectivity.

Table 1.5. Collagenase 1 (MMP1), gelatinase-A (MMP2), stromelysin 1 (MMP3), gelatinase-B (MMP9), collagenase 3 (MMP13) inhibition by *N*-arylsulfonylaziridine hydroxamic acid analogues

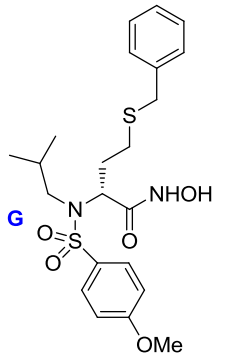

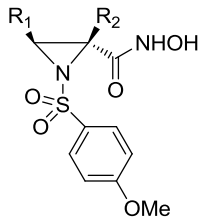

Ha: R_1= -H, R_2= -*i*-Bu
Hb: R_1= -H, R_2= -$(CH_2)_5$Ph
Hc: R_1= -H, R_2= -CH_2O-Ph-O-Ph

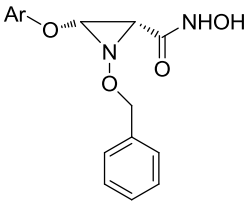

I: Ar= -Ph-O-Ph

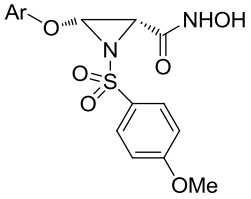

Ja: Ar= -Ph-O-Ph
Jb : Ar= -3-pyridyl

Compounds	IC_{50}, nM				
	MMP1	MMP2	MMP3	MMP9	MMP13
G	104	0.7	0.7	2.5	12
H_a	>10 000	617	213	184	380
H_b	26 400	259	595	203	231
H_c	>100 000	15 000	10 000	4 770	8 775
I	56 000	98 000	>100 000	>100 000	>100 000
J_a	50 000	3 600	2 000	500	>100 000
J_b	15 000	237	164	83	300

1.13 Evaluation of a pyridyl substituent on an HDAC inhibitor, Largazole

As the most recent example of the enhanced biological activity of an HDAC inhibitor containing nitrogen, natural product largazole analogues were reported with significant bioactivity (Figure 1.10).[42] Largazole was isolated from a marine cyanobacterium of the genus *Symploca* and showed selective activity against transformed human mammary epithelial cells (MDA-MB-231, GI_{50} 7.7 nM) over nontransformed murine mammary epithelial cells (NMuMG, GI_{50} 122 nM).[43] Also, the selectivity was displayed against transformed fibroblastic

osteosarcoma cells (U2OS, GI_{50} 55 nM) over nontransformed fibroblasts (NIH3T3, GI_{50} 480 nM). Analogues **K_a** and **K_b** showed significantly increased inhibitory activities for HDAC1 over HDAC6 (80%) while the parent compound (largazole) and analogue **K_c** displayed modest selective inhibition. Investigation of potential selective inhibitors has been an attractive target for chemists and biologists since specific isoforms might offer opportunities to develop selective anti-cancer drugs. With the biological activity trend, a compound containing a pyridyl group was synthesized, screened, and discussed in our research (Chapter 4).

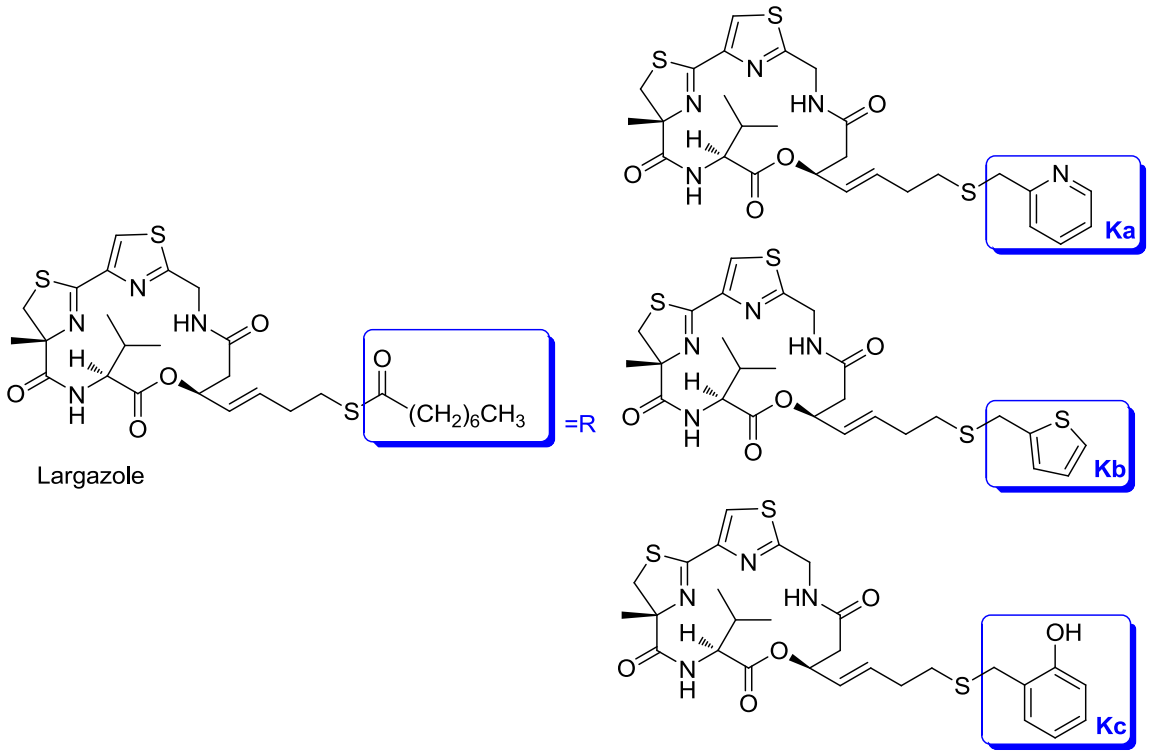

Figure 1.10. Structures of largazole and analogues

Currently, SAHA and the other candidates inhibit multiple HDAC members. However, isoform-specific HDAC inhibitors are promising targets with respect to clinical efficacy due to the fact that broad-spectrum inhibitors have demonstrated toxicities in the clinic.[44] The mechanism of relative action between the selectivity and toxicity of HDAC inhibitors in the clinic is not well-defined, but might reveal new mechanism-based therapeutics for cancers. Therefore, several studies have reported a link among different HDAC family members, specific tumor characteristics, and reduced toxicity profiles.[45] Specifically, HDAC inhibitor cytotoxicities of pediatric acute myeloid leukemia (AML) cell lines were tested by using MTT (3-[4,5-dimethyl-thiazol-2-yl]-2,5-diphenylterazolium-bromide) assays.[45e] At clinically practicable concentrations, dual HDAC inhibitors that inhibited both HDAC1 and HDAC6 displayed the best anti-leukemic activities in the four pediatric AML cell lines (THP-1, CMS, Kasumi-1, and MV4-11). As mentioned earlier, pre-clinical evaluation of HDAC6-selective inhibitors was highlighted in cardiovascular disease.[35] Furthermore, investigating HDAC inhibitors with hydrophilic substituents including a pyridyl group might enhance selective inhibition compared to common pan inhibitors. Even though the function or regulation of individual HDAC proteins is still not clear, the development of the specific-isoform HDAC protein inhibitors will lead optimal drugs for a variety of specific diseases.

CHAPTER 2 – SYNTHESIS OF SAHA ANALOGUES MODIFIED AT THE C3 POSITION

2.1 Rationale for design of the SAHA analogues containing substituents on the C3 position

Inhibitor binding to a zinc atom at the bottom of the active site plays a critical role in potency. Therefore, introducing substituents near hydroxamic acid would help understand structural requirements of HDAC inhibitors. The SAR study of SAHA on the linker area is relatively unexplored, in spite of it is being a fruitful potential area (Chapter 1.5). Especially, there is the possibility to develop isoform selective inhibitors through designing a library of SAHA analogues on the linker. When SAHA is present in HDAC active site, it has been observed that the linker is tightly surrounded by a hydrophobic tunnel (Figure 1.4). We theorized that hydrophobic substituents attached at the linker would display better interaction with the HDAC active site than hydrophilic substituents.

To explore the impact of substituents in the liker area, we previously studied SAHA analogues with hydrophobic substituents attached on the C2 position (Figure 2.1).[26] In this case, inhibitor potency was significantly reduced regardless of substituent size. The lack of potency of the C2-SAHA analogues indicates that limited flexibility exists in the HDAC active site near the hydroxamic acid group. In contrast, high potency (nM range) HDAC

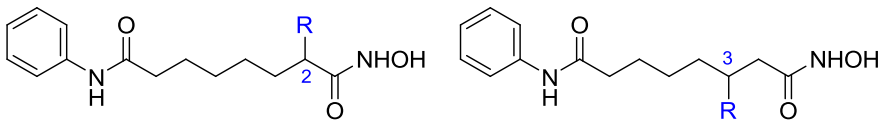

Figure 2.1. Structures of SAHA analogues containing substituents on the C2 and C3 position

inhibitors have been created with bulky substituent near the solvent-exposed region.[27c, 31, 46] Therefore, we proposed that HDAC proteins would be more tolerant of SAHA analogues containing substituents positioned closer to the solvent exposed surface.

To systematically probe the impact of substituents present in the linker, SAHA analogues with substituents on the C3 position were synthesized (Figure 2.1).[47] We theorized that analogues with substituents attached at the C3 position would display more potent inhibition compared to analogues with C2 substituents due to their location closer to the solvent-exposed region.

2.2 Initial synthesis

We initially synthesized the C3-SAHA *n*-butyl analogue **1a**, as shown Scheme 1. The ring of commercially available ε-caprolactone **2** was opened with aniline and trimethyl aluminum to give alcohol **3**, which was subjected to Swern oxidation to give aldehyde **4**. The Horner-Wadsworth-Emmons reaction with trimethyl phosphonoacetate gave the corresponding α,β-unsturated ester **5**. The (E) and (Z)-isomers of ester **5** were separated by column chromatography and then individually treated with a copper (I) bromide dimethylsulfide complex to give the *n*-butyl ester **6a**. Saponification of **6a** gave carboxylic acid **7**, which was coupled with *O*-benzyl-protected hydroxamine. *O*-benzyl-protected hydroxamic acid **8** was deprotected by hydrogenolysis to give the C3-*n*-butyl SAHA **1a**.

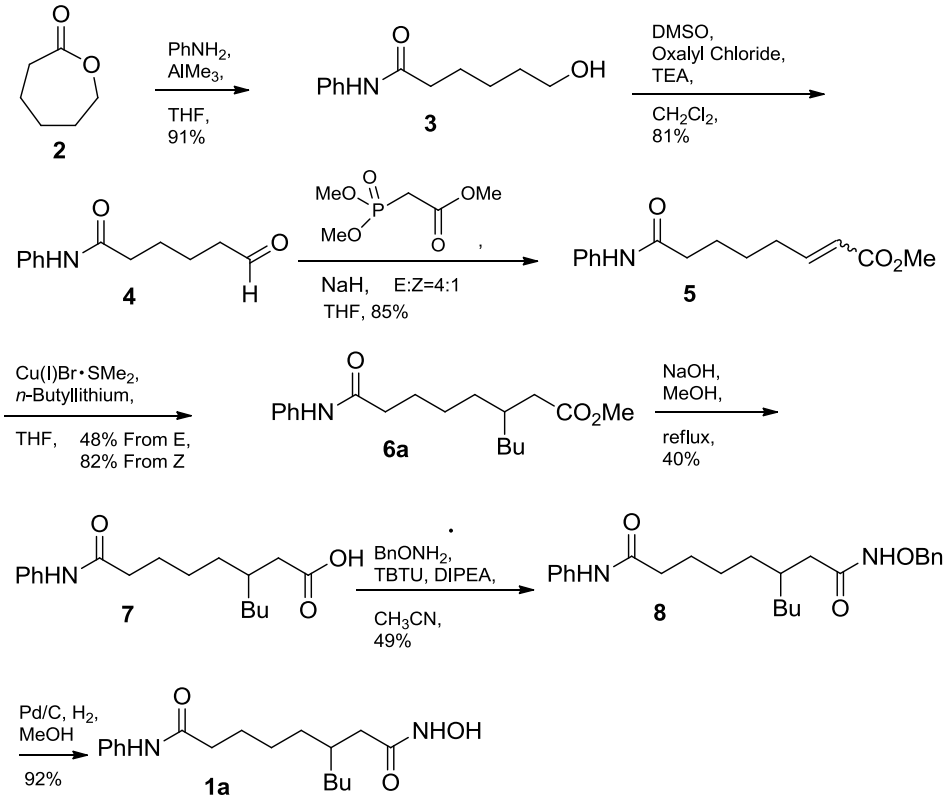

Scheme 2.1. Initial synthesis of C3-SAHA analogue (*n*-butyl derivative **1a**)

2.3 Optimized synthesis

To create the remaining C3-SAHA analogues, several aspects of the synthesis were improved (Scheme 2.2).

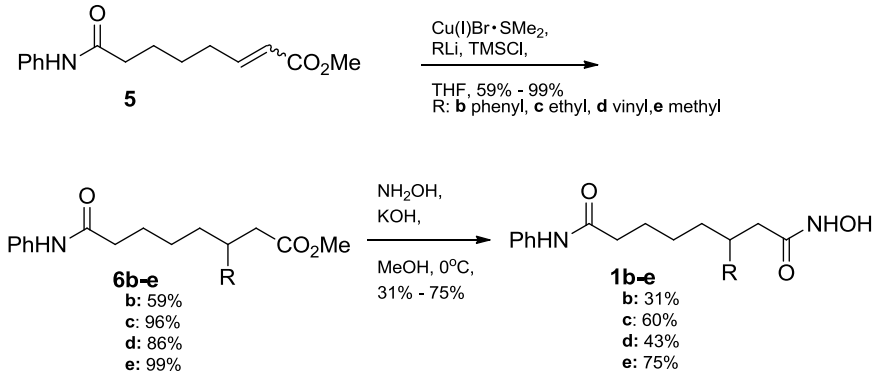

Scheme 2.2. Optimized synthesis of C3-SAHA analogues **1d** -**1e**

First, the 1,4-conjugate addition reaction (**5** to **6**) was performed using a mixture of (E) and (Z) isomers without the separation. Second, we found that when preparing compound **6e** from methyl lithium, no addition product was observed. However, addition of trimethylsilane chloride (TMSCl) to the reaction gave excellent yield.[48] With this success, TMSCl was included in the addition reaction with all remaining analogues. Finally, we used a direct, one-step conversion of ester **6** to the final product **1**. In the synthesis of C3-*n*-butyl SAHA **1a**, a benzyl-protected hydroxamic acid intermediate **8** was used en route to the hydroxamic acid final product, as previously reported (Scheme 1).[26] However, 40% yield after three steps (saponification, coupling *O*-benzyl hydroxylamine, and benzyl deprotection) was unsatisfying. The direct conversion using neutralized hydroxylamine in methanol was more efficient compared to the three-step conversion and was employed for all remaining analogues (**1b**-**1e**). Using theses modified conditions, the phenyl, ethyl, vinyl, and methyl analogues **1b**-**1e** were synthesized (Scheme 2.2).

2.4 Biological analysis

The inhibitory activities of the C3-SAHA were measured using Fluor de Lys™ *in vitro* fluorescence activity assay kit (Biomol) using HeLA cell lysates as the source of HDAC activity by Dr. Sujith Weerasinghe (Table 2.1).[26]

The methyl variant **1e** was the most potent analogue, displaying an IC_{50} of 350 nM, which is only 4-fold less potent than SAHA (90 nM). Theses results indicate that the active site of HDAC proteins can accommodate a small methyl

substituent at the C3 position. The potency of the remaining analogues decreased with increasing size of the C3 substituent. The *n*-butyl and phenyl analogues (**1a** and **1b**) displayed the weakest inhibitory activity (184 μM and 73 μM, respectively). Interestingly, the ethyl-substituted analogue **1c** displayed 91-fold decreased activity compared to the methyl analogue **1e**, despite containing only one additional methylene. Likewise, the vinyl analogue **1d** showed significantly reduce activity compared to the methyl analogue **1e**. In total, the data indicated that a C3-methyl substituted SAHA analogue maintains nM potency, but substituents larger than methyl result in a reduction in potency.

Table 2.1. HDAC inhibition by SAHA, MS-275, and the C3-SAHA analogues using HeLa cell lysates

Compounds	R	IC_{50}, μM[a]
SAHA		0.090 ± 0.004
MS-275		3.2 ± 0.1
1a	*n*-Butyl	184 ± 14
1b	Phenyl	73 ± 14
1c	Ethyl	32 ± 4
1d	Vinyl	15 ± 1
1e	Methyl	0.350 ± 0.05

[a]Values are the mean of three experiments with standard error given.

The inhibition results are consistent with the hypothesis that linker substituents are accommodated in the HDAC active site when positioned closer to the solvent exposed capping group of SAHA. While the C3-methyl analogue displayed potency comparable to SAHA (4-fold reduced), the previously reported

C2-methyl analogue (IC_{50} of 134 μM) displayed 1488-fold reduced activity versus SAHA.[26] Interestingly, the C3-*n*-butyl variant **1a** is less potent (184 μM IC_{50}) than the previously reported C2-*n*-butyl analogue (72 μM IC_{50}),[26] suggesting that the area of the HDAC active site near the C2 and C3 linker position displays structural differences.

We next tested the isoform selectivity of the C3-SAHA analogues. Creating isoform selective HDAC inhibitors has been challenging.[20] However, the availability of selective inhibitors would provide powerful chemical tools to dissect the individual functions of the HDAC isoforms, in addition to providing lead antitumor drug candidates. To assess the isoform selectivity of the C3-SAHA analogues, HDAC1 and HDAC3 representing class I and HDAC6 representing class II were tested at a single concentration near to their IC_{50} values using the Fluor de Lys™ kit (Figure 2.2). As expected, SAHA almost equally inhibited HDAC1, HDAC3, and HDAC6.[30] In contrast, the ethyl variant **1c** showed greater potency for HDAC6 over HDAC1 and HDAC3 at 32 μM. The butyl, phenyl, and vinyl variants (**1a**, **1b**, and **1c**) also showed similar, although more modest, preference for HDAC6 over HDAC3.

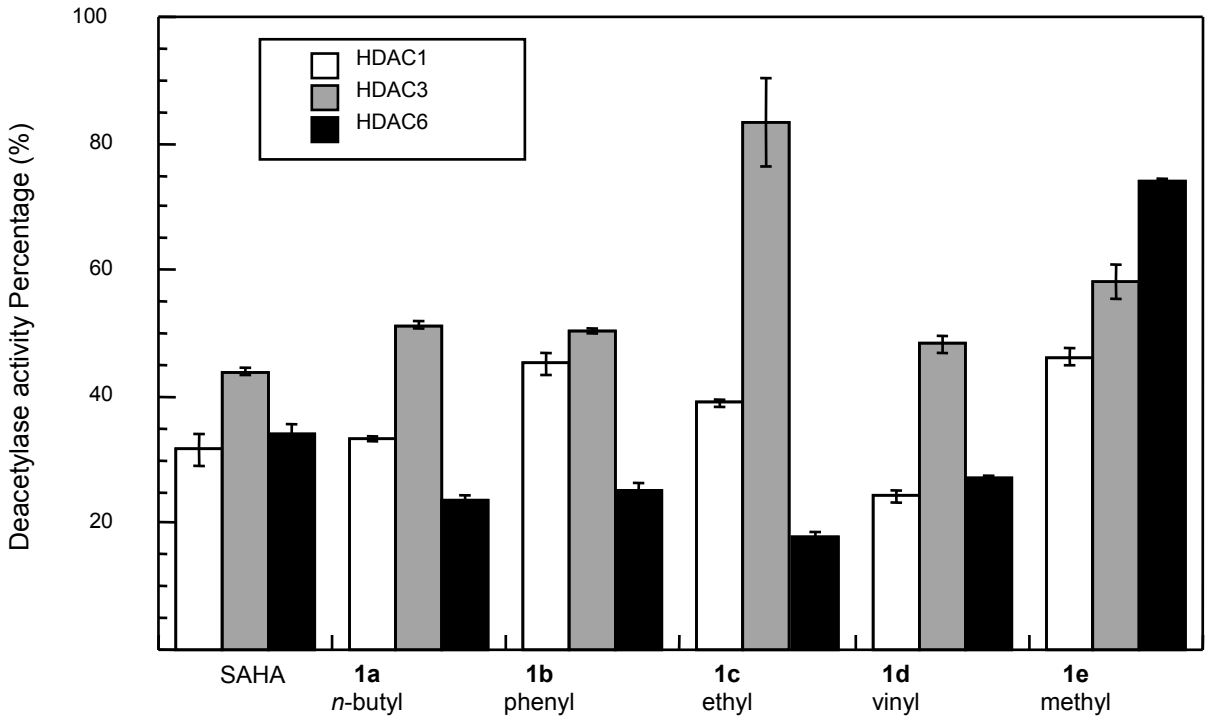

Figure 2.2. Screen of C3-SAHA analogues against HDAC1, HDAC3, and HDAC6 with 125 nM SAHA, 32 μM **1a-d**, and 375 nM **1e**.

To more rigorously assess the selectivity observed in the initial screen, we determined the IC_{50} values of the C3-ethyl variant **1c** because it displayed the most promising results in the initial screen. The C3-ethyl analogue **1c** displayed 12-fold selectivity for HDAC6 over HDAC3 and 3-fold selectivity for HDAC6 over HDAC1 (Table 2.2). In addition, it displayed selectivity within class I, with 4-fold preference for HDAC1 over HDAC3. As a control, SAHA displayed similar inhibitor activity against the isoform, as expected (Table 2.2).[30] The isoform selectivity analysis shows that a substituent on the C3 position can transform SAHA from non-selective inhibitor to an HDAC6-selective one. As a comparison, the HDAC6-selective inhibitor tubacin displays 7-fold selectivity for HDAC6 over

HDAC1[49] and has been used widely in cell biology studies.[50] Therefore, the data indicate that isoform selective SAHA analogues can be generated by attaching a substituent to the linker chain.

Table 2.2. IC_{50} values of SAHA and the C3-ethyl SAHA variant **1c** for HDAC1, HDAC3, and HDAC6

Compound	$IC_{50}/\mu M^a$		
	HDAC1	HDAC3	HDAC6
SAHA	0.096 ± 0.016	0.146 ± 0.012	0.074 ± 0.009
1c	22 ± 2	97 ± 6	8 ± 1

SAHA analogues with substituents on the C3 position displayed HDAC6-selective inhibition, in contrast to the broad-spectrum inhibitor SAHA. These results reveal that small structural changes in the linker region of SAHA can significantly influence selectivity.

2.5 Experimentals

2.5.1 General methods

Starting materials, reagents, and solvents for reactions obtained from Acros, Sigma-Aldrich, and VWR were used as purchased. Moisture-sensitive reactions were performed under argon with dried glassware and dry solvent. Iron-sensitive reactions were performed with acid-washed glassware and were purified with silica gel that was washed with 6M aqueous hydrochloric acid through at least 3 times. Thin-layer chromatography with 60Å, 250μm Partisil® K6F fluorescent indicator plates was used to monitor reactions. Flash

chromatography was performed with 60 Å, 230-400 mesh silica gel (Whatman). Solvents were removed by rotary evaporation (Büchi Rotavapor R-114 and Büchi Waterbath B-480) and a vacuum pump (Welch Vaccum, Thomas Industries, Inc.). NMR spectra were recorded in $CDCl_3$ or CD_3OD using a Varian Unity 300 MHz or Varian L900 400 MHz. Mass spectrometric analysis was performed at Wayne State University's Central Instrumentation facility using a Waters LCT Premier XE ESI-LC-MS TOF or a Waters GCT EI-TOF. IR spectra were recorded in Jasco FT/IR – 4100. HPLC analysis was performed with a Waters 1525 Binary HPLC pump, Waters 2998 Photodiode Array detector, and a Symmetry® Reverse Phase C_{18} 5µm column (4.6x150 mm Diameter) using a gradient of 10% Buffer A to 90% Buffer B over 20 min (Buffer A = water with 0.1% TFA; Buffer B = HPLC grade acetonitrile) at 1.0 mL/min at room temperature.

2.5.2 Experimental Procedures and Compound Characterization

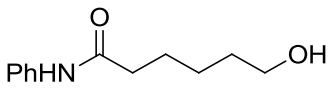

5-Hydroxy-*N*-phenylpentanamide (3). Trimethyl aluminum (1.88 mL, 3.75 mmol) and aniline (0.34 mL, 3.75 mmol) were stepwise added to a solution of *ε*–caprolactone (0.28 mL, 2.5 mmol) in dry THF (25 mL) at 0ºC. The mixture was stirred and warmed to room temperature over 3 h. The reaction mixture was quenched by a dropwise addition of 1.0 M aqueous hydrochloric acid until evolution of gas was not observed. The mixture was subsequently diluted with anhydrous diethyl ether (10 mL) and washed with distilled water (5 mL). The

aqueous layer was extracted with diethyl ether (10 mL) at least 3 times. The organic layer was dried over anhydrous Na_2SO_4, filtered, and concentrated. The residue was purified by column chromatography (20% acetone/CH_2Cl_2) on silica gel to give **3** (469 mg, 91%). ^{1}H-NMR (δ, ppm, CHLOROFORM-D): 1.41 (m, 2H), 1.58 (m, 2H), 1.71 (m, 2H), 2.39 (bs, 1H), 2.60 (m, 2H), 3.59 (m, 2H), 7.10 (t, 1H), 7.29 (t, 2H), 7.59 (d, 2H), 7.90 (bs, 1H); ^{13}C-NMR (δ, ppm, CHLOROFORM-D): 25.8, 25.9, 32.1, 39.1, 61.9, 120.2, 124.1, 128.9, 138.8, 173.5; IR: 3298, 3136, 3063, 2936, 2863, 1663, 1599, 1544, 1498, 1442, 1309, 908, 730 cm^{-1}; HRMS (EI-TOF, *m/z*): found [M] 207.1259, calc. for $C_{12}H_{17}NO_2$, 207.1259.

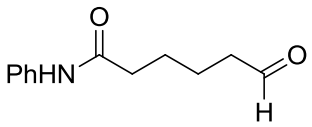

6-Oxo-6-(phenylamino)hexanal (4). To a solution of DMSO (1.75 mL, 24.62 mmol) in CH_2Cl_2 (75 mL) was added oxalyl chloride (5.60 mL, 11.19 mmol) dropwise and then 5-hydroxy-*N*-phenylpentanamide **3** (1.55 g, 7.46 mmol) stepwise at -78ºC. The reaction mixture was stirred for 45 min before triethylamine (TEA, 7.05 mL, 50.73 mmol) was added dropwise at -78 ºC. The mixture was warmed to room temperature and stirred for an additional 1 h. The reaction mixture was quenched by adding distilled water (75 mL). The mixture was diluted with CH_2Cl_2 (25mL) and washed with 1.0 M aqueous hydrochloric acid (25 mL), an aqueous solution of saturated $NaHCO_3$ (100 mL), and brine (100 mL). The organic layer was dried over anhydrous Na_2SO_4, filtered, and concentrated. The residue was purified by column chromatography (ether:petroleum ether 4:1) on silica gel to give **4** (1.25 g, 81%). ^{1}H-NMR (δ, ppm,

CHLOROFORM-D): 1.67-1.72 (m, 4H), 2.36 (t, 2H), 2.47 (t, 2H), 7.07 (t, 1H), 7.28 (t, 2H), 7.52 (d, 2H), 9.74 (bs, 1H); ^{13}C-NMR (δ, ppm, CHLOROFORM-D): 21.7, 25.1, 37.4, 43.8, 120.2, 124.5, 129.2, 138.2, 171.3, 202.7; IR: 3305, 3198, 3140, 3059, 2940, 2866, 2826, 2726, 1721, 1664, 1599, 1543, 1498, 1442, 1310, 909, 730 cm^{-1}; HRMS (EI-TOF, *m/z*): found [M] 205.1106, calc. for $C_{12}H_{15}NO_2$, 205.1103.

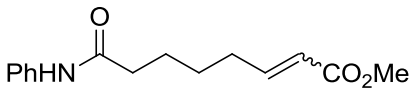

8-Oxo-8-(phenylamino)-oct-2-enoate (5). To a solution of NaH (435 mg, 10.88 mmol) in THF (64 mL) was added trimethyl phosphonoacetate (1.6 mL, 10.88 mmol) dropwise at 0 ºC and the mixture was stirred for 15 min. To the solution was added 6-oxo-6-(phenylamino)hexanal **4** (1.3 g, 6.40 mmol) at -78 ºC and the mixture was stirred for 15 min. The mixture was allowed to warm to room temperature and stirred for an additional 1 h. The mixture was quenched by addition of an aqueous solution of saturated NH_4Cl until evolution of gas was not observed. The mixture was washed with distilled H_2O (64 mL) at least 3 times. The organic layer was dried over anhydrous Na_2SO_4, filtered, and concentrated. The residue was purified by column chromatography (ether:petroleum ether 2:3) on silica gel to give **5** (E-isomer; 1,136 mg, 68%, Z-isomer; 289mg, 17%). For preparation of butyl derivative **6a**, the E and Z isomers were used separately, as described below. For the other derivatives **6b**-**e**, the E isomer alone or a mixture of E/Z isomers was used. Synthesis of the mixture of E/Z isomers was similar that of each isomer, except the following reagents were used: trimethyl

phosphonoacetate (391 mL, 2.57 mmol) in THF (15 mL), NaH (102 mg, 4.27 mmol) and 6-oxo-6-(phenylamino)hexanal **4** (310 mg, 1.51 mmol). The residue was purified by column chromatography (ether:petroleum ether 2:3) on silica gel to give **5 (E+Z)** (391 mg, 99%). (Z)-isomer ^{1}H-NMR (δ, ppm, CHLOROFORM-D): 1.54 (m, 2H), 1.76 (m, 2H), 2.38 (t, 2H), 2.68 (q, 2H), 3.71 (s, 3H), 5.79 (d, 1H, J=180 Hz), 6.24 (m, 1H), 7.09 (t, 1H), 7.29 (m, 2H), 7.51 (d, 2H), 7.64 (s, 1H); (E)-isomer ^{1}H-NMR (δ, ppm, CHLOROFORM-D): 1.54 (m, 2H), 1.76 (m, 2H), 2.21 (q, 2H), 2.38 (t, 2H), 3.71 (s, 3H), 5.82 (d, 1H, J=448 Hz), 6.94 (m, 1H), 7.08 (t, 1H) 7.27 (m, 2H), 7.49 (d, 2H); (E+Z)-isomer ^{13}C-NMR (δ, ppm, CHLOROFORM-D): 25.3, 27.8, 32.2, 37.5, 51.7, 120.1, 121.5, 124.3, 129.2, 138.2, 149.2, 150.4, 167.4, 171.3; IR: 3674, 3308, 2950, 1721, 1658, 1600, 1541, 1498, 1441, 1310, 910, 756, 693 cm^{-1}; HRMS (EI-TOF, *m/z*): found [M] 261.1361, calc. for $C_{15}H_{19}NO_3$, 261.1365.

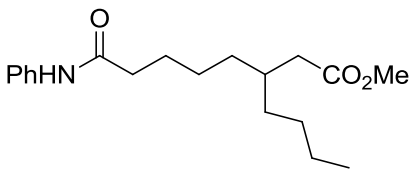

8-Oxo-8-(phenylamino)-3-*n*-butyloctanoate (6a). To a solution of Cu(I)Br·SMe_2 (880 mg, 4.28 mmol) in THF (14.3 mL) was added *n*-butyl lithium (5.35 mL, 8.56 mmol) dropwise at -15 ºC and the mixture was stirred for 20 min. The reaction mixture was cooled to -78 ºC before addition of (Z)-8-oxo-8-(phenylamino)-oct-2-enoate **5** (373 mg, 1.43 mmol, Z isomer only) at -78 ºC. The reaction was stirred for 3 h at -78 ºC to room temperature and then quenched by addition of 1.0 M

aqueous hydrochloric acid until a color of the mixture changed to blue ($CuCl_{2(aq)}$). The organic layer was dried over anhydrous Na_2SO_4, filtered, and concentrated. The residue was purified by column chromatography (ether:petroleum ether 2:3) on silica gel to give **6a** (378 mg, 83% from the Z isomer). The synthesis starting from the E isomer of **5** was similar to that above except the following reagents were used: Cu(I)Br·SMe_2 (470 mg, 2.28 mmol) in THF (11 mL), *n*-butyl lithium (2.85 mL, 4.56 mmol), and (E)-8-oxo-8-(phenylamino)-oct-2-enoate **5** (200 mg, 0.76 mmol, E isomer only) at -78 ºC. Chromatography gave **6a** (117 mg, 48% from the E isomer). ^{1}H-NMR (δ, ppm, CHLOROFORM-D): 0.87 (t, 3H), 1.24-1.32 (m, 10H), 1.70 (m, 2H), 1.84 (m, 1H), 2.21 (m, 2H), 2.33 (t, 2H), 3.65 (s, 3H), 7.07 (t, 1H), 7.29 (t, 2H), 7.51 (d, 2H), 7.62 (bs, 1H); ^{13}C-NMR (δ, ppm, CHLOROFORM-D): 14.3, 23.1, 25.9, 26.1, 29.0, 33.5, 33.7, 35.0, 37.7, 39.1, 51.7, 120.0, 124.3, 129.1, 138.3, 171.7, 174.4; IR: 3303, 3197, 3137, 3059, 2928, 2857, 1737, 1662, 1600, 1542, 1499, 1441, 1309, 903, 755, 693 cm^{-1}; HRMS (EI-TOF, *m/z*): found [M] 319.2143, calc. for $C_{19}H_{29}NO_3$, 319.2147.

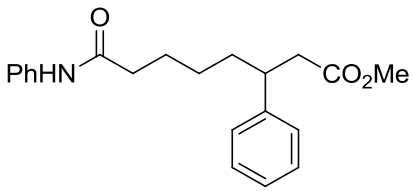

8-Oxo-8-(phenylamino)-3-phenyloctanoate (6b). To a solution of Cu(I)Br·SMe_2 (945 mg, 4.59 mmol) in THF (7.7 mL) was added phenyl lithium (4.59 mL, 9.19 mmol) dropwise at -15 ºC and the mixture was stirred for 20 min. The reaction mixture was cooled to -78 ºC. To the solution was added trimethylsilyl chloride (TMSCl, 1.76 mL, 13.78 mmol) dropwise and then 8-oxo-8-(phenylamino)-oct-2-

enoate **5** (200 mg, 0.77 mmol, only E isomer) stepwise at -78 ºC. Only the E isomer of **5** was used because the presence of the Z isomer complicated purification. The mixture was stirred for 3 h at -78 ºC and then quenched by addition of an aqueous solution of NH_4Cl:NH_4OH (1:1) until a color of the mixture turned to blue ($(NH_3)_4CuCl_{2(aq)}$). The mixture was washed with the aqueous solution of NH_4Cl:NH_4OH (1:1) (7.7 mL). The organic layer was dried over anhydrous Na_2SO_4, filtered, and concentrated. The residue was purified by column chromatography (ether:petroleum ether 1:1) on silica gel to give **6b** (154 mg, 59%). ^{1}H-NMR (δ, ppm, CHLOROFORM-D): 1.22 (m, 2H), 1.62-1.68 (m, 4H), 2.23 (m, 2H), 2.59 (m, 2H), 3.07 (m, 1H), 3.57 (s, 3H), 7.06 (t, 1H), 7.19 (m, 3H), 7.29 (m, 4H), 7.47 (d, 2H), 7.53 (bs, 1H); ^{13}C-NMR (δ, ppm, CHLOROFORM-D): 25.6, 27.0, 35.8, 37.6, 41.8, 42.1, 51.8, 120.1, 124.4, 126.8, 127.6, 128.7, 129.1, 138.3, 144.0, 171.6, 173.2; IR: 3310, 3045, 2924, 2857, 1698, 1603, 1600, 1456, 1378, 1265, 910, 755, 735 cm^{-1}. HRMS (EI-TOF, *m/z*): found [M+Na] 362.1732, calc. for $C_{21}H_{25}NO_3Na$, 362.1732;

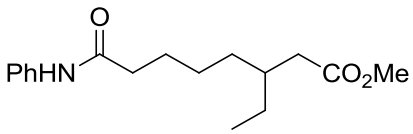

8-Oxo-8-(phenylamino)-3-ethyloctanoate (6c). The synthesis was similar that of **6b** except the following reagents were used: Cu(I)Br·SMe_2 (945 mg, 4.59 mmol) in THF (7.7 mL), ethyl lithium (5.41 mL, 9.19 mmol), TMSCl (1.76 mL, 13.78 mmol), and 8-oxo-8-(phenylamino)-oct-2-enoate **5** (200 mg, 0.77 mmol, E and Z mixture). The product was purified by column chromatography (ether:petroleum ether 1:1) on silica gel to give **6c** (215 mg, 96%). ^{1}H-NMR (δ,

ppm, CHLOROFORM-D): 0.85 (t, 3H), 1.23-1.38 (m, 6H), 1.9 (m, 2H), 1.78 (m, 1H), 2.21 (m, 2H), 2.32 (t, 2H), 3.64 (s, 3H), 7.07 (t, 1H), 7.28 (t, 2H), 7.51 (d, 2H), 7.77 (bs, 1H); ^{13}C-NMR (δ, ppm, CHLOROFORM-D): 11.0, 25.9, 26.2, 26.5, 33.1, 36.5, 37.7, 38.7, 51.7, 120.1, 124.3, 129.1, 138.4, 171.8, 174.4; IR: 3675, 3308, 3198, 3139, 3061, 2960, 2934, 1734, 1665, 1601, 1543, 1499, 1442, 1309, 911, 756, 733 cm^{-1}; HRMS (EI-TOF, *m/z*): found [M] 291.1830, calc. for $C_{17}H_{25}NO_3$, 291.1834.

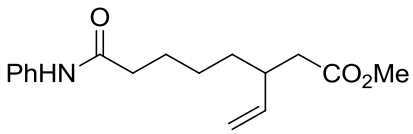

8-Oxo-8-(phenylamino)-3-vinyloctanoate (6d). The synthesis was similar to that of **6b** except the following reagents were used: CuI (875 mg, 4.59 mmol) in THF (7.7 mL), vinyl magnesium bromide (6.56 mL, 4.59 mmol), TMSCl (1.76 mL, 13.78 mmol), and 8-oxo-8-(phenylamino)-oct-2-enoate **5** (200 mg, 0.77 mmol, only E isomer). Only the E isomer of **5** was used because the presence of the Z isomer complicated purification. The product was purified by column chromatography (ether:petroleum ether 1:1) on silica gel to give **6d** (191 mg, 86%). ^{1}H-NMR (δ, ppm, CHLOROFORM-D): 1.33 (m, 2H), 1.39 (m, 2H), 1.70 (m, 2H), 2.30-2.34 (m, 4H), 2.50 (m, 1H), 3.64 (s, 3H), 5.00 (m, 2H), 5.57 (m, 1H), 7.08 (t, 1H), 7.29 (t, 2H), 7.50 (d, 2H), 7.57 (bs, 1H); ^{13}C-NMR (δ, ppm, CHLOROFORM-D): 25.6, 26.7, 34.1, 37.7, 40.1, 40.4, 51.7, 115.6, 120.0, 124.4, 129.2, 138.3, 140.9, 171.7, 173.3; IR: 3315, 3199, 3138, 3076, 2939, 2859, 1737, 1601, 1543, 1499, 1442, 1308, 915, 755 cm^{-1}; HRMS (EI-TOF, *m/z*): found [M] 312.1564, calc. for $C_{17}H_{23}NO_3Na$, 312.1576.

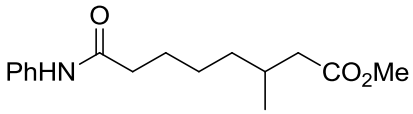

8-oxo-8-(phenylamino)-3-methyloctanoate (6e). The synthesis was similar that of **6b** except the following reagents were used: Cu(I)Br·SMe_2 (945 mg, 4.59 mmol) in THF (7.7 mL), methyl lithium (5.74 mL, 9.19 mmol), TMSCl (1.76 mL, 13.78 mmol) and 8-oxo-8-(phenylamino)-oct-2-enoate **5** (200 mg, 0.77 mmol, E and Z mixture). The residue was purified by column chromatography (ether:petroleum ether 2:3) on silica gel to give **6e** (232 mg, 99%). ^{1}H-NMR (δ, ppm, CHLOROFORM-D): 0.92 (d, 3H), 1.21-1.40 (m, 4H), 1.72 (m, 2H), 1.95 (m, 1H), 2.11-2.36 (m, 4H), 3.66 (s, 3H), 7.09 (t, 1H), 7.31 (t, 2H), 7.51 (d, 2H), 7.68 (bs, 1H); ^{13}C-NMR (δ, ppm, CHLOROFORM-D): 19.9, 25.8, 26.6, 30.3, 36.3, 37.7, 41.7, 51.7, 120.0, 124.3, 129.2, 138.3, 171.7, 174.1; IR: 3305, 3197, 3137, 3060, 2931, 2859, 1738, 1662, 1600, 1539, 1499, 1442, 1309, 1008, 902, 756 cm^{-1}; HRMS (EI-TOF, *m/z*): found [M] 277.1678, calc. for $C_{16}H_{23}NO_3$, 277.1678.

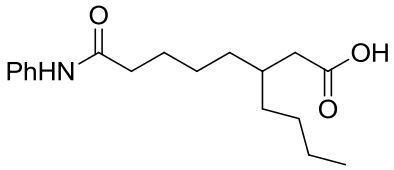

3-*n*-Butyl-*N*^{1}-hydroxyl-*N*^{8}-phenyloctanoic acid (7). To a solution of 8-oxo-8-(phenylamino)-3-*n*-butyloctanoate **6a** (492mg, 1.54mmol) was added NaOH (6.16 mL, 30.79 mmol) in MeOH (15 mL) and the mixture was refluxed overnight. The reaction was quenched by adding conc. aqueous hydrochloric acid (up to pH 6) and then extracting with H_2O (5 mL) and ethyl acetate (20 mL). The organic layer was dried over anhydrous Na_2SO_4, filtered, and concentrated. The residue

was purified by column chromatography (20% acetone/CH_2Cl_2) on silica gel to give **7** (189 mg, 40%). ^{1}H-NMR (δ, ppm, CHLOROFORM-D): 0.87 (t, 3H), 1.27-1.37 (m, 10H), 1.63 (m, 2H), 1.86 (m, 1H), 2.17-2.36 (m, 4H), 7.09 (t, 1H), 7.30 (t, 2H), 7.50 (d, 2H), 7.71 (bs, 1H); ^{13}C-NMR (δ, ppm, CHLOROFORM-D): 14.3, 23.1, 25.9, 26.1, 29.0, 33.5, 33.7, 35.0, 37.7, 39.1, 120.2, 124.5, 129.1, 138.2, 172.1, 179.5; IR: 3306, 3195, 3137, 3060, 2928, 2858, 1705, 1662, 1599, 1543, 1499, 1442, 1309, 907, 755, 692 cm^{-1}; HRMS (EI-TOF, *m/z*): found [M] 305.1993, calc. for $C_{18}H_{27}NO_3$, 305.1991.

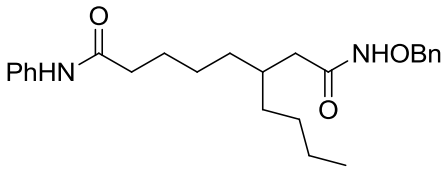

3-*n*-Butyl-*N*^{1}-benzyloxy-*N*^{8}-phenyloctanediamide (8). *O*-benzylhydroxylamine hydrochloride salt (144g, 0.9mmol) and Na_2CO_3 (47g, 0.45mmol) were dissolved in distill H_2O (9 mL), extracted with diethyl ether (9 mL) and concentrated. TBTU (289g, 0.9 mmol) and 3-*n*-butyl-*N*^{1}-hydroxyl-*N*^{8}-phenyloctanoic acid **7** (189mg, 0.6mmol) were added to the neutralized O-benzylhydroxylamine residue in CH_3CN (6mL). The reaction mixture was stirred overnight at room temperature and then quenched by adding $NaHCO_3$ (6 mL). The mixture was extracted with H_2O and DCM (1:1). The organic layer was dried over anhydrous Na_2SO_4, filtered, and concentrated. The residue was purified by column chromatography (10% acetone/DCM) on silica gel to give **8** (121 mg, 49%). ^{1}H-NMR (δ, ppm, CHLOROFORM-D): 0.86 (t, 3H), 1.22-1.35 (m, 12H), 1.66 (m, 1H), 1.94 (m, 2H), 2.30 (m, 2H), 5.29 (s, 2H), 7.07 (t, 1H), 7.28 (m, 7H), 7.55 (d, 2H), 8.12 (bs, 1H);

^{13}C-NMR (δ, ppm, CHLOROFORM-D): 14.3, 23.1, 25.3, 25.7, 29.1, 32.5, 33.7, 35.0, 37.2, 37.9, 78.4, 120.1, 124.3, 128.8, 129.1, 129.4, 138.5, 171.0, 172.3; IR: 3724, 3195, 3140, 3064, 2929, 2858, 1656, 1620, 1600, 1544, 1498, 1442, 1380, 1309, 1253, 1046, 1030, 975, 911, 734, 695 cm^{-1}; HRMS (EI-TOF, *m/z*): found [M] 410.2566, calc. for $C_{25}H_{34}N_2O_3$, 410.2569.

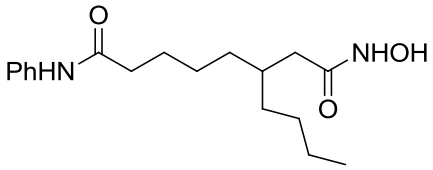

3-*n*-Butyl-*N*^{1}-hydroxyl-*N*^{8}-phenyloctandiamide (1a). To a solution of 3-*n*-butyl-*N*^{1}-benzyloxy-*N*^{8}-phenyloctanediamide **8** (121 mg, 0.3 mmol) in methanol (3mL) was added 20% $Pd(OH)_2/C$ (32 mg, 0.03 mmol) in an acid-washed 25mL round-bottom flask and the reaction mixture was purged with $H_{2\,(g)}$ for 30 s. The reaction solution was stirred under $H_{2\,(g)}$ for 30 min and then filtered through a plug of Celite with MeOH (9 mL). The filtrate was concentrated to give **1a** (89 mg, 92%) as a clear oil. ^{1}H-NMR (δ, ppm, METHANOL-D4): 0.88 (t, 3H), 1.28-1.39 (m, 10H), 1.68 (m, 2H), 1.86 (m, 1H), 2.02 (d, 2H), 2.37 (t, 2H), 7.07 (t, 1H), 7.28 (t, 2H), 7.52 (d, 2H); ^{13}C-NMR (δ, ppm, METHANOL-D4): 13.2, 22.8, 25.9, 28.6, 33.1, 33.2, 35.0, 36.7, 37.6, 120.1, 123.9, 128.6, 138.7, 171.4, 173.5; IR: 3384, 3044, 2929, 2858, 1640, 1600, 1546, 1499, 1468, 1309, 976, 903, 755, 693 cm^{-1}; HRMS (EI-TOF, *m/z*): found [M] 320.2108, calc. for $C_{18}H_{28}N_2O_3$, 320.2100; HPLC analytical purity analysis: 92%.

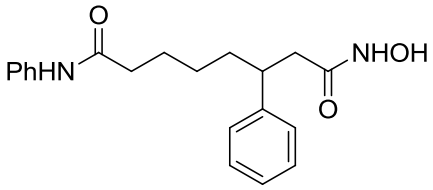

3-Phenyl-*N*^{1}-hydroxyl-*N*^{8}-phenyloctandiamide (1b). To a solution of $NH_2OH{\cdot}HCl$ (315 mg, 4.54 mmol) in methanol (4.5 mL) was added KOH (509 mg, 9.08 mmol) at 0 ˚C in an acid-washed 25mL round-bottom flask. After stirring for 20 min, 8-oxo-8-(phenylamino)-3-phenyloctanoate **(6b)** (154 mg, 0.45 mmol) was added and the mixture was stirred for 8 h at 0°C. The reaction mixture was quenched by adding 1mL of distilled water and adjusting to pH 6 by adding concentrated aqueous hydrochloric acid. The mixture was diluted with 30 mL of ethyl acetate, and washed with distilled water. The organic layer was dried over anhydrous Na_2SO_4, filtered and concentrated. The residue was purified by column chromatography (10% methanol/CH_2Cl_2) on acid-washed silica gel to give **1b** (48 mg, 31%). ^{1}H NMR (δ, ppm, METHANOL-D4): 1.22 (m, 2H), 1.55-1.73 (m, 4H), 2.25-2.43 (m, 4H), 3.09 (m, 1H), 7.06 (t, 1H), 7.12-7.29 (m, 7H), 7.47 (d, 2H); ^{13}C-NMR (δ, ppm, METHANOL-D4): 25.6, 26.8, 35.4, 36.6, 40.2, 42.3, 120.1, 124.0, 126.4, 127.5, 128.3, 128.5, 138.6, 143.9, 170.1, 173.4; IR: 3256, 3030, 2932, 2860, 2559, 1646, 1600, 1545, 1499, 1468, 1442, 1420, 1372, 1310, 1253, 906, 758 cm^{-1}; HRMS (EI-TOF, *m/z*): found [M] 340.1789, calc. for $C_{20}H_{24}N_2O_3$, 340.1787; HPLC analytical purity analysis: 91%.

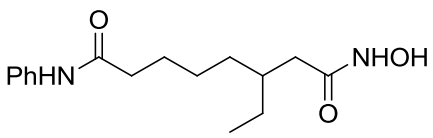

3-Ethyl-*N*^{1}-hydroxyl-*N*^{8}-phenyloctandiamide (1c). A similar procedure to that for **1b** was used, except for the following reagents: $NH_2OH{\cdot}HCl$ (520 mg, 7.48 mmol) in methanol (7.4 mL), KOH (839 mg, 14.96 mmol), 8-oxo-8-(phenylamino)-3-ethyloctanoate **(6c)** (218 mg, 0.75 mmol) and stirring for 4 h. In this case, the product was purified by column chromatography (8 % methanol/CH_2Cl_2) on acid-washed silica gel to give **1c** (130 mg, 60%). ^{1}H-NMR (δ, ppm, METHANOL-D4): 0.88 (t, 3H), 1.28-1.41 (m, 6H), 1.68 (m, 2H), 1.81 (m, 1H), 2.01 (m, 2H), 2.36 (t, 2H), 7.07 (t, 1H), 7.28 (t, 2H), 7.52 (d, 2H); ^{13}C-NMR (δ, ppm, METHANOL-D4): 9.8, 25.9, 32.6, 36.5, 36.7, 37.1, 120.1, 123.9, 128.6, 138.7, 171.4, 173.5; IR: 3857, 3404, 2935, 2862, 1649, 1600, 1544, 1501, 1469, 1311, 978, 904, 758, 691 cm^{-1}; HRMS (EI-TOF, *m/z*): found [M-H] 292.1718, calc. for $C_{16}H_{23}N_2O_3$, 292.1709; HPLC analytical purity analysis: 99%.

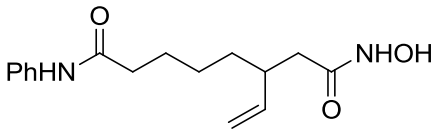

3-Vinyl-*N*^{1}-hydroxyl-*N*^{8}-phenyloctandiamide (1d). A similar procedure to that for **1b** was used, except for the following reagents: $NH_2OH{\cdot}HCl$ (456 mg, 6.57 mmol) in methanol (6.6 mL), KOH (737 mg, 13.13 mmol), 8-oxo-8-(phenylamino)-3-vinyloctanoate **(6d)** (190 mg, 0.66 mmol), and stirring for 6 h. In this case, the product was purified by column chromatography (8 % methanol/CH_2Cl_2) on acid-washed silica gel to give **1d** (83 mg, 43%). ^{1}H-NMR (δ, ppm, METHANOL-D4): 1.33-1.47 (m, 4H),1.70 (m, 2H), 2.08 (m, 2H), 2.35 (t, 2H), 2.50 (m, 1H), 5.00 (q, 2H), 5.58 (m, 1H), 7.07 (t, 1H), 7.28 (t, 2H), 7.52 (d, 2H); ^{13}C-NMR (δ, ppm,

METHANOL-D4): 25.6, 26.5, 33.9, 36.6, 38.3, 40.8, 115.0, 120.1, 124.0, 128.6, 138.7, 140.7, 170.3, 173.4; IR: 3299, 3079, 2931, 1647, 1600, 1542, 1500, 1442, 1312, 920, 758, 692 cm^{-1}; HRMS (EI-TOF, *m/z*): found [M+Na] 313.1533, calc. for $C_{16}H_{22}N_2O_3Na$, 313.1528; HPLC analytical purity analysis: 94%.

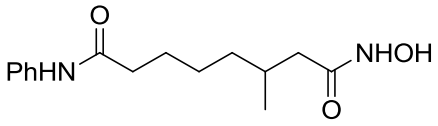

3-Methyl-*N*^{1}-hydroxyl-*N*^{8}-phenyloctandiamide (1e). A similar procedure to that for **1b** was used, except for the following reagents: $NH_2OH{\cdot}HCl$ (533 mg, 7.67 mmol) in methanol (7.7 mL), KOH (860 mg, 15.33 mmol), 8-oxo-8-(phenylamino)-3-methyloctanoate **(6e)** (213 mg, 0.77 mmol), and stirring for 2 h. In this case, the product was purified by column chromatography (10 % methanol/CH_2Cl_2) on acid-washed silica gel to give **1e** (160 mg, 75%). ^{1}H-NMR (δ, ppm, METHANOL-D4): 0.93 (d, 3H), 1.28 (m, 2H), 1.40 (m, 2H), 1.68 (m, 2H), 1.89 (m, 2H), 2.07 (m, 1H), 2.36 (t, 2H), 7.07 (t, 1H), 7.28 (t, 2H), 7.52 (d, 2H); ^{13}C-NMR (δ, ppm, METHANOL-D4): 18.6, 25.8, 26.4, 30.4, 36.2, 36.7, 40.1, 120.1, 123.9, 128.6, 138.7, 171.1, 173.4; IR: 3198, 2927, 2855, 2359, 1657, 1598, 1544, 1499, 1443, 755, 691 cm^{-1}; HRMS (EI-TOF, *m/z*): found [M] 278.1635, calc. for $C_{15}H_{22}N_2O_3$, 278.1630; HPLC analytical purity analysis: 98%.

2.6 HDAC high-throughput assay

2.6.1 Fluorescence activity assay for libraries of SAHA analogues

A number of HDAC inhibitors have been attractive targets as chemotherapeutic drugs due to that the overexpression activity of HDAC, which leads malignant diseases, as discussed (Section 1.2). Our research is also focused on development of novel HDAC inhibitors based on SAHA. Therefore, SAHA analogues were screened compared to SAHA using a Fluorescence high-throughput assay. The deacetylase activity was measured using the Fluor de Lys® activity assay (Enzo) using the manufacturer's protocol(Figure 2.3).[51]

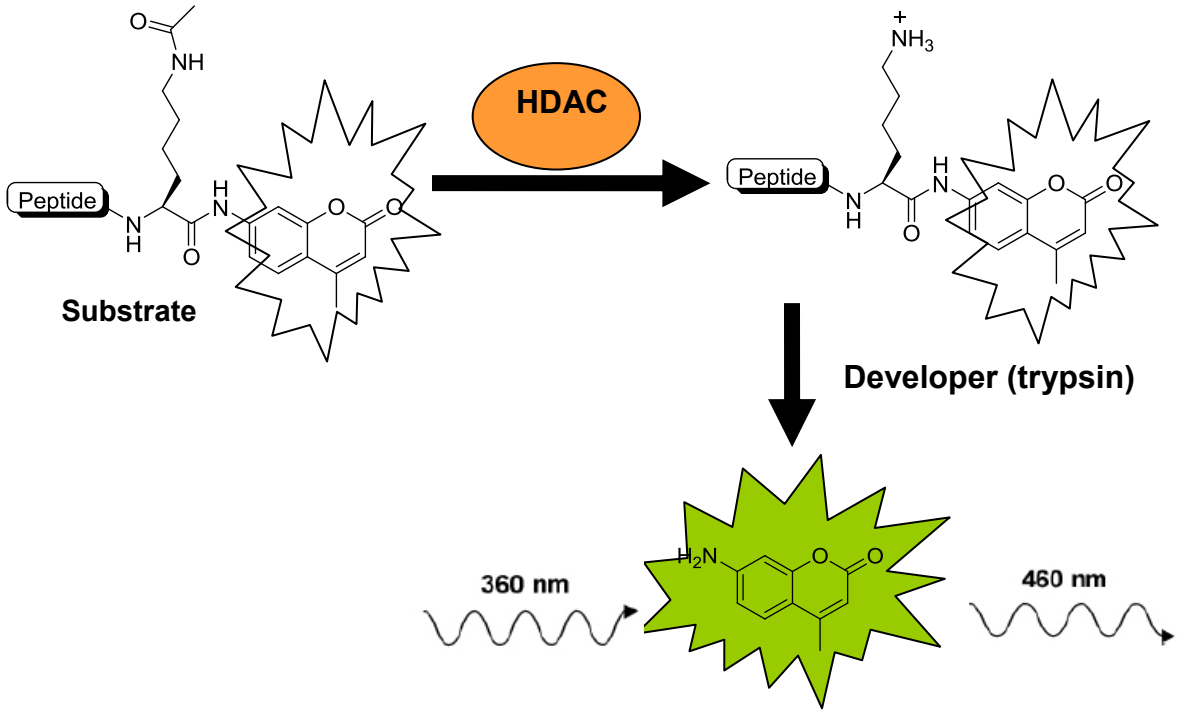

Figure 2.3. HDAC Fluorescent activity assay. Deacetylation of the substrate sensitizes to the developer.

To measure global HDAC inhibition, HeLa lysates, which contains a mixture of HDAC1-8 and HDAC10-11, were incubated with or without SAHA

analogues in HDAC assay buffer solution. After the initial incubation, Fluor de Lys® substrate in HDAC assay buffer was added to the reaction. The peptidic substrates consisted of an ε-acetylated lysine residue and a 4-methylcoumarin-7-amide at the carboxy terminal unit. In the reaction catalyzed by HDACs, the acetylated lysine residue of the substrate was deacetylated, while acetylated lysine would remain in the reaction when inhibited by the SAHA analogues. To quench the reaction and allow color development, Fluor de Lys® developer was added to the reaction mixture. In this reaction, the only deacetylated peptidic lysine substrates containing the methylcoumarinamide were cleaved by trypsin to release the fluorescence molecule, methylcoumarin. In other word, the acetylated lysine substrate present when the reaction was inhibited by the SAHA analogues did not result in measurable cleavage by trypsin and did not release the fluorescence molecule (no fluorescence activity). As a result, the high level of deacetylated activity of the substrates indicated low inhibitory activity of the SAHA analogues. The fluorescence intensity was determined using a Geniosplus Fluorimeter (Tecan) with excitation at 360 nm and emission at 465 nm.

2.6.2 HDAC assay procedure

HDAC activity of the C3-SAHA analogues was measured using the Fluor de Lys™ activity assay (Biomol) using the manufacturer's protocol by Dr. Sujith Weerasinghe. To measure global HDAC inhibition, HeLa lysates (approximately 4μg of total protein) were incubated with small molecule inhibitor or without small molecule inhibitor (2% DMSO) in HDAC assay buffer (50 mM Tris/Cl, pH 8.0, 137

mM NaCl, 2.7 mM KCl, 1 mM $MgCl_2$) at a final volume of 25 µL for 30 min at 30 ˚C with shaking. Concentrations of small molecule between 1 nM and 1 mM final concentration were used to determine IC_{50} values. Because the small molecules were stored in DMSO, dilution with HDAC buffer ensured that a maximum of 2% DMSO was present in the final reaction mixture. After the initial incubation, Fluor de Lys™ substrate in HDAC assay buffer (100 µM final concentration) was added to make a total reaction volume of 50µL. The reaction mixture was incubated at 30˚C for 45 min with shaking. To quench the reaction and allow color development, Fluor de Lys™ developer (2.5 µL of 20X diluted up to 50 µL in HDAC assay buffer) was added to give a final 100 µL volume and incubated with shaking for 5 min at room temperature. The fluorescence intensity was determined using a Geniosplus Fluorimeter (Tecan) with excitation at 360 nm and emission at 465 nm.

To perform the isoform selectivity studies, the procedure was similar except that the HeLa cell lysates were replaced with 0.2 µg HDAC1 (specific activity = 42.5 pmol/min/µg), 0.05 µg HDAC3 (specific activity = 249 pmol/min/µg) or 0.25 µg HDAC6 (specific activity = 257 pmol/min/µg), purchased from BPS Biosciences. In addition, the Fluor de Lys™ substrate was used at a final concentration of 50 µM for HDAC1 or 25µM for HDAC3 and HDAC6.

For each trial, a no enzyme control sample was used to assess the background. The background-corrected fluorescence units of small molecule-treated samples were then compared to that of untreated samples (set to 100%) to give a percentage deacetylase activity. IC_{50} values were obtained by plotting

the percentage deacetylase activity versus the small molecule concentration and fitting the data to a sigmoidal dose-response curve ($y=100/(1+(x/m3)^{m4}$) using KaleidaGraph software where m1 is the IC_{50} value in Molar units. All experiments were performed in triplicate with the mean and standard error reported in the tables and figures.

CHAPTER 3 – SYNTHESIS OF SAHA ANALOGUES MODIFIED AT THE C6 POSITION

3.1 Rationale for design of SAHA analogues modified at the C6 position

A limited number of structure activity relationship (SAR) studies on the linker area of SAHA have been performed, even though the linker region might influence inhibitory activity and selectivity (Section 1.7). In fact, many number of inhibitors that have substituents on the linker have been discovered with great potency and selective inhibition when substituents were attached near or on the capping group (Section 1.9). Specifically, tubacin with a bulky substituent at the capping group has been used in pharmacokinetic and clinical studies (Figure 1.9). Also, based on data from previous C2 and C3-SAHA libraries[26, 47], substituents on the C6 position might lead to potent inhibitory activities because C6-SAHA substituents would be located close to the solvent-exposed region of the active site. As discussed in the chapter 2, the C3-SAHA ethyl analogue showed selective inhibition for HDAC6 over HDAC1 and HDAC3.[47] To expand our understanding of the impact of substituents, synthesis of C6-SAHA analogues with hydrophobic substituents was achieved because the carbon linker is surrounded by a hydrophobic tunnel.

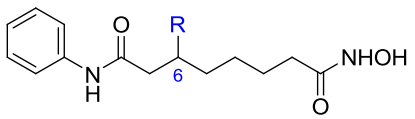

Figure 3.1. Structure of SAHA analogues containing substituents on the C6 position

The earlier results from the C2 and C3-SAHA libraries showed that the steric environment on the SAHA carbon linker caused reduced inhibitory activity, in

addition to influencing selective inhibition.[26, 52] With the potential to improve selectivity, the C6-SAHA library (Figure 3.1) was synthesized. We proposed that the HDAC protein active site would not only be more tolerant of bulkier substituents on the C6 position near the solvent-exposed area but the C6-SAHA analogues would also display more selectivity compared to the C2 and C3-SAHA analogues based on the previous reports about several class-selective inhibitors with bulky substituents in the capping group region (Section 1.9).[20]

3.2 Initial synthesis

To elucidate the impact of substituents present near the solvent-exposed area, C6-SAHA analogues were synthesized. Like C2 and C3-SAHA analogues (Chapter 1 and 2), we selected hydrophobic substituents since the carbon linker is surrounded by a hydrophobic tunnel (Figure 1.4). Also, we theorized that bulky analogues on the C6 position would display more potent inhibition compared to C2 and C3-SAHA analogues due to their proximity to the solvent-exposed surface.

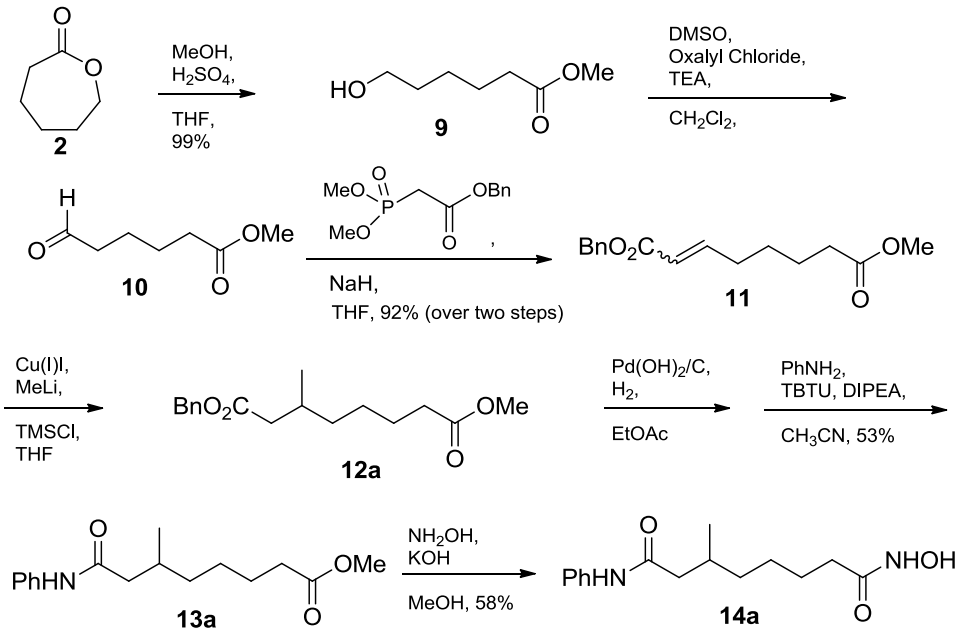

Scheme 3.1. Initial synthesis of C6-SAHA analogue (methyl derivative **14a**)

Initially, we synthesized the C6-SAHA methyl analogue **14a**, as outlined in Scheme 3.1. Due to symmetry compared to the C3-SAHA analogues, synthesis of the C6-SAHA analogues was straightforward and similar to that of the C3-SAHA library. The major differences between two syntheses are the following. Commercially available ε-caprolactone **2** was opened to give methyl 6-hydrohexanoate **9** under Fisher conditions instead of building the anilide derivative. The alcohol compound **9** was subjected to Swern oxidation to give aldehyde **10** similar to the C3-aldehyde formation. For the Horner-Wadsworth-Emmons reaction, using benzyl dimethyl phosphonoacetate instead of using trimethyl phosphonoacetate gave the corresponding α,β-unsturated benzyl ester **11** that allowed incorporation of substituents, which provided the precursor for anilide derivative **13a**. A mixture of (E) and (Z)-isomers of ester **11** were treated with a copper (I) iodide to give the methyl substituted ester **12a**. Similar to the

previous optimized synthesis of the C3-methyl SAHA analogue (Scheme 2) where the 1,4-addition demonstrated quantitative yield, the C6-methyl ester **12a** was synthesized and characterized without impurities according to thin layer chromatography (TLC) and ^{1}H & ^{13}C NMR spectra analysis. Therefore, the methyl ester **12a** without purification was deprotected by hydrogenolysis and coupled with aniline in 53% yield (over the three steps). In contrast to the C3-SAHA library where the anilide derivative was installed at the beginning stage, the anilide **13a** was created from benzyl ester **12a** at a late stage, which attached substituents near the capping group. The methyl ester derivative **13a** was directly converted to the methyl hydroxamic acid **14a**.

3.3 Modified synthesis

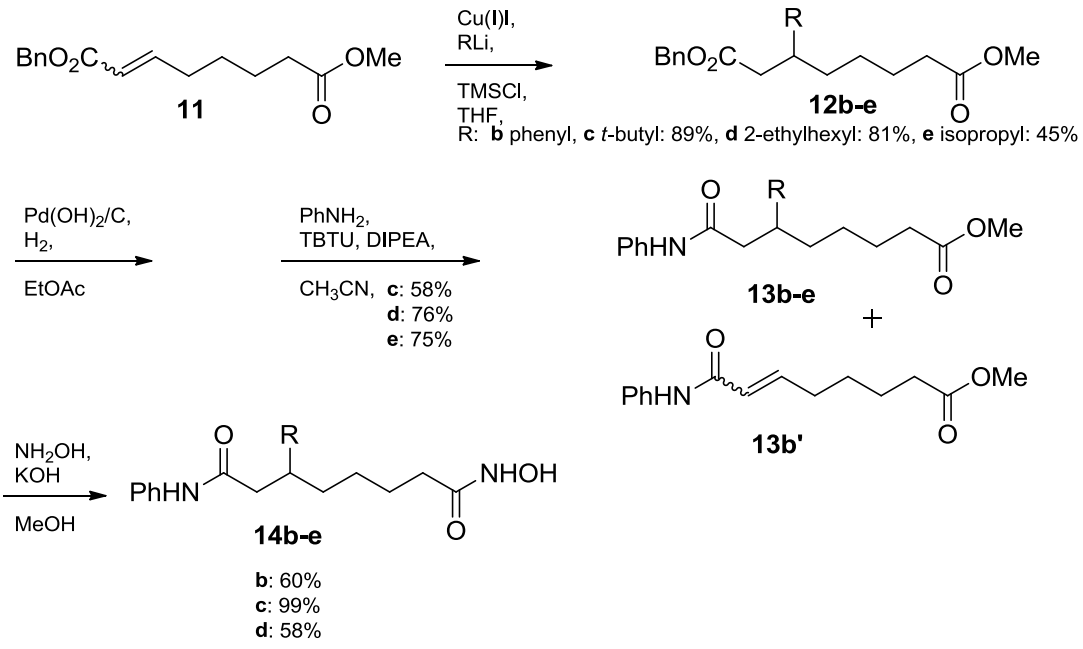

Scheme 3.2. Modified synthesis of C6-SAHA analogue **14b** - **14d**

To create the remaining C6-SAHA analogues, first, purification by column chromatography was required after 1,4-addition since the mixture of (E) and (Z)

isomers **11** were unable to completely react to produce phenyl ester **12b**, as was observed with the methyl derivative **12a** (Scheme 3.2). Using the additional purification step after the 1,4-addition, the *t*-butyl ester **12c**, 2-ethylhexyl ester **12d,** and isopropyl ester **12e** were synthesized. The rest of syntheses for hydrogenolysis, coupling, and conversion to hydroxamic acid were similar to the methyl analogue synthesis. However, despite the purification, there was still remaining unsaturated ester **11** after 1, 4-addition for obtaining phenyl ester **12b** due to the similar polarity. The mixture of unsaturated ester **11** and phenyl ester **12b** were subjected to hydrogenolysis and coupling to give anilide **13b** and unsaturated anilide compound **13b´**. Fortunately, **14b** was completely purified after conversion to hydroxamic acid in 60% yield (over the four steps).

3.4 Biological analysis

The HDAC inhibitory activities of the C6-SAHA library were measured using the Fluor de Lys® *in vitro* fluorescence activity assay kit (Enzo). Unlike the C3-SAHA library, the C6-SAHA analogue biological activities were performed by Sun Ea Choi. The activities of the C6-SAHA compounds are summarized in Table 3.1. Interestingly, the planar phenyl variant **14b** was the most potent analogue displaying an IC_{50} of 344 nM similar to the C3-methyl variant **1e** (IC_{50} of 350 nM) and comparable to SAHA (4-fold reduced), IC_{50} of 86 nM. This is in contrast to the C3-phenyl variant **1b** (IC_{50} of 73000 nM), which displayed 811-fold reduced activity versus SAHA.[53] In addition, the smallest C6-methyl variant **14a** (IC_{50} of 349 nM) displayed similar potency to the phenyl variant. These results indicate that the active site of HDAC proteins can accommodate a bulky

substituent at the C6 position. Moreover, the longest analogues, the 2-ethylhexyl variant **14d**, still displayed potent inhibitory activity in the nM range. Likewise, the bulkiest substituent with three methyl groups at the α-carbon, the *t*-butyl variant **14c**, displayed only 20-fold reduced activity versus SAHA. In summary, the inhibition data show that most C6-SAHA analogues maintain nM potency, but substitution at the α-carbon decreases potent inhibitory activity.

Table 3.1. HDAC inhibition by SAHA, MS-275, and the C6-SAHA analogues using HeLa cell lysates

Compounds	R	IC_{50}, nM[a]
SAHA		86 ± 4
MS-275		3200 ± 100
14a	Methyl	349 ± 20
14b	Phenyl	344 ± 40
14c	*t*-Butyl	1940 ± 300
14d	2-Ethylhexyl	456 ± 30

[a]Values are the mean of at least three experiments with standard error given.

These results are consistent with the hypothesis that the active site of HDAC proteins accommodates large substituents near the solvent exposed area. As expected, one trend for the C6-SAHA analogues is that the increasing size of substituents has less influence on inhibitory activity compared to the C2 and C3-SAHA analogues.

As mentioned earlier, the presence of methyl groups at the α-carbon decreased inhibitory activity. We speculate that the *t*-butyl variant **14c** might display specific selectivity since the C3-ethyl variant **1c**, which contains an α-

methyl group, displayed selective inhibition for HDAC6 over HDAC1 and HDAC 3 and also showed significantly decreased inhibitory activity compared with the C3-methyl variant **1e**. To explore the role of an α-methyl group on selectivity, synthesis of the isopropyl derivative would reveal the effect of α-carbon substituents. Another possibility is that the hybridization at the α-carbon might influence selectivity. For example, the C6-SAHA phenyl **14b** and methyl variant **14a** have sp^2 and sp^3 orbital structures. The data might provide key structural information for binding site recognition. The long chain of the C6-SAHA 2-ethyl hexyl analogue **14d** might also affect isoform selectivity. To verify the influence of sterics on isoform selectivity, testing the isoform selectivity of C6-SAHA analogues is described. The results of the isoform selectivity of the C6-SAHA analogues are outlined in Figure 3.2.

The isoform selectivity of C6-SAHA analogues was tested with HDAC1 and HDAC3 representing class I and HDAC6 representing class II. To assess the isoform selectivity, all compounds were tested at a single concentration near to their IC_{50} values using the Fluor de Lys® kit (Figure 3.2). As observed from previous data, SAHA exhibited roughly equal inhibition against HDAC1, HDAC3, and HDAC6. The phenyl variant **14b**, which displayed the most potent inhibition among the C6-SAHA analogues with HeLa cell lysates, similarly inhibited HDAC1, HDAC3, and HDAC6 as well. In contrast, the methyl variant **14a** showed dual-preference for HDAC1 and HDAC3 over HDAC6 at 500 nM even though the methyl **14a** (IC_{50} of 349 nM) and phenyl variant **14b** (IC_{50} of 344 nM) displayed equal inhibition in the HeLa cell lysates. The difference between sp^3 and sp^2

orbital structures might affect selectivity but not potency. The 2-ethylhexyl variant **14d** with an additional carbon chain displayed selectivity for HDAC3 over HDAC1 and HDAC6 compared to the methyl variant **14a**. Similar to the methyl variant **14a** (IC_{50} of 349 nM), the 2-ethylhexyl variant **14d** (IC_{50} of 456 nM) imparted selectivity but not potency. However, the bulkiest analogue at the α–carbon position, *t*-butyl variant **14c**, displayed the opposite selectivity with preference for HDAC1 and HDAC6 over HDAC3. In this case, the α-carbon substituent lead to different interactions with each isoform HDAC active sites. The *t*-butyl substituent encouraged dual-selectivity toward HDAC1 and HDAC6 over HDAC3, while the inhibitory activity of *t*-butyl variant **14c** (IC_{50} of 1.9 μM) showed 5-fold reduced activity compared to the 2-ethylhexyl variant **14d** (IC_{50} of 456 nM) and 20-fold less potent than SAHA (IC_{50} of 86 nM). In summary, the data indicated that the methyl, *t*-butyl, and 2-ethylhexyl variants (**14a**, **14c**, and **14d**) showed dissimilar preference for each isoform HDAC proteins despite parallel potency. The deacetylase activity of individual trial is summarized in Table C.5 in Appendix C.

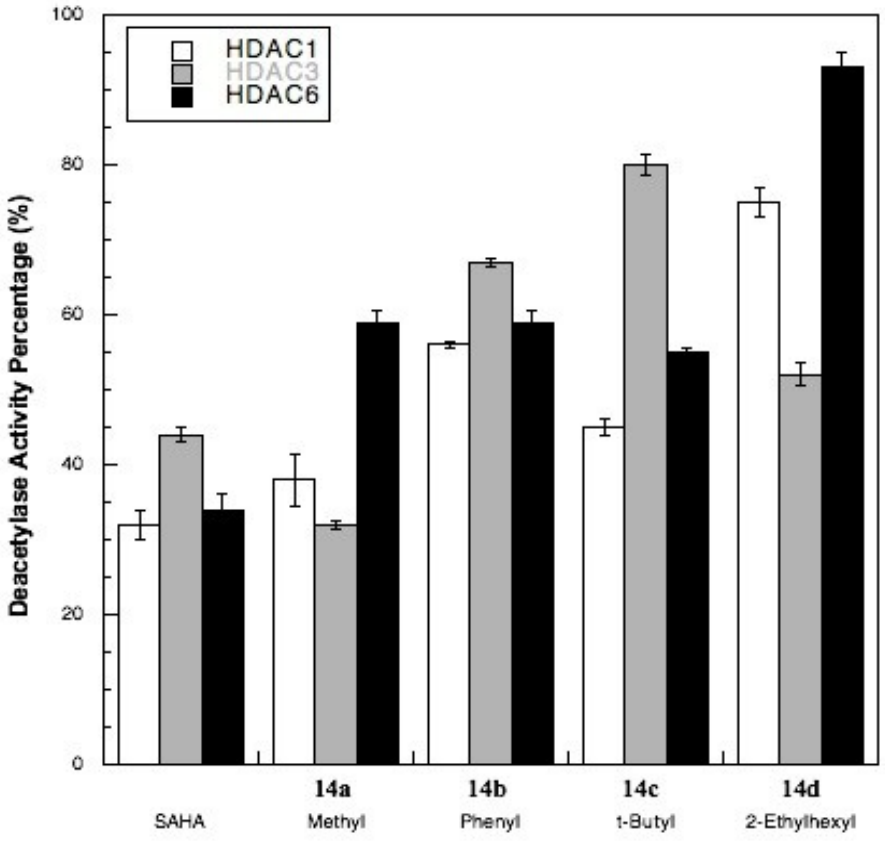

Figure 3.2. Initial screen of isoform selectivity of C6-SAHA analogues against HDAC1, HDAC3, and HDAC6 with 125 nM SAHA, 500 nM **14a**, **b**, **d**, and 2 μM **14c**.

To more thoroughly assess the selectivity observed in the initial screen, we determined the HDAC1, HDAC3, and HDAC6 IC_{50} values of the C6-*t*-butyl variant **14c** because it showed the most potential to create a dual-selective inhibitor. The C6-*t*-butyl analogue **14c** displayed 6-fold greater potency for HDAC1 over HDAC3 and 2-fold greater potency for HDAC6 over HDAC3 (Table 3.2). In addition, it displayed selectivity within class I for HDAC1 over HDAC3. As a control, SAHA displayed non-selective inhibitor activity against the isoform, as expected (Table 3.2).[30] The selectivity analysis shows that a substituent on the C6 position can influence the selectivity of SAHA from non-selective inhibitor to a dual-selective HDAC1 and HDAC6 inhibitor. Furthermore, the C6-SAHA *t*-butyl

analogue displays an IC_{50} value of 1.9 μM in the lowmicromolar range, while the C3-SAHA ethyl analogue (HDAC6-selective inhibitor) displayed 16-fold decreasing potency (IC_{50} of 32 μM).[47] Therefore, the data indicate that attaching the *t*-butyl substituent to the linker chain on the C6 position may promote dual-selective inhibition as well as potency on SAHA.

Table 3.2. IC_{50} values of SAHA and the C6-SAHA *t*-butyl variant **14c** for HDAC1, HDAC3, and HDAC6

Compound	IC_{50}/μM		
	HDAC1	HDAC3	HDAC6
SAHA	0.096 ± 0.016	0.136 ± 11	0.074 ± 0.009
14c	0.993 ± 0.061	5.4 ± 0.7	2.4 ± 0.5

Specific selective HDAC inhibitors support pathological cardiac remodeling studies. For example, a recent cardiac study reported that stressed myocardium increased the catalytic activity of the class IIb HDAC, HDAC6.[35] Moreover, the best anti-leukemic activities in the four pediatric AML cell lines were observed by dual HDAC1 and HDAC6 inhibitors that inhibited both.[45e] . The function or regulation of dual-selective HDAC inhibitors is not well informed in present even though dual-selective HDAC inhibitors might guide development of prospective drugs of anti-diverse diseases.

From the initial isoform selectivity screen (Figure 3.2), SAHA analogues with substituents on the C6 position displayed diverse selective inhibitions, such as class I selectivity (methyl **14a**), dual-class I, II selectivity (*t*-butyl **14c**), and isoform selectivity for HDAC3 (2-ethylhexyl **14d**). Our results reveal that small

structural changes in the C6 position linker region of SAHA can significantly influence selectivity with suitable potency.

3.5 Experimental

3.5.1 General methods

Additional details were shown in Section 2.5.1 of Chapter 2.

3.5.2 Experimental Procedures and Compound Characterization

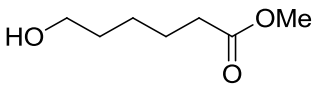

Methyl 6-hydroxyhexanoate (9). Concentrated aqueous sulfuric acid (adjusted to pH 6 using neutral pH meter paper (pH 1 to pH 14 range) as assessed with) was dropwise added to a solution of *ε*–caprolactone (5.54 mL, 50 mmol) in MeOH (50 mL). The mixture was stirred for 20 min. The mixture was subsequently diluted with anhydrous diethyl ether (25 mL) and washed with distilled water (equal volume to organic layer). The aqueous layer was extracted with diethyl ether (equal volume to organic layer) at least 3 times. The combined organic layers were dried over anhydrous Na_2SO_4, filtered, and concentrated. The residue was purified by column chromatography (12% acetone/CH_2Cl_2) on silica gel to give **9** (7.23 g, 99%). ^{1}H-NMR (δ, ppm, CHLOROFORM-D): 1.30 (m, 2H), 1.50 (m, 2H), 1.56 (m, 2H), 2.24 (m, 2H), 2.59 (bs, 1H), 3.52 (m, 2H), 3.58 (s, 3H); ^{13}C-NMR (δ, ppm, CHLOROFORM-D): 24.8, 25.5, 32.4, 34.1, 51.8, 62.5, 174.5; IR: 3424, 2940, 2866, 1738, 1438, 1205, 857, 744 cm^{-1}; HRMS (EI-TOF, *m/z*): found [M+Na] 169.0840, calc. for $C_7H_{14}O_3$, 169.0841.

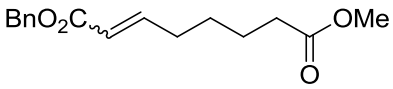

1-Benzyl 8-methyl oct-2-enedioate (11). To a solution of DMSO (1.02 mL, 14.39 mmol) in CH_2Cl_2 (44 mL) was added 2 M oxalyl chloride in dichloromethane (3.27 mL, 6.54 mmol) dropwise and then methyl 6-hydroxyhexanoate **9** (0.638 g, 4.36 mmol) stepwise at -78ºC. The reaction mixture was stirred for 45 min before triethylamine (TEA, 4.12 mL, 29.66 mmol) was added dropwise at -78 ºC. The mixture was warmed to room temperature and stirred for an additional 1 h. The reaction mixture was quenched by adding distilled water (44 mL). The mixture was washed with 1.0 M aqueous hydrochloric acid (44 mL), an aqueous solution of saturated $NaHCO_3$ (44 mL), and brine (44 mL). The organic layer **10** was dried over anhydrous Na_2SO_4, filtered, and concentrated.

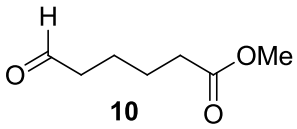

10

To a solution of NaH (0.513 g, 12.8 mmol) in THF (85 mL) was added benzyl dimethyl phosphonoacetate (3.31 g, 12.8 mmol) dropwise at 0 ºC and the mixture was stirred for 15 min. To the solution was added crude methyl 6-oxohexanoate **10** (1.23 g, 8.55 mmol) at -78 ºC and the mixture was stirred for 15 min. The mixture was allowed to warm to room temperature and stirred for an additional 1 h. The mixture was quenched by addition of an aqueous solution of saturated NH_4Cl until evolution of gas was not observed. The mixture was washed with distilled H_2O (85 mL). The organic layer was collected and the aqueous layer was extracted with diethyl ether (equal volume to aqueous layer) at least 3 times. The combined organic layers were dried over anhydrous

Na_2SO_4, filtered, and concentrated. The residue was purified by column chromatography (diethyl ether: petroleum ether 1:6) on silica gel to give **11** (2.17 g, 92%). (E+Z)-isomer ^{1}H-NMR (δ, ppm, CHLOROFORM-D): 1.48 (m, 2H), 1.63 (m, 2H), 2.20 (q, 2H), 2.30 (t, 2H), 3.64 (s, 3H), 5.16 (s, 2H), 5.84 (d, 1H, J=180 Hz), 6.98 (m, 1H), 7.35 (m, 5H); ^{13}C-NMR (δ, ppm, CHLOROFORM-D): 24.6, 27.6, 32.1, 33.9, 51.7, 66.2, 121.6, 128.3, 128.4, 128.8, 136.3, 149.5, 166.6, 174.0; IR: 3671, 2974, 1735, 1455, 1258, 1066, 907, 748, 698 cm^{-1}; HRMS (EI-TOF, *m/z*): found [M+Na] 299.1269, calc. for $C_{16}H_{20}O_4Na$, 299.1259.

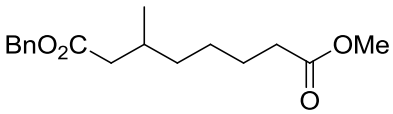

1-Benzyl 8-methyl 3-methyloctanedioate (12a). To a solution of Cu(I)I (1.06 g, 5.57 mmol) in THF (19 mL) was added 1.6M methyllithium in diethyl ether (6.97 mL, 11.15 mmol) dropwise at -15 ºC and the mixture was stirred for 20 min. The reaction mixture was cooled to -78 ºC before addition of trimethylsilyl chloride (TMSCl, 4.25 mL, 33.48 mmol). To the reaction mixture was dropwise added 1-benzyl 8-methyl oct-2-enedioate **11** (513 mg, 1.86 mmol) at -78 ºC. The reaction was stirred for 3 h at -78 ºC to room temperature and then quenched by addition of 1.0 M aqueous hydrochloric acid until a color of the mixture changed to blue ($CuCl_{2(aq)}$). The organic layer was collected and the aqueous layer was extracted with diethyl ether (equal volume to aqueous layer) at least 3 times. The combined organic layers were dried over anhydrous Na_2SO_4, filtered, and concentrated. ^{1}H-NMR (δ, ppm, CHLOROFORM-D): 0.91 (d, 3H), 1.30 (m, 4H), 1.58 (m, 2H), 1.96

(m, 1H), 2.19 (q, 1H), 2.32 (m, 3H), 3.65 (s, 3H), 5.10 (s, 2H), 7.34 (m, 5H); ^{13}C-NMR (δ, ppm, CHLOROFORM-D): 19.9, 25.2, 26.6, 30.4, 34.2, 36.4, 42.0, 51.7, 66.3, 128.4, 128.5, 128.8, 136.3, 173.2, 174.4; HRMS (EI-TOF, *m/z*): found [M+Na] 315.1569, calc. for $C_{17}H_{24}O_4Na$, 315.1572.

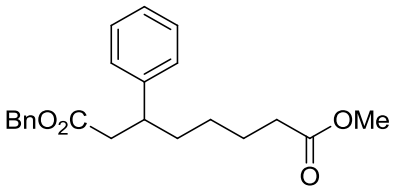

1-Benzyl 8-methyl 3-phenyloctanedioate (12b). To a solution of Cu(I)I (827 mg, 4.34 mmol) in THF (14.5 mL) was added phenyl lithium 2.0M (4.34 mL, 8.69 mmol) dropwise at -15 ºC and the mixture was stirred for 20 min. The reaction mixture was cooled to -78 ºC. To the solution was added trimethylsilyl chloride (TMSCl, 1.67 mL, 13.03 mmol) dropwise and then 1-benzyl 8-methyl oct-2-enedioate **11** (400 mg, 1.45 mmol) stepwise at -78 ºC. The mixture was stirred for 3 h at -78 ºC and then quenched by addition of an aqueous solution of saturated NH_4Cl: saturated NH_4OH (1:1) until the color of the mixture turned to blue ($(NH_3)_4CuCl_{2(aq)}$). The mixture was washed with the aqueous solution of saturated NH_4Cl: NH_4OH (1:1) (14.5 mL). The organic layer was collected and the aqueous layer was extracted with diethyl ether (equal volume to the aqueous layer). The combined organic layers were dried over anhydrous Na_2SO_4, filtered, and concentrated. The residue was purified by column chromatography (diethyl ether: petroleum ether 1:6) on silica gel to give **12b** + **11** (3:1).

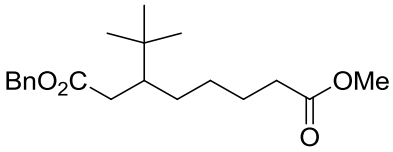

1-Benzyl 8-methyl 3-(*tert*-butyl)octanedioate (12c). The synthesis was similar that of **12b** except the following reagents were used: Cu(I)I (827 mg, 4.34 mmol) in THF (10.9 mL), *tert*-butyllithium 1.6M (5.43 mL, 8.69 mmol), TMSCl (1.67 mL, 13.03 mmol), and 1-benzyl 8-methyl oct-2-enedioate **11** (300 mg, 1.09 mmol). The product was purified by column chromatography (diethyl ether: petroleum ether 1:6) on silica gel to give **12c** (313 mg, 89%). ^{1}H-NMR (δ, ppm, CHLOROFORM-D): 0.84 (s, 9H), 1.05 (m, 1H), 1.17-1.35 (m, 2H), 1.47-1.62 (m, 3H), 1.68 (m, 1H), 2.10 (q, 1H), 2.23 (t, 2H), 2.41 (q, 1H), 3.64 (s, 3H), 5.09 (s, 2H), 7.34 (m, 5H); ^{13}C-NMR (δ, ppm, CHLOROFORM-D): 25.5, 27.6, 28.5, 31.0, 33.8, 34.2, 36.3, 45.2, 51.6, 66.4, 128.4, 128.6, 128.7, 136.3, 174.3, 174.5; IR: 2952, 2869, 1737, 1457, 1367, 1151, 914, 737 cm^{-1}. MS (ESI, *m/z*): found [M^{+} +Li] 341.28, calc. for $C_{20}H_{30}O_4Li$, 341.23.

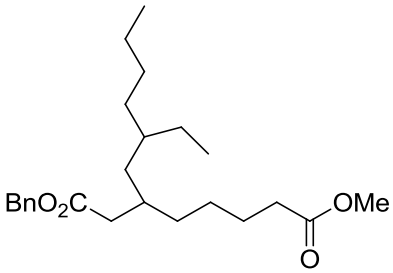

1-Benzyl 8-methyl 3-(2-ethylhexyl)octanedioate (12d). The synthesis was similar to that of **12b** except the following reagents were used: Cu(I)Br·SMe_2 (1.89 g, 9.19 mmol) in THF (15.3 mL), 2-ethylhexyllithium (10.09 mL, 18.38 mmol), TMSCl (3.52 mL, 27.57 mmol), and 1-benzyl 8-methyl oct-2-enedioate **11**

(400 mg, 1.53 mmol). The product was purified by column chromatography (diethyl ether: petroleum ether 1:8) on silica gel to give **12d** (485 mg, 81%). ^{1}H-NMR (δ, ppm, CHLOROFORM-D): 0.79 (m, 3H), 0.88 (t, 3H), 1.23-1.31 (m, 15H), 1.58 (m, 2H), 1.91 (m, 1H), 2.25-2.30 (m, 4H), 3.66 (s, 3H), 5.11 (s, 2H), 7.35 (m, 5H); ^{13}C-NMR (δ, ppm, CHLOROFORM-D): 10.7, 14.40, 23.4, 25.4, 26.1, 28.9, 32.8, 33.1, 34.2, 36.1, 38.5, 44.4, 66.3, 128.4, 128.6, 128.8, 129.2, 130.4, 173.2, 173.5; IR: 2956, 2858, 1739, 1457, 1167, 912, 741 cm^{-1}. MS (ESI, *m/z*): found [M^{+}+K] 429.29, [M^{+}+Li] 397.36, [M^{+}+Na] 413.31, calc. for $C_{24}H_{38}O_4K$, 429.65, $C_{24}H_{38}O_4Li$, 397.50, $C_{24}H_{38}O_4Na$, 413.55.

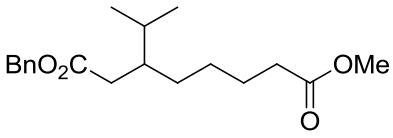

1-Benzyl 8-methyl 3-isopropyloctanedioate (12e). The synthesis was similar that of **12b** except the following reagents were used: Cu(I)I (875 mg, 4.59 mmol) in THF (7.7 mL), isopropyl magnesium bromide 1.94M (2.37 mL, 4.59 mmol), TMSCl (1.76 mL, 13.78 mmol) and 1-benzyl 8-methyl oct-2-enedioate **11** (200 mg, 0.77 mmol). The residue was purified by column chromatography (diethyl ether: petroleum ether 1:6) on silica gel to give **12e** (109 mg, 45%). ^{1}H-NMR (δ, ppm, CHLOROFORM-D): 0.80 (d, 3H), 0.84 (d, 3H), 1.16-1.33 (m, 4H), 1.59 (m, 2H), 1.70 (m, 1H), 1.78 (m, 1H), 2.18 (m, 1H), 2.27 (m, 3H), 3.65 (s, 3H), 5.10 (s, 2H), 7.35 (m, 5H); ^{13}C-NMR (δ, ppm, CHLOROFORM-D): 18.4, 19.4, 25.1, 26.8, 29.7, 30.7, 34.0, 36.0, 40.7, 51.5, 66.1, 128.2, 128.3, 128.5, 136.1, 173.9, 174.2; IR: 3033, 2954, 2873, 1737, 1458, 1332, 1261, 1008, 905, 750 cm^{-1}; HRMS (EI-TOF, *m/z*): found [M+Na] 343.1883, calc. for $C_{19}H_{28}O_4Na$, 343.1885.

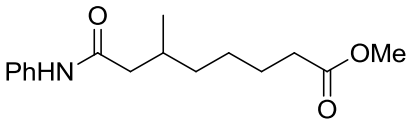

Methyl 6-methyl-8-oxo-8-(phenylamino)octanoate (13a). To a solution of crude 1-benzyl 8-methyl 3-methyloctanedioate **12a** (513 mg, 1.86 mmol) in ethyl acetate (19 mL) was added 20% $Pd(OH)_2/C$ (261 mg, 0.372 mmol) and the reaction mixture was purged with H_2 gas for 30 s. The reaction solution was stirred under H_2 gas for 3 h and then filtered through a plug of Celite with ethyl acetate (57 mL). The filtrate was concentrated to give 8-methoxy-3-methyl-8-oxooctanoic acid as clear oil. The crude residue, 8-methoxy-3-methyl-8-oxooctanoic acid, was transferred to a flask and dissolved in 19 mL of acetonitrile. TBTU (895 mg, 2.79 mmol), diisopropylethylamine (647 mL, 3.72 mmol), and aniline (254 mL, 2.79 mmol) was added to the flask. The reaction mixture was stirred for 3 h. The mixture was then quenched with 19 mL of saturated $NaHCO_3$ solution, transferred to a separatory funnel and extracted with ethyl acetate (equal volume to aqueous layer) at least 3 times. The combined organic layers were dried over magnesium sulfate, filtered, and evaporated to oil. Flash silica gel chromatography (1:6 diethyl ether: petroleum ether → 1:1 diethyl ether: petroleum ether) afforded 274 mg of the anilide **13a** as a clear oil (53% over 3 steps). ^{1}H-NMR (δ, ppm, CHLOROFORM-D): 0.91 (d, 3H), 1.13-1.34 (m, 4H), 1.56 (m, 2H), 2.09 (m, 2H), 2.27 (m, 3H), 3.61 (s, 3H), 7.02 (t, 1H), 7.24 (t, 2H), 7.52 (d, 2H), 8.27 (bs, 1H); ^{13}C-NMR (δ, ppm, CHLOROFORM-D): 19.9, 25.1, 26.6, 30.9, 34.2, 36.5, 45.6, 51.8, 120.0, 124.4, 129.2, 138.2, 171.1, 175.3;

IR: 3306, 2952, 2868, 1739, 1601, 1544, 1151, 913, 757 cm^{-1}; HRMS (EI-TOF, *m/z*): found [M+H] 278.1764, calc. for $C_{16}H_{24}NO_3$, 278.1756, found [M+Na] 300.1584, calc. for $C_{16}H_{24}NO_3Na$, 300.1576.

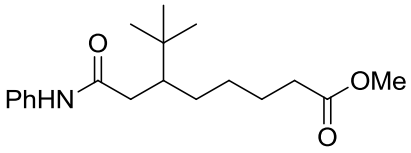

Methyl 6-(*tert*-butyl)-8-oxo-8-(phenylamino)octanoate (13c). A similar procedure to that for **13a** was used, except for the following reagents: 20% $Pd(OH)_2/C$ (210 mg, 0.299 mmol) and 1-benzyl 8-methyl 3-(*tert*-butyl)octanedioate **12c** (414 mg, 0.748 mmol) in ethyl acetate (7.5 mL), TBTU (360 mg, 1.121 mmol) in acetonitrile (7.5 mL), diisopropyethylamine (521 mL, 2.99 mmol), aniline (102 mL, 0.748 mmol) and stirring for 4 h. The mixture was then quenched with 7.5 mL of saturated $NaHCO_3$ solution, transferred to a separatory funnel and extracted with ethyl acetate (equal volume to aqueous layer) at least 3 times. The organic layer was dried over magnesium sulfate, filtered, and evaporated to oil. In this case, flash silica gel chromatography (1:6 diethyl ether: petroleum ether → 1:1 diethyl ether: petroleum ether) afforded 185 mg of the anilide **13c** as a clear oil (58% over 2 steps). ^{1}H-NMR (δ, ppm, CHLOROFORM-D): 0.91 (s, 9H), 1.13 (m, 1H), 1.33 (m, 1H), 1.42 (m, 1H), 1.55 (m, 3H), 1.82 (m, 1H), 2.09 (q, 1H), 2.28 (t, 2H), 2.49 (q, 1H), 3.62 (s, 3H), 7.09 (t, 1H), 7.21 (bs, 1H), 7.31 (t, 2H), 7.50 (d, 2H); ^{13}C-NMR (δ, ppm, CHLOROFORM-D): 25.5, 27.8, 28.4, 31.2, 34.0, 34.1, 45.1, 56.1, 62.8, 119.2, 124.3, 129.2, 134.7, 168.5, 171.3; IR: 3055, 2952, 2865, 1732, 1600, 1265, 741,

706 cm^{-1}; HRMS (EI-TOF, *m/z*): found [M+H] 320.2229, calc. for $C_{19}H_{29}NO_3$, 320.2226, found [M+Na] 342.2048, calc. for $C_{19}H_{29}NO_3Na$, 342.2045.

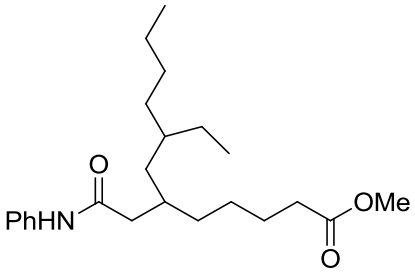

Methyl 8-ethyl-6-(2-oxo-2-(phenylamino)ethyl)dodecanoate (13d). A similar procedure to that for **13a** was used, except for the following reagents: 20% $Pd(OH)_2/C$ (345 mg, 0.492 mmol) and 1-benzyl 8-methyl 3-(2-ethylhexyl)octanedioate **12d** (463 mg, 1.229 mmol) in ethyl acetate (12.3 mL), TBTU (592 mg, 1.844 mmol) in acetonitrile (12.3 mL), diisopropyethylamine (856 mL, 4.916 mmol), aniline (168 mL, 1.844 mmol) and stirring for 3 h. In this case, the mixture was quenched with 12.3 mL of saturated $NaHCO_3$ solution, transferred to a separatory funnel and extracted with CH_2Cl_2 (equal volume to aqueous layer) at least 3 times. The organic layer was dried over magnesium sulfate, filtered, and evaporated to oil. The product was purified by column chromatography (diethyl ether: petroleum ether 1:8) on silica gel to give **13d** (349 mg, 76%). ^{1}H-NMR (δ, ppm, CHLOROFORM-D): 0.81-0.87 (m, 6H),1.10-1.34 (m, 15H), 1.60 (m, 2H), 2.03 (m, 1H), 2.22-2.32 (m, 4H), 3.65 (s, 3H), 7.08 (t, 1H), 7.32 (t, 2H), 7.51 (d, 2H); ^{13}C-NMR (δ, ppm, CHLOROFORM-D): 10.7, 14.4, 23.4, 25.3, 25.8, 26.0, 28.9, 33.1, 33.2, 33.6, 33.8, 36.2, 38.5, 43.2, 51.7, 120.0, 124.3, 129.2, 138.3, 171.4, 174.6; IR: 3322, 3066, 2956, 1740, 1661,

1171, 912, 746, 694 cm^{-1}; MS (ESI, *m/z*): found $[M^+ + Li]$ 382.41, $[M^+ + Na]$ 398.35, $[M^+ + K]$ 414.31, calc. for $C_{23}H_{37}NO_3Li$, 382.49, $C_{23}H_{37}NO_3Na$, 398.53, $C_{23}H_{37}NO_3K$, 414.64.

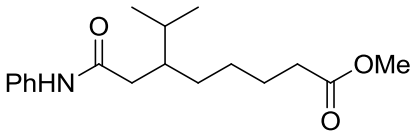

Methyl 6-isopropyl-8-oxo-8-(phenylamino)octanoate (13e). A similar procedure to that for **13a** was used, except for the following reagents: 20% $Pd(OH)_2/C$ (88 mg, 0.125 mmol) and 1-benzyl 8-methyl 3-isopropyloctanedioate **12e** (0.312 mmol) in ethyl acetate (3 mL), TBTU (150 mg, 0.468 mmol) in acetonitrile (3 mL), diisopropyethylamine (218 mL, 1.248 mmol), aniline (43 mL, 0.468 mmol) and stirring for 3 h. In this case, the product was purified by column chromatography (1:6 diethyl ether: petroleum ether → 1:1 diethyl ether: petroleum ether) on silica gel to give **13e** (71 mg, 75%). ^{1}H-NMR (δ, ppm, CHLOROFORM-D): 0.84 (d, 3H), 0.89 (d, 3H), 1.25-1.38 (m, 4H), 1.61 (m, 2H), 1.81 (m, 1H), 1.90 (m, 1H), 2.15 (q, 1H), 2.30 (t, 2H), 2.34 (q, 1H), 3.64 (s, 3H), 7.09 (t, 1H), 7.31 (t, 2H), 7.41 (bs, 1H), 7.51 (d, 2H); ^{13}C-NMR (δ, ppm, CHLOROFORM-D): 18.9, 19.5, 25.3, 26.9, 29.7, 30.6, 34.1, 39.6, 41.1, 51.8, 120.0, 124.4, 129.2, 138.3, 171.8, 174.6; IR: 3297, 3140, 2954, 2870, 1739, 1601, 1368, 906, 757, 693 cm^{-1}; HRMS (EI-TOF, *m/z*): found [M+H] 306.2071, calc. for $C_{18}H_{28}NO_3$, 306.2069, found [M+Na] 328.1884, calc. for $C_{18}H_{28}NO_3Na$, 328.1889.

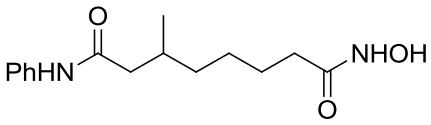

***N*^{8}-Hydroxyl-3-methyl-*N*^{1}-phenyloctanediamide (14a).** To a solution of $NH_2OH{\cdot}HCl$ (677 mg, 9.735 mmol) in methanol (10 mL) was added KOH (1.092 g, 19.469 mmol) at 0 ˚C in an acid-washed 25mL round-bottom flask. After stirring for 20 min, methyl 6-methyl-8-oxo-8-(phenylamino)octanoate **13a** (270 mg, 0.974 mmol) was added and the mixture was stirred for 8 h at 0°C. The reaction mixture was adjusting to pH 6 by adding concentrated aqueous hydrochloric acid. The mixture was diluted with 30 mL of ethyl acetate, and washed with 30 mL of distilled water. The organic layer was dried over anhydrous Na_2SO_4, filtered, and concentrated. The residue was purified by column chromatography (9% methanol/CH_2Cl_2) on acid-washed silica gel to give **14a** (159 mg, 58%) as a clear oil. ^{1}H-NMR (δ, ppm, METHANOL-D4): 0.98 (d, 3H), 1.24-1.44 (m, 4H), 1.61 (m, 2H), 2.02 (m, 1H), 2.09 (t, 2H), 2.16 (q, 1H), 2.34 (q, 1H), 7.07 (t, 1H), 7.29 (t, 2H), 7.52 (d, 2H); ^{13}C-NMR (δ, ppm, METHANOL-D4): 18.7, 25.7, 26.3, 30.8, 32.5, 36.3, 44.4, 120.2, 124.0, 128.6, 138.6, 171.8, 172.9; IR: 3270, 2928, 2868, 1643, 1600, 1500, 1418, 1116, 977, 759, 693 cm^{-1}; HRMS (EI-TOF, *m/z*): found [M+H] 279.1710, calc. for $C_{15}H_{23}N_2O_3$, 279.1709, found [M+Na] 301.1531, calc. for $C_{15}H_{23}N_2O_3Na$, 301.1528.

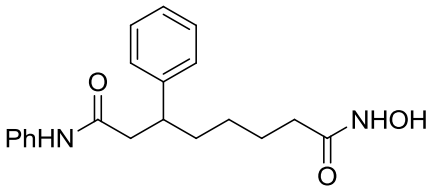

***N*^{8}-Hydroxyl-*N*^{8}, 3-diphenyloctanediamide (14b).** The synthesis of methyl 6-phenyl-8-oxo-8-(phenylamino)octanoate **13b** was similar to that of **14a** except the following reagents were used: 20% $Pd(OH)_2/C$ (153 mg, 0.218 mmol) and 1-benzyl 8-methyl 3-phenyloctanedioate **12b** (0.546 mmol) in ethyl acetate (5.5 mL), TBTU (263 mg, 0.818 mmol) in acetonitrile (5.5 mL), diisopropyethylamine (190 mL, 1.09 mmol), aniline (75 mL, 0.818 mmol) and stirring for 4 h. In this case, the reaction mixture was quenched with 5.5 mL of saturated $NaHCO_3$ solution, transferred to a separatory funnel and extracted with CH_2Cl_2 (equal volume to aqueous layer) at least 3 times. The organic layer was dried over magnesium sulfate, filtered, and evaporated to oil. Flash silica gel chromatography (diethyl ether: petroleum ether 1:1) afforded the mixture of phenyl substituted anilide **13b** and α, β unsaturated anilide **13b´** as a clear oil.

To a solution of $NH_2OH{\cdot}HCl$ (696 mg, 10.721 mmol) in methanol (10.7 mL) was added KOH (1.203 g, 21.442 mmol) at 0 ˚C in an acid-washed 25mL round-bottom flask. After stirring for 20 min, the mixture of methyl 6-phenyl-8-oxo-8-(phenylamino)octanoate **13b** and α, β unsaturated anilide **13b´** (1.072 mmol) was added and the reaction mixture was stirred for 8 h at 0°C. The rest of the reaction procedure was similar to that for **14a**. The residue was purified by column chromatography (4% methanol/CH_2Cl_2) on acid-washed silica gel to give **14b** (221 mg, 60% over 4 steps). ^{1}H NMR (δ, ppm, DIMETHYLSULFOXIDE-

D6): 0.85-1.25 (m, 3H), 1.42 (m, 2H), 1.58 (m, 2H), 1.83 (t, bs, 2H), 2.57 (m, 2H), 3.07 (m, 1H), 6.97 (t, 1H), 7.14-7.27 (m, 7H), 7.47 (d, 2H), 8.61 (s, 1H), 9.80 (s, 1H), 10.25 (s, 1H); ^{13}C-NMR (δ, ppm, METHANOL-D4): 25.5, 26.9, 32.5, 35.5, 42.8, 44.5, 120.4, 124.1, 126.4, 127.5, 128.4, 128.5, 138.4, 144.1, 171.7, 171.9; IR: 3235, 3027, 2928, 2859, 1874, 1641, 1599, 1544, 1498, 1467, 1116, 977, 757,699 cm^{-1}; HRMS (EI-TOF, *m/z*): found [M+H] 341.1877, calc. for $C_{20}H_{25}N_2O_3$, 341.1865, found [M+Na] 363.1697, calc. for $C_{20}H_{25}N_2O_3Na$, 363.1685.

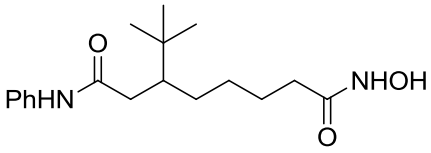

3-(*tert*-Butyl)-*N*^{8}-hydroxyl-*N*^{1}-phenyloctanediamide (14c). A similar procedure to that for **14a** was used, except for the following reagents: $NH_2OH{\cdot}HCl$ (348 mg, 5.008 mmol) in methanol (7.4 mL), KOH (562 mg, 10.018 mmol), methyl 6-(*tert*-butyl)-8-oxo-8-(phenylamino)octanoate **13c** (160 mg, 0.501 mmol) and stirring for 4 h. In this case, the product was purified by column chromatography (4 % methanol/CH_2Cl_2) on acid-washed silica gel to give **14c** (158 mg, 99%). ^{1}H-NMR (δ, ppm, METHANOL-D4): 0.92 (s, 9H), 1.15 (m, 1H), 1.28 (m, 1H), 1.40 (m, 1H), 1.58 (m, 3H), 1.77 (m, 1H), 2.04 (t, 2H), 2.16 (q, 1H), 2.53 (q, 1H), 7.07 (t, 1H), 7.29 (t, 2H), 7.50 (d, 2H); ^{13}C-NMR (δ, ppm, METHANOL-D4): 26.1, 26.7, 28.6, 30.8, 32.6, 33.3, 38.5, 45.0, 120.2, 123.9, 128.6, 138.8, 171.8, 173.9; IR: 3350, 2956, 2870, 1938, 1648, 1547, 1500, 1119, 976, 757, 693 cm^{-1}; HRMS (EI-TOF, *m/z*): found [M+H] 321.2180, calc. for $C_{18}H_{29}N_2O_3$, 321.2178, found [M+Na] 343.1998, calc. for $C_{18}H_{29}N_2O_3Na$, 343.1988.

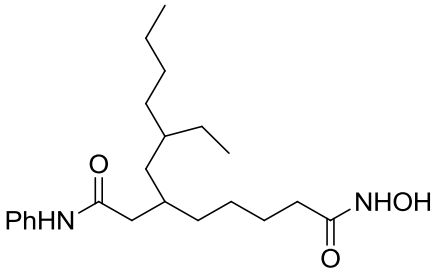

3-(2-Ethylhexyl)-*N*^{8}-hydroxyl-*N*^{1}-phenyloctanediamide (14d). A similar procedure to that for **14a** was used, except for the following reagents: $NH_2OH{\cdot}HCl$ (629 mg, 9.054 mmol) in methanol (9 mL), KOH (1.016 g, 18.108 mmol), methyl 8-ethyl-6-(2-oxo-2-(phenylamino)ethyl)dodecanoate **13d** (340 mg, 0.905 mmol), and stirring for 6 h. In this case, the product was purified by column chromatography (4 % methanol/CH_2Cl_2) on acid-washed silica gel to give **14d** (199 mg, 58%). ^{1}H-NMR (δ, ppm, METHANOL-D4): 0.85 (m, 6H), 1.19-1.37 (m, 16H),1.61 (m, 2H), 2.02 (bs, 1H), 2.09 (t, 2H), 2.24 (m, 2H), 7.07 (t, 1H), 7.29 (t, 2H), 7.53 (d, 2H); ^{13}C-NMR (δ, ppm, METHANOL-D4): 9.7, 9.9, 13.4, 23.0, 26.0, 28.5, 28.8, 32.6, 32.8, 33.0, 34.0, 36.1, 38.4, 42.3, 120.1, 124.0, 128.6, 138.7, 171.8, 173.1; IR: 3391, 3256, 3065, 2956, 1643, 1600, 1539, 1500, 1308, 903, 756, 692 cm^{-1}; HRMS (EI-TOF, *m/z*): found [M+H] 377.2798, calc. for $C_{22}H_{37}N_2O_3$, 377.2804.

3.5 HDAC assay procedure

HDAC activity was measured using the Fluor de Lys® activity assay (Enzo) using the manufacturer's protocol. To measure global HDAC inhibition, HeLa lysates (approximately 4μg of total protein) were incubated with small

molecule inhibitor or without small molecule inhibitor (2% DMSO) in HDAC assay buffer (50 mM Tris/Cl, pH 8.0, 137 mM NaCl, 2.7 mM KCl, 1 mM $MgCl_2$) in a final volume of 25 µL for 20 min at 23 ˚C with 600 rmp shaking. Concentrations of small molecule between 1 nM and 1 mM were used to determine IC_{50} values (Appendix C. Table C.1-C.6). Because the small molecules were stored in DMSO, dilution with HDAC buffer ensured that a maximum of 2% DMSO was present in the final reaction mixture. After the initial incubation, Fluor de Lys® substrate in HDAC assay buffer (100 µM final concentration) was added to make a total reaction volume of 50µL. The reaction mixture was incubated at 30˚C for 30 min with 600 rmp shaking. To quench the reaction and allow color development, Fluor de Lys® developer (2.5 µL of 20X diluted up to 50 µL in HDAC assay buffer) was added to give a final 100 µL volume and incubated with shaking for 5 min at room temperature. The fluorescence intensity was determined using a Geniosplus Fluorimeter (Tecan) with excitation at 360 nm and emission at 465 nm.

To perform the isoform selectivity studies, the procedure was similar except that the HeLa cell lysates were replaced with 0.2 µg HDAC1 (specific activity = 42.5 pmol/min/µg), 0.05 µg HDAC3 (specific activity = 249 pmol/min/µg) or 0.25 µg HDAC6 (specific activity = 257 pmol/min/µg), purchased from Enzo Life Sciences. In addition, the Fluor de Lys® substrate was used at a final concentration of 50 µM for HDAC1 and HDAC6 or 25µM for HDAC3.

For each trial, a no enzyme control sample was used to assess the background. The background-corrected fluorescence units of small molecule-

treated samples were then compared to that of untreated samples (set to 100%) to give a percentage deacetylase activity. IC_{50} values were obtained by plotting the percentage deacetylase activity versus the small molecule concentration and fitting the data to a sigmoidal dose-response curve ($y=100/(1+(x/m3)^{m4}$) using KaleidaGraph software where m1 is the IC_{50} value in Molar units. All experiments were performed in triplicate with the mean and standard error reported in the tables and figures.

CHAPTER 4 – SYNTHESIS OF SAHA ANALOGUES MODIFIED AT THE C7 POSITION

4.1 Rationale for design of the SAHA analogues modified at the C7 position

SAHA analogues with substituents on C2 and C3 position displayed decreasing inhibitory activity while C6-SAHA analogues displayed similar potency to the parent compound, SAHA. These results indicate that only limited steric environment exists near hydroxamic acid. For example, the C6-SAHA analogue with the phenyl substituent displayed only 4-fold decreased inhibition while the C3-SAHA analogue with the phenyl substituent displayed more 800-fold decreased inhibitory activity compared to SAHA. Based on an analysis of the HDAC crystal structure (Figure 1.4)[54], more space near the capping group area is available to accommodate bulky groups compared to the area near the hydroxamic acid. Moreover, large capping groups have been synthesized and displayed nM range inhibition.[21b, 38] Several class-selective HDAC inhibitors have been synthesized that contain large groups in capping group region.[20] Therefore, design, synthesis, and evaluation of a C7-SAHA library (Figure 4.1) are necessary to elucidate the structural requirement of HDAC inhibitors, since C7-SAHA analogues are located closest to the solvent-exposed region through the linker area.

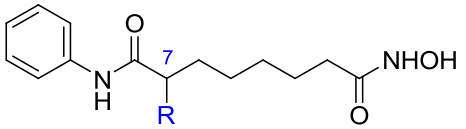

Figure 4.1. Structure of SAHA analogues containing substituents on the C7 position

C7-SAHA analogues with hydrophobic substituents were generated. Synthesizing C7-SAHA analogues with

only hydrophobic substituents might be sub-optimal since the C7 position is between the hydrophobic tunnel and the solvent exposed area. Therefore, we synthesized the methyl pyridyl variant to study the influence of polar groups. In addition, since medicinal and natural compounds containing nitrogen were involved in diverse therapeutic areas (Chapter 1), we chose the pyridyl derivative.[41-42, 55] Since hydrophobic substituents attached at the C6 position, a position that is close to the solvent-exposed location, displayed more potent inhibition compared to the C2 and C3-SAHA libraries, C7-SAHA analogues might also display potent inhibition compared to the C2, C3, and C6-SAHA analogues. Therefore, large aromatic groups should be incorporated on the C7 position. We designed a variety of substituents from the small methyl substituent to the large 4-methylnaphthyl, methylbiphenyl, methylanthracene, and methyltetrahydroanthracene substituents to address what effect large groups impart on potency. Due to the structural similarity to the previously reported C2-SAHA analogues, a straightforward synthetic approach was envisioned.

4.2 Initial synthesis of C7-SAHA analogues

Initially, C7-SAHA analogues with methyl **22a**, benzyl **22b**, and 4-methylnaphthyl **22c** substituents were synthesized by Dr. A. Bieliauskas. The early synthetic route for C7-SAHA analogues is outlined in Scheme 4.1.

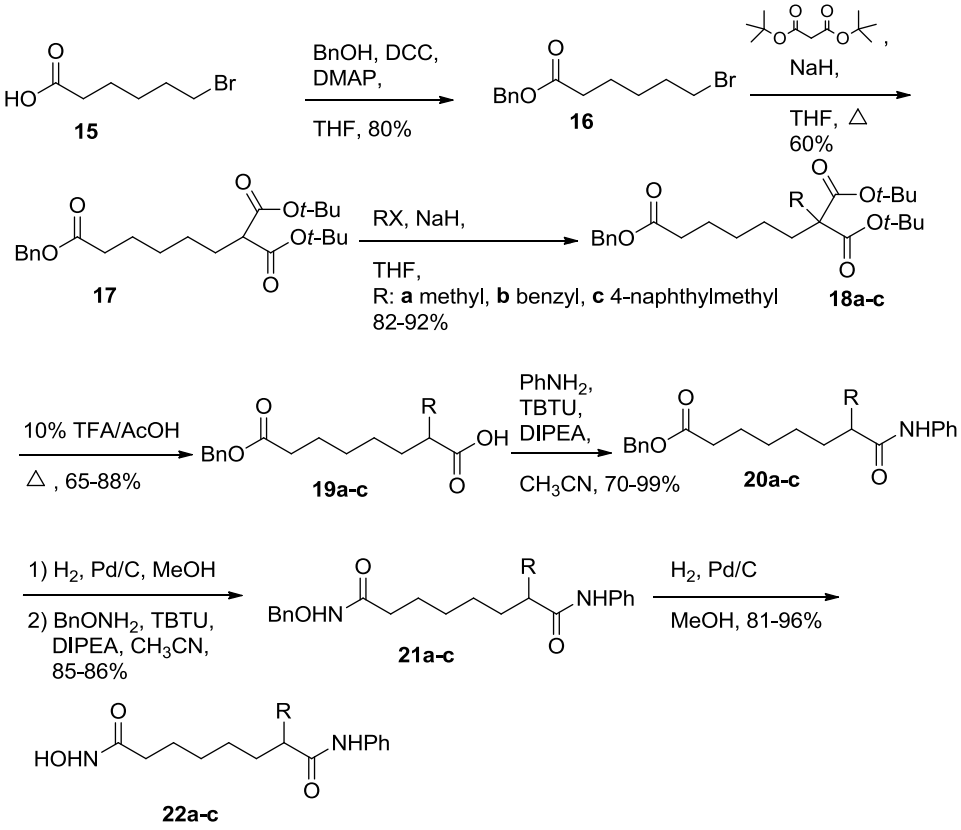

Scheme 4.1. Initial synthesis of C7-SAHA analogues **22a**-**22c**

Benzyl ester **16** was obtained by coupling conditions with benzyl alcohol and 6-bromohexanoic acid **15**. *t*-Butyl malonate derivatives **17** after nucleophilic substitution reaction provided the scaffold to create alkylated malonate derivatives **18a-c**. In acidic conditions, the *t*-butyl groups in **18a-c** were deprotected and decarboxylation was accomplished under reflux to give monocarboxylic acid **19a-c**, which was coupled with aniline. The benzyl group in **20a-c** was removed by Pd/C, and was coupled with *O*-benzyl-protected hydroxamine. *O*-benzyl-protected hydroxamic acid **21a-c** was deprotected by hydrogenolysis to give the C7- SAHA methyl, benzyl, and methylnaphthyl **22a-c**.

HDAC inhibitory activities of the C7-methyl, benzyl, and 4-methylnaphthyl SAHA analogues **22a-c** were measured using the Fluor de Lys™ *in vitro* fluorescence activity assay kit (Biomol) by Dr. S. V. W. Weerasinghe (Table 4.1).

Table 4.1. HDAC inhibition by SAHA, C7-methyl, benzyl, and 4-naphthyl variants using HeLa cell lysates

Compounds	R	IC_{50}, nM[a]
SAHA		86 ± 4
22a	Methyl	105 ± 6
22b	Benzyl	109 ± 5
22c	1-Naphthylmethyl	16 ± 1

[a]Values are the mean of at least three experiments with standard error given.

The C7-methyl and benzyl analogues **22a-b** were equipotent in 100 nM range similar to SAHA (86 nM). The inhibition results are consistent with the hypothesis that greater steric tolerance exists in HDAC active site at the entrance area of capping group than the metal binding moiety region. Moreover, the largest compound, C7-SAHA naphthylmethyl analogue **22c** among three analogues, displayed greater than 5-fold increasing inhibitory activity compared to SAHA. The addition of certain groups at the C7 position showed favourable interaction between the entrance area of HDAC active site and large bulky groups at the C7 position.

4.3 Synthesis of the C7-SAHA analogues with pyridyl and bulky substituents

To thoroughly explore the impact of the large bulky groups at the C7 position, additional large groups should be investigated. For example, the 4-methylbiphenyl and 9-methylanthracene variants **22e-f** should be synthesized to verify how large groups at the C7 position could interact with the HDAC active site. In addition, the inclusion of polar groups should be included to validate interaction between HDAC active site and hydrophilic substituents at the C7 position, the end edge of the hydrophobic channel. However, the synthesis of C7-SAHA analogues containing bulkier and larger substituents than the methyl, benzyl, and 4-methylnaphthyl variants **22a-c** faced issue in the nucleophilic substitution reaction (**17**->**18**) (Scheme 4.1). Therefore, the synthesis methodology was redesigned (Scheme 4.2). First of all, we used commercially available methyl 6-bromohexanoate **23** as the starting material instead of using coupling reaction to obtain benzylester **16** (two-step) (Scheme 4.1). Second, the nucleophilic substitution reaction was accomplished with dibenzylmalonate, which has a planar structure compared to the bulky *t*-butylmalonate (Scheme 4.1) to give the dibenzylmalonate derivatives **24** (Scheme 4.2). Finally, direct conversion to hydroxamic acid **22** was accomplished in one step without saponification, coupling *O*-benzyl hydroxylamine, and benzyl deprotection.[47] The 4-(1,1'-Biphenyl)methyl variant **22e** was synthesized by Geetha Padige, the 9-anthracenylmethyl **22f** and 9-(1,2,3,4-tetrahydroanthracenyl)methyl **22g**

derivatives were synthesized by Satish Garre, and the 4-pyridylmethyl variant **22d** was synthesized under my responsibility.

The alternative synthetic route of the C7-SAHA library had been designed by the main concern for bulky subsitutuent attachment when the nucleophilic substitution (**24**->**25**) reaction was performed with large groups. Additionally, several steps were improved in Scheme 4.2.

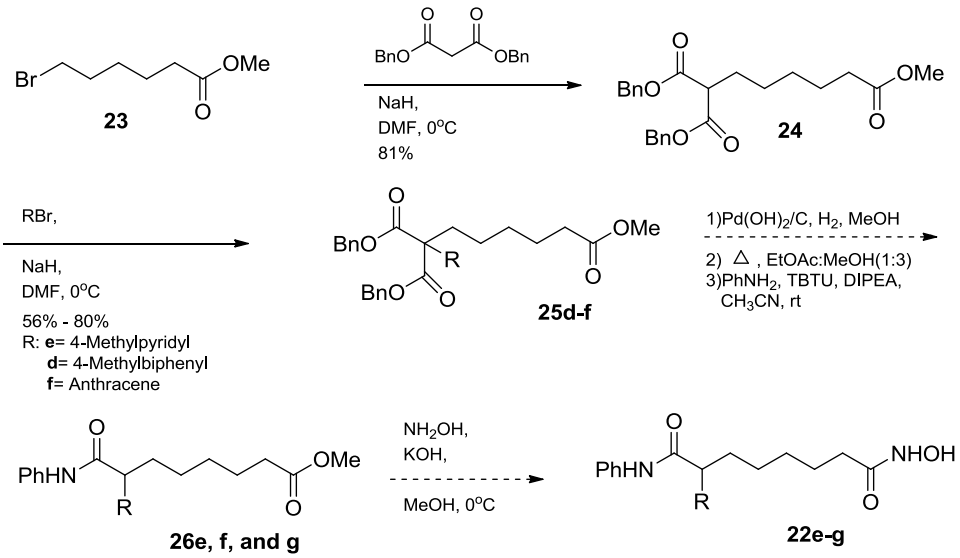

Scheme 4.2. Redesigned synthesis of C7-SAHA library for bulky groups

After successful nucleophilic substitution reaction with the dibenzylmalonate derivatives **24** and remaining substituents (pyridylmethyl, biphenylmethyl, and anthracenylmethyl groups), alkylated malonate derivatives **25d-f** were deprotected by Pd/C under hydrogen gas. Interestingly, the pyridyl and anthracenylmethyl groups were reduced when the dibenzyl groups of compounds **25d-f** were deprotected. Zacharie and co-workers have proven the reduction from pyridine derivatives to piperidine derivatives in the mild condition.[56] After deprotection by Pd/C, decarboxylation under the reflux condition, and coupling with aniline (three-step), there were additional anilide

products, the anthracenylmethyl anilide derivative **26f** and the tetrahydro-anthracenylmethyl anilide derivative **26g**. In contrast, pyridyl and piperidylmethyl anilide derivatives **26d**, **26d´** were unable to be isolated. The anthracenylmethyl and tetrahydroanthracenylmethyl anilide derivatives **26f**, **26g** were directly convert to hydroxamic acid **22f**, **22g**.

4.4 Optimized synthesis for the C7-pyridyl analogue

To synthesize the C7-pyridyl hydroxamic acid **22d**, the synthetic method was redesigned since the pyridyl and piperidylmethyl anilide derivatives were not isolated (Scheme 4.3). The initial synthesis performed by Dr. Bieliauskas was modified since the pyridylmethyl group is smaller than naphthylmethyl group. However, several reaction conditions were improved.

First of all, benzyl ester **16** was obtained under Fisher condition (95% yield) with benzyl alcohol and 6-bromohexanoic acid **15** instead of the coupling reaction (80% yield). The nucleophilic substitution reaction with *t*-butyl malonate generated derivative **17**, which was alkylated with bromomethyl pyridine to produce alkylated malonate derivatives **18d**. Compared to Dr. Bieliaskas' synthesis, the alkylation was performed under the kinetic condition in DMF at 0 ºC (**16** in 99% yield and **18d** in 55% yield) for shorter time (2-3h). Under acidic condition, the *t*-butyl groups on compound **18d** were deprotected and decarboxylation was observed under reflux to give the monocarboxylated derivative. Without purification, the coupling reaction was performed to give anilide **20d** (yield 99% over three steps). To obtain the final C7-SAHA

pyridylmethyl hydroxamic acid **22d**, direct conversion was achieved in one step (43%).

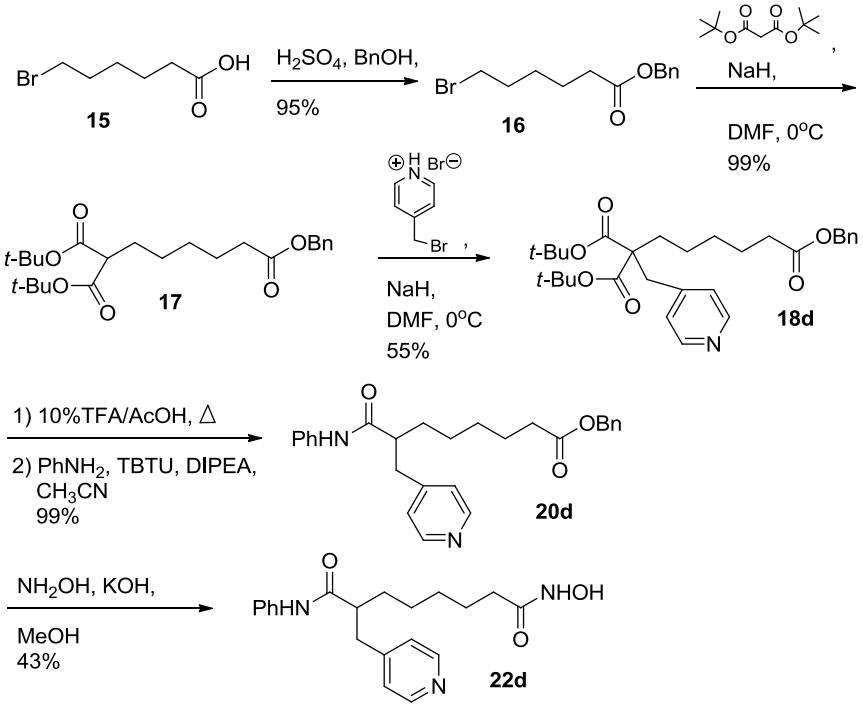

Scheme 4.3. Redesigned and optimized synthesis for C7-SAHA pyridylmethyl analogue **22d**

4.5 Biological analysis

HDAC inhibitory activities of the remaining C7-SAHA analogues were measured using the Fluor de Lys® *in vitro* fluorescence activity assay kit using Hela cell lysates (Table 4.2). HDAC inhibition of biphenylmethyl variant **22e** was tested by Geetha Padige.

Table 4.2. HDAC inhibition by C7-SAHA analogues and SAHA using HeLa cell lysates

Compounds	R	IC_{50}, nM[a]
SAHA		86 ± 4
22d	4-Pyridylmethyl	450 ± 35
22e	4-(1,1'-Biphenyl)methyl	4 ± 0.3
22f	9-Anthracenylmethyl	20 ± 1
22g	9-(1,2,3,4-Tetrahydroanthracenyl)methyl	102 ± 30

[a]Values are means of more than three experiments with standard error given.

One of the large compounds, C7-SAHA 4-(1,1´-biphenyl)methyl analogue **22e** displayed greater than 22-fold increase in inhibitory activity compared to SAHA (86 nM) or the smallest compound C7-SAHA methyl analogue **22a** (105 nM). Variants **22b**, **22e** with the large groups, such as naphthylmethyl and biphenylmethyl, were more potent than the smallest variant **22a** with methyl group for C7-SAHA inhibitory activities (Table 4.2). However, the bulky tetrahydroanthracenylmethyl subtituents displayed potency similar to SAHA. The data suggest that C7-SAHA analogues with planar aromatic groups interacted favourably in the binding area of HDAC active site. Moreover, the addition of certain groups at the C7 position likely promotes interaction between the entrance area of HDAC active site and the inhibitor.

Even though we found that greater steric tolerance exists in the HDAC active site in the entrance area of the capping group than the metal binding moiety region, the pyridylmethyl analogue displayed the weakest inhibitory activity (IC_{50} 450 nM). The polarity of the nitrogen atom might interact

unfavorably the binding area of the HDAC active site. As a result, the potency was influenced not only by the size of subsitutuents, but also the polarity, as shown by the fact that the pyridylmethyl group of equal size to the benzyl group (IC_{50} 109 nM).

To more thoroughly verify the structural requirements of SAHA analogues, the isoform selectivity of the C7-SAHA analogues was tested by using HDAC1 and HDAC3 representing class I and HDAC6 representing class II (Figure 4.2). To assess the isoform selectivity of the C7-SAHA analogues, all compounds were initially tested at a single concentration near to their IC_{50} values using the Fluor de Lys® kit (Enzo).

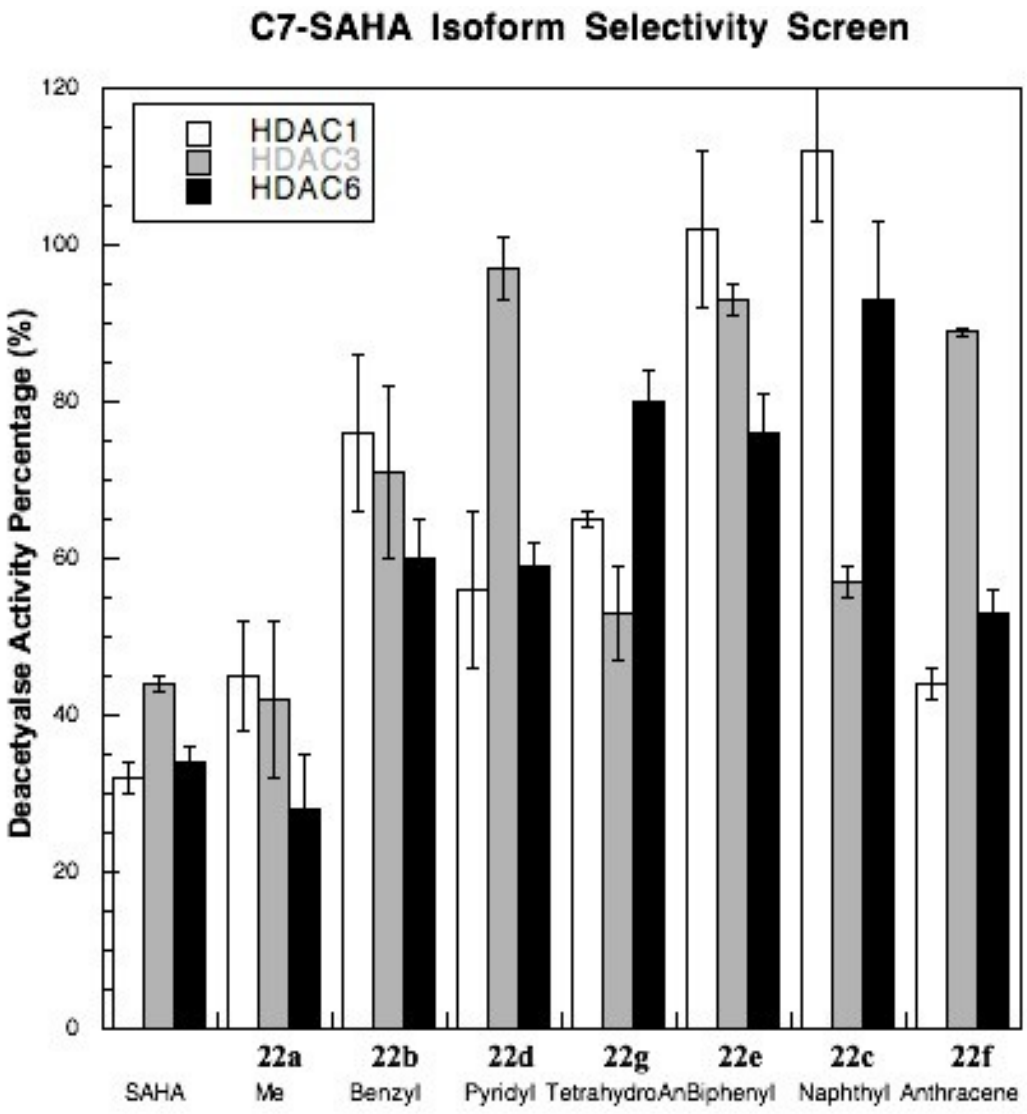

Figure 4.2. Screen of C7-SAHA analogues against HDAC1, HDAC3, and HDAC6 with 100 nM methyl, benzyl, tetrahydroanthracenylmethyl, and biphenylmethyl (**22a**, **22b**, **22g**, and **22e**) variants, 500 nM pyridylmethyl and anthracenylmethyl variants (**22d** and **22f**), and 10 nM naphthylmethyl variant (**22c**).

The methyl **22a**, and benzyl **22b** variants showed similar inhibition for HDAC1, HDAC3, and HDAC6 at 100 nM, despite slight selectivity for HDAC6 over HDAC1 and HDAC3. The biphenyl variant **22e**, which displayed the most potent inhibition from using Hela cell lysates, showed a slightly preference for

HDAC6 over HDAC1 and HDAC3 as well. In this case, however, two flexible perpendicular aromatic groups might enhance interaction with all of HDAC protein active sites to increase potency, not selectively. In addition, the biphenylmethyl variant **22e** did not show inhibition at 10 nM concentration near to the Hela cell lysate IC_{50} value (4 nM) for HDAC1, HDAC3, and HDAC6. In contrast, the naphthylmethyl **22c** and tetrahydroanthracenylmethyl **22g** variants showed greater potency for HDAC3 over HDAC1 and HDAC6 at 10 nM and 100 nM. Interestingly, both compounds contain two planar aromatic groups. Moreover, the pyridylmethyl **22d** and anthracenylmethyl **22f** variants showed unique dual-selective inhibition at 500 nM for HDAC1 and HDAC6 over HDAC3. Surprisingly, the C7-SAHA anthracenylmethyl compound **22f** was unable to inhibit when tested at 10 nM concentration near to the Hela cell lysate IC_{50} value (20 nM). After several screening, we found that the anthracenylmethyl variant **22f** inhibited 50% at 500 nM against HDAC1 and HDAC6. The biphenylmethyl **22e** and anthracenylmethyl **22f** variants might display more selective inhibition for other HDAC proteins, such as HDAC2, HDAC4, HDAC5, HDAC7, HDAC8, and HDAC10 due to the fact that showed inhibition at 25-time higher concentration (100 nM and 500 nM) against HDAC1, HDAC3, and HDAC6 than their Hela cell lysate IC_{50} values (4 nM and 20 nM).

With the potential of chemotherapeutic use of selective HDAC inhibitors, several class-selective and isoform-selective HDAC inhibitors have been studied. Most of selective HDAC inhibitors displayed preference for HDAC1 or HDAC8 against HDAC3.[17b, 20, 38b, 57-58] For example, compounds **27a** and **27b**, which have two-aromatic group, showed preference for HDAC8 (Figure 4.3).[38b] Nevertheless, the C7-SAHA naphthylmethyl analogue **22c** and tetrahydroanthracenylmethyl analogue **22g** containing similar structures to the compounds **27a** and **27b** display unique HDAC3 selectivity. Two parallel aligned aromatic group subsitutuents on the linker region may influence selectivity due to the presence of favorable π-π interactions with particular HDAC active site. Additionally, a dual-selective HDAC1 and HDAC6 inhibitor (pyridyl **22d** and anthracene **22f**) might promote design of drugs. Therefore, studying the C7-SAHA analogues, which displayed HDAC3 selective inhibition (the naphthylmethyl **22c** and tetrahydro-anthracenylmethyl **22g**) and dual-HDAC1 and HDAC6 selective inhibition (the pyridylmethyl **22d** and anthracenylmethyl **22f** variants), might be a great starting point to develop a variety of dual or isoform-selective HDAC inhibitors.

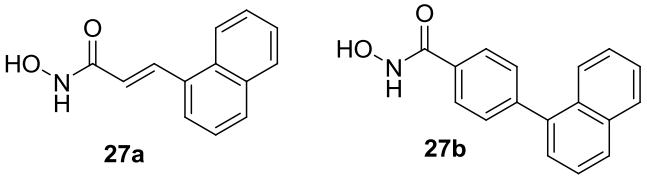

Figure 4.3. HDAC inhibitors modified at the linker regions with two parallel aligned aromatic groups

To more thoroughly assess the selectivity observed in the initial screen, we determined individual HDAC1, HDAC3, and HDAC6 IC_{50} values of the anthracene variant **22f**, and SAHA as a comparison. Pathological cardiac remodeling studies have been reported using selective HDAC inhibitors (Section

1.9). Specifically, development of dual-selective inhibitors has been an attractive target in pharmacokinetic study due to the hypothesis by that cancer formation is more complex than related to only single isoform HDAC protein. However, a lack of information on dual-selective HDAC inhibitors is a current challenge. For promising chemotherapeutic use, the anthracenylmethyl analogue **22f** among C7-SAHA analogues, which displayed dual-selective inhibition for HDAC1 and HDAC6, was analyzed by using the Fluor de Lys® kit (Enzo). The C7-anthracenylmethyl analogue **22f** displayed 4-fold selectivity for HDAC1 over HDAC3 and 3-fold class selectivity for HDAC6 over HDAC3 (Table 4.3). In addition, it displayed selectivity within class I, with 4-fold preference for HDAC1 over HDAC3. As a control, SAHA displayed non-selective inhibitor activity against the isoform, as expected (Table 4.3).[30] The selectivity analysis shows that substituents on the C7 position can influence selectivity. As a comparison, the C6-SAHA *t*-butyl analogue (dual-HDAC1 and HDAC6 selective inhibitor, IC_{50} value of 1.9 μM) displayed 22-fold less potency compared to SAHA (86 nM) while the C7-SAHA anthracene analogue **22f** (20 nM) showed 4-fold better potency compared to SAHA. Therefore, the data indicate that attaching the anthracene substituent on the linker chain on the C7 position promotes selectivity with potency.

Table 4.3. IC_{50} values of SAHA and the C7-SAHA anthracene **22f** for HDAC1, HDAC3, and HDAC6

Compound	IC_{50}/nM		
	HDAC1	HDAC3	HDAC6
SAHA	96 ± 16	136 ± 11	74 ± 9
22f	300 ± 66	1200 ± 50	443 ± 73

SAHA analogues with substituents on the C7 position displayed selective inhibition, including dual-class I, II selectivity (pyridyl **22d** and anthracene **22f** variants) and isoform selectivity for HDAC3 (naphthyl **22c** and tetrahydroanthracne **22g** variants) and HDAC6 (biphenyl variant **22e**). The results reveal that small structural changes in the C7 position linker region of SAHA will lead in designing drugs by improving selectivity and potency compared to the broad-spectrum inhibitor SAHA. Furthermore, studying selective inhibitor structures in detail will be able to be explored through our selective compound analysis in a variety of scope.

4.6 Future direction

We have synthesized and analyzed SAHA analogues that placed a variety of substituents in the carbon linker. The results from the C3, C6, and C7 library suggest that SAHA analogues with substituents on the carbon linker are promising to develop new anti-cancer drugs. To more systematically assess the structural effect in HDAC active site, more analogues positioning subsituetns at the C4, and C5 positions should be synthesized (Figure 4.4). In addition, analysis of isoform selectivity of the C3-SAHA analogues suggests that substituents on the SAHA linker influence selectivity. We have shown that the

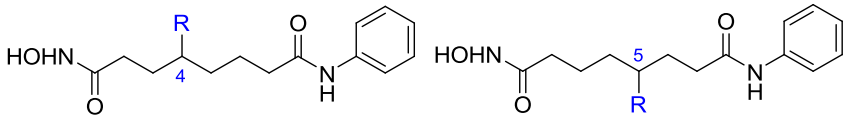

Figure 4.4. Structures of SAHA analogues containing substituents on the C4 and C5

steric environment of the C6 position displays less influences on potency compared to SAHA analogues with substituents near the hydroxamic acid. However, substituents at α-carbon on C6 position still decreased inhibitory activity. Interestingly, despite the poor potency of the C6-SAHA *t*-butyl analogue, it displayed selectivity. Likewise, the C3-SAHA ethyl analogue with an additional methylene group at the α–carbon compared to the C3-SAHA methyl analogue displayed selective inhibition (HDAC6 selectivity). The effect of the α-carbon on C6 substituents could be thoroughly investigated with the synthesis of isopropyl and adamantyl group analogues. Besides, the long chain of the 2-ethyl hexyl SAHA analogues on the C6 position also affected isoform selectivity (HDAC3-selectivity) with potency. Favourable interactions of the long aliphatic chain in HDAC active site could be verified through synthesis of C6-SAHA octyl to undecyl analogues. Furthermore, C7-SAHA analogues show potent inhibition with large and polar group substituents. The influence of the enantiomers with bulky or polar groups near the capping group would allow assessing the structural requirements of the compounds in detail. Therefore, screening the enantiomers of all SAHA analogues might show promising properties. Moreover, testing the inhibitory activities against all HDAC proteins, from HDAC1 to HDAC11, will provide the structures of selective inhibitors. Developing new cost-effective, high through-put screening methods are needed to test selectivity against all HDAC1-11. Therefore, the biological evaluation of the current compound enantiomers, the additional synthesis of different structural

compounds, and the development of easy-access high through-put assay will contribute to develop promising cancer drugs.

4.7 Experimental

4.7.1 General methods

Additional details were shown in Section 2.5.1 of Chapter 2.

4.7.2 Experimental Procedures and Compound Characterizations

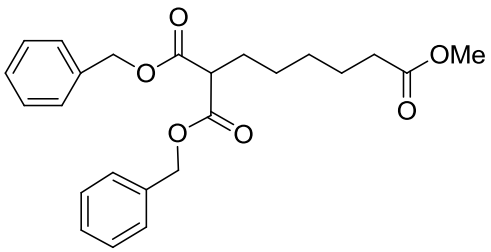

1, 1-Dibenzyl 6-methyl hexane-1, 1, 6-tricarboxylate (24). To a solution of NaH (144 mg, 6 mmol) in DMF (20 mL) was added dibenzylmalonate (1.14 mL, 6 mmol) dropwise at 0 ºC and the mixture was stirred for 15 min. To the solution was added methyl 6-bromohexanoate **23** (0.57 g, 2 mmol) and the mixture was stirred for 3 h. The mixture was filtered through celite with ethyl acetate and concentrated. The residue was purified by column chromatography (diethyl ether:petroleum ether 1:19) on silica gel to give **24** (682 mg, 81%). ^{1}H-NMR (δ, ppm, CHLOROFORM-D): 1.31 (m, 4H), 1.58 (m, 2H), 1.94 (q, 2H), 2.26 (t, 2H), 3.43 (t, 1H), 3.65 (s, 3H), 5.14 (s, 4H), 7.31 (m, 10H); ^{13}C-NMR (δ, ppm, CHLOROFORM-D): 24.8, 27.1, 28.8, 28.9, 34.1, 51.7, 52.1, 67.3, 128.4, 128.6, 128.8, 135.6, 169.4, 174.3; IR: 3033, 2949, 2862, 1734, 1498, 1456, 1333, 1214,

1156, 907, 741, 698 cm^{-1}; HRMS (EI-TOF, *m/z*): found [M+Na] 435.1767, calc. for $C_{24}H_{28}O_6$, 435.1784.

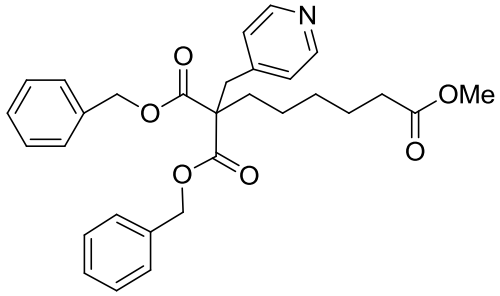

6, 6-Dibenzyl 1-methyl 7-(pyridine-4-yl)heptane-1, 6, 6-tricarboxylate (25). To a solution of NaH (256 mg, 6.4 mmol) in DMF (53 mL) was added 1, 1-dibenzyl 6-methyl hexane-1, 1, 6-tricarboxylate **24** (2.20 g, 5.33 mmol) dropwise at 0 ºC and the mixture was stirred for 15 min. Separately, 1.5 equivalents of 4-bromo-methylpyridine hydrobromide salt (2.02 g, 8.00 mmol) was dissolved in distilled water (8 mL) and added to a separatory funnel, followed by 0.7 equivalent of Na_2CO_3 (396 mg, 3.74 mmol). After the separatory funnel was shaken until gas evolution was not observed, the mixture was extracted with ethyl acetate (8 mL) at least 4 times. The organic layers were dried over magnesium sulfate, filtered, and concentrated by rotary evaporation. To the flask containing the activated dibenzyl malonate derivatives solution **24** was added the solution of the neutralized and concentrated 4-bromo-methylpyridine and the mixture was stirred for 4h at 0 ºC. The reaction was quenched with distilled water (26.5 mL) and extracted with ethyl acetate (equal volume to aqueous layer). The organic layer was pooled and extracted with distilled water (equal volume to organic layer) at least 4 times. The organic layer was dried over magnesium sulfate, filtered, and concentrated to oil. The residue was purified by column chromatography (ethyl

acetate:hexanes 1:3) on silica gel to give **25** (1.61 g, 60%). ^{1}H-NMR (δ, ppm, CHLOROFORM-D): 1.21 (m, 4H), 1.50 (m, 2H), 1.75 (t, 2H), 2.20 (t, 2H), 3.19 (s, 2H), 3.64 (s, 3H), 5.08 (s, 4H), 6.82 (d, 1H), 6.91 (d, 1H), 7.24-7.31 (m, 7H), 8.35 (d, 1H), 8.36 (d, 1H); ^{13}C-NMR (δ, ppm, CHLOROFORM-D): 24.1, 24.8, 29.3, 32.3, 34.0, 37.8, 51.7, 58.7, 67.5, 125.3, 128.765, 128.787, 128.816, 135.3, 145.3, 149.9, 170.6, 174.1; IR: 3032, 2951, 1731, 1601, 1455, 1218, 1170, 912, 733, 698 cm^{-1}; HRMS (EI-TOF, *m/z*): found [M+H] 504.2387, calc. for $C_{30}H_{34}NO_6$, 504.2386.

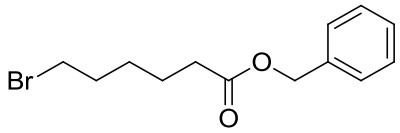

Benzyl 6-bromohexanoate (16). Benzyl alcohol (0.07 mL, 0.68 mmol) and concentrated aqueous sulfuric acid (3 µL, 0.056 mmol) were stepwise added to a solution of 6-bromohexanoic acid **15** (0.11 g, 0.56 mmol) in diethyl ether (5 mL) at 0ºC. The mixture was stirred for 30min and warmed to room temperature. The reaction mixture was quenched with distilled water (5 mL). The mixture was extracted with diethyl ether (5 mL) at least 4 times. The organic layer was evaporated. The concentrated organic layer was extracted with distilled water (equal volume to the concentrated organic layer) at least 3 times. The organic layer was dried over anhydrous Na_2SO_4, filtered, and concentrated. The residue was purified by column chromatography (diethyl ether:petroleum ether 1:19) on silica gel to give **16** (153 mg, 95%). ^{1}H-NMR (δ, ppm, CHLOROFORM-D): 1.47

(m, 2H), 1.68 (m, 2H), 1.86 (m, 2H), 2.38 (t, 2H), 3.38 (t, 2H), 5.12 (s, 2H), 7.36 (m, 5H); ^{13}C-NMR (δ, ppm, CHLOROFORM-D): 24.3, 27.9, 32.6, 33.7, 34.3, 66.4, 128.5, 128.8, 136.3, 173.5; IR: 3033, 2939, 1733, 1455, 1254, 1165, 736, 697 cm^{-1}; HRMS (EI-TOF, *m/z*): found [M+Na] 307.0314, calc. for $C_{13}H_{17}O_2NaBr$, 307.0310.

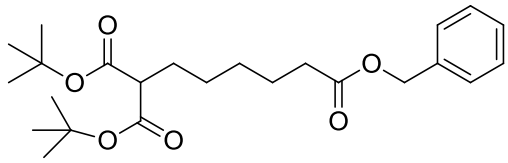

6-Benzyl 1,1-di-*tert*-butyl hexane-1,1,6-tricarboxylate (17). To a solution of NaH (589 mg, 14.7 mmol) in DMF (49 mL) was added di-*t*-butylmalonate (3.30 mL, 14.7 mmol) dropwise at 0 ºC and the mixture was stirred for 15 min. To the solution was added benzyl 6-bromohexanoate **16** (1.4 g, 4.91 mmol) at 0 ºC and the mixture was stirred for 3 h at room temperature. The mixture was filtered through celite with ethyl acetate and concentrated. The residue was purified by column chromatography (diethyl ether:petroleum ether 1:19) on silica gel to give **17** (2.04 g, 99%).^{1}H-NMR (δ, ppm, CHLOROFORM-D): 1.34 (m, 4H), 1.45 (s, 18H), 1.65 (m, 2H), 1.79 (q, 2H), 2.34 (t, 2H), 3.10 (t, 1H), 5.11 (s, 2H), 7.35 (m, 5H); ^{13}C-NMR (δ, ppm, CHLOROFORM-D): 24.9, 27.1, 28.2, 28.6, 29.0, 34.4, 54.1, 66.3, 81.5, 128.4, 128.8, 135.6, 169.1, 173.7; IR: 3033, 2979, 2935, 2861, 1729, 1498, 1369, 1256, 1169, 1139, 748 cm^{-1}; found MS(ESI): m/z = 427.30 (M^++Li), 443.30 (M^++Na), 459.27 (M^++K), calc. for $C_{24}H_{36}LiO_6$, 427.48, $C_{24}H_{36}NaO_6$, 443.53, $C_{24}H_{36}KO_6$, 459.64.

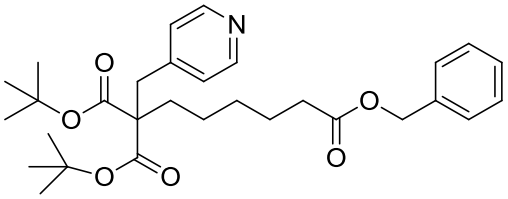

1-Benzyl 6,6-di-tert-butyl 7-(pyridine-4-yl)heptane-1,6,6-tricaboxylate (18d). To NaH (171 mg, 4.28 mmol) and 4-bromo-methylpyridine hydrobromide salt (1.0 g, 4.28 mmol) was added DMF (16 mL) dropwise at 0 ºC and the mixture was stirred for 20min. Separately, to NaH (171 mg, 4.28 mmol) in DMF (20 mL) was added 6-benzyl 1,1-di-*tert*-butyl hexane-1,1,6-tricarboxylate **17** (1.5 g, 3.57 mmol) dropwise at 0 ºC and the mixture was stirred for 20 min. To the solution of the activated 6-benzyl 1,1-di-*tert*-butyl hexane-1,1,6-tricarboxylate **17** was added the solution of the neutralized 4-bromo-methylpyridine dropwise at 0 ºC and the mixture was stirred for 3h at room temperature. The reaction mixture was filtered through celite with ethyl acetate and concentrated. The residue was purified by column chromatography (diethyl ether:petroleum ether 1:5) on silica gel to give **18d** (513 mg, 55%). ^{1}H-NMR (δ, ppm, CHLOROFORM-D): 1.29 (m, 4H), 1.43 (s, 18H), 1.65 (m, 4H), 2.34 (t, 2H), 3.12 (s, 2H), 5.10 (s, 2H), 7.07 (d, 2H), 7.34 (m, 5H), 8.47 (d, 2H); ^{13}C-NMR (δ, ppm, CHLOROFORM-D): 24.0, 24.9, 28.1, 29.5, 32.2, 34.4, 37.4, 59.1, 66.4, 82.0, 125.6, 128.4, 128.8, 136.2, 146.3, 149.7, 170.3, 173.6; IR: 3036, 2976, 2935, 2867, 1727, 1605, 1248, 1159, 846, 737, 696 cm^{-1}; HRMS (EI-TOF, *m/z*): found [M+H] 512.3016, calc. for $C_{30}H_{42}NO_6$, 512.3012.

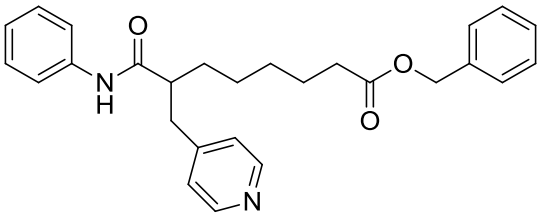

Benzyl 8-oxo-8-(phenylamino)-7-(pyridine-4-ylmethyl)octanoate (20d). To a flask equipped with a reflux condenser and containing 1-benzyl 6,6-di-tert-butyl 7-(pyridine-4-yl)heptane-1,6,6-tricaboxylate **18d** (510 mg, 997 mmol) was added 10 mL of 10% TFA in acetic acid. The reaction mixture was refluxed overnight and evaporated to oil. The residue was dissolved in ethyl acetate (10 mL) and transferred to a separatory funnel. The solution was extracted with saturated $NaHCO_{3(aq)}$ (equal volume to organic layer) at least 4 times. The organic layer was dried over magnesium sulfate, filtered, and evaporated. The crude residue was dissolved in acetonitrile (10 mL). To the solution of crude carboxylic acid derivative was added individually in order listed in a stepwise: TBTU (480 mg), diisopropylethylamine (695 mL), and aniline (136 mL). The reaction mixture was stirred overnight at room temperature. The reaction was quenched by addition of an aqueous solution of saturated $NaHCO_3$ (10 mL). The mixture was extracted with CH_2Cl_2 (equal volume to aqueous layer) at least 4 times. The organic layer was dried over magnesium sulfate, filtered, and concentrated to an oil. The residue was purified by column chromatography (ether:petroleum ether 1:1) on silica gel to give **20d** (572 mg, 99%). ^{1}H-NMR (δ, ppm, CHLOROFORM-D): 1.34 (m, 4H), 1.49 (m, 1H), 1.61 (m, 2H), 1.79 (m, 1H), 2.33 (t, 2H), 2.47 (m, 1H), 2.69 (q, 1H), 3.02 (q, 1H), 5.09 (s, 2H), 7.09 (m, 3H), 7.25 (m, 2H), 7.32 (m, 4H), 7.38 (d, 2H), 7.89 (m, 1H), 8.40 (d, 2H); ^{13}C-NMR (δ, ppm, CHLOROFORM-

D): 24.8, 27.1, 29.0, 33.1, 34.3, 38.6, 49.9, 66.4, 120.4, 124.7, 128.3, 128.4, 128.5, 128.8, 129.2, 136.2, 137.9, 149.4, 149.8, 173.0, 173.9; IR: 3304, 3221, 3035, 2931, 2858, 1734, 1602, 1443, 1173, 912, 752, 696 cm^{-1}. HRMS (EI-TOF, *m/z*): found [M+H] 431.2331, calc. for $C_{27}H_{31}N_2O_3$, 431.2335.

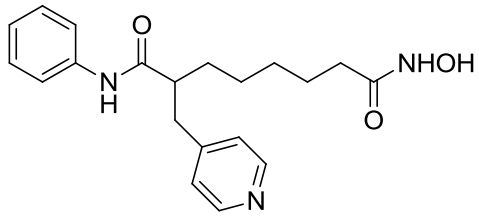

***N*^{8}-hydroxy-*N*^{1}-phenyl-2-(pyridin-4-ylmethyl)octanediamide (22d).** To a solution of $NH_2OH{\cdot}HCl$ (536 mg, 7.67 mmol) in methanol (8 mL) was added KOH (860 mg, 15.3 mmol) at 0 ˚C in an acid-washed 25mL round-bottom flask. After stirring for 20 min, benzyl 8-oxo-8-(phenylamino)-7-(pyridine-4-ylmethyl)octanoate **20d** (330 mg, 0.767 mmol) was added and the mixture was stirred for 8h at 0°C. The reaction mixture was quenched by adding 1mL of distilled water and adjusting to pH 6 by adding concentrated aqueous hydrochloric acid. The mixture was diluted with 8 mL of ethyl acetate, and extracted with distilled water (equal volume to organic layer) at least 4 times. The organic layer was dried over magnesium sulfate, filtered and concentrated. The residue was purified by column chromatography (8% methanol/CH_2Cl_2 with 0.1% Et_3N) on acid-washed silica gel to give **22d** (116 mg, 43%). ^{1}H-NMR (δ, ppm, METHANOL-D): 1.39 (m, 4H), 1.60 (m, 3H), 1.77 (m, 1H), 2.08 (t, 2H), 2.86 (m, 2H), 2.93-3.00 (m, 2H), 7.06 (t, 1H), 7.25 (t, 2H), 7.43 (d, 2H), 7.50 (d, 2H), 8.48 (d, 2H); ^{13}C-NMR (δ, ppm, CHLOROFORM-D): 25.4, 26.9, 28.8, 32.4, 32.8, 38.4, 120.3, 124.3, 125.8, 128.6, 138.1, 146.7, 153.8, 171.7, 174.1; IR: 3440, 3335,

2866, 1720, 1641, 1528, 1442, 1133, 759, 660 cm^{-1}; HRMS (EI-TOF, *m/z*): found [M+H] 356.1966, calc. for $C_{20}H_{26}N_3O_3$, 356.1974. HPLC analytical purity analysis: 90%.

4.8 HDAC assay procedure

HDAC activity was measured using the Fluor de Lys® activity assay (Biomol & Enzo) using the manufacturer's protocol. Additional details were shown in Section 3.6 of Chapter 3.

APPENDIX A. DOSE RESPONSE GRAPHS AND DATA FOR C3-SAHA LIBRARY

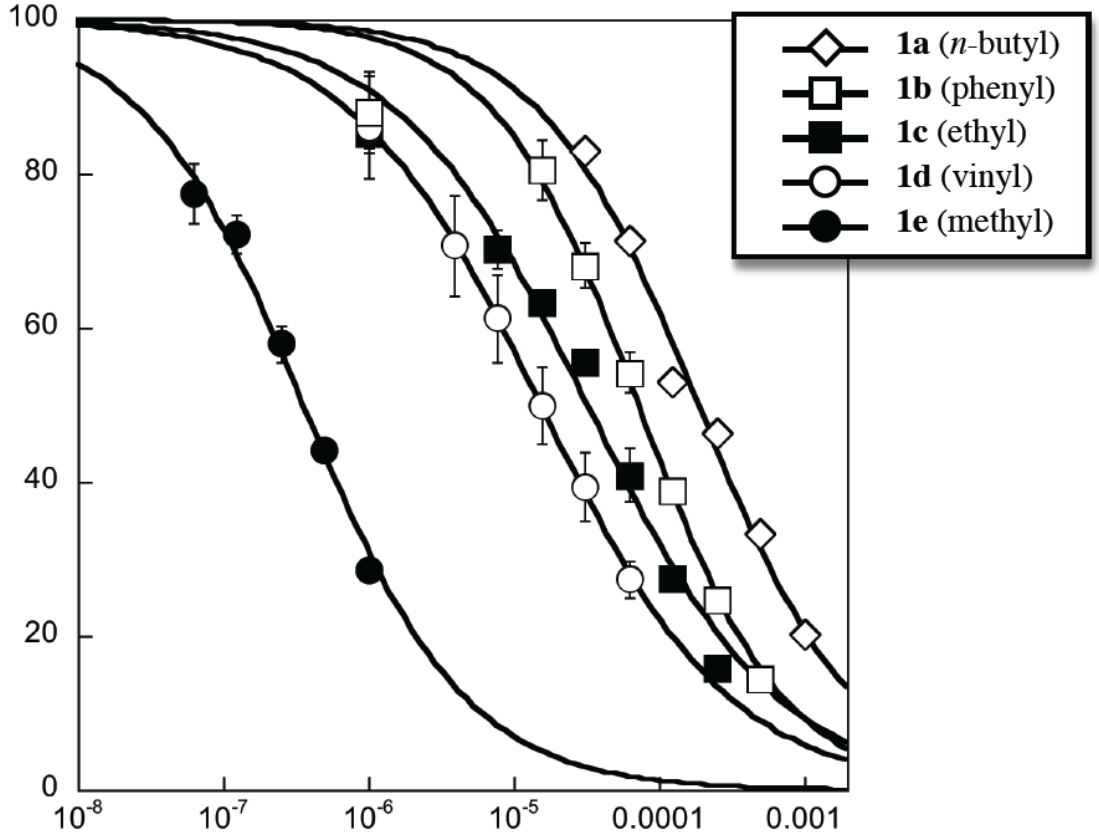

Figure A.1. Dose response curve of C3-SAHA analogue **1a**-**e** tested using the HDAC activity from HeLa cells lysates from three independent trials with error bars indicating standard error. In some case, the error bars are smaller than the marker size. Data were fit to the sigmoidal curve using Kaleidograph 4.0 (Synergy Software) to determine the IC_{50}. The insets were the results of the data analysis. The data are reported in Table 2.1.

Table A.1 Inhibition of HDAC Activity of SAHA C3-Butyl with Hela Lysate

Concentration (M)	Trial 1	Trial 2	Trial 3	Mean	S.E
3.125×10^{-5}	83	85	81	83	1
6.25×10^{-5}	72	69	73	71	1
1.25×10^{-4}	54	54	51	53	1
2.50×10^{-4}	47	46	46	46	1
5.00×10^{-4}	31	35	34	33	1
1.00×10^{-4}	19	22	20	20	1

Table A.2 Inhibition of HDAC Activity of SAHA C3-Phenyl with Hela Lysate

Concentration (M)	Trial 1	Trial 2	Trial 3	Mean	S.E
1.00×10^{-6}	98	80	86	88	5
1.5625×10^{-5}	88	79	74	80	4
3.125×10^{-5}	74	65	66	68	3
6.25×10^{-5}	59	54	50	54	3
1.25×10^{-4}	40	38	38	37	1
2.50×10^{-4}	25	26	24	25	1
5.00×10^{-4}	15	14	14	14	1

Table A.3 Inhibition of HDAC Activity of C3-SAHA Ethyl with Hela Lysate

Concentration (M)	Trial 1	Trial 2	Trial 3	Mean	S.E
1.00×10^{-6}	88	85	82	85	2
7.8125×10^{-5}	75	69	67	70	2
1.5625×10^{-5}	67	62	61	63	1
3.125×10^{-5}	52	57	57	55	2
6.25×10^{-5}	42	46	34	41	4
1.25×10^{-4}	27	28	28	28	1
2.50×10^{-4}	18	15	14	16	1

Table A.4 Inhibition of HDAC Activity of SAHA C3-Vinyl with Hela Lysate

Concentration (M)	Trial 1	Trial 2	Trial 3	Mean	S.E
1.00×10^{-6}	84	75	99	86	7
3.906×10^{-6}	83	60	69	71	7
7.8125×10^{-6}	72	55	57	61	5
1.5625×10^{-5}	60	43	47	50	5
3.125×10^{-5}	48	34	37	40	4
6.25×10^{-5}	32	23	27	27	3

Table A.5 Inhibition of HDAC Activity of C3-SAHA Methyl with Hela Lysate

Concentration (M)	Trial 1	Trial 2	Trial 3	Mean	S.E
1.00×10^{-9}	95	93	77	88	4
6.25×10^{-8}	85	75	72	77	4
1.25×10^{-7}	77	72	62	72	3
2.50×10^{-7}	62	58	54	58	2
5.00×10^{-7}	45	46	43	44	1
1.00×10^{-6}	31	28	29	29	1

Table A.6 Isoform Selective HDAC Inhibition of SAHA C3 Analogues

Compound	HDAC Isoform	Trial 1	Trial 2	Mean	S.E
SAHA (125 nM)	HDAC1	27	35	31	4
	HDAC3	44	45	45	1
	HDAC6	32	37	35	3
C3-Methyl (375 nM)	HDAC1	44	47	46	2
	HDAC3	53	62	57	5
	HDAC6	73	75	74	1
C3-Ethyl (32 μM)	HDAC1	38	39	39	1
	HDAC3	71	95	83	12
	HDAC6	17	18	18	1
C3-Vinyl (32 μM)	HDAC1	23	26	25	2
	HDAC3	47	51	49	2
	HDAC6	26	28	27	1
C3-Butyll (32 μM)	HDAC1	33	33	33	0
	HDAC3	52	52	52	0
	HDAC6	22	25	24	2
C3-Phenyl (32 μM)	HDAC1	42	48	45	3
	HDAC3	50	51	51	1
	HDAC6	24	27	26	2

Deacetylase activity of HDAC1, HDAC3 and HDAC6 was determined with SAHA and with SAHA C3 analogs at given concentration using an in vitro fluorescence assay as described. The background fluorescence activity (No enzyme added) was subtracted and the percentage deacetylase activity was calculated with compared to the No small molecule treated (100%). Percentage deacetylase activity of each independent trial, mean percentage deacetylase activity and standard error (S.E) are shown.

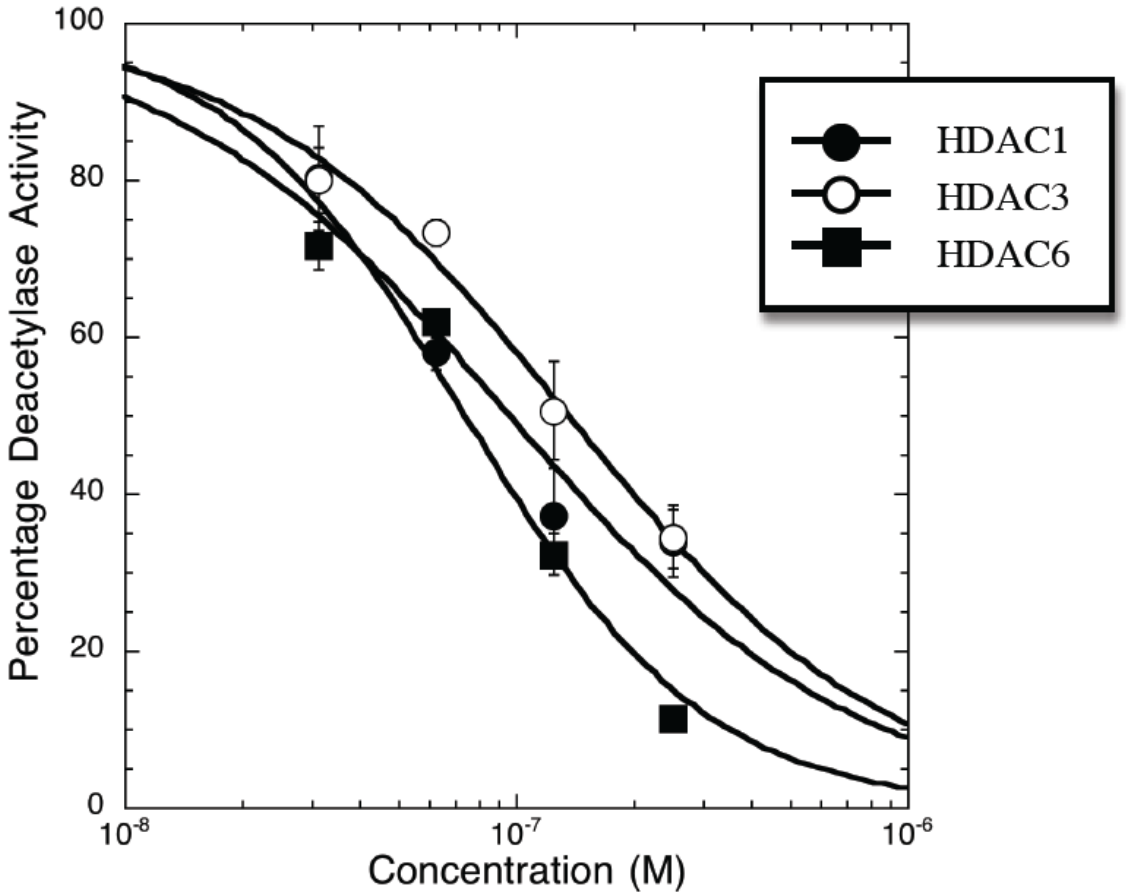

Figure A.2. Dose response curves of SAHA tested against HDAC1, HDAC3, and HDAC6 from three independent trials with error bars indicating standard error. In some cases, the error bars are smaller than the marker size. The data is reported in the manuscript in Table 2.2.

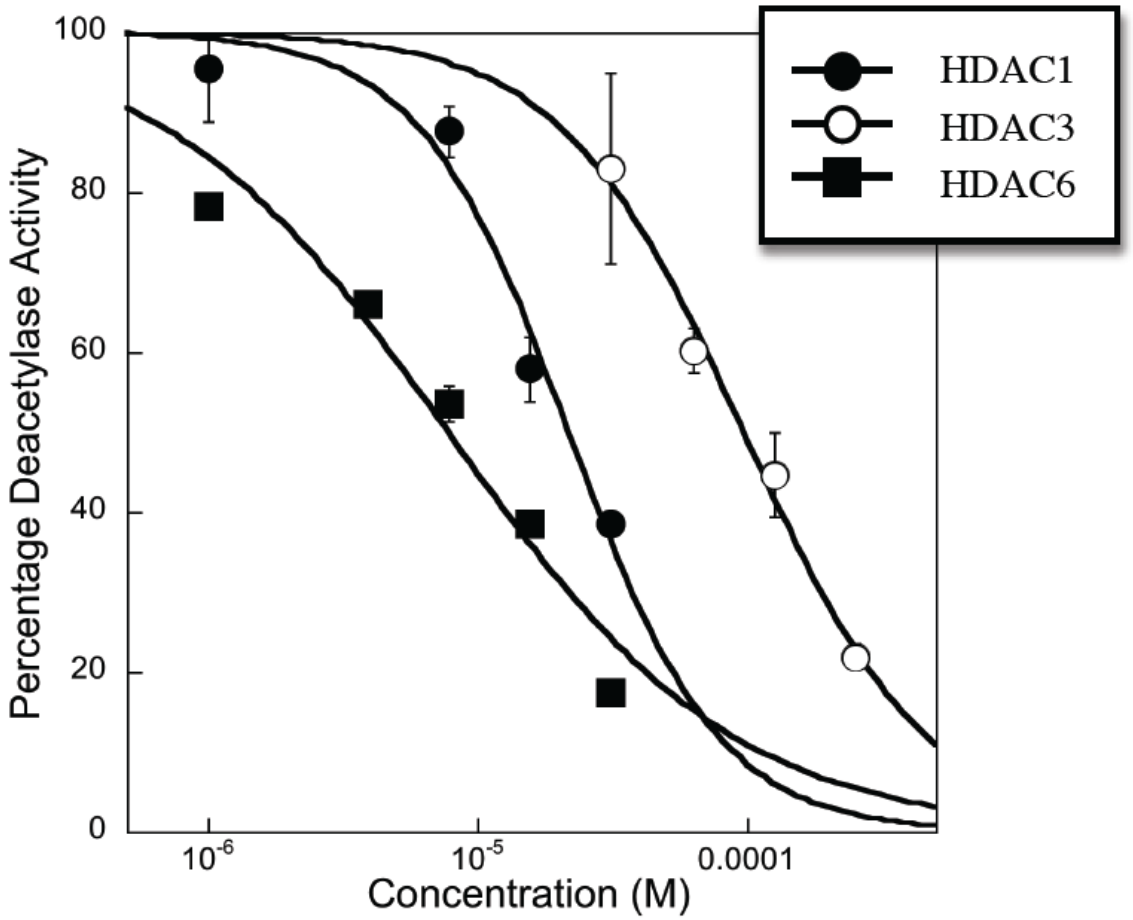

Figure A.3. Dose response curves of the C3- SAHA ethyl analogue **1c** tested against HDAC1, HDAC3, and HDAC6 from three independent trials with error bars indicating standard error. In some cases, the error bars are smaller than the marker size. The data is reported in the manuscript in Table 2.2.

Table A.7 Inhibition of HDAC1 Activity by SAHA

Concentration (M)	Trial 1	Trial 2	Trial 3	Mean	S.E
3.125×10^{-8}	68	91	82	80	7
6.25×10^{-8}	55	62	57	58	2
1.25×10^{-7}	48	27	37	37	6
2.50×10^{-7}	37	40	25	34	5

Table A.8 Inhibition of HDAC3 Activity by SAHA

Concentration (M)	Trial 1	Trial 2	Trial 3	Mean	S.E
3.125×10^{-8}	88	78	74	80	4
6.25×10^{-8}	76	74	70	73	2
1.25×10^{-7}	63	45	44	56	5
2.50×10^{-7}	27	39	37	34	4

Table A.9 Inhibition of HDAC6 Activity by SAHA

Concentration (M)	Trial 1	Trial 2	Trial 3	Mean	S.E
3.125×10^{-8}	66	76	73	72	3
6.25×10^{-8}	64	62	60	62	1
1.25×10^{-7}	37	28	32	32	2
2.50×10^{-7}	13	12	9	11	1

Table A.10 Inhibition of HDAC1 Activity by SAHA C3-Ethyl

Concentration (M)	Trial 1	Trial 2	Trial 3	Mean	S.E
1.00×10^{-6}	102	89	ND	96	9
7.8125×10^{-6}	83	94	86	88	6
1.5625×10^{-5}	58	65	51	58	7
3.125×10^{-5}	39	38	ND	39	1

Table A.11 Inhibition of HDAC3 Activity by SAHA C3-Ethyl

Concentration (M)	Trial 1	Trial 2	Trial 3	Mean	S.E
3.125×10^{-5}	95	71	ND	83	12
62.50×10^{-5}	58	57	66	60	3
1.25×10^{-4}	46	35	53	45	5
$2.50x\ 10^{-5}$	20	21	25	22	2

Table A.12 Inhibition of HDAC6 Activity by SAHA C3-Ethyl

Concentration (M)	Trial 1	Trial 2	Trial 3	Mean	S.E
1.000×10^{-6}	81	76	78	78	1
3.906×10^{-6}	69	65	64	66	2
7.812×10^{-6}	52	58	51	54	2
1.562×10^{-5}	38	40	38	39	1
3.125×10^{-5}	17	18	ND	18	1

APPENDIX B. SUPPLEMENTARY INFORMATION FOR C3-SAHA LIBRARY

B.1 5-Hydroxy-*N*-phenylpentanamide (**3**)

B.1.1 ^{1}H NMR

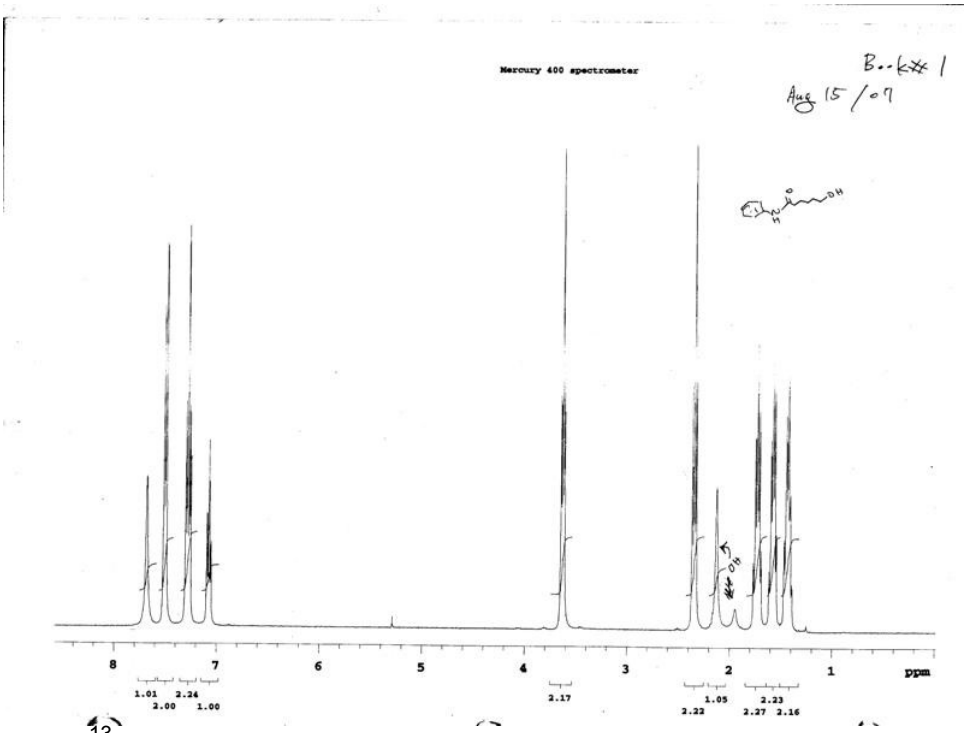

B.1.2 ^{13}C NMR

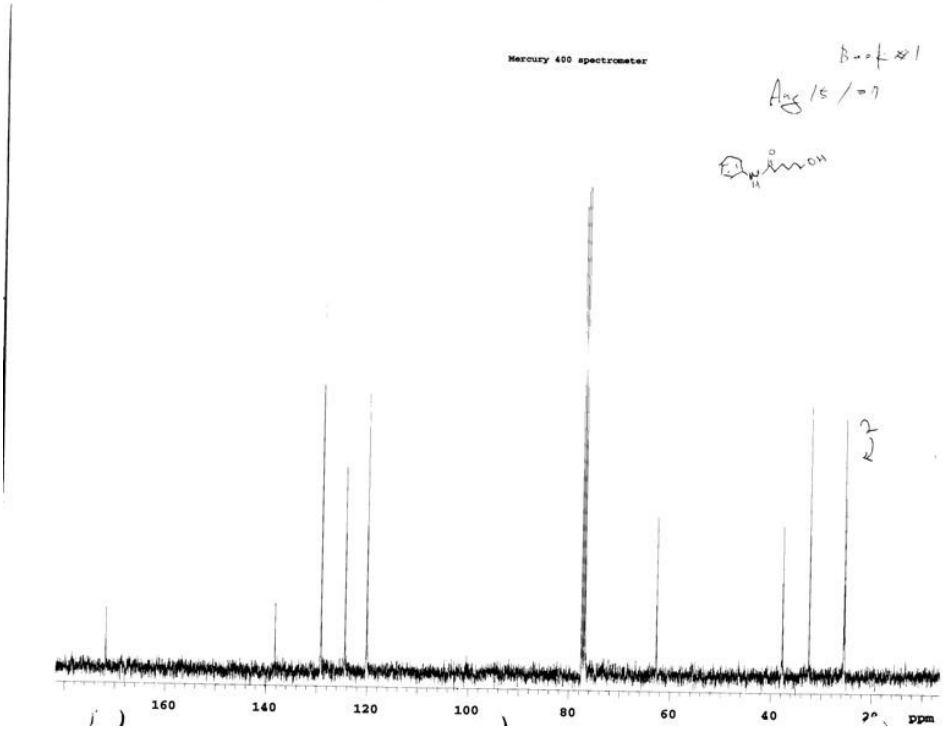

B.1.3 IR

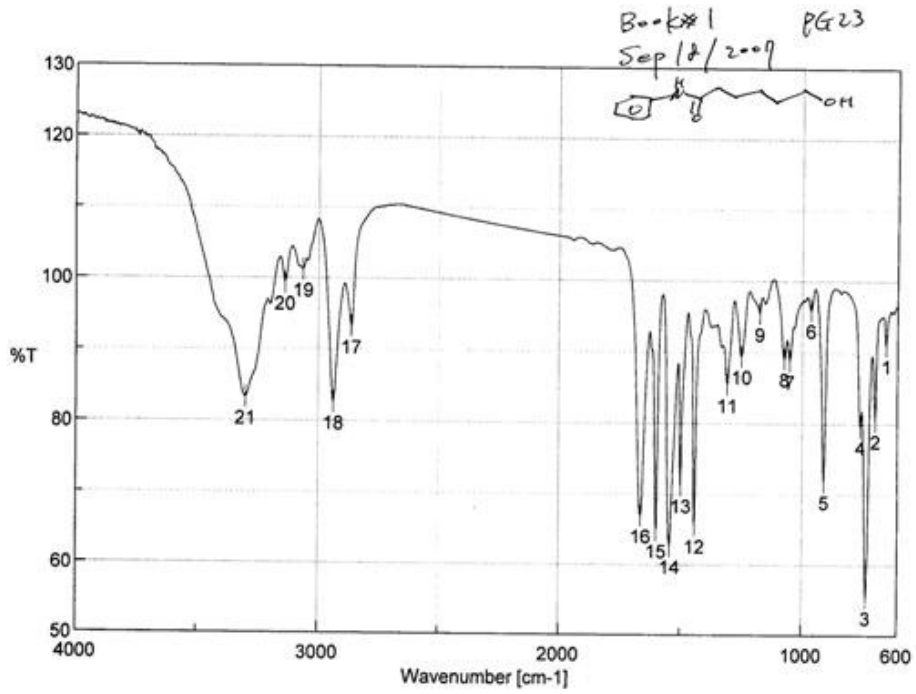

Result of Peak Picking

No.	Position	Intensity	No.	Position	Intensity
1	647.001	91.0387	2	692.32	80.474
3	729.925	55.4341	4	754.995	79.59
5	908.308	71.8178	6	961.341	95.907
7	1051.01	88.7738	8	1074.16	89.0851
9	1177.33	95.3979	10	1251.58	89.3905
11	1309.43	85.4377	12	1442.49	65.4784
13	1498.42	71.2467	14	1543.74	62.6047
15	1598.7	64.7477	16	1663.3	66.9215
17	2862.81	93.2437	18	2936.09	82.5852
19	3063.37	101.173	20	3136.65	99.3077
21	3297.68	83.2347			

[Comment]
Sample Name
Comment
User
Division
Company Wayne State

[Measurement Information]
Model Name FT/IR-4100typeA
Serial Number B071461016

Light Source Standard
Detector TGS
Accumulation Auto (66)
Resolution 4 cm-1
Zero Filling On
Apodization Cosine
Gain Auto (4)
Aperture Auto (7.1 mm)
Scanning Speed Auto (2 mm/sec)
Filter Auto (30000 Hz)

B.1.4 HRMS

Elemental Composition Report **Page 1**

Single Mass Analysis (displaying only valid results)
Tolerance = 4.0 mDa / DBE: min = -1.5, max = 50.0
Isotope cluster parameters: Separation = 1.0 Abundance = 1.0%

Monoisotopic Mass, Odd and Even Electron Ions
72 formula(e) evaluated with 3 results within limits (all results (up to 1000) for each mass)

Sun Ea Choi 091807 PG 23 Alcohol
SPEI 70eV
L071005_904 120 (2.000) Cm (94:122-260:298x2.000)
GC-TOF
05-Oct-2007 10:36:24
TOF MS EI+
4.64e5

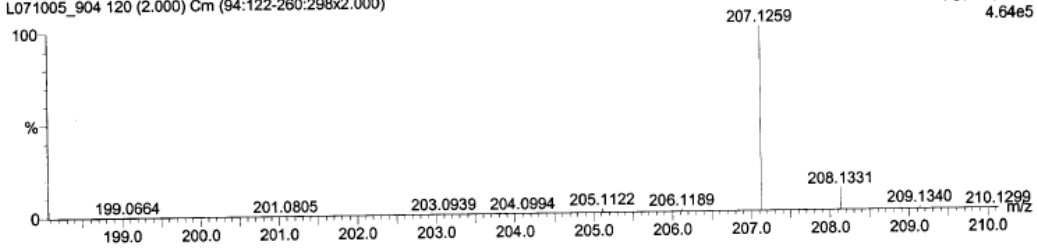

Minimum:				-1.5		
Maximum:		4.0	5.0	50.0		
Mass	Calc. Mass	mDa	PPM	DBE	Score	Formula
207.1259	207.1259	-0.1	-0.3	5.0	2	C12 H17 N O2
	207.1246	1.3	6.2	5.5	1	C10 H15 N4 O
	207.1219	4.0	19.1	1.0	3	C7 H17 N3 O4

B.2 6-Oxo-6-(phenylamino)hexanal (**4**)

B.2.1 ^{1}H NMR

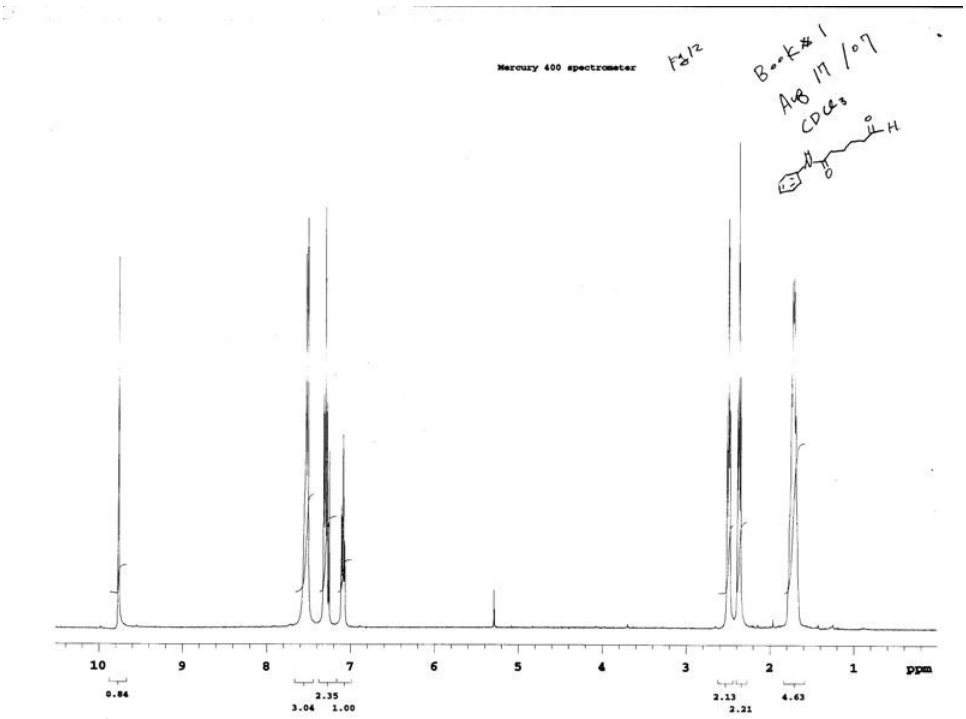

B.2.2 ^{13}C NMR

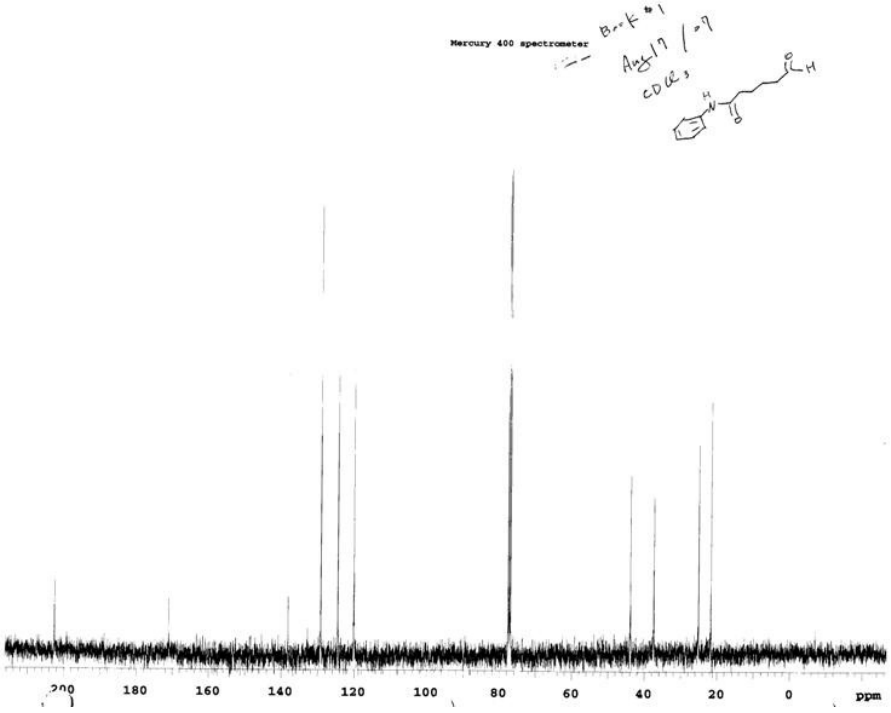

B.2.3 IR

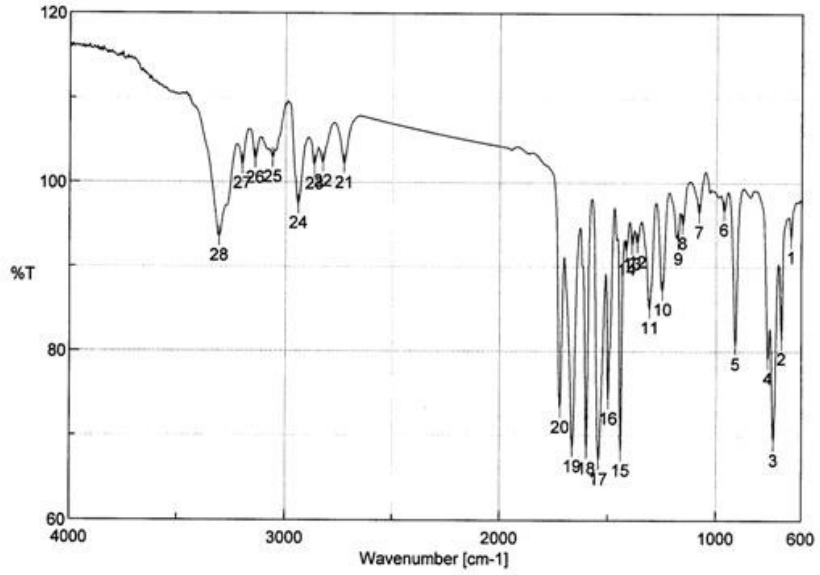

Result of Peak Picking

No.	Position	Intensity	No.	Position	Intensity
1	647.965	93.4442	2	693.284	81.3578
3	729.925	69.3754	4	755.959	79.0068
5	909.272	80.7072	6	961.341	96.6682
7	1078.98	96.3849	8	1156.12	95.0621
9	1177.33	93.2351	10	1250.61	87.1809
11	1310.39	85.0071	12	1366.32	92.8652
13	1389.46	92.6047	14	1416.46	92.0052
15	1441.53	68.1541	16	1498.42	74.2736
17	1542.77	67.1488	18	1598.7	68.4163
19	1664.27	68.6768	20	1721.16	73.2593
21	2725.89	102.202	22	2826.17	102.371
23	2865.7	102.048	24	2939.95	97.4177
25	3058.55	102.895	26	3139.54	102.79
27	3198.36	102.098	28	3305.39	93.5273

[Comment]	
Sample Name	
Comment	
User	
Division	
Company	Wayne State
[Measurement Information]	
Model Name	FT/IR-4100typeA
Serial Number	B071461016
Light Source	Standard
Detector	TGS
Accumulation	Auto (71)
Resolution	4 cm-1
Zero Filling	On
Apodization	Cosine
Gain	Auto (8)
Aperture	Auto (7.1 mm)
Scanning Speed	Auto (2 mm/sec)
Filter	Auto (30000 Hz)

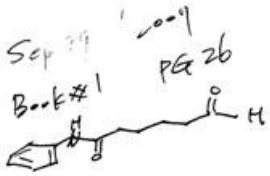

B.2.4 HRMS

Elemental Composition Report Aug 16 /07 **Page 1**

Book #1 P.g 12

Single Mass Analysis
Tolerance = 5.0 mDa / DBE: min = -1.5, max = 50.0
Isotope cluster parameters: Separation = 1.0 Abundance = 1.0%

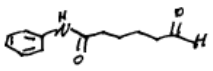

Monoisotopic Mass, Odd and Even Electron Ions
190 formula(e) evaluated with 4 results within limits (all results (up to 1000) for each mass)

Anton Blellauskas 081707 PG12 17-Aug-2007 13:43:43
SPEI 70eV GC-TOF TOF MS EI+
L070817_866 89 (1.908) Cm ((84+86:90)-13:29x2.000) 560

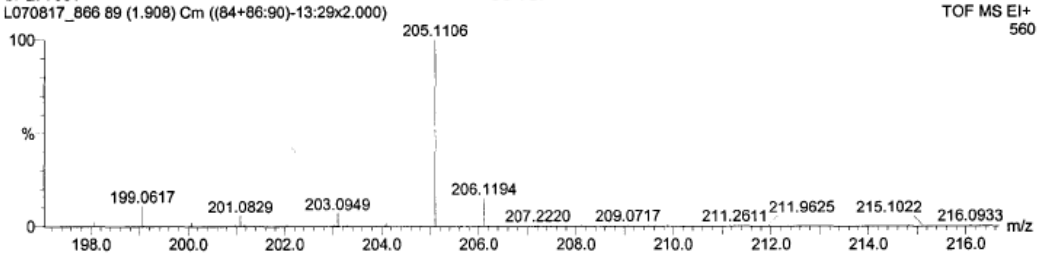

Minimum:				-1.5		
Maximum:		5.0	10.0	50.0		
Mass	Calc. Mass	mDa	PPM	DBE	Score	Formula
205.1106	205.1103	0.3	1.6	6.0	1	C12 H15 N O2
	205.1089	1.7	8.2	6.5	2	C10 H13 N4 O
	205.1076	3.0	14.7	1.5	3	C9 H17 O5
	205.1063	4.4	21.2	2.0	4	C7 H15 N3 O4

B.3 8-Oxo-8-(phenylamino)-oct-2-enoate (**5**)

B.3.1 ^{1}H NMR (E)

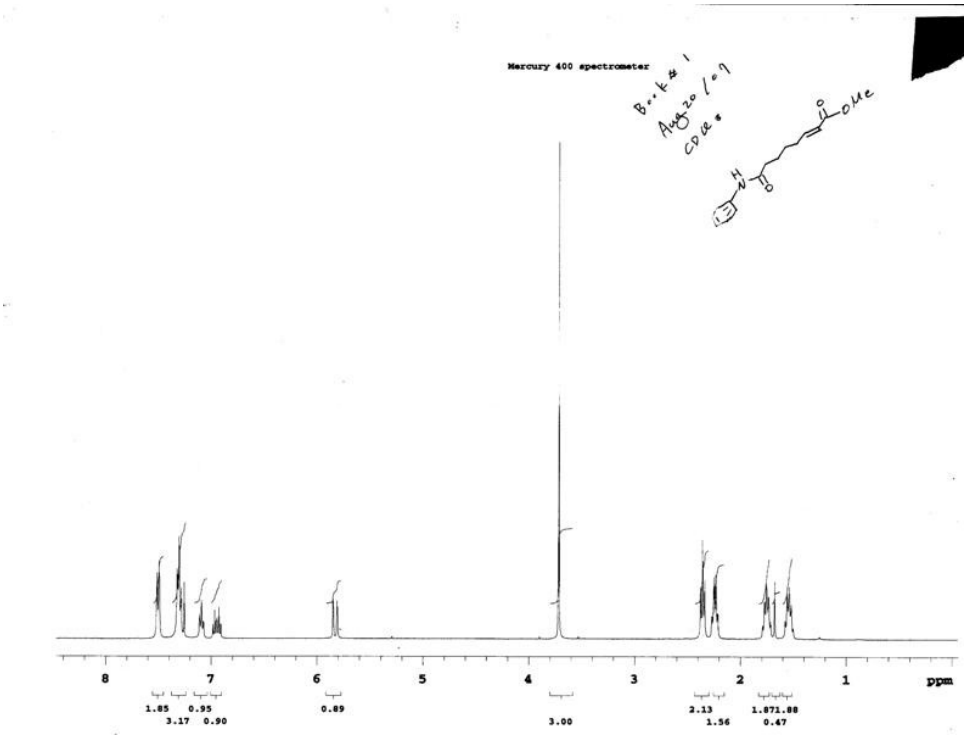

B.3.2 ^{1}H NMR (**Z**)

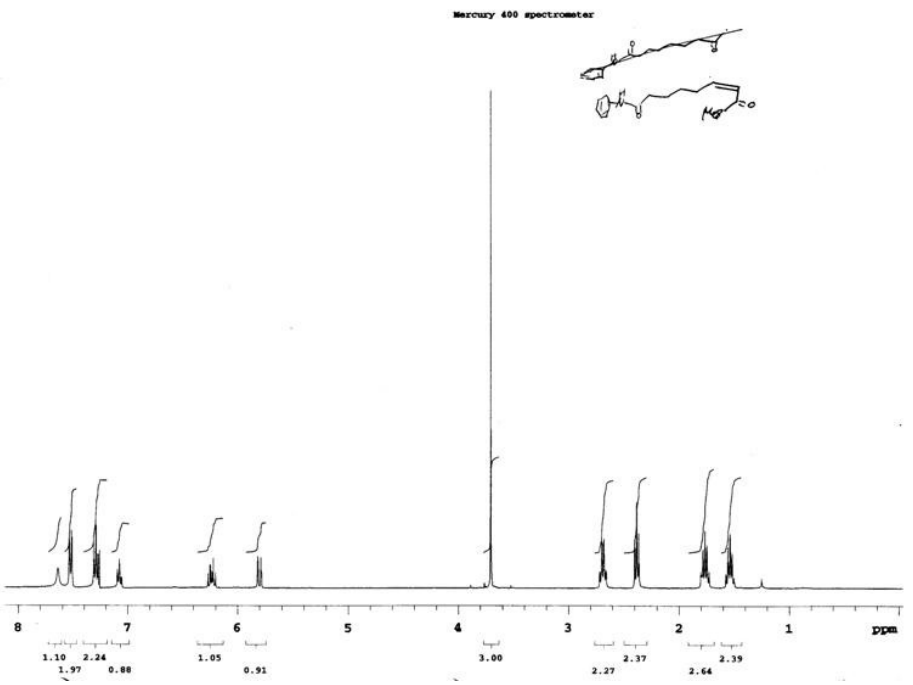

B.3.3 ^{13}C NMR

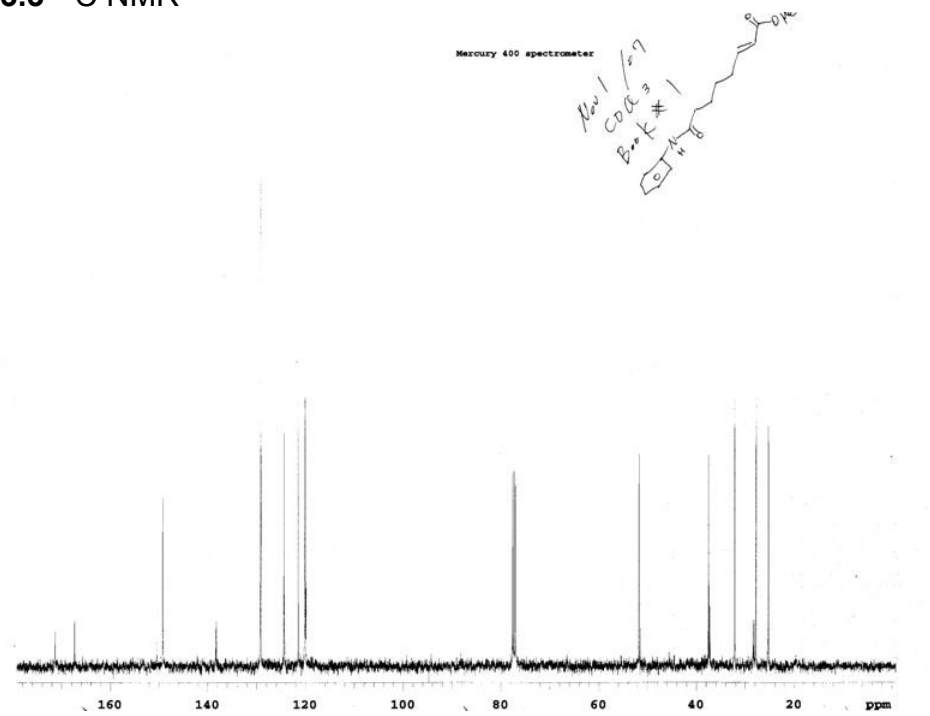

B.3.4 IR

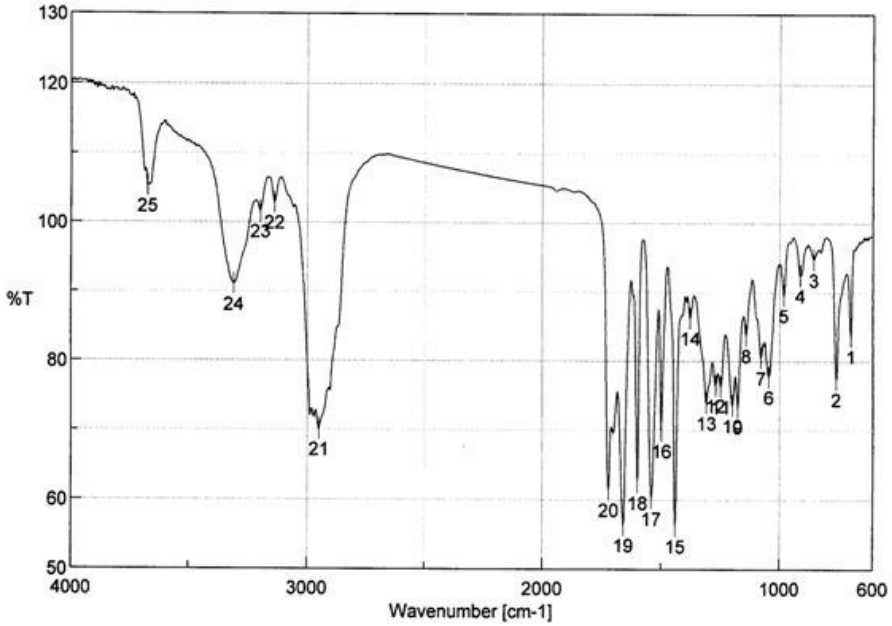

Result of Peak Picking

No.	Position	Intensity	No.	Position	Intensity
1	693.284	83.6407	2	755.959	77.3382
3	851.418	94.7337	4	910.236	92.4506
5	980.625	89.5229	6	1045.23	77.7072
7	1078.01	80.4314	8	1141.65	83.7083
9	1176.36	73.341	10	1199.51	73.5611
11	1249.65	76.2745	12	1270.86	76.4486
13	1310.39	73.9157	14	1377.89	86.1727
15	1440.56	56.2537	16	1498.42	69.8914
17	1540.85	60.2037	18	1599.66	62.4347
19	1658.48	56.3849	20	1721.16	61.3994
21	2949.59	70.0954	22	3136.65	102.866
23	3197.4	101.578	24	3308.29	91.0283
25	3673.73	105.197			

[Comment]	
Sample Name	
Comment	
User	
Division	
Company	Wayne State
[Measurement Information]	
Model Name	FT/IR-4100typeA
Serial Number	B071461016
Light Source	Standard
Detector	TGS
Accumulation	Auto (71)
Resolution	4 cm-1
Zero Filling	On
Apodization	Cosine
Gain	Auto (8)
Aperture	Auto (7.1 mm)
Scanning Speed	Auto (2 mm/sec)
Filter	Auto (30000 Hz)

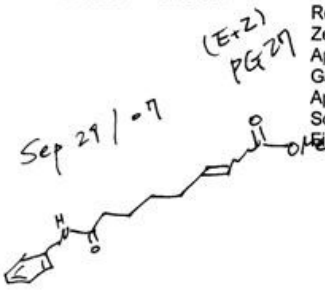

B.3.5 HRMS

Elemental Composition Report **Page 1**

Single Mass Analysis (displaying only valid results)
Tolerance = 4.0 mDa / DBE: min = -1.5, max = 50.0
Isotope cluster parameters: Separation = 1.0 Abundance = 1.0%

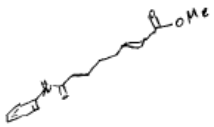

Monoisotopic Mass, Odd and Even Electron Ions
77 formula(e) evaluated with 3 results within limits (all results (up to 1000) for each mass)

Sun Ea Choi 092907 PG 27
SPEI 70eV
L071005_905 49 (0.801) Cm (30:50-153:182x2.000)
GC-TOF
05-Oct-2007 10:56:53
TOF MS EI+
2.79e5

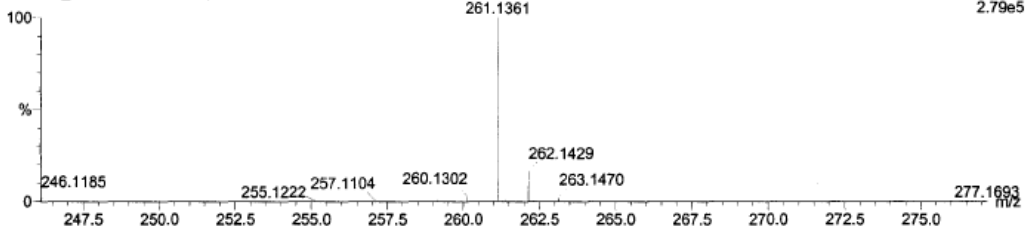

Minimum:				-1.5		
Maximum:		4.0	5.0	50.0		
Mass	Calc. Mass	mDa	PPM	DBE	Score	Formula
261.1361	261.1365	-0.4	-1.5	7.0	2	**C15 H19 N O3**
	261.1352	1.0	3.7	7.5	1	C13 H17 N4 O2
	261.1392	-3.1	-11.7	11.5	3	C18 H17 N2

B.4 8-Oxo-8-(phenylamino)-3-*n*-butyloctanoate (**6a**)

B.4.1 ^{1}H NMR

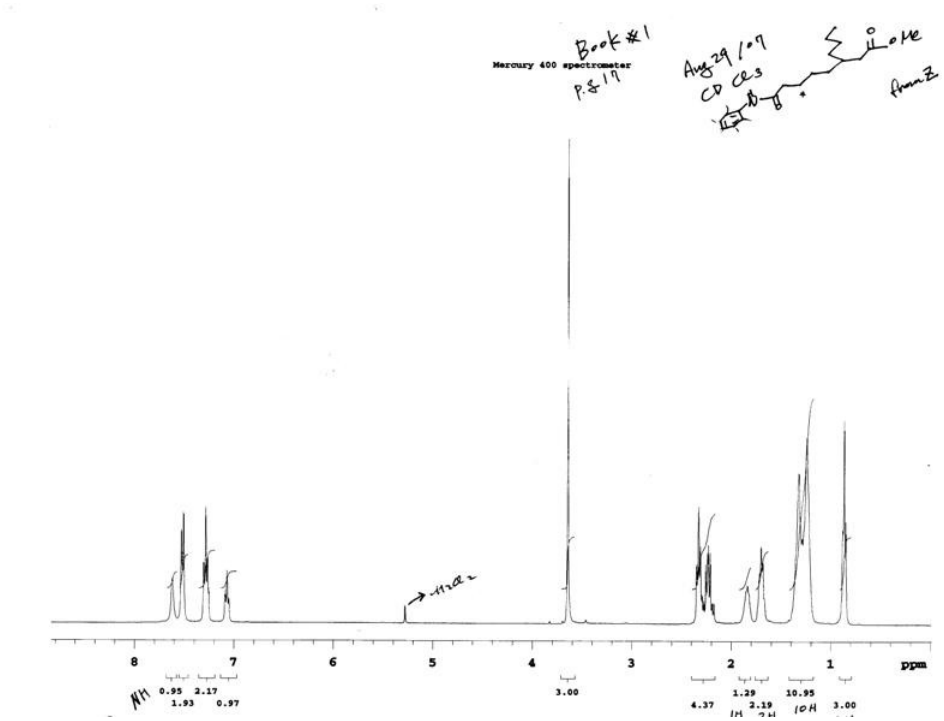

B.4.2 ^{13}C NMR

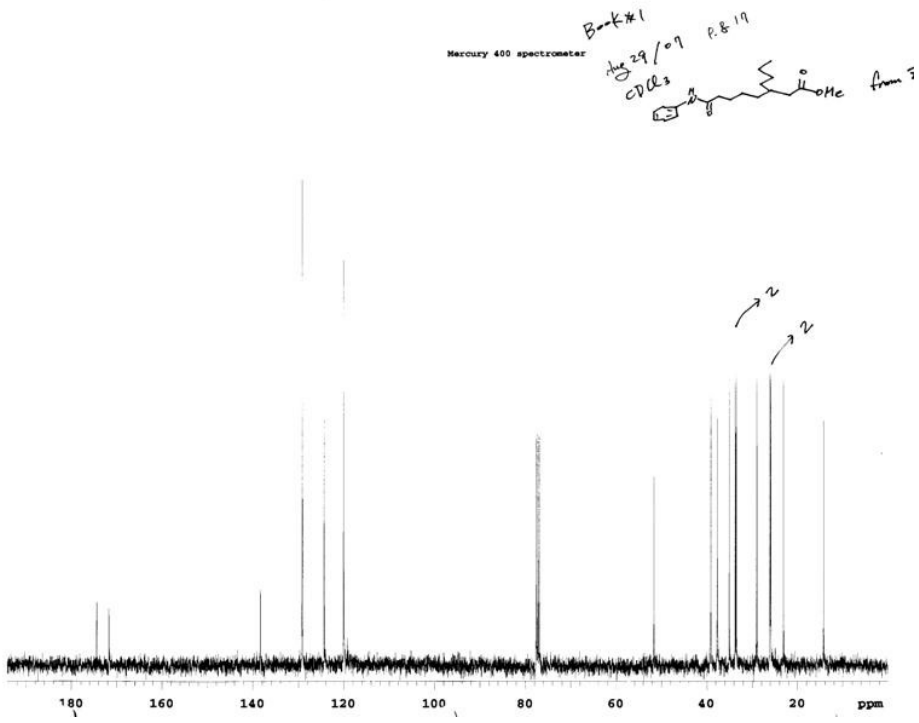

B.4.3 IR

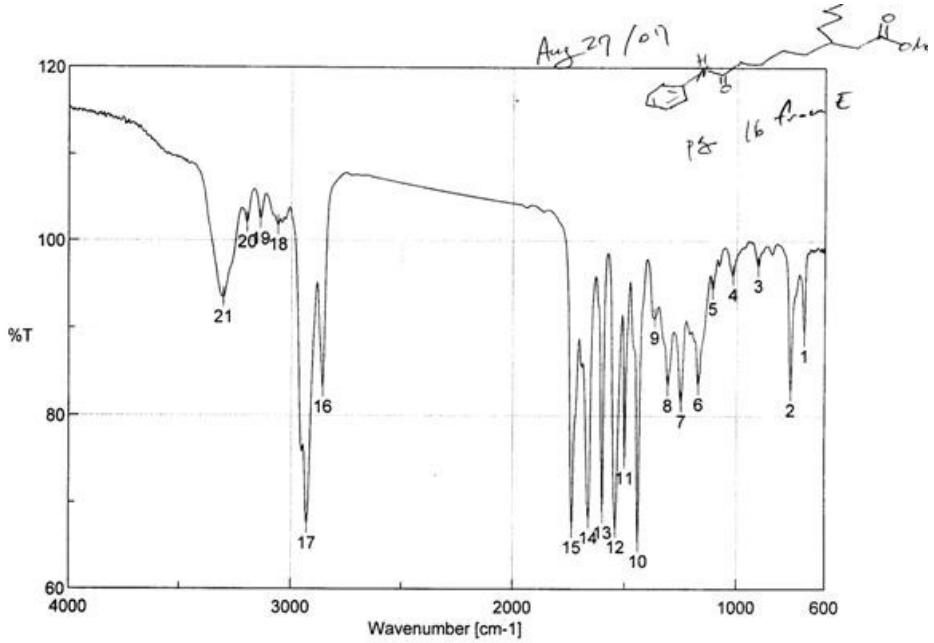

Result of Peak Picking

No.	Position	Intensity	No.	Position	Intensity
1	693.284	89.0843	2	754.995	82.8636
3	902.523	97.0722	4	1017.27	96.0388
5	1106.94	94.4572	6	1171.54	83.5348
7	1250.61	81.5591	8	1309.43	83.3787
9	1367.28	91.1232	10	1440.56	65.4473
11	1499.38	75.0844	12	1541.81	67.0899
13	1599.66	68.805	14	1662.34	68.1755
15	1736.58	67.0555	16	2857.99	83.1721
17	2928.38	67.5274	18	3058.55	101.764
19	3136.65	102.456	20	3197.4	102.06
21	3302.5	93.4479			

[Comment]

Sample Name	
Comment	
User	
Division	
Company	Wayne State

[Measurement Information]

Model Name	FT/IR-4100typeA
Serial Number	B071461016
Light Source	Standard
Detector	TGS
Accumulation	Auto (64)
Resolution	4 cm-1
Zero Filling	On
Apodization	Cosine
Gain	Auto (4)
Aperture	Auto (7.1 mm)
Scanning Speed	Auto (2 mm/sec)
Filter	Auto (30000 Hz)

B.4.4 HRMS

Elemental Composition Report **Page 1**

Single Mass Analysis
Tolerance = 5.0 mDa / DBE: min = -1.5, max = 50.0
Isotope cluster parameters: Separation = 1.0 Abundance = 1.0%

Monoisotopic Mass, Odd and Even Electron Ions
228 formula(e) evaluated with 5 results within limits (all results (up to 1000) for each mass)

Sun Ea Choi 082707 PG 16 28-Aug-2007 11:42:48
SPEI 70eV GC-TOF TOF MS EI+
L0708223_877 90 (1.944) Cm ((71+76+80+88+90+100)-16:29x2.000) 399

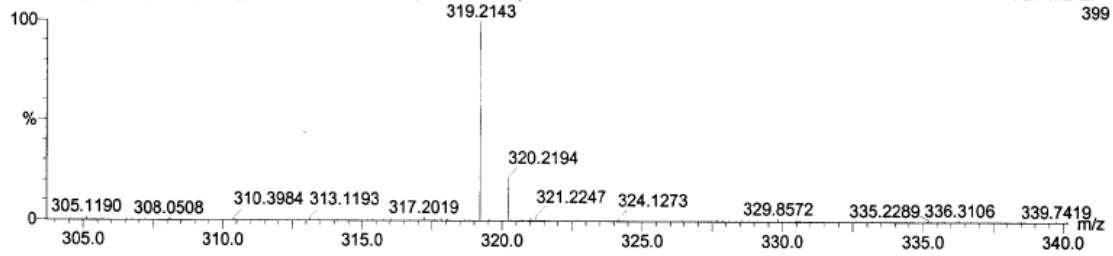

Minimum:				-1.5		
Maximum:		5.0	10.0	50.0		
Mass	Calc. Mass	mDa	PPM	DBE	Score	Formula
319.2143	319.2147	-0.5	-1.5	6.0	1	C19 H29 N O3
	319.2134	0.9	2.7	6.5	2	C17 H27 N4 O2
	319.2121	2.2	6.9	1.5	3	C16 H31 O6
	319.2174	-3.2	-9.9	10.5	4	C22 H27 N2
	319.2107	3.5	11.1	2.0	5	C14 H29 N3 O5

B.5 8-Oxo-8-(phenylamino)-3-phenyloctanoate (**6b**)
B.5.1 ^{1}H NMR

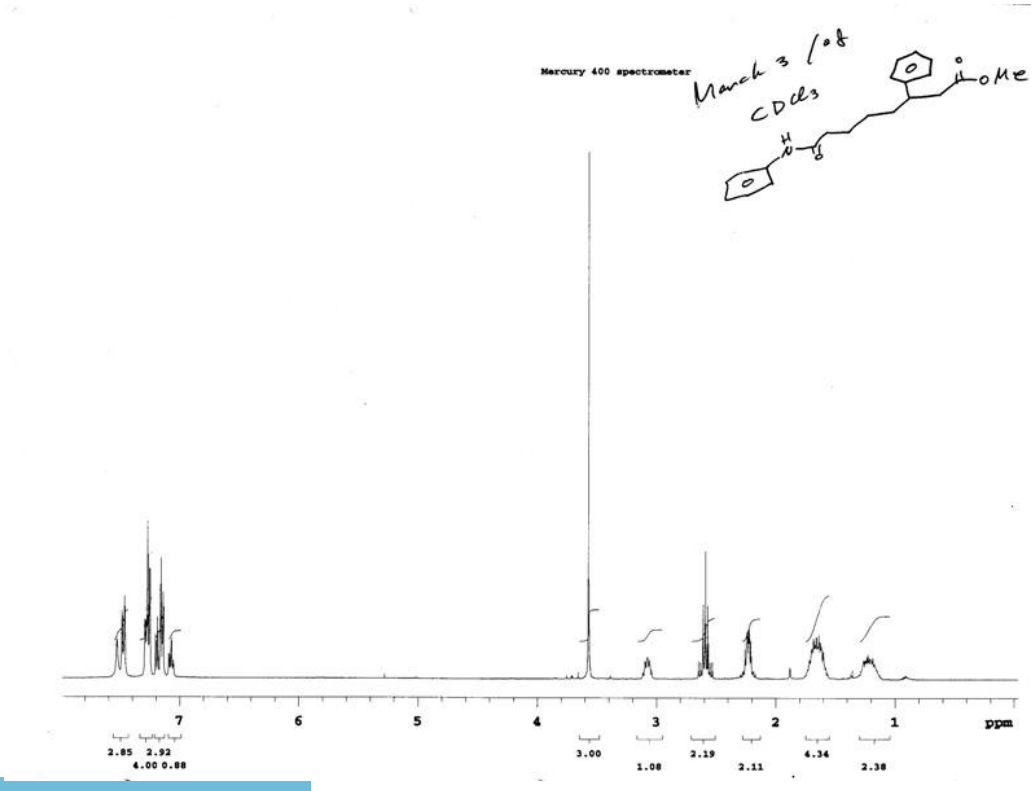

B.5.2 ^{13}C NMR

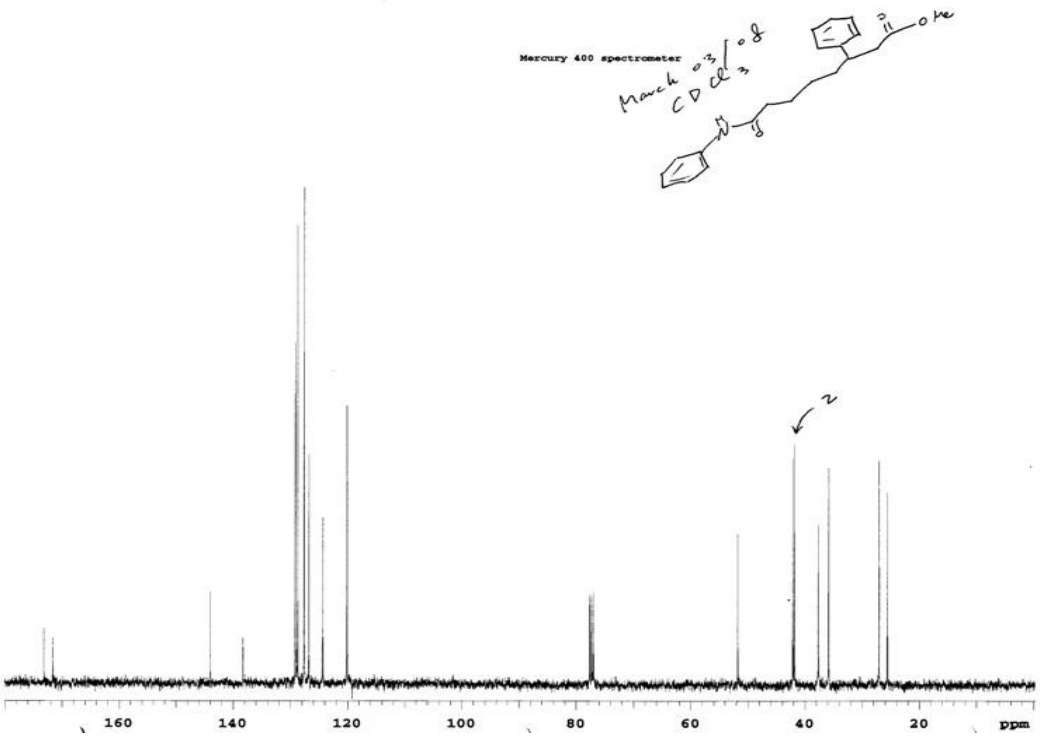

B.5.3 IR

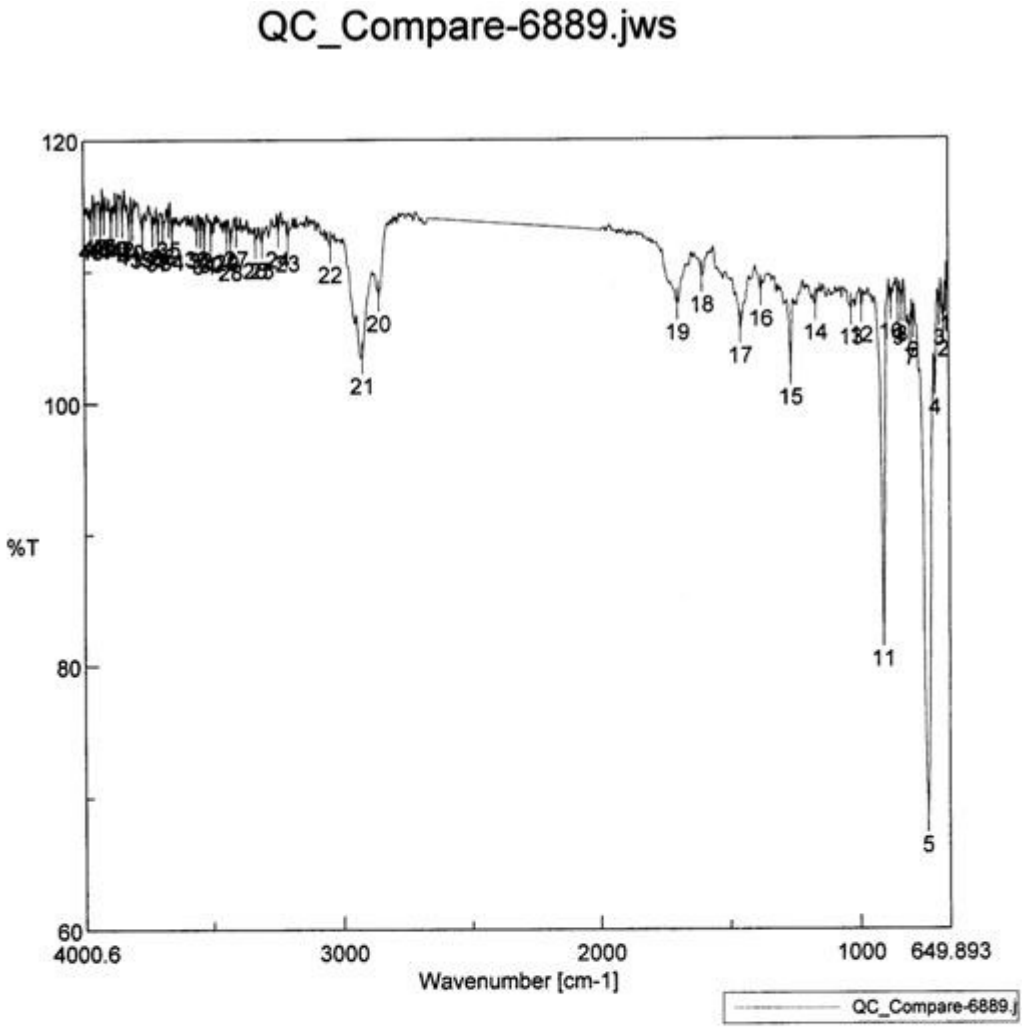

[Comment]
Sample Name
Comment
User
Division
Company wsu

[Data Information]
Creation Date 11/20/2009 4:23 PM
Data array type Linear data array
Horizontal Wavenumber [cm-1]
Vertical %T
Start 649.893 cm-1
End 4000.6 cm-1
Data pitch 0.964233 cm-1
Data points 3476

Result of Peak Picking

No.	Position	Intensity	No.	Position	Intensity	No.	Position	Intensity
1	660.5	107.96	2	668.214	106.047	3	684.606	106.906
4	703.89	101.656	5	734.746	68.4042	6	787.779	105.976
7	800.314	105.45	8	831.169	107.216	9	846.597	106.95
10	876.488	107.402	11	910.236	82.531	12	990.268	107.149
13	1030.77	107.015	14	1168.65	107.382	15	1265.07	102.444
16	1378.85	108.438	17	1456.96	105.638	18	1603.52	109.511
19	1698.02	107.413	20	2857.02	108.132	21	2923.56	103.351
22	3045.05	111.847	23	3209.93	112.69	24	3246.57	112.991
25	3310.21	112.174	26	3335.28	112.174	27	3408.57	113.013
28	3430.74	112.024	29	3446.17	112.78	30	3505.95	112.662
31	3531.99	112.548	32	3546.45	112.942	33	3561.88	113.007
34	3657.34	112.806	35	3670.84	113.75	36	3692.05	113.225
37	3711.33	112.763	38	3733.51	113.051	39	3772.08	113.044
40	3810.65	113.565	41	3823.19	113.235	42	3850.18	113.799
43	3870.43	113.848	44	3893.57	113.703	45	3921.54	114.015
46	3935.04	113.818	47	3956.25	113.976	48	3970.71	113.639

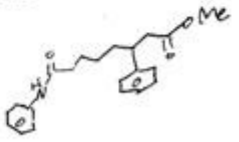

B.5.4 HRMS

Elemental Composition Report **Page 1**

Single Mass Analysis
Tolerance = 5.0 PPM / DBE: min = -1.5, max = 100.0
Element prediction: Off
Number of isotope peaks used for i-FIT = 3

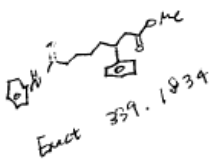

Monoisotopic Mass, Even Electron Ions
942 formula(e) evaluated with 3 results within limits (all results (up to 1000) for each mass)
Elements Used:
C: 0-200 H: 0-250 N: 0-7 O: 0-23 Na: 0-1

SUN, CHOI C3-Phenylester-PG 83
2008-07b.pro
2009_1116_0691 11 (0.229) Cm (11:18-(1:6+36:45)x2.000)

LCT Premier 16-Nov-2009 15:09:45
1: TOF MS ES+
2.95e+003

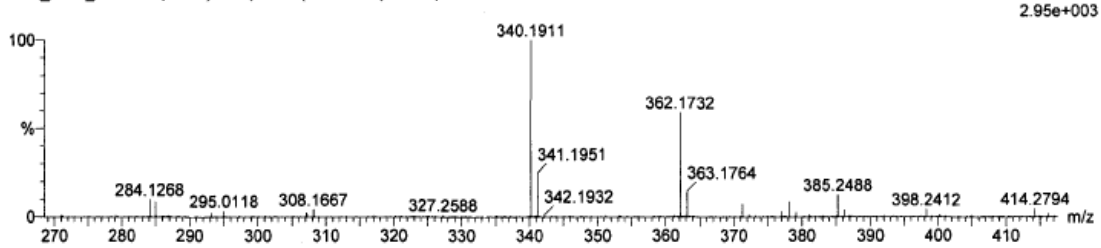

Minimum:				-1.5			
Maximum:		5.0	5.0	100.0			
Mass	Calc. Mass	mDa	PPM	DBE	i-FIT	i-FIT (Norm)	Formula
362.1732	362.1729	0.3	0.8	13.5	60.3	0.6	C19 H20 N7 O
	362.1732	0.0	0.0	9.5	60.6	0.9	C21 H25 N O3 Na
	362.1716	1.6	4.4	8.5	62.6	3.0	C18 H24 N3 O5

B.6 8-Oxo-8-(phenylamino)-3-ethyloctanoate (**6c**)
B.6.1 ^{1}H NMR

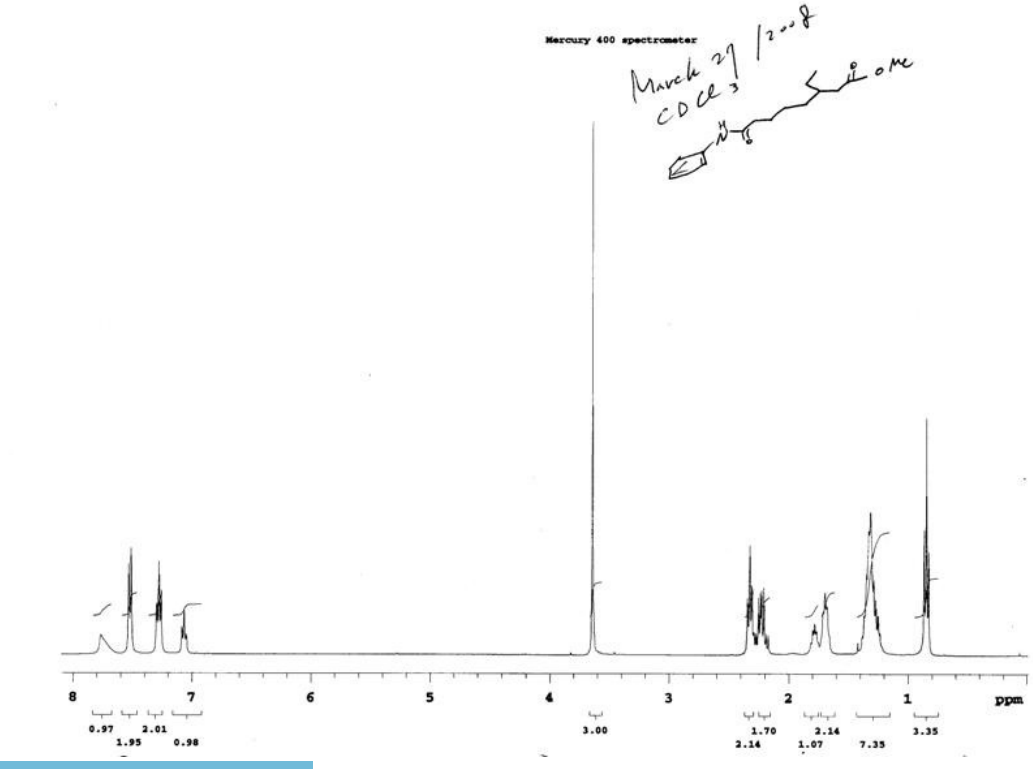

B.6.2 ^{13}C NMR

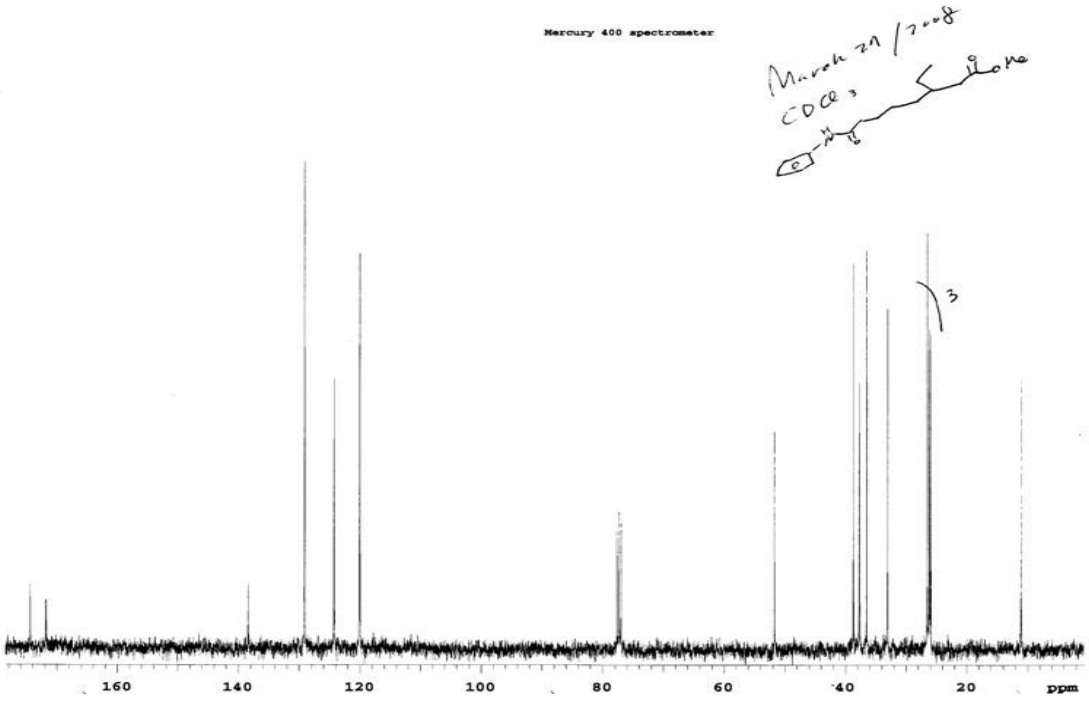

B.6.3 IR

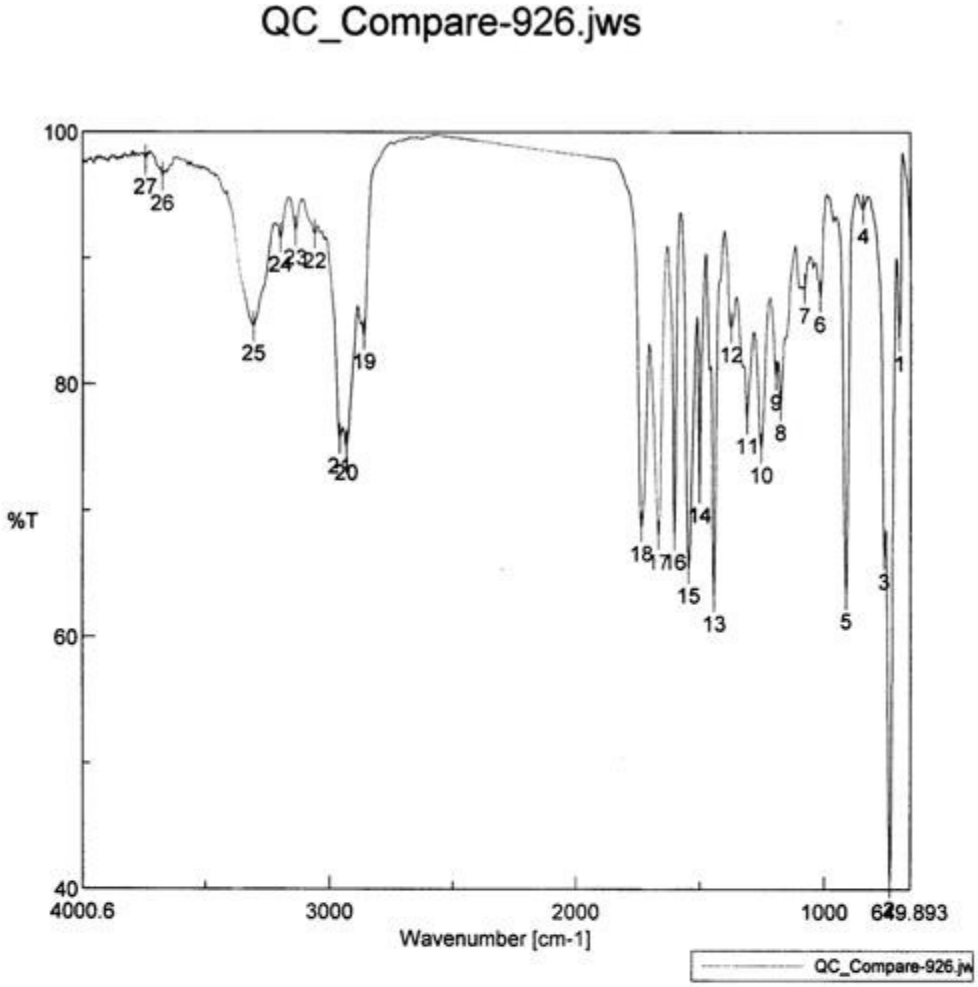

[Comment]	
Sample Name	
Comment	
User	
Division	
Company	wsu

[Data Information]	
Creation Date	3/7/2008 3:01 PM
Data array type	Linear data array
Horizontal	Wavenumber [cm-1]
Vertical	%T
Start	649.893 cm-1
End	4000.6 cm-1
Data pitch	0.964233 cm-1
Data points	3476

Result of Peak Picking

No.	Position	Intensity	No.	Position	Intensity	No.	Position	Intensity
1	696.177	83.7483	2	732.817	40.5363	3	755.959	66.4865
4	842.74	93.8612	5	911.201	63.3521	6	1017.27	86.8497
7	1080.91	87.5446	8	1175.4	78.2486	9	1193.72	80.6471
10	1252.54	74.9075	11	1309.43	77.229	12	1375	84.4272
13	1441.53	63.1383	14	1499.38	71.7377	15	1542.77	65.362
16	1600.63	68.0072	17	1665.23	68.0121	18	1733.69	68.6931
19	2861.84	83.8827	20	2934.16	75.0602	21	2960.2	75.6272
22	3061.44	91.8606	23	3138.58	92.1175	24	3198.36	91.5703
25	3308.29	84.5458	26	3674.69	96.4706	27	3742.19	97.7793

March 07/2008

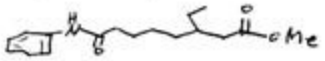

B.6.4 HRMS

Elemental Composition Report **Page 1**

Single Mass Analysis
Tolerance = 5.0 mDa / DBE: min = -1.5, max = 50.0
Isotope cluster parameters: Separation = 1.0 Abundance = 1.0%

Monoisotopic Mass, Odd and Even Electron Ions
238 formula(e) evaluated with 6 results within limits (all results (up to 1000) for each mass)

Sun Choi Feb 22 08-ethyl-C3-ester 03-Mar-2008 11:48:39
GCEI 70eV GC-TOF
L080303_1015 132 (2.184) Cm ((15:18+25:27+52:54+125:132)-313:353x2.000) TOF MS EI+ 8.84e4

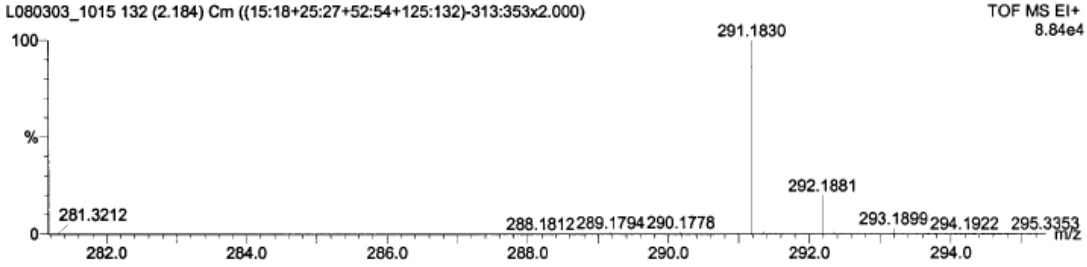

Minimum:				-1.5		
Maximum:		5.0	10.0	50.0		
Mass	Calc. Mass	mDa	PPM	DBE	Score	Formula
291.1830	291.1834	-0.5	-1.7	6.0	1	C17 H25 N O3
	291.1821	0.9	2.9	6.5	2	C15 H23 N4 O2
	291.1808	2.2	7.5	1.5	4	C14 H27 O6
	291.1861	-3.2	-10.9	10.5	3	C20 H23 N2
	291.1794	3.5	12.1	2.0	5	C12 H25 N3 O5
	291.1781	4.9	16.7	2.5	6	C10 H23 N6 O4

B.7 8-Oxo-8-(phenylamino)-3-vinyloctanoate (**6d**)
B.7.1 ^{1}H NMR

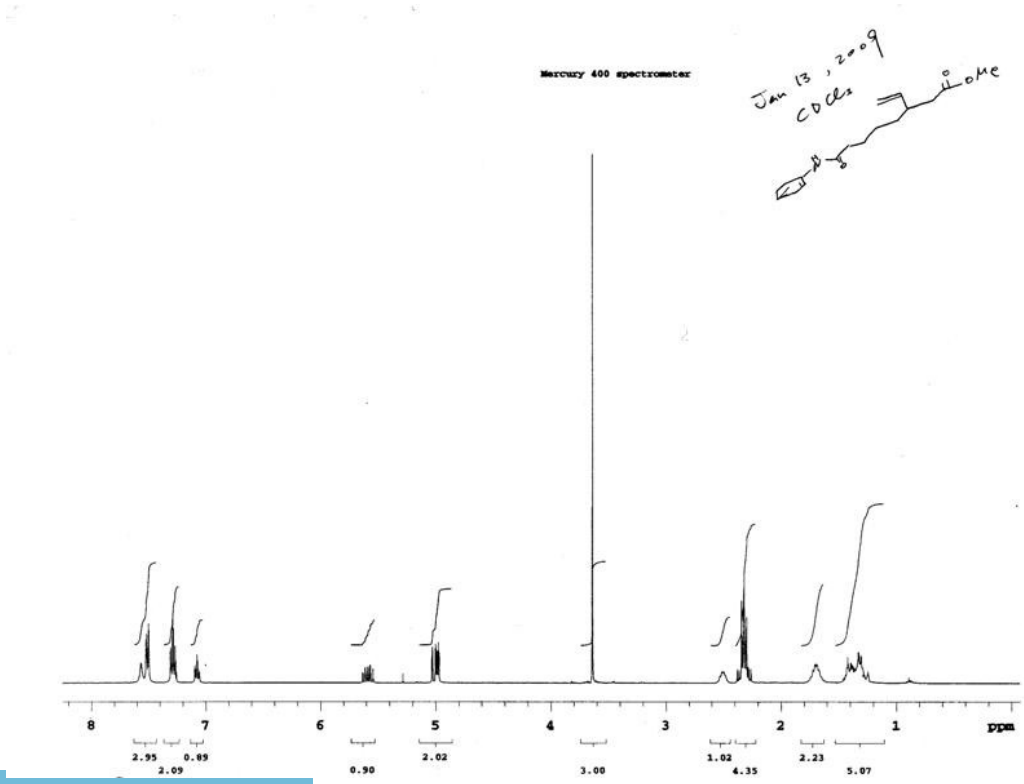

B.7.2 ^{13}C NMR

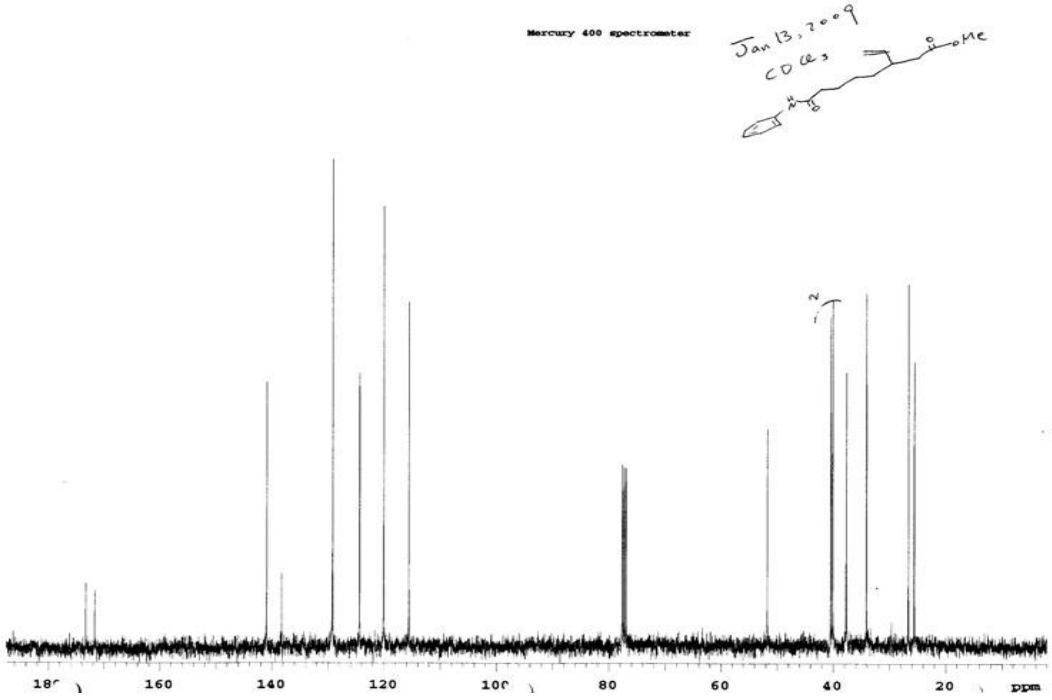

B.7.3 IR

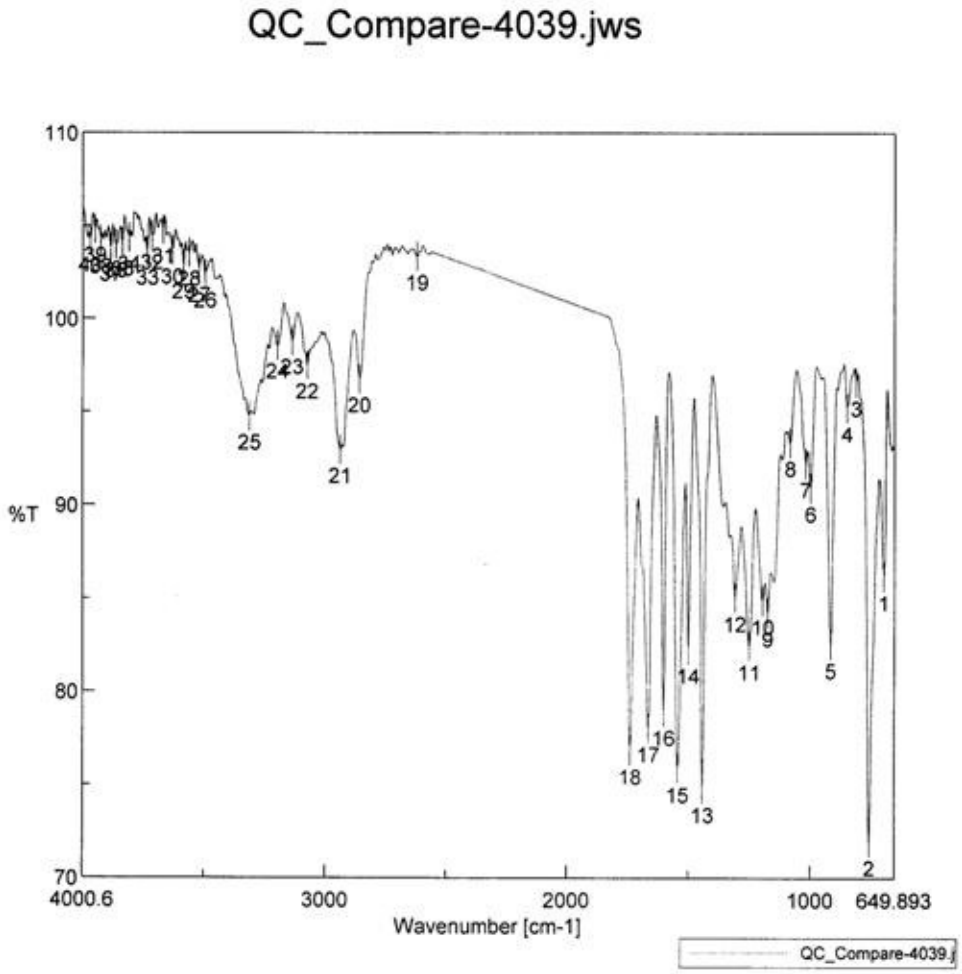

[Comment]
Sample Name
Comment
User
Division
Company wsu

[Data Information]

Creation Date	1/6/2009 11:22 AM
Data array type	Linear data array
Horizontal	Wavenumber [cm-1]
Vertical	%T
Start	649.893 cm-1
End	4000.6 cm-1
Data pitch	0.964233 cm-1
Data points	3476

Result of Peak Picking

No.	Position	Intensity	No.	Position	Intensity	No.	Position	Intensity
1	693.284	86.1446	2	754.995	71.9561	3	808.028	96.5997
4	846.597	95.2202	5	915.058	82.5058	6	997.982	90.9202
7	1017.27	92.2293	8	1081.87	93.3688	9	1174.44	84.2327
10	1196.61	84.8495	11	1250.61	82.4451	12	1308.46	85.0198
13	1441.53	74.7878	14	1499.38	82.2452	15	1542.77	75.8466
16	1600.63	78.9195	17	1663.3	78.0231	18	1737.55	76.815
19	2620.79	103.329	20	2858.95	96.7437	21	2938.98	92.9393
22	3075.9	97.4824	23	3137.62	98.8101	24	3199.33	98.5508
25	3315.03	94.7254	26	3496.31	102.387	27	3521.38	102.661
28	3562.84	103.538	29	3585.98	102.855	30	3631.3	103.644
31	3669.87	104.752	32	3716.16	104.423	33	3735.44	103.596
34	3809.69	104.328	35	3837.65	104.068	36	3865.61	103.983
37	3884.9	103.791	38	3926.36	104.182	39	3950.46	104.797
40	3970.71	104.282						

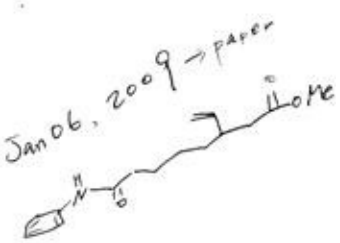

B.7.4 HRMS

Elemental Composition Report **Page 1**

Single Mass Analysis
Tolerance = 5.0 PPM / DBE: min = -1.5, max = 50.0
Element prediction: Off
Number of isotope peaks used for i-FIT = 3

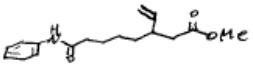

Monoisotopic Mass, Even Electron Ions
266 formula(e) evaluated with 2 results within limits (up to 50 best isotopic matches for each mass)
Elements Used:
C: 0-500 H: 0-1000 N: 0-4 O: 0-6 23Na: 0-1
Pflum- Sun Choi Sep0408-C3-vinylester mw289 LCT0133 1uL meoh
Shay 2008-07b.pro
2008_0909_0133_01 14 (0.300) Cm (11:17-(1:8+22:33)x1.200)

LCT Premier 09-Sep-2008 13:45:10
1: TOF MS ES+
2.65e+004

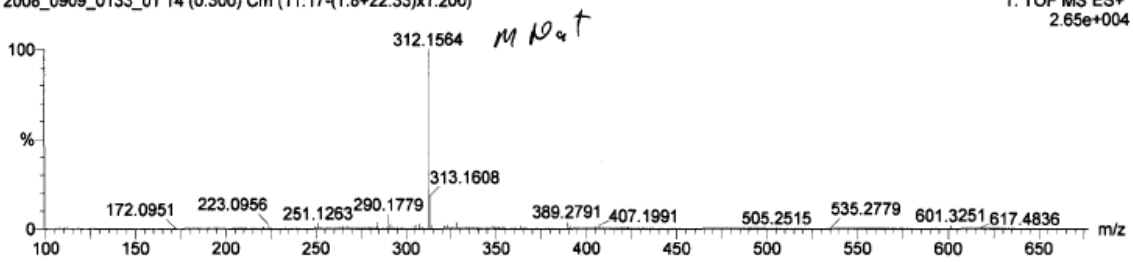

Minimum:				-1.5			
Maximum:		5.0	5.0	50.0			
Mass	Calc. Mass	mDa	PPM	DBE	i-FIT	i-FIT (Norm)	Formula
312.1564	312.1559	0.5	1.6	5.5	51.4	0.5	C14 H22 N3 O5
	312.1576	-1.2	-3.8	6.5	51.9	1.0	C17 H23 N O3 23Na

B.8 8-Oxo-8-(phenylamino)-3-methyloctanoate (**6e**)
B.8.1 ^{1}H NMR

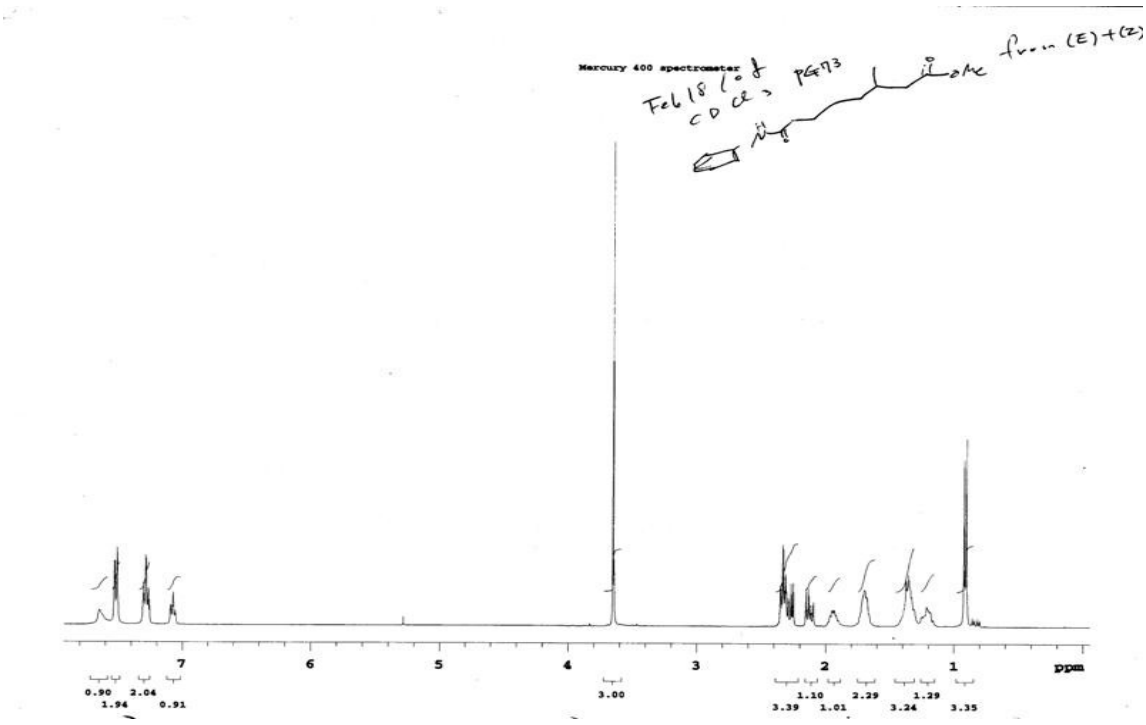

B.8.2 ^{13}C NMR

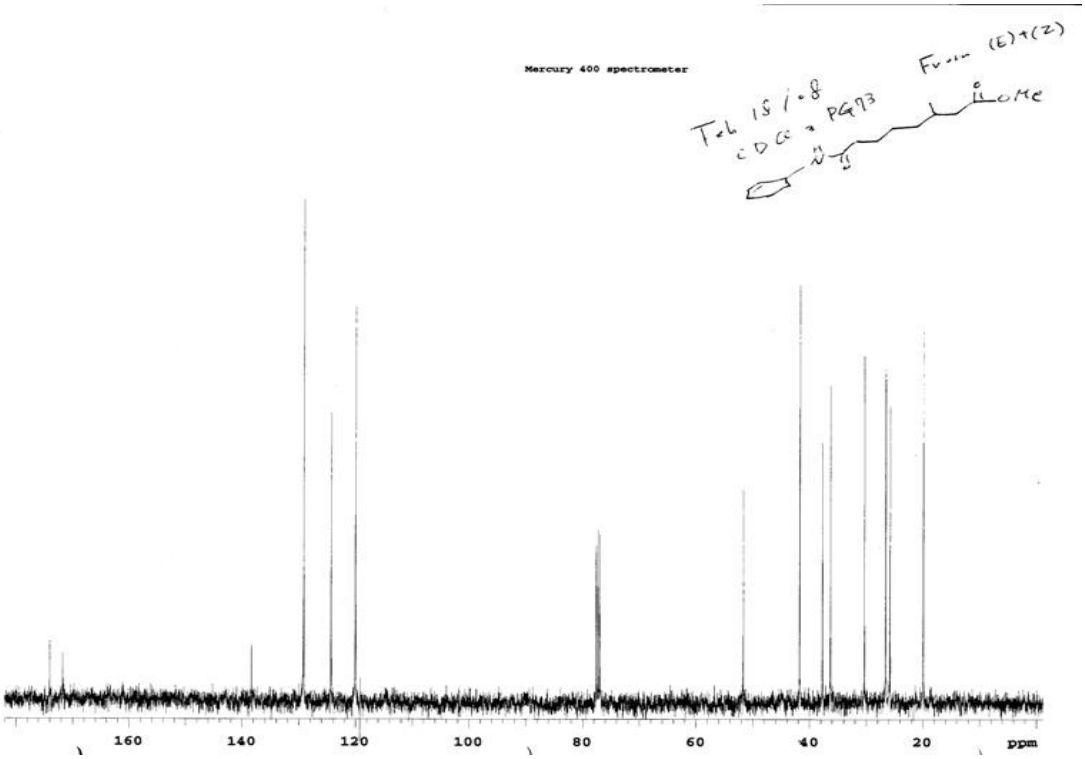

B.8.3 IR

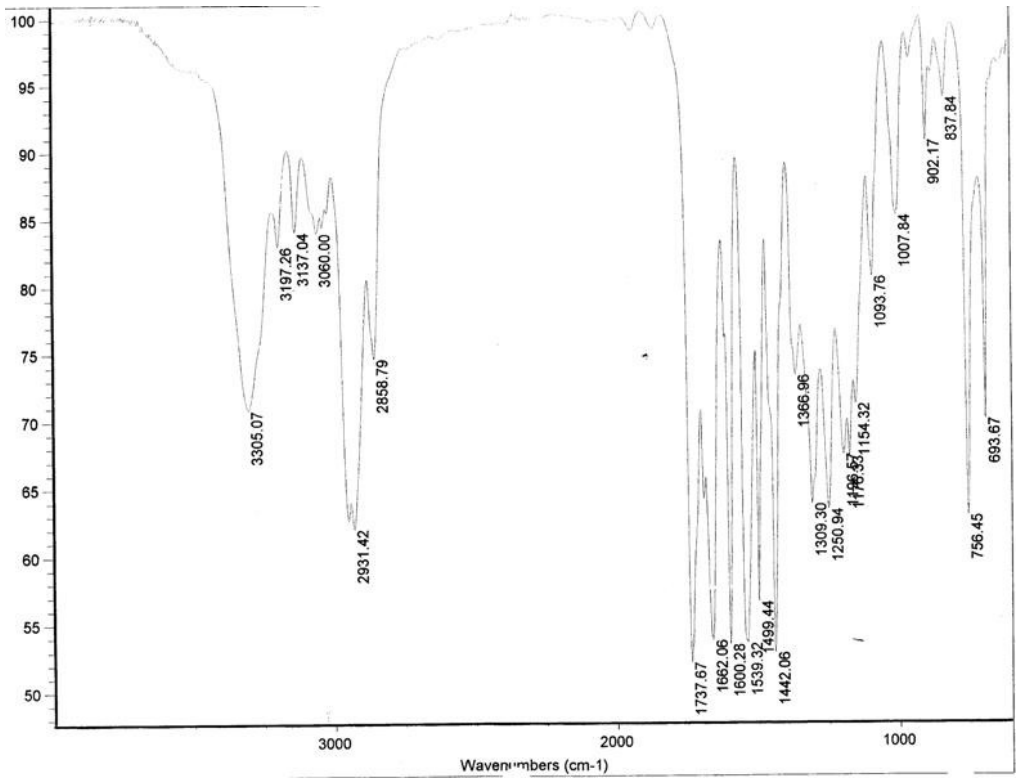

B.8.1 HRMS

Elemental Composition Report **Page 1**

Single Mass Analysis
Tolerance = 5.0 mDa / DBE: min = -1.5, max = 50.0
Isotope cluster parameters: Separation = 1.0 Abundance = 1.0%

Monoisotopic Mass, Odd and Even Electron Ions
225 formula(e) evaluated with 5 results within limits (all results (up to 1000) for each mass)

Sun Choi Feb 18 08-Methyl-C3-ester
GCEI 70eV GC-TOF
L080214_1002 79 (1.317) Cm ((63:64+67+77+79+88+122:123)-258:292x2.000)
19-Feb-2008 13:18:19
TOF MS EI+
1.07e5

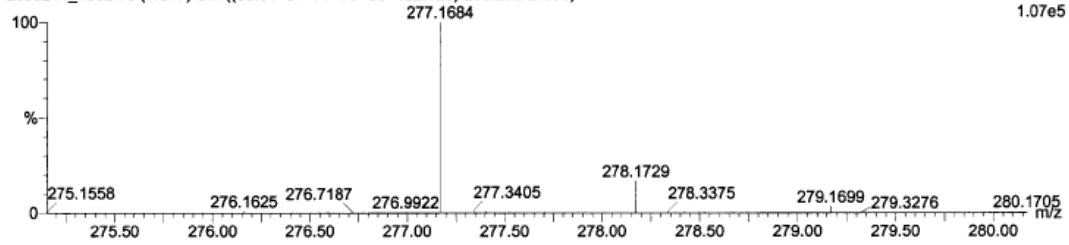

Minimum:				-1.5		
Maximum:		5.0	10.0	50.0		
Mass	Calc. Mass	mDa	PPM	DBE	Score	Formula
277.1684	277.1678	0.6	2.2	6.0	3	C16 H23 N O3
	277.1665	1.9	7.0	6.5	1	C14 H21 N4 O2
	277.1705	-2.1	-7.5	10.5	5	C19 H21 N2
	277.1651	3.3	11.8	1.5	2	C13 H25 O6
	277.1638	4.6	16.7	2.0	4	C11 H23 N3 O5

B.9 3-*n*-Butyl-N^1-hydroxyl-N^8-phenyloctanoic acid (**7**)
B.9.1 ^{1}H NMR

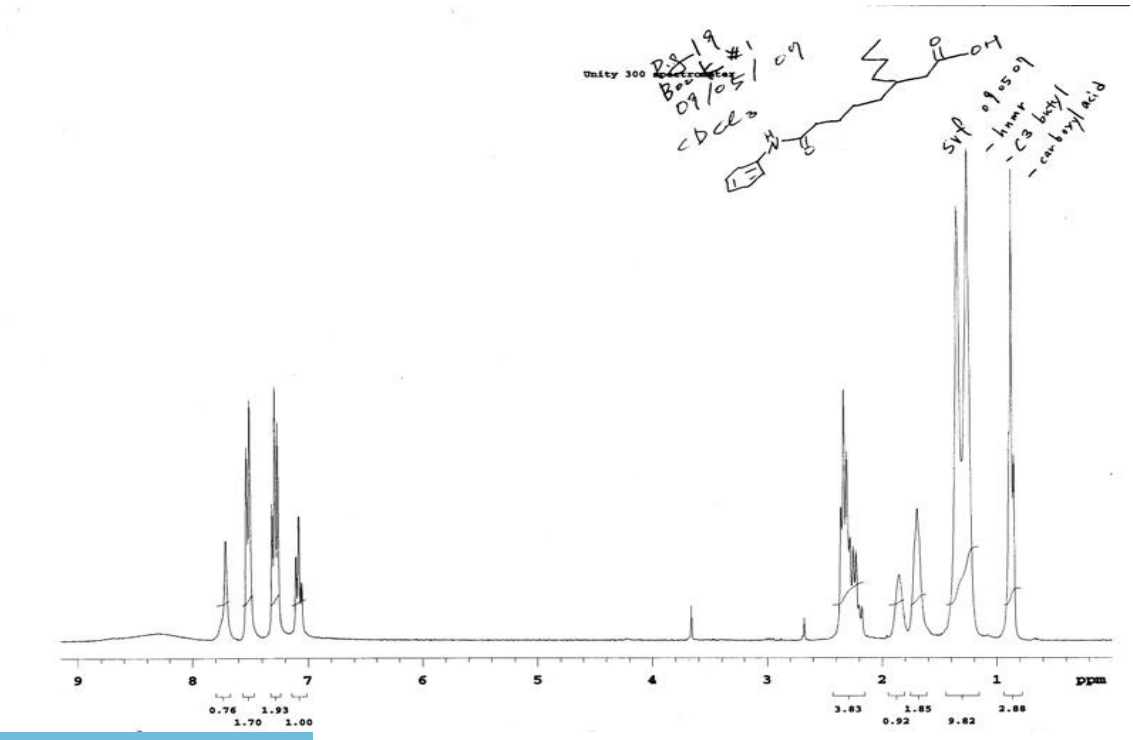

B.9.2 ^{13}C NMR

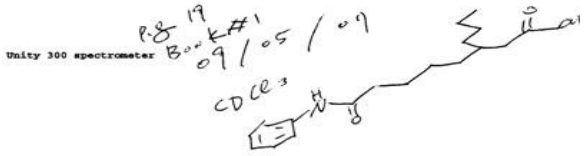

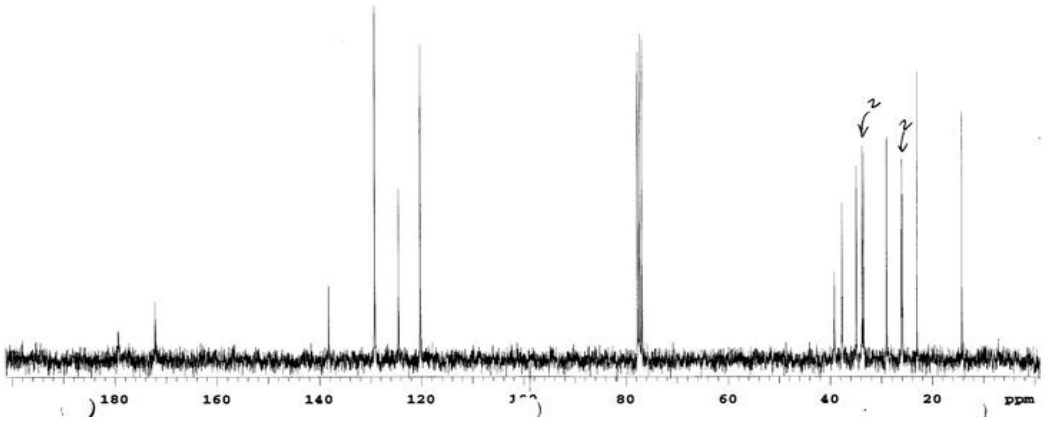

B.9.3 IR

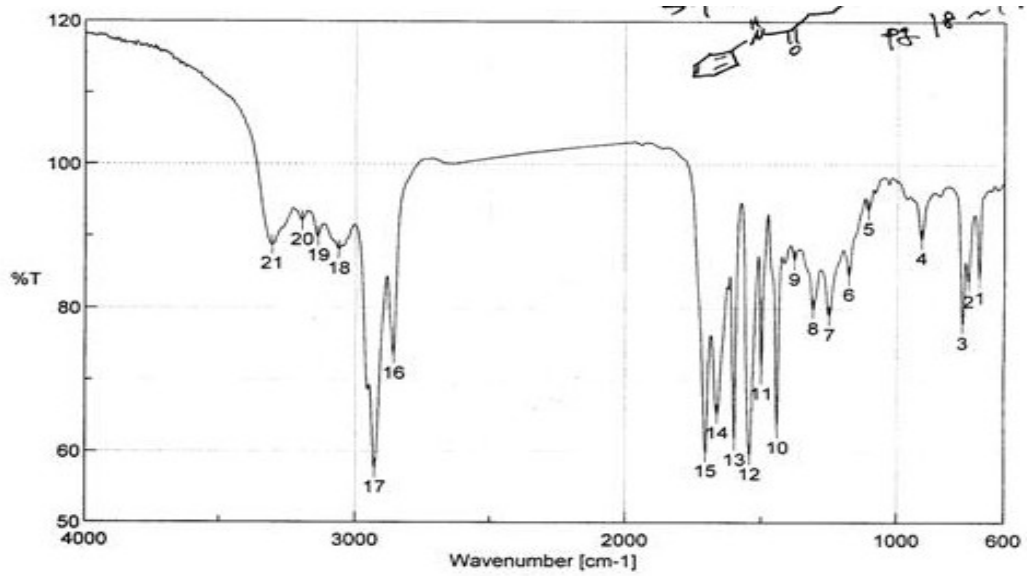

Result of Peak Picking

No.	Position	Intensity	No.	Position	Intensity
1	692.32	84.0953	2	732.817	83.5965
3	754.995	77.7589	4	907.344	89.5454
5	1105.98	93.611	6	1176.36	84.4641
7	1250.61	78.9063	8	1309.43	79.8208
9	1377.89	86.6497	10	1442.49	63.1385
11	1499.38	70.6946	12	1542.77	59.4345
13	1598.7	61.4726	14	1662.34	65.2417
15	1704.76	59.8978	16	2857.99	73.4995
17	2928.38	57.537	18	3060.48	88.0579
19	3137.62	89.8364	20	3195.47	92.0541
21	3306.36	88.7473			

[Comment]
Sample Name
Comment
User
Division
Company Wayne State

[Measurement Information]
Model Name FT/IR-4100typeA
Serial Number B071461016

Light Source Standard
Detector TGS

B.9.4 HRMS

Elemental Composition Report **Page 1**

Single Mass Analysis (displaying only valid results)
Tolerance = 4.0 mDa / DBE: min = -1.5, max = 50.0
Isotope cluster parameters: Separation = 1.0 Abundance = 1.0%

Monoisotopic Mass, Odd and Even Electron Ions
52 formula(e) evaluated with 2 results within limits (all results (up to 1000) for each mass)

Sun Ea Choi 090507-C3 butylcarboxilic acid 05-Oct-2007 11:10:57
SPEI 70eV GC-TOF TOF MS EI+
L071005_906 125 (2.084) Cm (107:126-7:32x2.000) 7.71e4

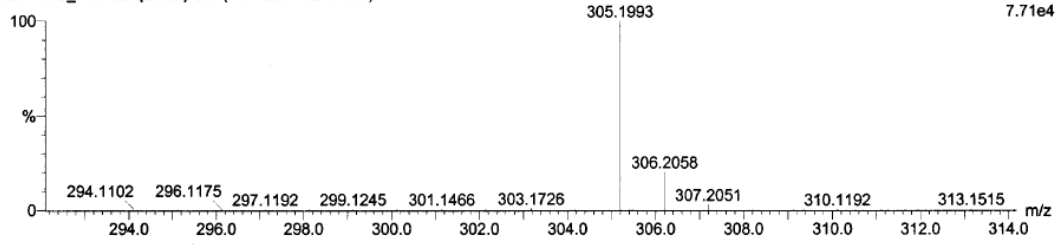

Minimum:				-1.5		
Maximum:		4.0	5.0	50.0		
Mass	Calc. Mass	mDa	PPM	DBE	Score	Formula
305.1993	305.1991	0.2	0.8	6.0	1	**C18 H27 N O3**
	305.1978	1.6	5.2	6.5	2	C16 H25 N4 O2

B.10 3-*n*-Butyl-N^1-benzyloxy-N^8-phenyloctanediamide (**8**)
B.10.1 ^{1}H NMR

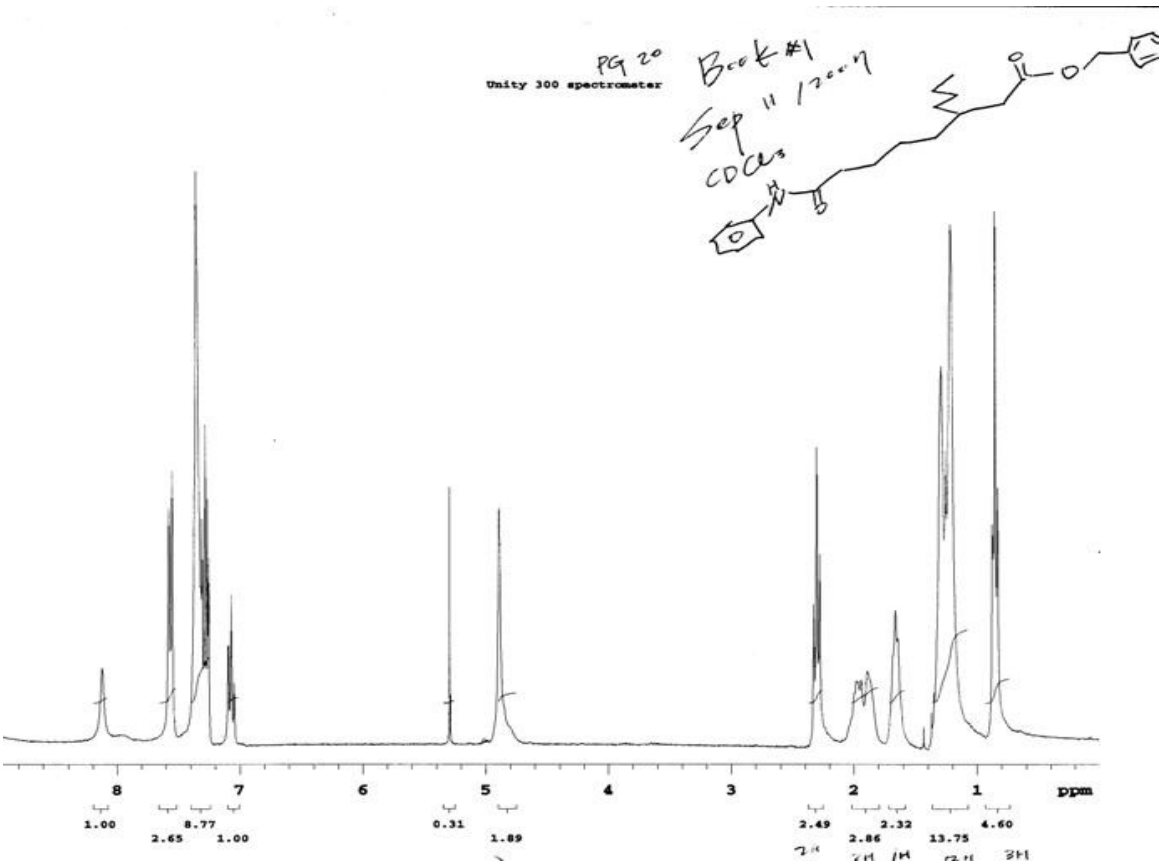

B.10.2 ^{13}C NMR

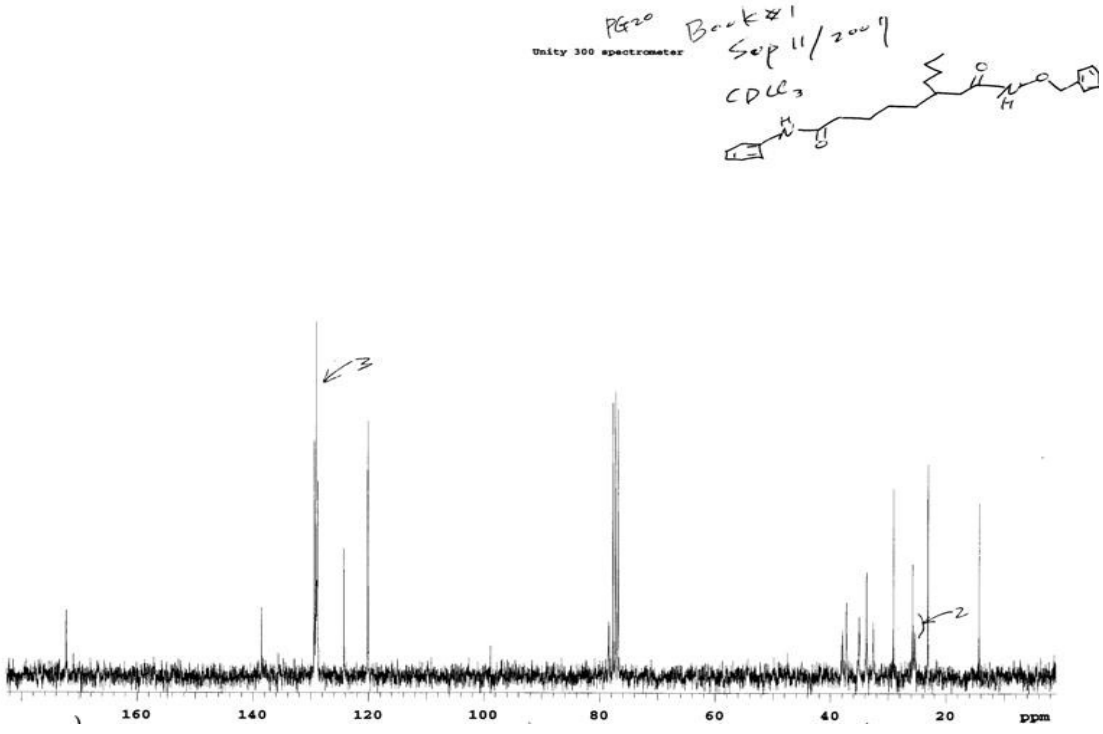

B.10.3 IR

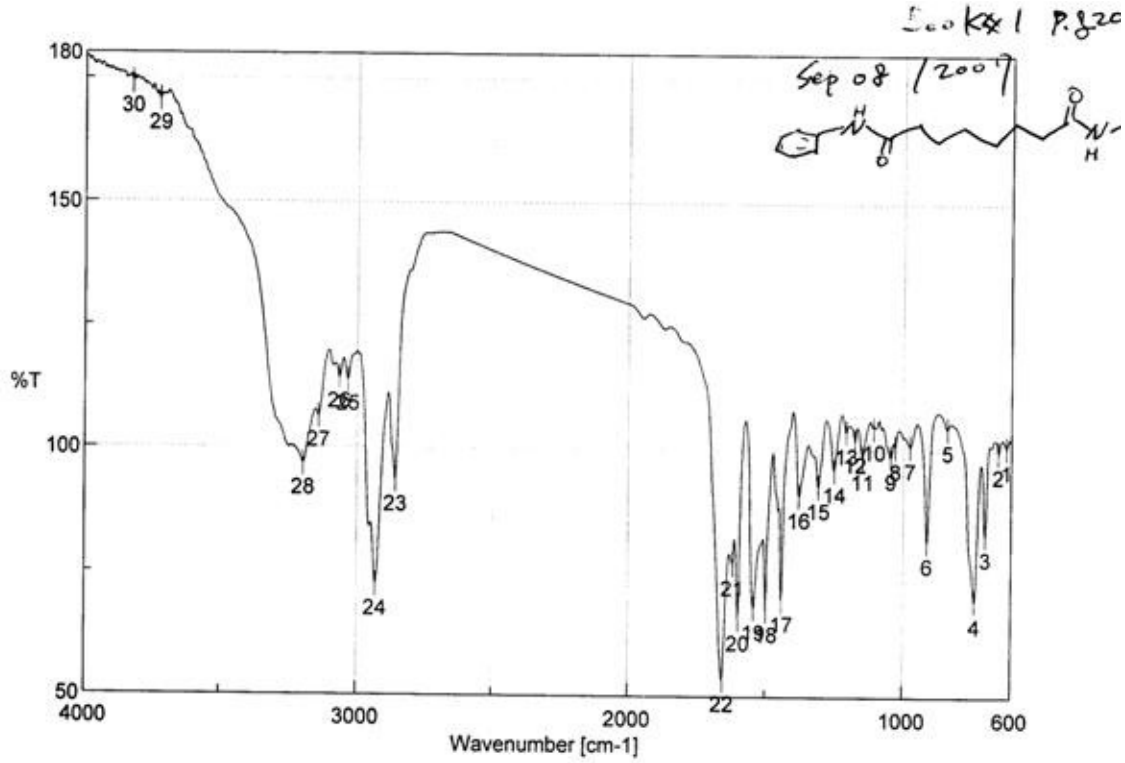

Result of Peak Picking

No.	Position	Intensity	No.	Position	Intensity
1	618.074	100.423	2	647.965	99.5156
3	695.212	82.8082	4	733.782	69.2952
5	836.955	104.304	6	911.201	81.4994
7	974.84	100.684	8	1029.8	100.493
9	1046.19	98.4892	10	1107.9	104.443
11	1148.4	98.422	12	1176.36	101.871
13	1209.15	103.565	14	1252.54	95.8236
15	1309.43	92.4519	16	1379.82	90.6013
17	1442.49	69.6131	18	1498.42	67.5212
19	1543.74	67.9726	20	1599.66	65.7706
21	1619.91	76.8858	22	1655.59	53.4272
23	2857.99	93.3939	24	2929.34	72.3348
25	3033.48	113.73	26	3064.33	114.247
27	3139.54	106.298	28	3194.51	96.6941
29	3723.87	170.564	30	3826.08	174.068

[Comment]
Sample Name
Comment
User
Division
Company Wayne State

[Measurement Information]

Model Name	FT/IR-4100typeA
Serial Number	B071861016
Light Source	Standard
Detector	TGS
Accumulation	Auto (80)
Resolution	4 cm-1
Zero Filling	On
Apodization	Cosine
Gain	Auto (8)
Aperture	Auto (7.1 mm)
Scanning Speed	Auto (2 mm/sec)
Filter	Auto (30000 Hz)

B.10.4 HRMS

Elemental Composition Report **Page 1**

Single Mass Analysis
Tolerance = 5.0 mDa / DBE: min = -1.5, max = 50.0
Isotope cluster parameters: Separation = 1.0 Abundance = 1.0%

Monoisotopic Mass, Odd and Even Electron Ions
329 formula(e) evaluated with 7 results within limits (all results (up to 1000) for each mass)

Sun Ea Choi 091007-C3 butyl-benzylhydroxylamine 08-Oct-2007 11:03:42
SPEI 70eV GC-TOF
L071008_915 142 (2.367) Cm ((122:126+133+142+146+202)-15:45x2.000) TOF MS EI+
1.86e3

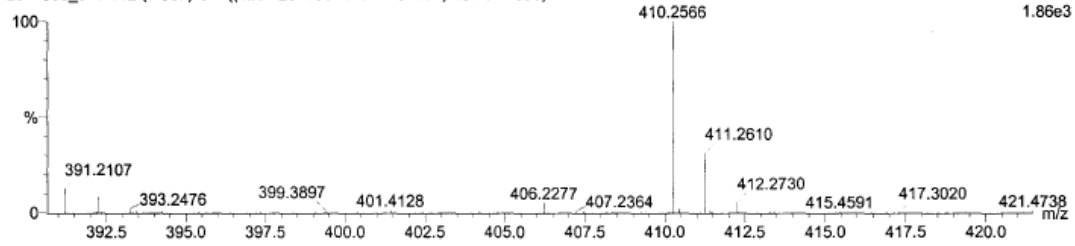

Minimum:				-1.5		
Maximum:		5.0	10.0	50.0		
Mass	Calc. Mass	mDa	PPM	DBE	Score	Formula
410.2566	410.2569	-0.4	-0.9	10.0	3	C25 H34 N2 O3
	410.2556	1.0	2.4	10.5	4	C23 H32 N5 O2
	410.2543	2.3	5.7	5.5	5	C22 H36 N O6
	410.2596	-3.0	-7.4	14.5	1	C28 H32 N3
	410.2529	3.7	8.9	6.0	6	C20 H34 N4 O5
	410.2610	-4.4	-10.7	14.0	2	C30 H34 O
	410.2615	-4.9	-11.9	1.5	7	C16 H36 N5 O7

B.11 3-*n*-Butyl-N^1-hydroxyl-N^8-phenyloctandiamide (**1a**)
B.11.1 ^{1}H NMR

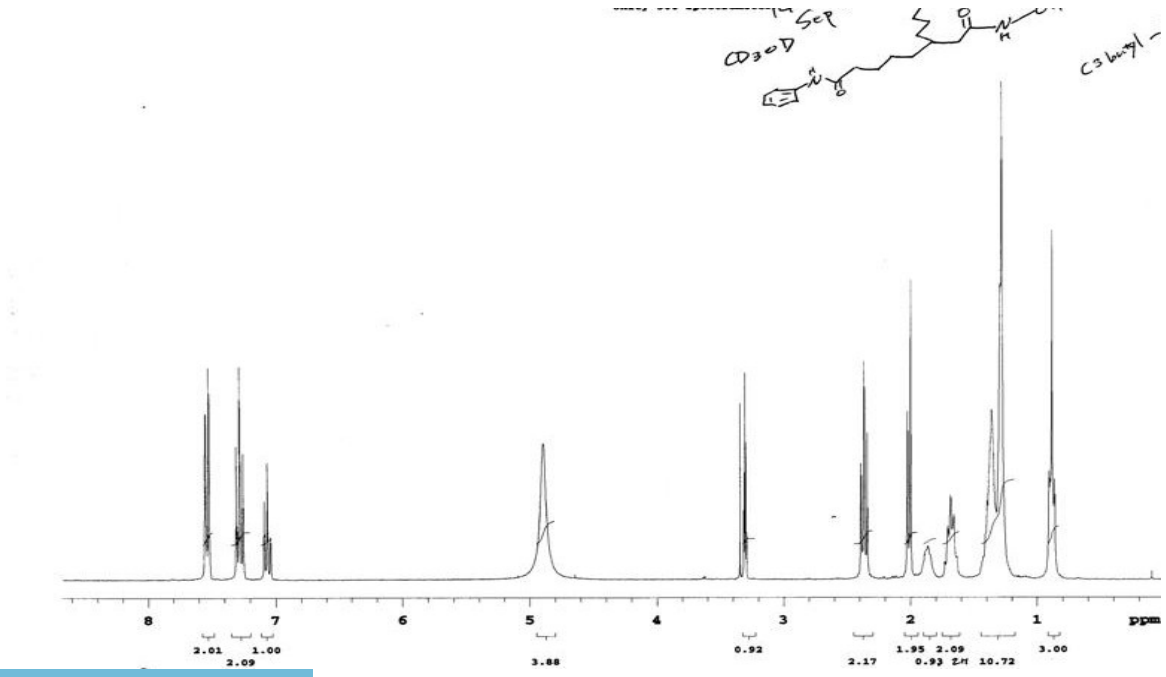

B.11.2 ^{13}C NMR

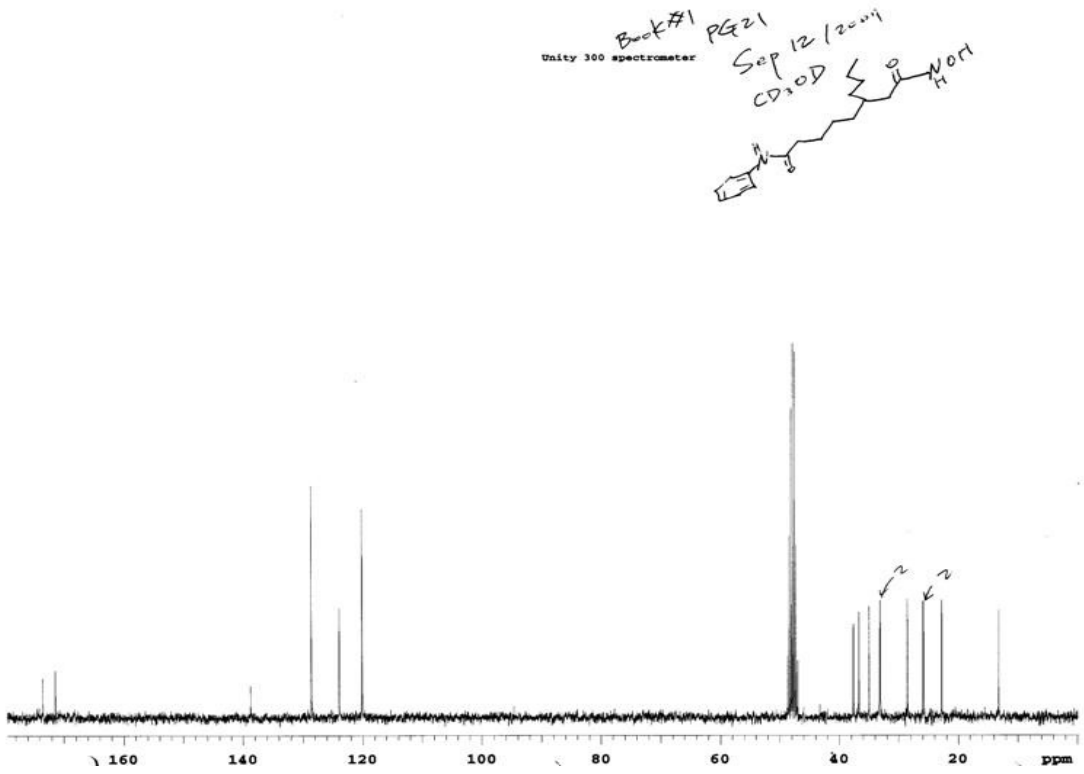

B.11.3 IR

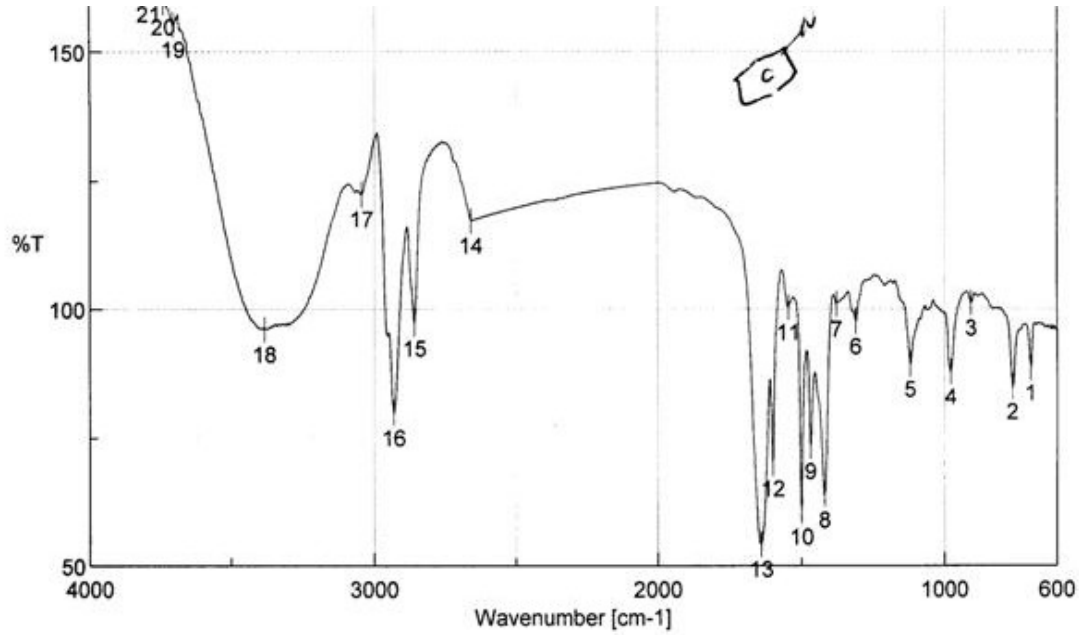

Result of Peak Picking

No.	Position	Intensity	No.	Position	Intensity
1	693.284	88.3224	2	755.959	84.7511
3	903.487	101.069	4	975.804	87.656
5	1118.51	89.12	6	1309.43	97.54
7	1376.93	100.839	8	1420.32	63.7517
9	1467.56	73.1938	10	1499.38	60.4673
11	1545.67	100.26	12	1599.66	69.8524
13	1640.16	54.2248	14	2660.32	117.131
15	2857.99	97.0537	16	2929.34	79.6486
17	3044.09	122.24	18	3383.5	95.8697

[Comment]
Sample Name
Comment
User
Division
Company Wayne State

[Measurement Information]
Model Name FT/IR-4100typeA
Serial Number B071861016

B.11.4 HRMS

Single Mass Analysis (displaying only valid results)
Tolerance = 4.0 mDa / DBE: min = -1.5, max = 50.0
Isotope cluster parameters: Separation = 1.0 Abundance = 1.0%

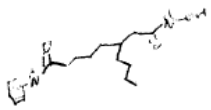

Monoisotopic Mass, Odd and Even Electron Ions
41 formula(e) evaluated with 1 results within limits (all results (up to 1000) for each mass)

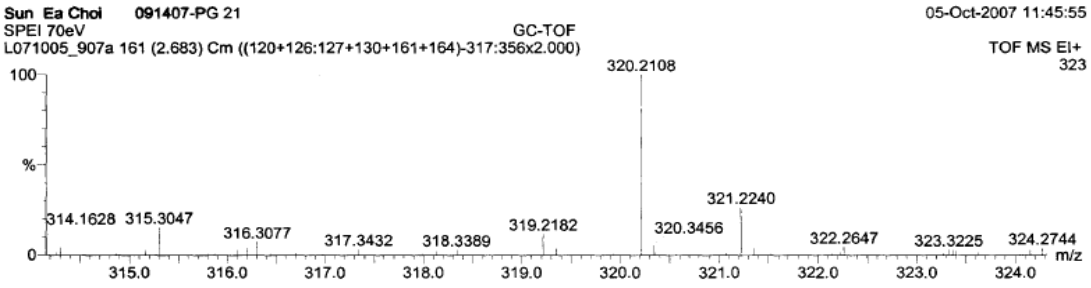

Minimum:				-1.5		
Maximum:		4.0	5.0	50.0		
Mass	**Calc. Mass**	**mDa**	**PPM**	**DBE**	**Score**	**Formula**
320.2108	320.2100	0.8	2.6	6.0	1	C18 H28 N2 O3

B.11.5 HPLC

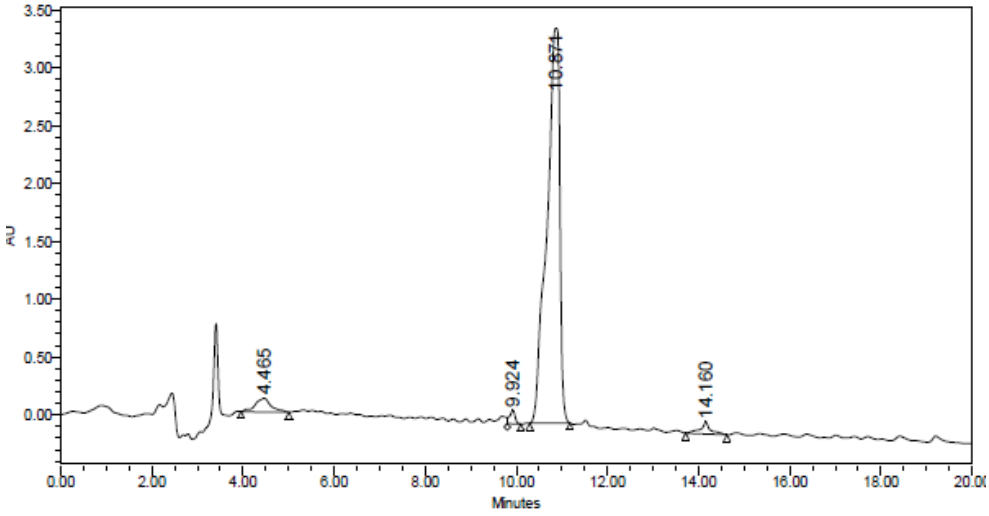

	RT	Area	% Area	Height
1	4.465	2883957	3.97	119017
2	9.924	979572	1.35	118509
3	10.871	67201132	92.46	3412411
4	14.160	1619846	2.23	105570

B.12 3-Phenyl-N^1-hydroxyl-N^8-phenyloctandiamide (**1b**)

B.12.1 ^{1}H NMR

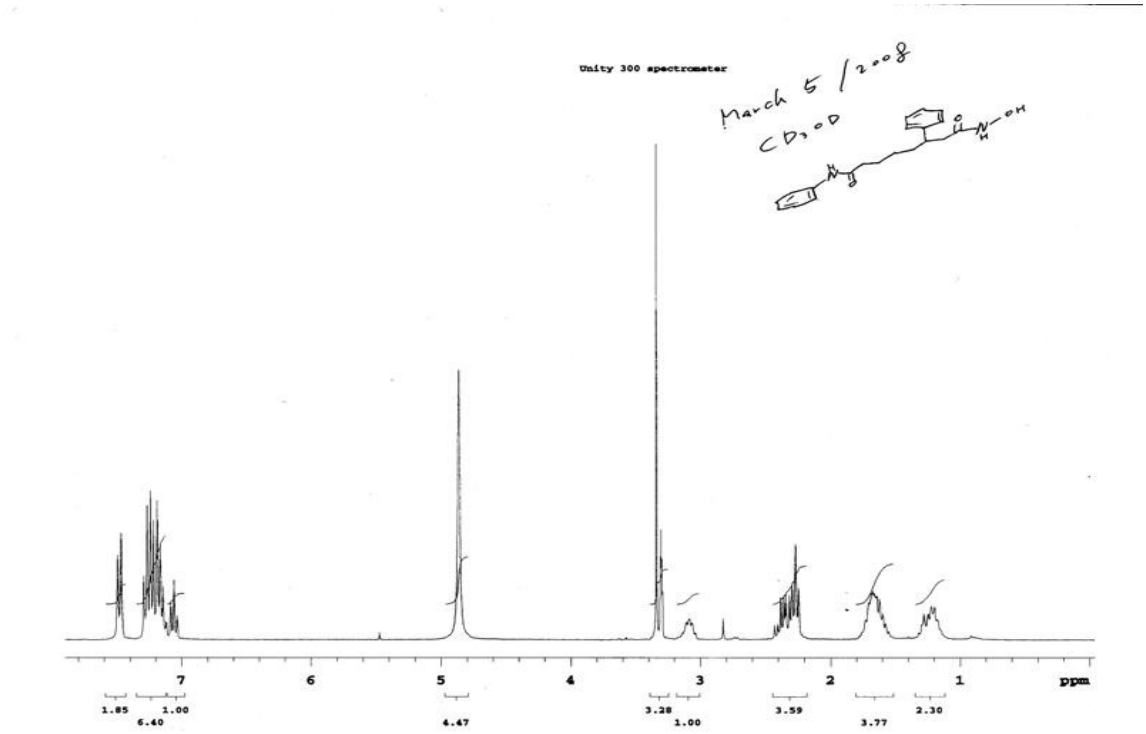

B.12.2 ^{13}C NMR

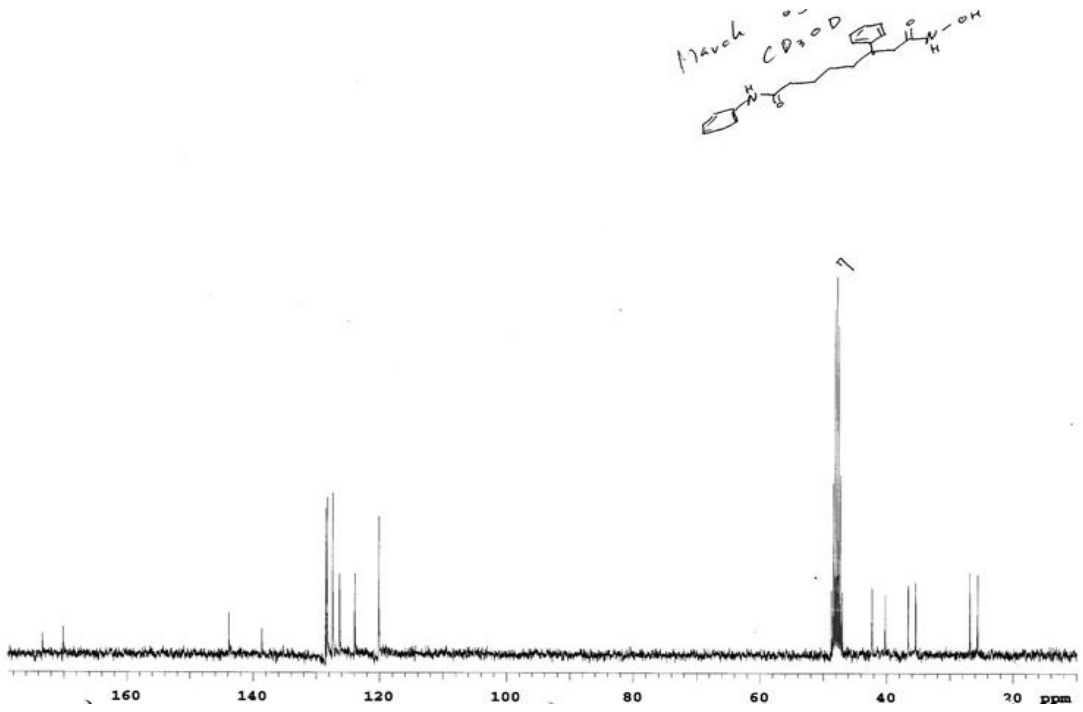

B.12.3 IR

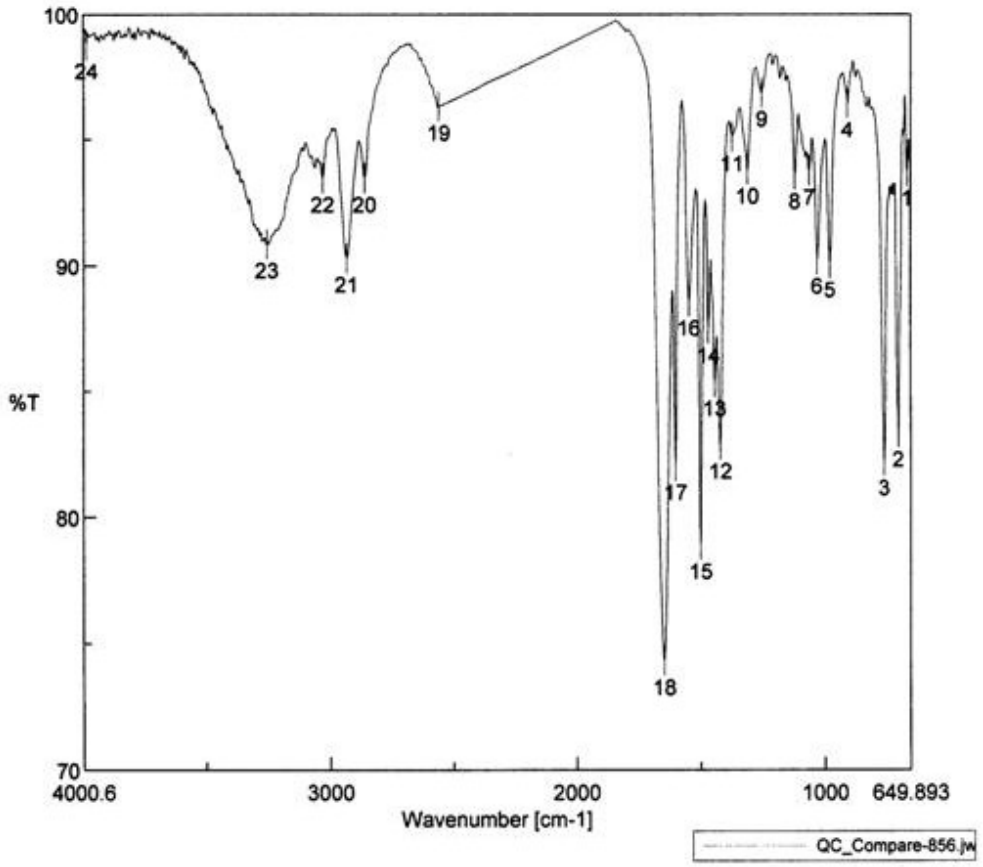

[Comment]	
Sample Name	
Comment	
User	
Division	
Company	wsu

[Data Information]	
Creation Date	3/5/2008 4:27 PM
Data array type	Linear data array
Horizontal	Wavenumber [cm-1]
Vertical	%T
Start	649.893 cm-1
End	4000.6 cm-1
Data pitch	0.964233 cm-1
Data points	3476

Result of Peak Picking

No.	Position	Intensity	No.	Position	Intensity	No.	Position	Intensity
1	665.321	93.7268	2	700.998	83.3563	3	757.888	82.2192
4	906.379	96.4265	5	978.697	90.0889	6	1029.8	90.2342
7	1062.59	93.7749	8	1120.44	93.6069	9	1253.5	96.8625
10	1310.39	93.816	11	1372.1	95.08	12	1420.32	82.8693
13	1442.49	85.3707	14	1467.56	87.4727	15	1499.38	78.885
16	1544.7	88.5676	17	1599.66	82.0265	18	1645.95	74.3198
19	2559.08	96.2967	20	2859.92	93.4684	21	2932.23	90.2789
22	3029.62	93.4632	23	3256.22	90.8424	24	3988.07	98.7856

B.12.4 HRMS

Elemental Composition Report **Page 1**

Single Mass Analysis
Tolerance = 5.0 mDa / DBE: min = -1.5, max = 50.0
Isotope cluster parameters: Separation = 1.0 Abundance = 1.0%

Monoisotopic Mass, Odd and Even Electron Ions
330 formula(e) evaluated with 7 results within limits (all results (up to 1000) for each mass)

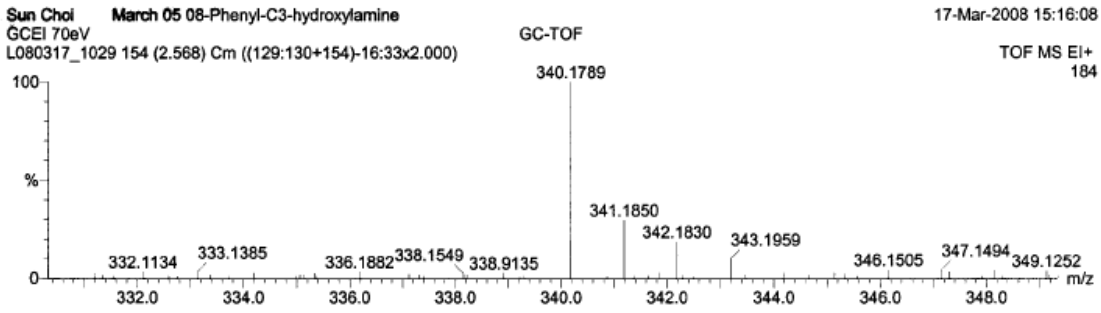

Minimum:				-1.5		
Maximum:		5.0	10.0	50.0		
Mass	Calc. Mass	mDa	PPM	DBE	Score	Formula
340.1789	340.1787	0.2	0.7	10.0	3	C20 H24 N2 O3
	340.1774	1.6	4.6	10.5	4	C18 H22 N5 O2
	340.1814	-2.4	-7.2	14.5	2	C23 H22 N3
	340.1760	2.9	8.6	5.5	5	C17 H26 N O6
	340.1827	-3.8	-11.1	14.0	1	C25 H24 O
	340.1747	4.3	12.5	6.0	6	C15 H24 N4 O5
	340.1832	-4.3	-12.6	1.5	7	C11 H26 N5 O7

B.12.5 HPLC

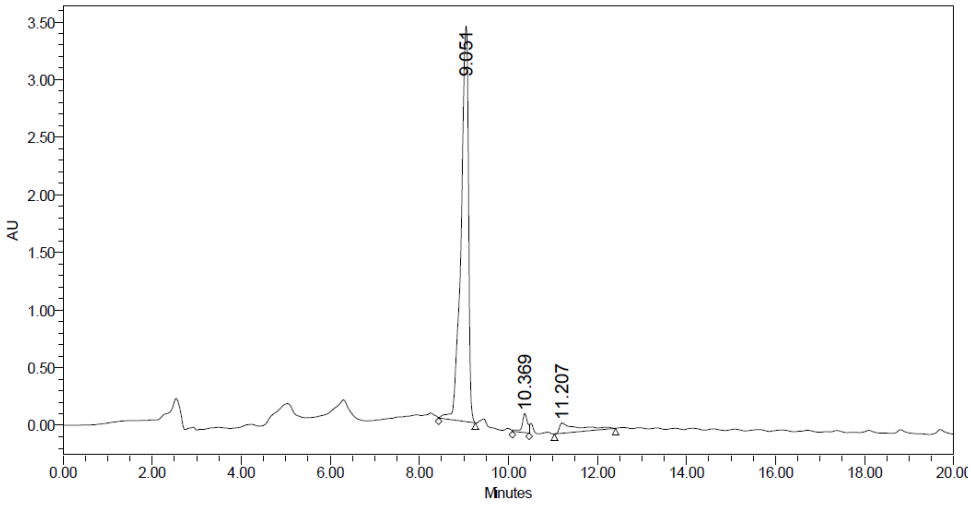

	RT	Area	% Area	Height
1	9.051	39873149	90.86	3433268
2	10.369	1369440	3.12	166207
3	11.207	2642112	6.02	87326

B.13 3-Ethyl-N^1-hydroxyl-N^8-phenyloctandiamide (**1c**)

B.13.1 ^{1}H NMR

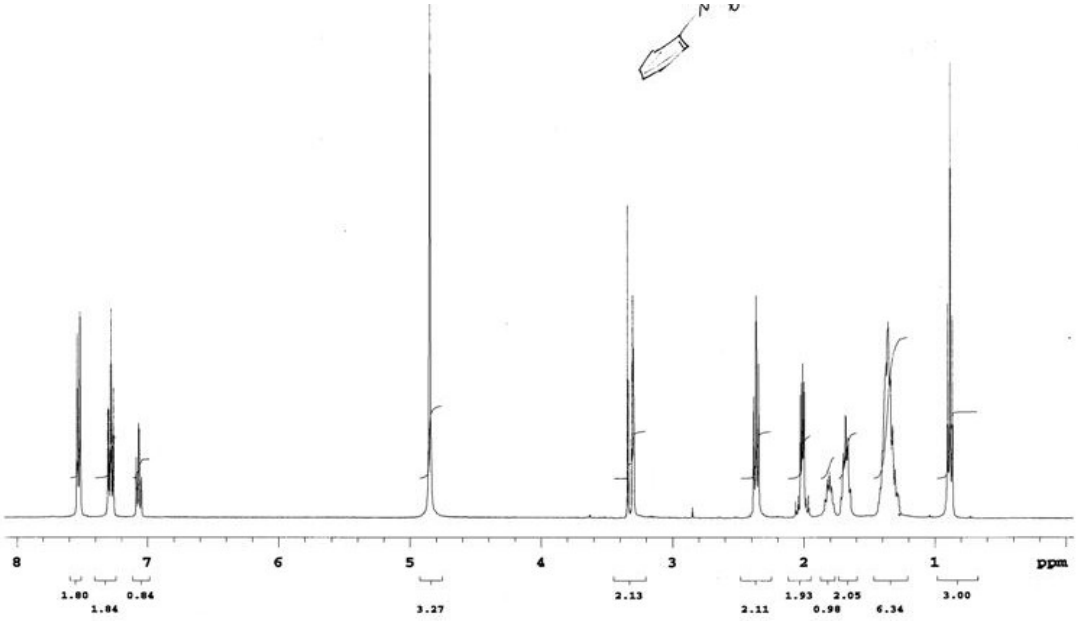

B.13.2 ^{13}C NMR

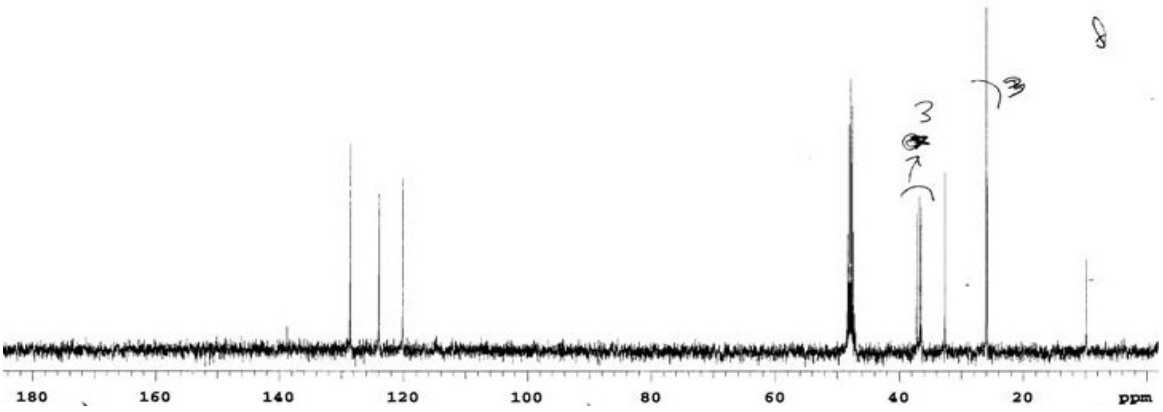

B.13.3 IR

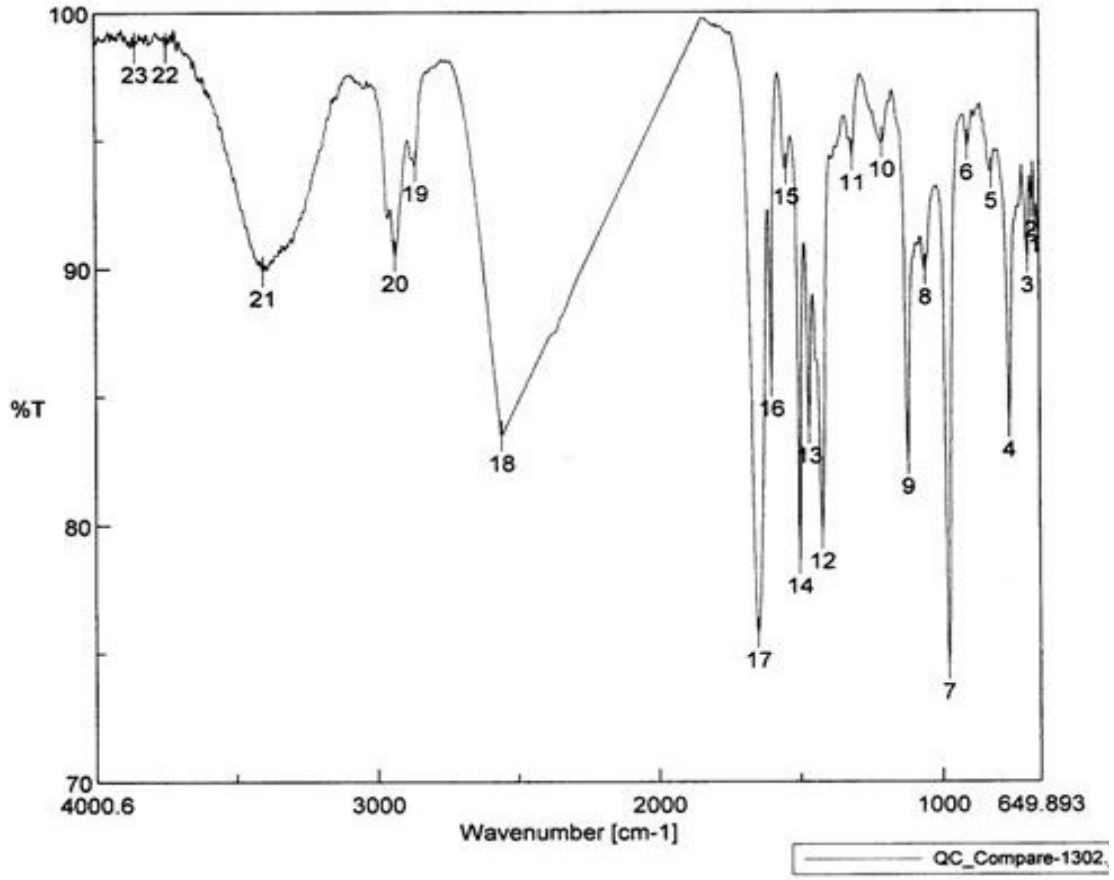

[Comment]	
Sample Name	
Comment	
User	
Division	
Company	wsu

[Data Information]	
Creation Date	4/18/2008 11:25 AM
Data array type	Linear data array
Horizontal	Wavenumber [cm-1]
Vertical	%T
Start	649.893 cm-1
End	4000.6 cm-1
Data pitch	0.964233 cm-1
Data points	3476

Result of Peak Picking

No.	Position	Intensity	No.	Position	Intensity	No.	Position	Intensity
1	665.321	91.8889	2	677.856	92.51	3	691.355	90.3449
4	757.888	83.9773	5	819.598	93.6244	6	904.451	94.73
7	976.769	74.5239	8	1056.8	89.8947	9	1119.48	82.5492
10	1207.22	94.858	11	1311.36	94.3431	12	1421.28	79.6257
13	1468.53	83.7494	14	1501.31	78.6569	15	1543.74	93.8118
16	1599.66	85.5489	17	1648.84	75.7582	18	2558.11	83.4513
19	2861.84	93.9587	20	2935.13	90.4381	21	3403.74	89.8635
22	3745.08	98.6405	23	3856.93	98.6377			

B.13.4 HRMS

Single Mass Analysis
Tolerance = 6.0 PPM / DBE: min = -1.5, max = 50.0
Element prediction: Off
Number of isotope peaks used for i-FIT = 3

Monoisotopic Mass, Even Electron Ions
348 formula(e) evaluated with 2 results within limits (up to 50 closest results for each mass)
Elements Used:
C: 0-500 H: 0-1000 N: 0-4 O: 0-10 Na: 0-1

pflum; sun choi Apr1808C3ethylhydroxylamine mw292 LCT0001 10pg/ul meoh 10ul full 150ul/min meoh
LeuEnk 100pg/ul LCT Premier
2008-0507-0001-31 21 (0.477) Cm (19:25-1:13x2.000)

2::0::5 07-May-2008
1: TOF MS ES-
1.80e+004

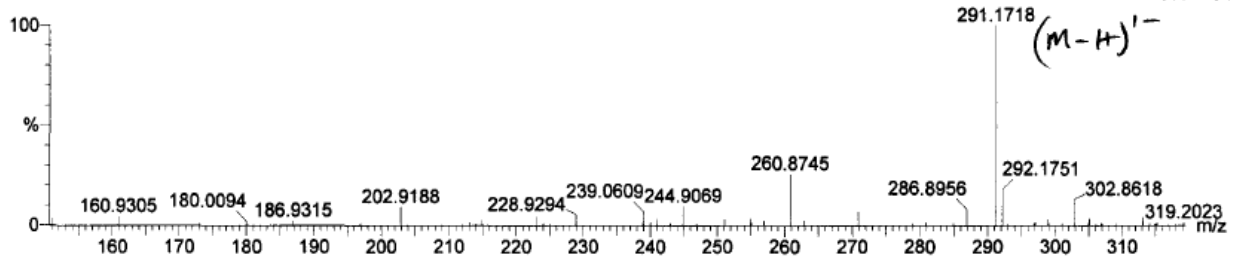

Minimum:				-1.5		
Maximum:		6.0	6.0	50.0		
Mass	Calc. Mass	mDa	PPM	DBE	i-FIT	Formula
291.1718	291.1725	-0.7	-2.4	7.5	n/a	C19 H24 O Na
	291.1709	0.9	3.1	6.5	n/a	C16 H23 N2 O3

B.13.5 HPLC

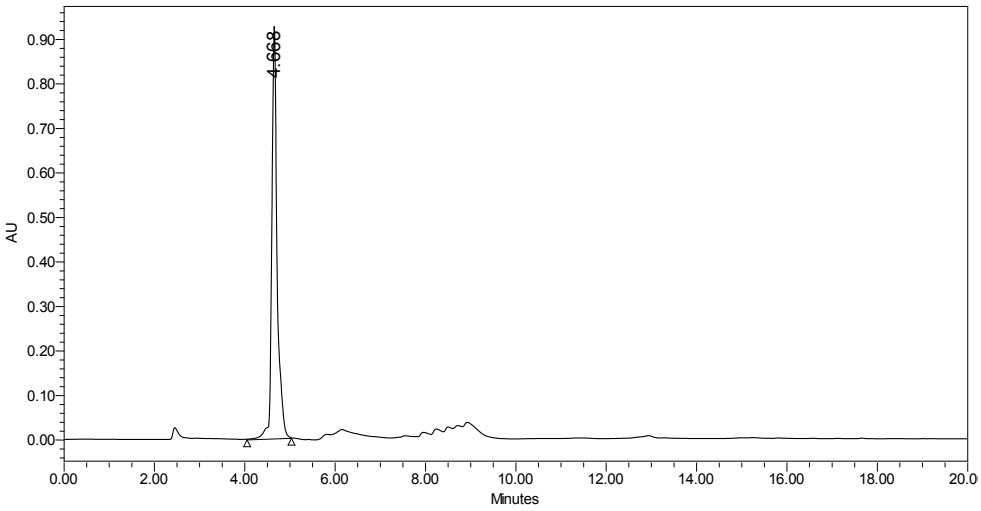

	RT	Area	% Area	Height
1	4.668	7510006	100.00	924974

B.14 3-Vinyl-N^1-hydroxyl-N^8-phenyloctandiamide (**1d**)

B.14.1 ^{1}H NMR

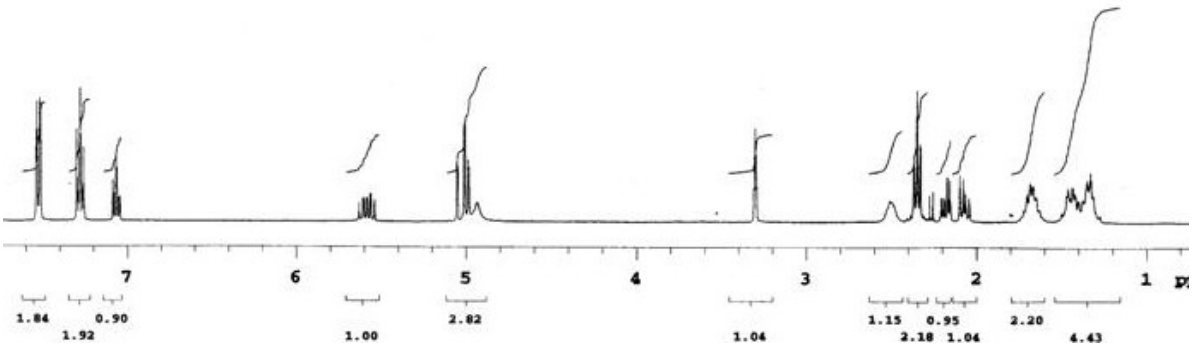

B.14.2 ^{13}C NMR

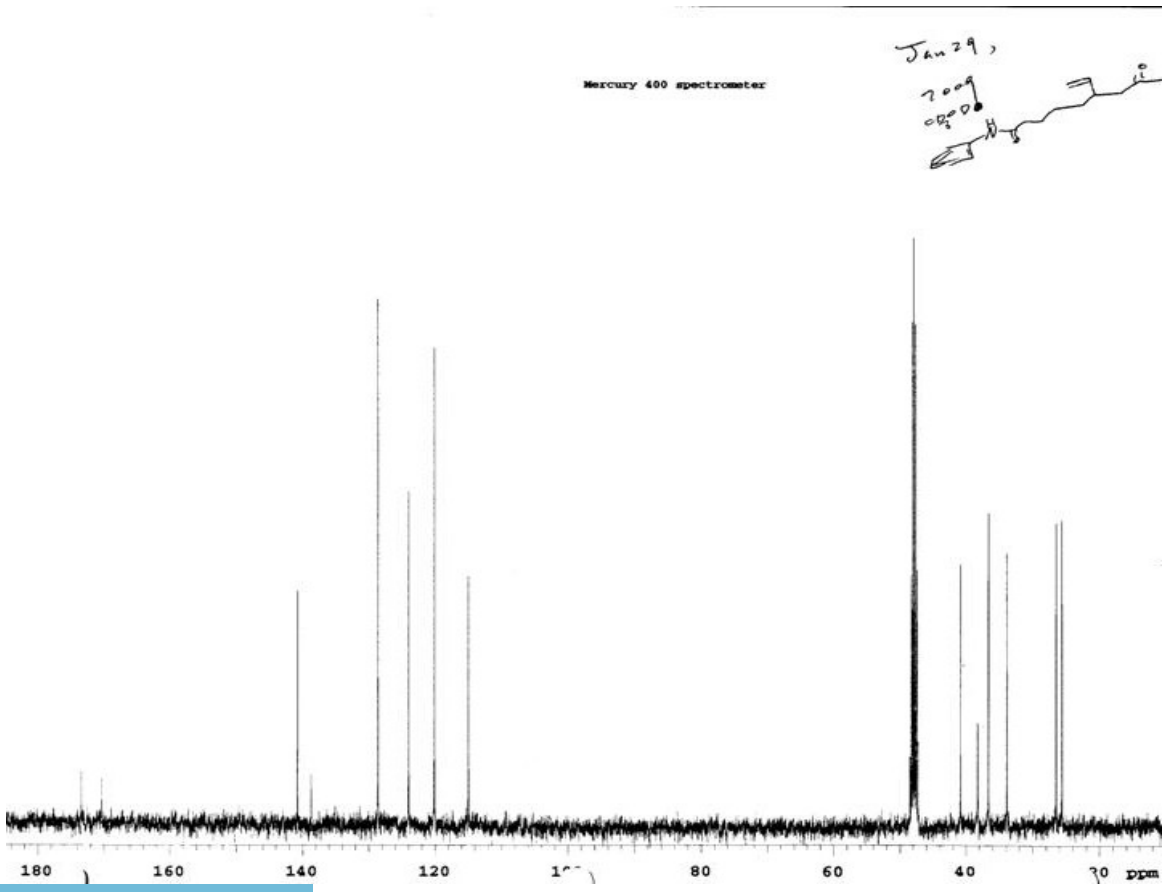

B.14.3 IR

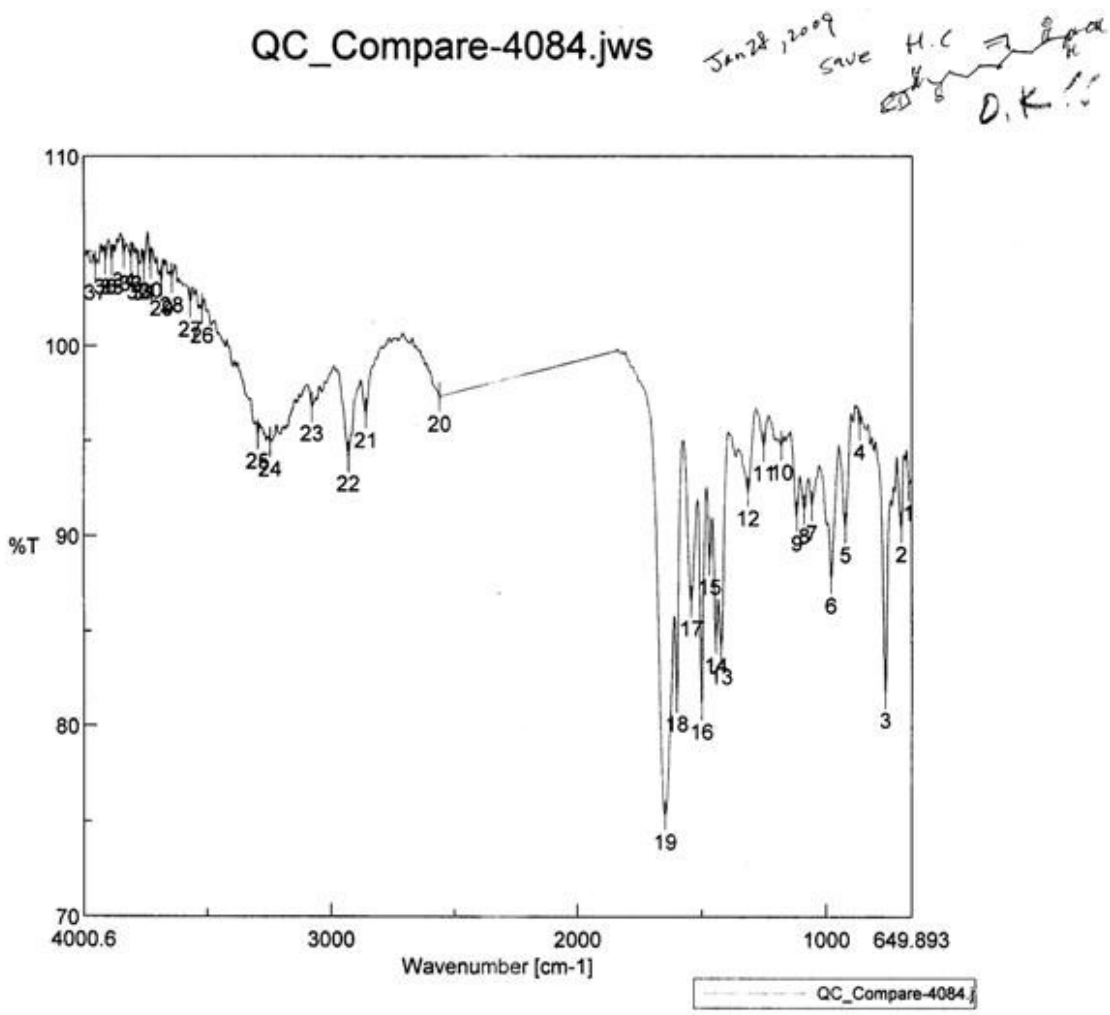

[Comment]
Sample Name
Comment
User
Division
Company wsu

[Data Information]

Creation Date	1/28/2009 11:22 AM
Data array type	Linear data array
Horizontal	Wavenumber [cm-1]
Vertical	%T
Start	649.893 cm-1
End	4000.6 cm-1
Data pitch	0.964233 cm-1
Data points	3476

Result of Peak Picking

No.	Position	Intensity	No.	Position	Intensity	No.	Position	Intensity
1	661.464	92.6312	2	692.32	90.4452	3	757.888	81.6979
4	862.025	95.8221	5	919.879	90.4263	6	977.733	87.7524
7	1055.84	91.563	8	1086.69	91.4003	9	1117.55	91.0162
10	1178.29	94.7709	11	1247.72	94.7005	12	1312.32	92.3315
13	1421.28	84.0141	14	1442.49	84.596	15	1467.56	88.7097
16	1500.35	81.0939	17	1541.81	86.5281	18	1599.66	81.5018
19	1646.91	75.3255	20	2561	97.2887	21	2860.88	96.4044
22	2931.27	94.119	23	3078.8	96.7797	24	3249.47	94.8895
25	3298.64	95.3182	26	3523.31	101.927	27	3570.56	102.273
28	3644.8	103.524	29	3687.23	103.358	30	3731.58	104.31
31	3757.62	104.201	32	3780.76	104.232	33	3810.65	104.66
34	3839.58	104.828	35	3887.79	104.491	36	3913.82	104.51
37	3955.29	104.205						

B.14.4 HRMS

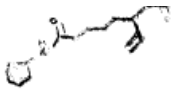

Single Mass Analysis
Tolerance = 5.0 PPM / DBE: min = -1.5, max = 50.0
Element prediction: Off
Number of isotope peaks used for i-FIT = 3

Monoisotopic Mass, Even Electron Ions
352 formula(e) evaluated with 1 results within limits (up to 50 best isotopic matches for each mass)
Elements Used:
C: 0-50 H: 0-50 N: 0-5 O: 0-7 Na: 0-1
Sun Choi U_Jan 30 09-C3-vinylhydroxamic PG37
Lew 2008-07b.pro
2009_0202_0297 15 (0.318) Cm (12:17-(1:9+29:36)x2.000)

LCT Premier 02-Feb-2009 14:39:14
1: TOF MS ES+
9.88e+002

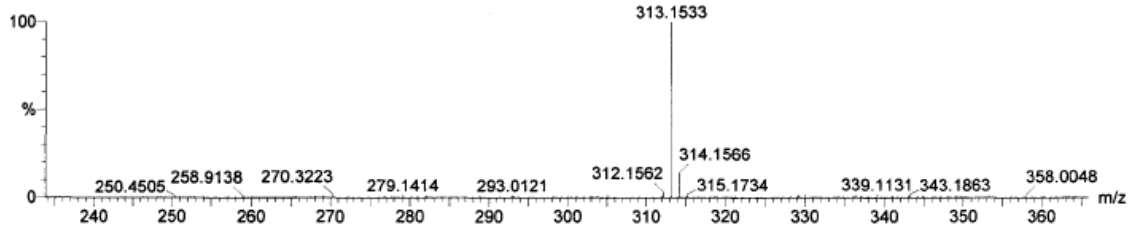

Minimum:				-1.5			
Maximum:		5.0	5.0	50.0			
Mass	Calc. Mass	mDa	PPM	DBE	i-FIT	i-FIT (Norm)	Formula
313.1533	313.1528	0.5	1.6	6.5	41.7	0.0	C16 H22 N2 O3 Na

B.14.5 HPLC

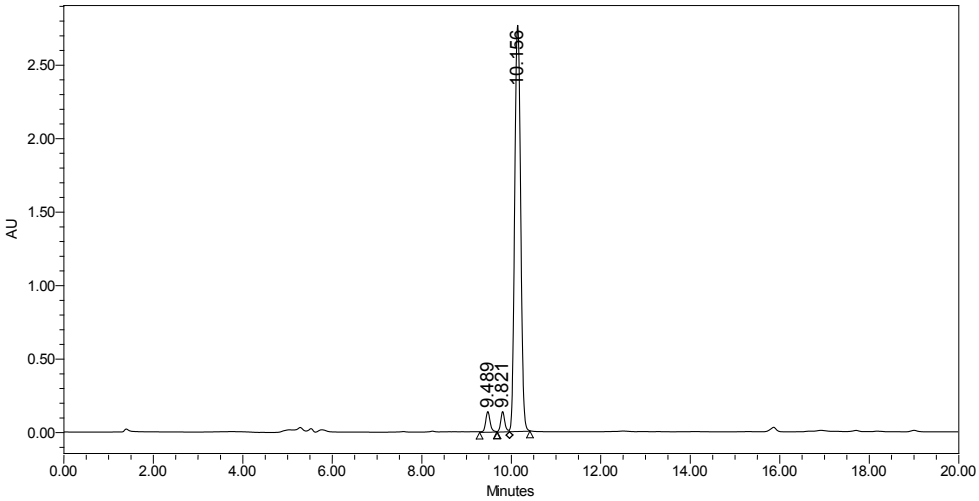

	RT	Area	% Area	Height
1	9.489	888985	3.29	135811
2	9.821	803374	2.97	134069
3	10.156	25352757	93.74	2759849

B.15 3-Methyl-N^1-hydroxyl-N^8-phenyloctandiamide (**1e**)

B.15.1 ^{1}H NMR

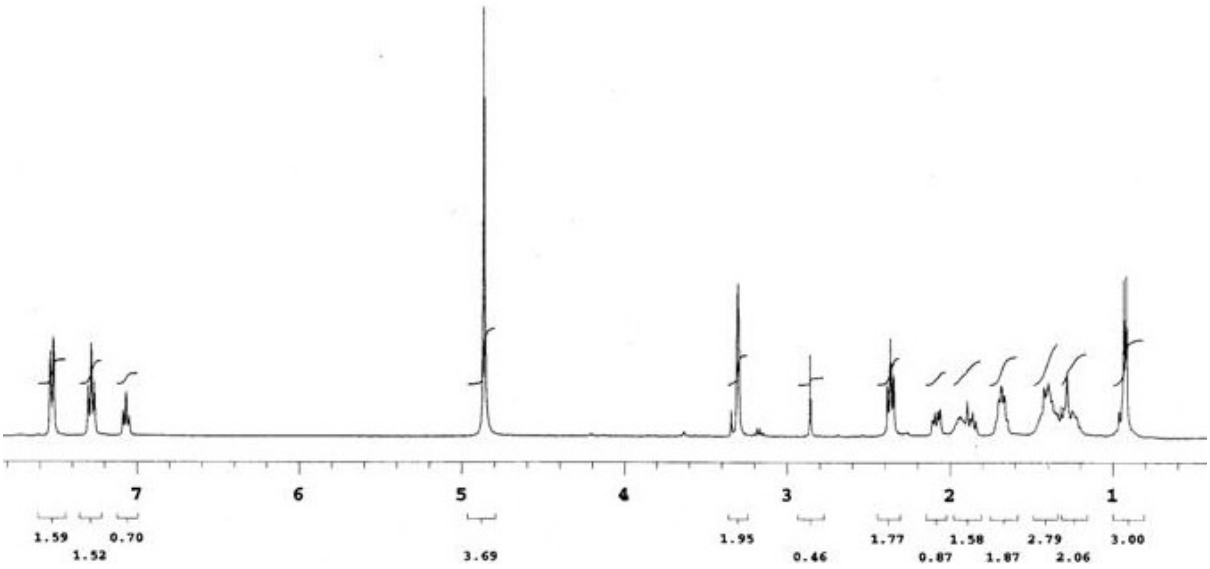

B.15.2 ^{13}C NMR

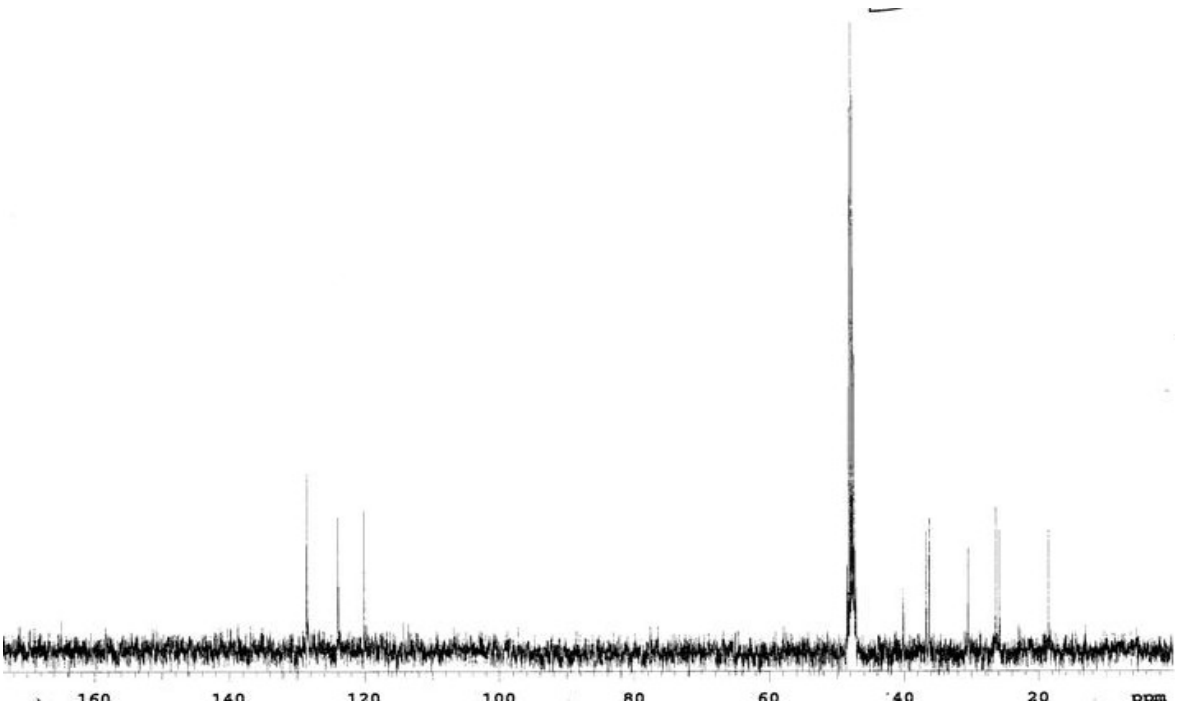

B.15.3 IR

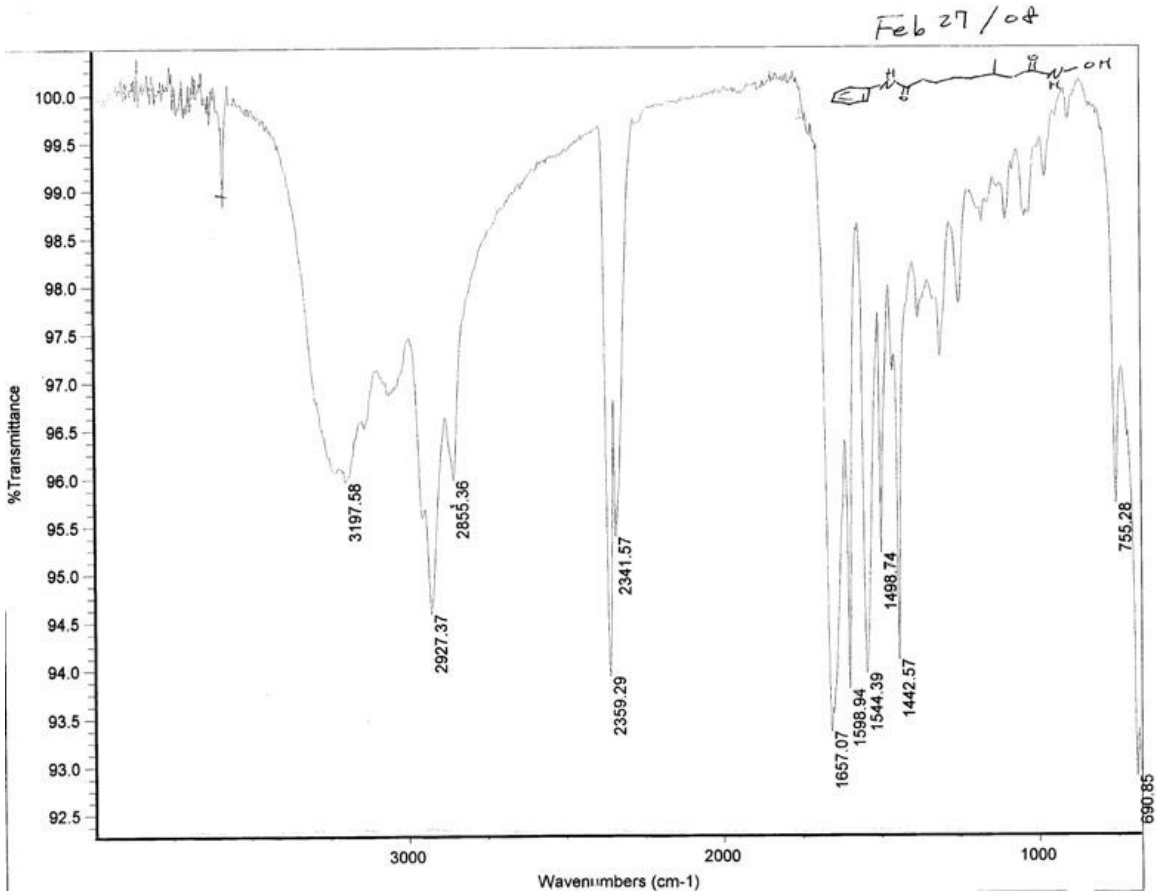

B.15.4 HRMS

Elemental Composition Report **Page 1**

Single Mass Analysis
Tolerance = 5.0 mDa / DBE: min = -1.5, max = 50.0
Isotope cluster parameters: Separation = 1.0 Abundance = 1.0%

Monoisotopic Mass, Odd and Even Electron Ions
222 formula(e) evaluated with 6 results within limits (all results (up to 1000) for each mass)

Sun Choi Feb21 08-methyl-C3-hydroxylamine
GCEI 70eV
L080221_1006b 92 (1.533) Cm ((92+100+103:104)-440:480x2.000)
GC-TOF
22-Feb-2008 11:09:55
TOF MS EI+
5.91e3

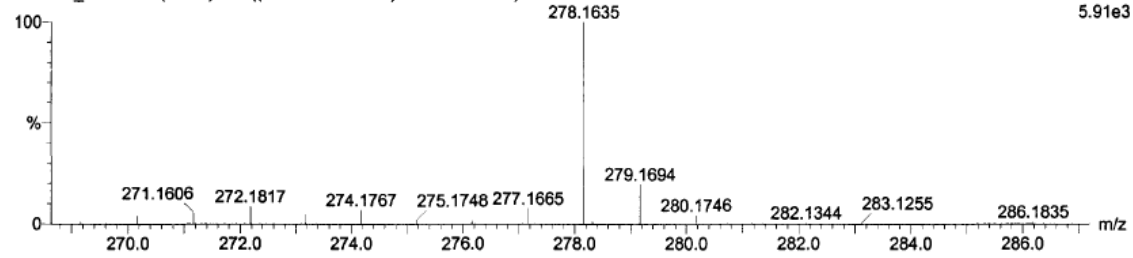

Minimum:				-1.5		
Maximum:		5.0	10.0	50.0		
Mass	Calc. Mass	mDa	PPM	DBE	Score	Formula
278.1635	278.1630	0.4	1.6	6.0	1	C15 H22 N2 O3
	278.1617	1.8	6.4	6.5	4	C13 H20 N5 O2
	278.1657	-2.2	-8.1	10.5	2	C18 H20 N3
	278.1604	3.1	11.2	1.5	5	C12 H24 N O6

B.15.5 HPLC

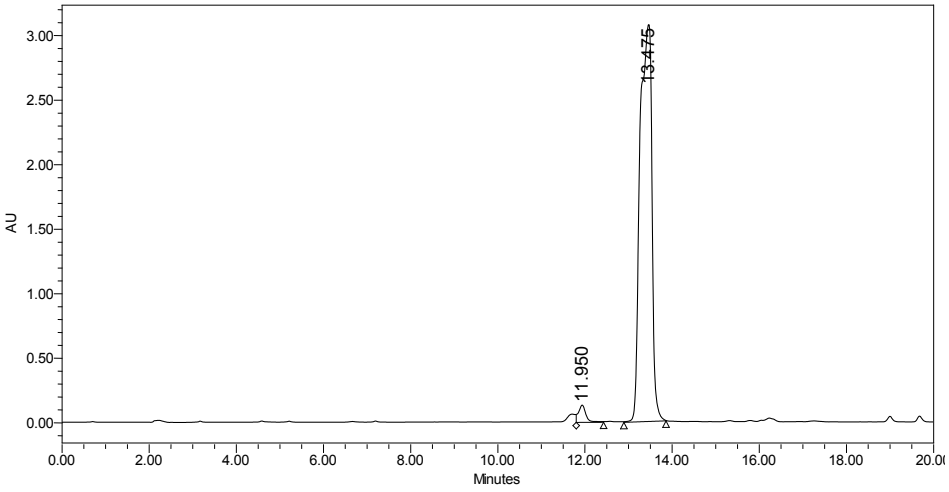

	Peak Name	RT	Area	% Area	Height
1	Peak2	9.489			
2	Peak3	9.821			
3	Peak4	10.156			
4	Peak1	10.871			
5		11.950	1469677	2.48	129416
6		13.475	57777809	97.52	3069522

APPENDIX C. DOSE RESPONSE GRAPHS AND DATA FOR C6-SAHA LIBRARY

Table C.1. Percentage HDAC activity after incubation of SAHA with Hela Lysate

Concentration (M)	Trial 1	Trial 2	Trial 3	Mean	Standard Error (S.E.)
3.125×10^{-8}	75	75	ND	75	0
6.25×10^{-8}	63	56	51	57	3
1.25×10^{-7}	44	35	40	40	3
2.5×10^{-7}	31	21	26	26	3
5.0×10^{-7}	20	16	15	17	2

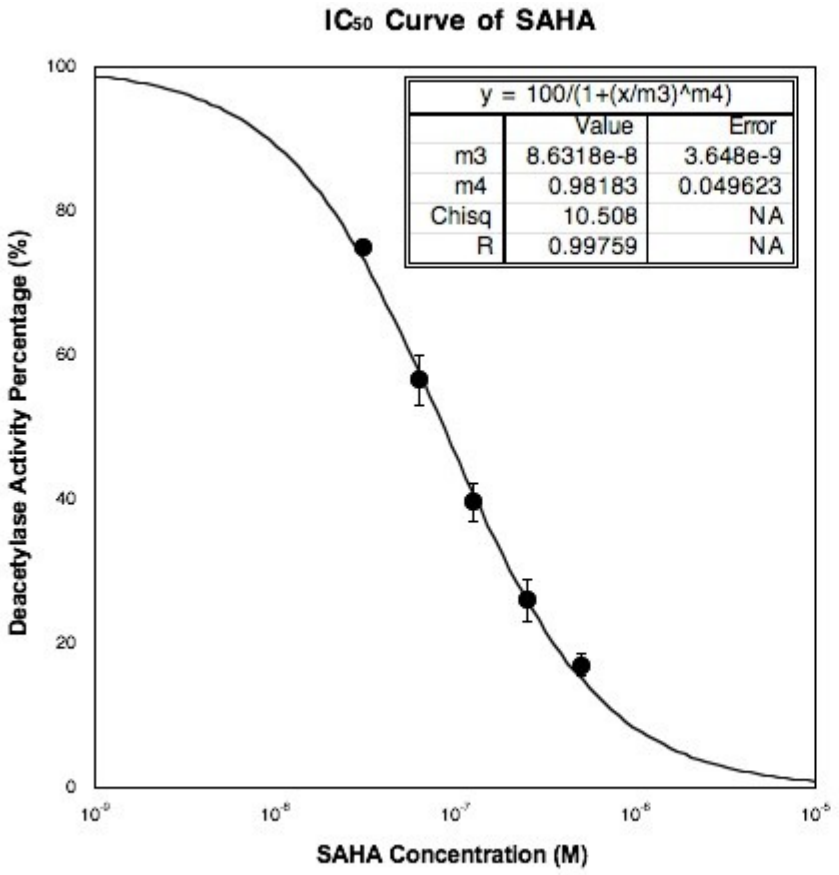

Figure C.1. Dose response curve of SAHA tested using the HDAC activity from HeLa cells lysates from three independent trials In some case, the error bar is smaller than the marker size. Data were fit to the sigmoidal curve using Kaleidograph 4.0 (Synergy Software) to determine the IC_{50}. The insets were the results of the data analysis. The data are reported in Table 3.1.

Table C.2. Percentage HDAC activity after incubation of MS-275 with Hela Lysate

Concentration (M)	Trial 1	Trial 2	Trial 3	Mean	Standard Error (S.E.)
1.95×10^{-6}	58	59	58	58	0.3
3.91×10^{-6}	44	47	49	47	1
7.81×10^{-6}	32	35	33	33	1
1.56×10^{-5}	27	27	26	27	0.3
6.25×10^{-5}	9	12	11	11	1

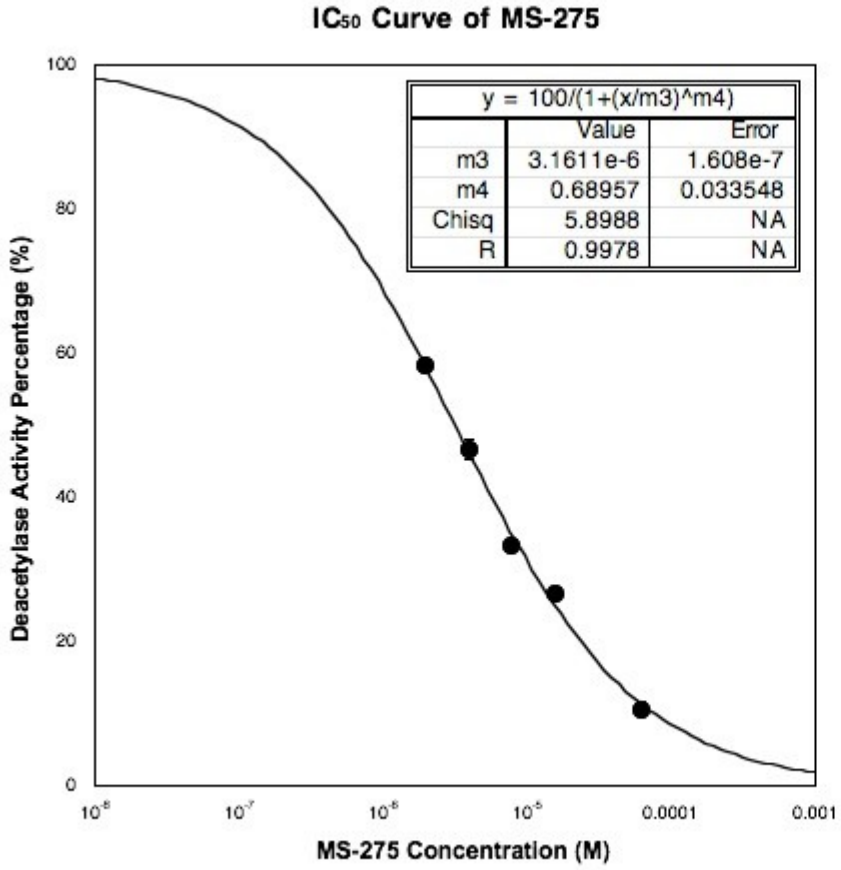

Figure C.2. Dose response curve of MS-275 tested using the HDAC activity from HeLa cells lysates from three independent trials. In some cases, the error bars are smaller than the marker size. Data were fit to the sigmoidal curve using Kaleidograph 4.0 (Synergy Software) to determine the IC_{50}. The insets were the results of the data analysis. The data are reported in Table 3.1.

Table C.3. Percentage HDAC activity after incubation of C6-SAHA methyl analogue **14a** with Hela Lysate

Concentration (M)	Trial 1	Trial 2	Trial 3	Mean	Standard Error (S.E.)
6.25×10^{-8}	104	72	102	92	10
1.25×10^{-7}	94	50	85	76	13
2.5×10^{-7}	66	51	79	65	8
5.0×10^{-7}	30	32	40	34	3
1.0×10^{-6}	24	20	22	22	1

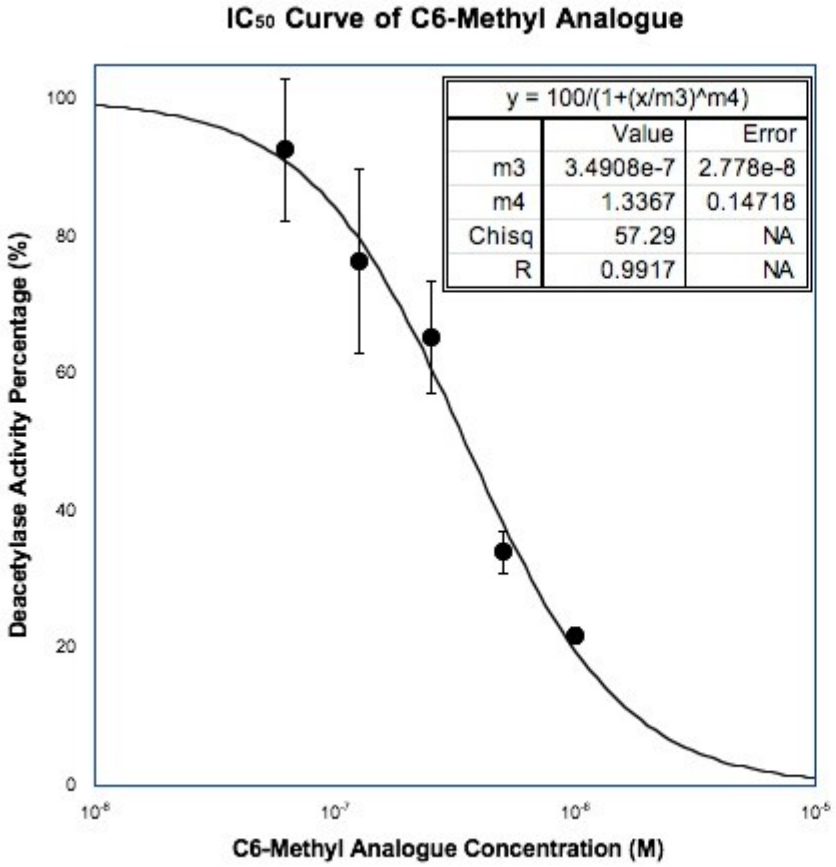

Figure C.3. Dose response curve of C6-SAHA methyl analogue **14a** tested using the HDAC activity from HeLa cells lysates from three independent trials. In some case, the error bar is smaller than the marker size. Data were fit to the sigmoidal curve using Kaleidograph 4.0 (Synergy Software) to determine the IC_{50}. The insets were the results of the data analysis. The data are reported in Table 3.1.

Table C.4. Percentage HDAC activity after incubation of C6-SAHA phenyl analogue **14b** with Hela Lysate

Concentration (M)	Trial 1	Trial 2	Trial 3	Mean	Standard Error (S.E.)
6.25×10^{-8}	87	87	82	85	1
1.25×10^{-7}	75	73	75	74	0.7
2.5×10^{-7}	59	41	54	51	5
5.0×10^{-7}	45	47	51	47	1
1.0×10^{-6}	27	23	20	23	2

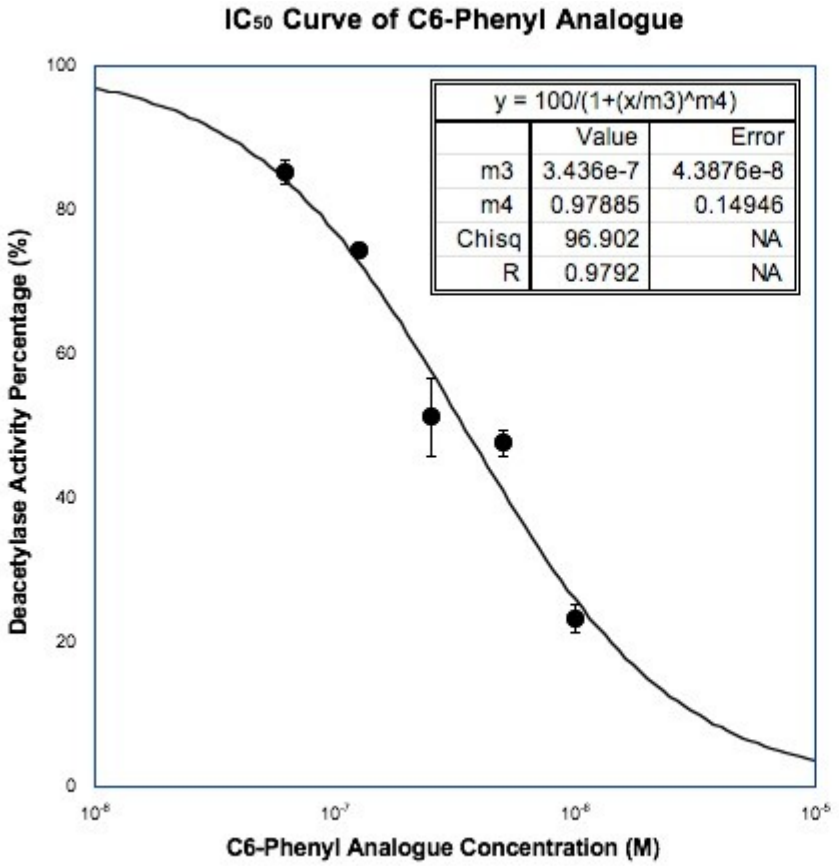

Figure C.4. Dose response curve of C6-SAHA phenyl analogue **14b** tested using the HDAC activity from HeLa cells lysates from three independent trials with error bars indicating standard error. In some case, the error bar is smaller than the marker size. Data were fit to the sigmoidal curve using Kaleidograph 4.0 (Synergy Software) to determine the IC_{50}. The insets were the results of the data analysis. The data are reported in Table 3.1.

Table C.5. Percentage HDAC activity after incubation of C6-SAHA *t*-butyl analogue **14c** with Hela Lysate

Concentration (M)	Trial 1	Trial 2	Trial 3	Mean	Standard Error (S.E.)
1.11×10^{-7}	94	99	114	102	6
3.33×10^{-7}	65	87	103	85	11
1.0×10^{-6}	55	58	71	61	4
3.0×10^{-6}	40	37	41	39	1
9.0×10^{-6}	28	20	18	22	3

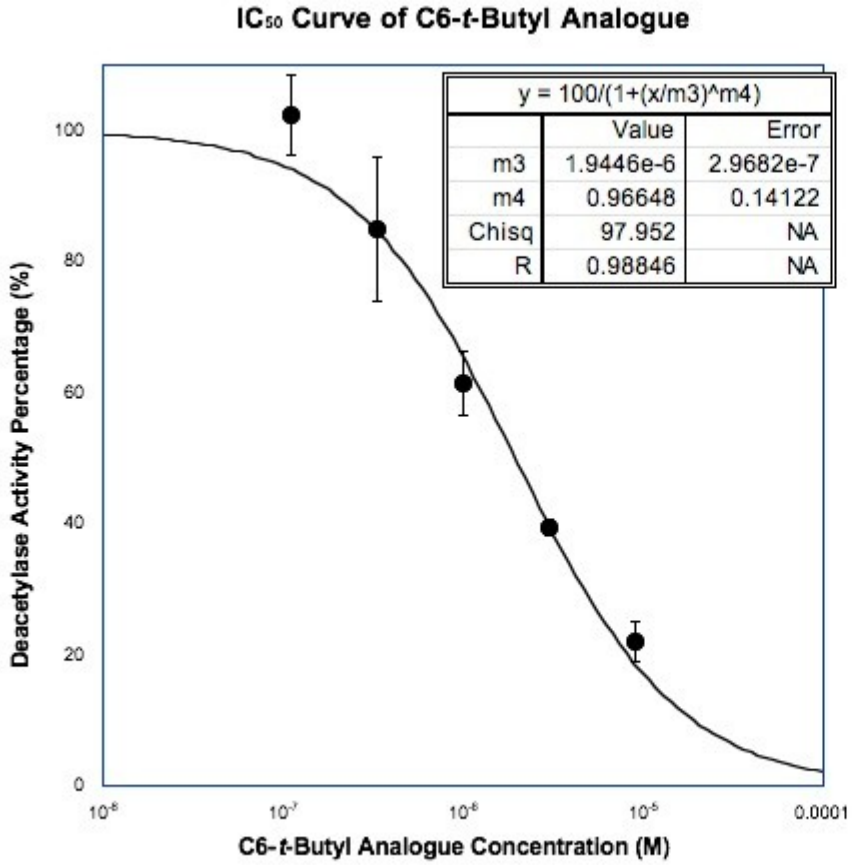

Figure C.5. Dose response curve of C6-SAHA *t*-butyl analogue **14c** tested using the HDAC activity from HeLa cells lysates from three independent trials. In some case, the error bar is smaller than the marker size. Data were fit to the sigmoidal curve using Kaleidograph 4.0 (Synergy Software) to determine the IC_{50}. The insets were the results of the data analysis. The data are reported in Table 3.1.

Table C.6. Percentage HDAC activity after incubation of C6-SAHA 2-ethylhexyl analogue **14d** with Hela Lysate

Concentration (M)	Trial 1	Trial 2	Trial 3	Mean	Standard Error (S.E.)
1.11×10^{-7}	93	69	78	80	7
3.33×10^{-7}	62	54	55	57	2
1.0×10^{-6}	42	22	38	34	6
3.0×10^{-6}	12	8	13	11	1
9.0×10^{-6}	4	2	2	2.7	0.7

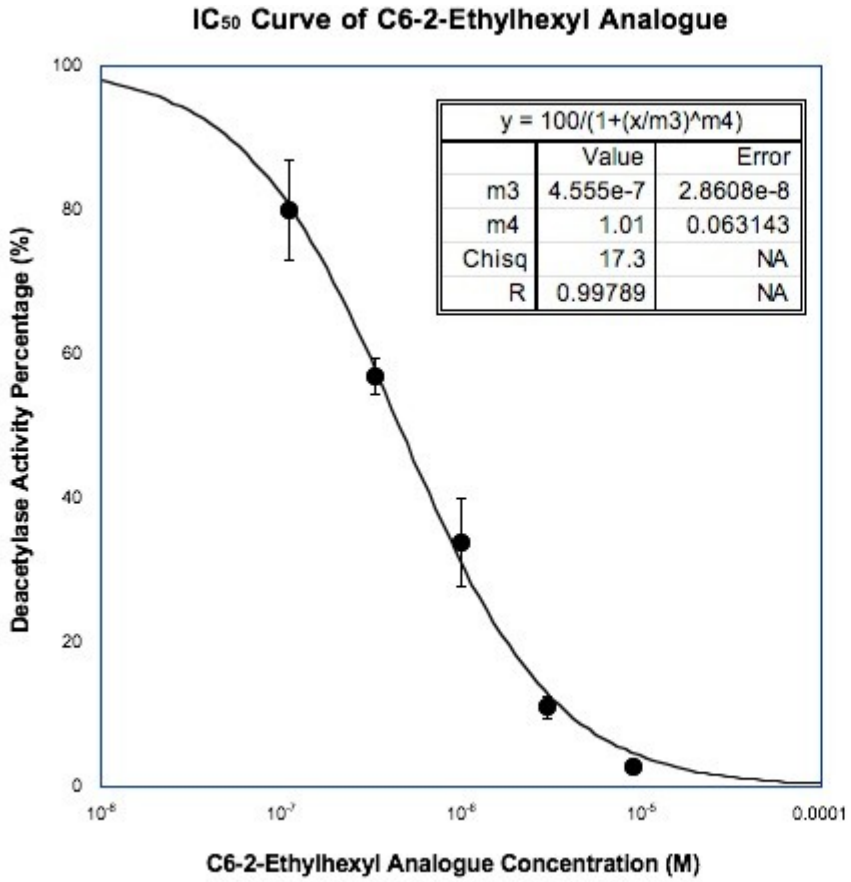

Figure C.6. Dose response curve of C6-SAHA 2-ethylhexyl analogue **14d** tested using the HDAC activity from HeLa cells lysates from three independent trials with error bars indicating standard error. In some case, the error bar is smaller than the marker size. Data were fit to the sigmoidal curve using Kaleidograph 4.0 (Synergy Software) to determine the IC_{50}. The insets were the results of the data analysis. The data are reported in Table 3.1.

Table C.7. Deacetylase activity percentage remaining after incubation of HDAC1, HDAC3, or HDAC6 with SAHA or the C6-SAHA analogues **14a-e**.

Compound	HDAC Isoform	Trial 1	Trial 2	Mean	S.E.
SAHA (125 nM)	HDAC1	30	35	32	2
	HDAC3	44	45	44	1
	HDAC6	32	36	34	2
C6-Methyl (500 nM)	HDAC1	35	42	38	3
	HDAC3	32	33	32	0.5
	HDAC6	61	58	59	1
C6-Phenyl (500 nM)	HDAC1	57	56	56	0.5
	HDAC3	68	67	67	0.5
	HDAC6	61	58	59	1
C6-*t*-Butyl (2 μM)	HDAC1	44	46	45	1
	HDAC3	79	82	80	1
	HDAC6	56	55	55	0.5
C6-2-Ethylhexyl (500 nM)	HDAC1	77	73	75	2
	HDAC3	51	54	52	1
	HDAC6	91	95	93	2
C6-Isopropyl (μM)	HDAC1	42	48	45	3
	HDAC3	50	51	51	1
	HDAC6	24	27	26	2

Deacetylase activity of HDAC1, HDAC3 and HDAC6 was determined with SAHA and with C6-SAHA analogues at given concentration using an in vitro fluorescence assay as described (Section 3.6). The fluorescence activity of background (No enzyme added) was subtracted from the no small molecule treated (positive control) and the percentage of the deacetylase activity was set to 100%. Deacetylase activity percentage of each independent trial, mean percentage of deacetylase activity, and standard error (S.E.) are illustrated. The data are reported in the manuscript in Figure 3.2.

Table C.8. HDAC1 activity percentage after incubation of SAHA.

Concentration (M)	Trial 1	Trial 2	Trial 3	Mean	Standard Error (S.E.)
3.125×10^{-8}	68	91	82	80	7
6.25×10^{-8}	55	62	57	58	2
1.25×10^{-7}	48	27	37	37	6
2.50×10^{-7}	37	40	25	34	5

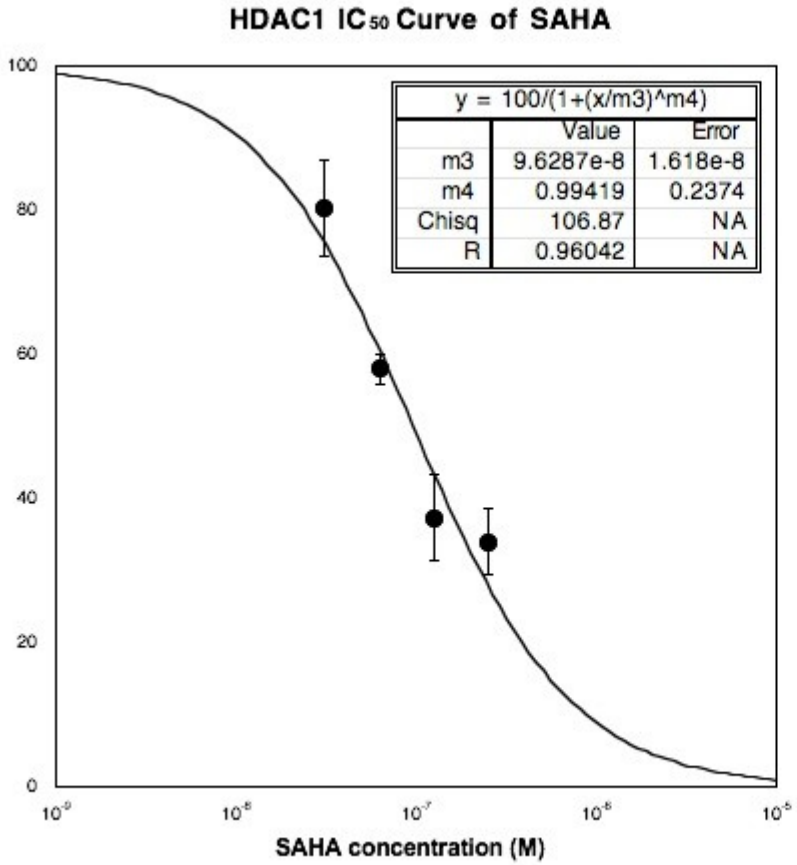

Figure C.7. Dose response curve of SAHA tested using the HDAC1 activity from three independent trials with error bars indicating standard error. Data were fit to the sigmoidal curve using Kaleidograph 4.0 (Synergy Software) to determine the IC_{50}. The insets were the results of the data analysis. The data are reported in Table 3.2.

Table C.9. HDAC3 activity percentage after incubation of SAHA.

Concentration (M)	Trial 1	Trial 2	Trial 3	Mean	Standard Error (S.E.)
3.125×10^{-8}	88	78	74	80	4
6.25×10^{-8}	76	74	70	73	2
1.25×10^{-7}	63	45	44	56	5
2.50×10^{-7}	27	39	37	34	4

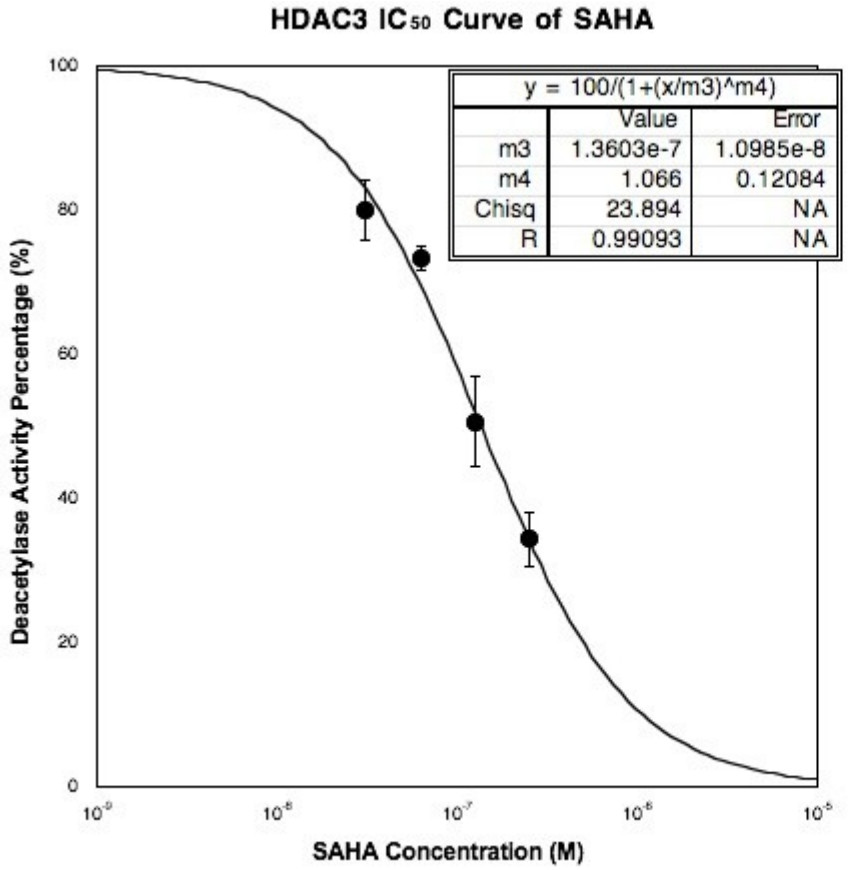

Figure C.8. Dose response curve of SAHA tested using the HDAC3 activity from three independent trials with error bars indicating standard error. Data were fit to the sigmoidal curve using Kaleidograph 4.0 (Synergy Software) to determine the IC_{50}. The insets were the results of the data analysis. The data are reported in Table 3.2.

Table C.10. HDAC6 activity percentage after incubation of SAHA.

Concentration (M)	Trial 1	Trial 2	Trial 3	Mean	Standard Error (S.E.)
3.125×10^{-8}	66	76	73	72	3
6.25×10^{-8}	64	62	60	62	1
1.25×10^{-7}	37	28	32	32	2
2.50×10^{-7}	13	12	9	11	1

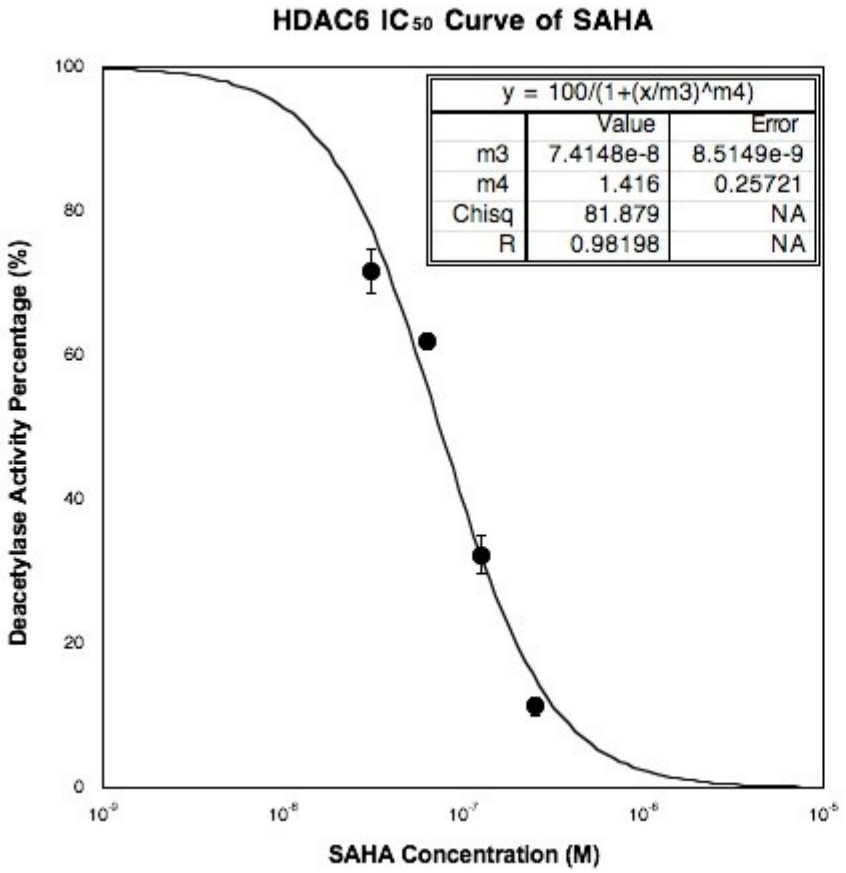

Figure C.9. Dose response curve of SAHA tested using the HDAC6 activity from three independent trials with error bars indicating standard error. In some case, the error bars are smaller than the marker size. Data were fit to the sigmoidal curve using Kaleidograph 4.0 (Synergy Software) to determine the IC_{50}. The insets were the results of the data analysis. The data are reported in Table 3.2.

Table C.11. HDAC1 activity percentage after incubation of C6-SAHA *t*-butyl analogue **14c**.

Concentration (M)	Trial 1	Trial 2	Trial 3	Mean	Standard Error (S.E.)
2.50×10^{-7}	102	92	82	92	5
5.00×10^{-7}	86	85	80	84	1
1.00×10^{-6}	68	44	35	49	9
3.125×10^{-5}	7	1	1	3	2

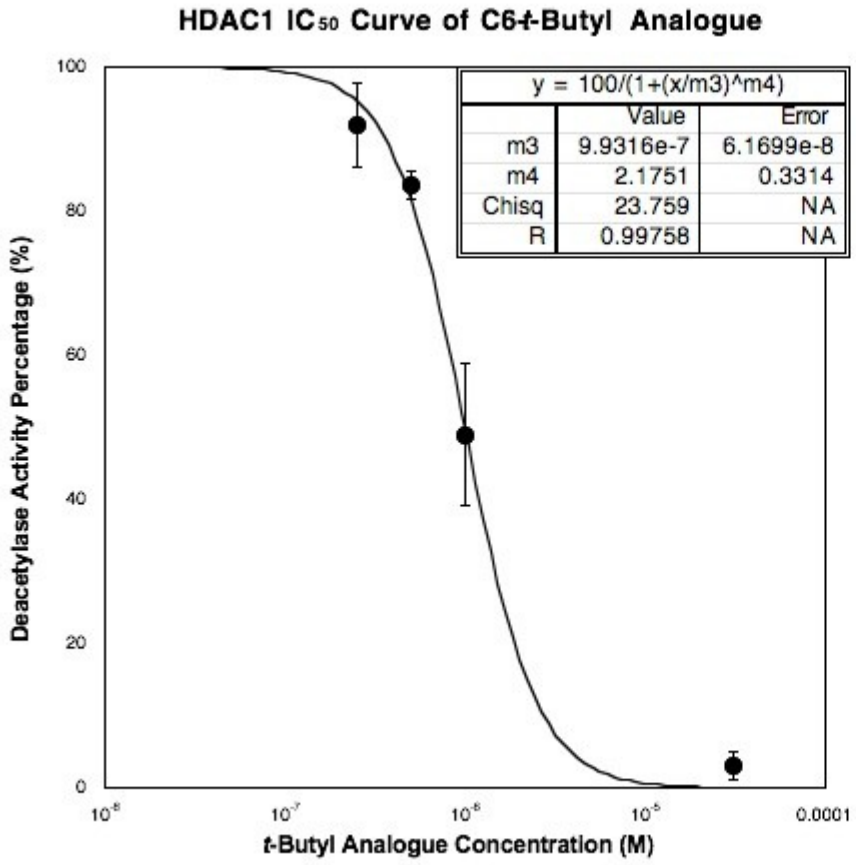

Figure C.10. Dose response curve of C6-SAHA *t*-butyl analogue **14c** tested using the HDAC1 activity from three independent trials with error bars indicating standard error. Data were fit to the sigmoidal curve using Kaleidograph 4.0 (Synergy Software) to determine the IC_{50}. The insets were the results of the data analysis. The data are reported in Table 3.2.

Table C.12. HDAC3 activity percentage after incubation of C6-SAHA *t*-butyl analogue **14c**.

Concentration (M)	Trial 1	Trial 2	Trial 3	Mean	Standard Error (S.E.)
1.00×10^{-6}	87	85	81	84	1
4.00×10^{-6}	76	63	52	64	6
1.5625×10^{-5}	21	20	13	18	2
3.125×10^{-5}	7	6	6	6	-

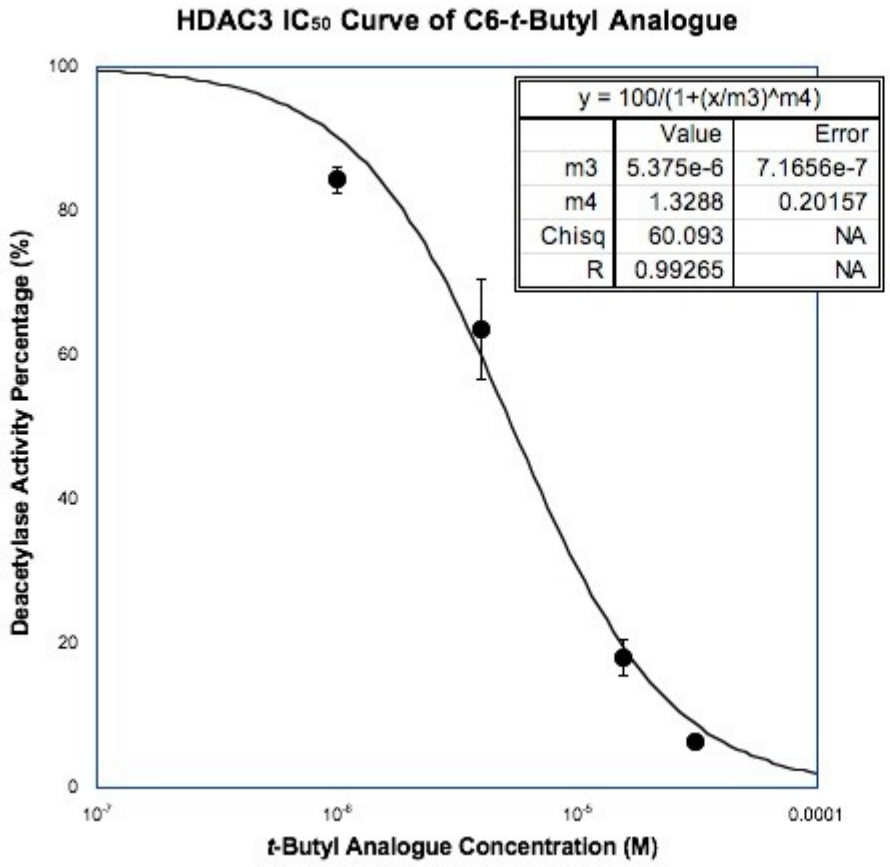

Figure C.11. Dose response curve of C6-SAHA *t*-butyl analogue **14c** tested using the HDAC3 activity from three independent trials. In some case, the error bar is smaller than the marker size. Data were fit to the sigmoidal curve using Kaleidograph 4.0 (Synergy Software) to determine the IC_{50}. The insets were the results of the data analysis. The data are reported in Table 3.2.

Table C.13. HDAC6 activity percentage after incubation of C6-SAHA *t*-butyl analogue **14c**.

Concentration (M)	Trial 1	Trial 2	Trial 3	Mean	Standard Error (S.E.)
5.00×10^{-7}	98	90	88	92	3
1.00×10^{-6}	89	82	86	85	2
2.00×10^{-6}	48	35	48	44	4
4.00×10^{-6}	45	29	45	40	5

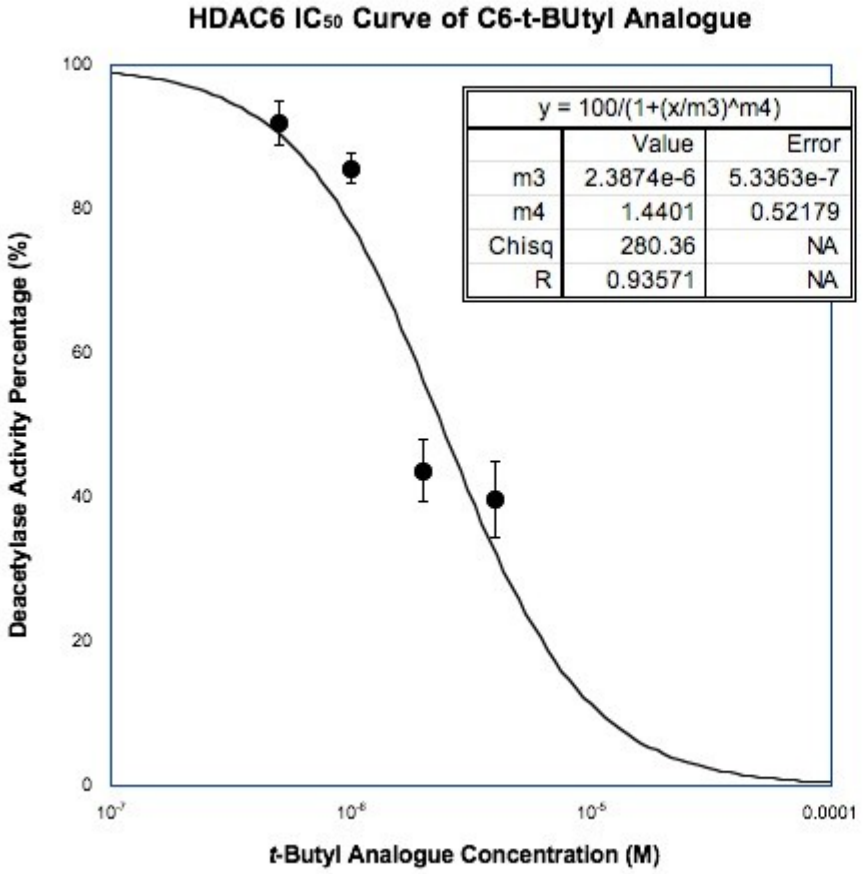

Figure C.12. Dose response curve of C6-SAHA *t*-butyl analogue **14c** tested using the HDAC6 activity from three independent trials with error bars indicating standard error. Data were fit to the sigmoidal curve using Kaleidograph 4.0 (Synergy Software) to determine the IC_{50}. The insets were the results of the data analysis. The data are reported in Table 3.2.

APPENDIX D. SUPPLEMENTARY INFORMATION FOR C6-SAHA LIBRARY

D.1 Methyl 6-hydroxyhexanoate (**9**)

D.1.1 ^{1}H NMR

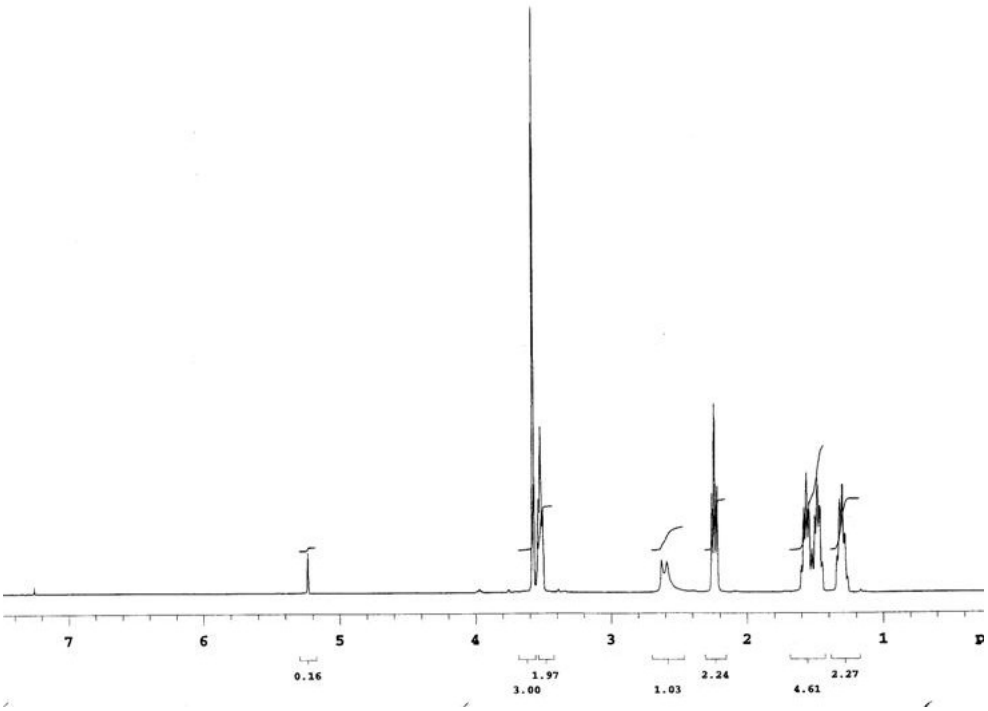

D.1.2 ^{13}C NMR

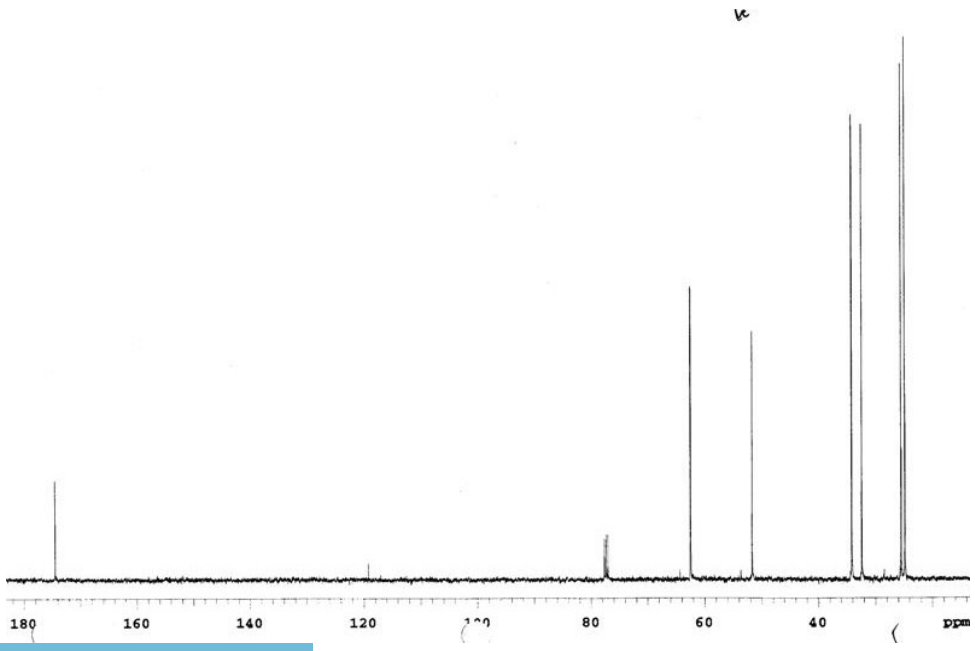

D.1.3 IR

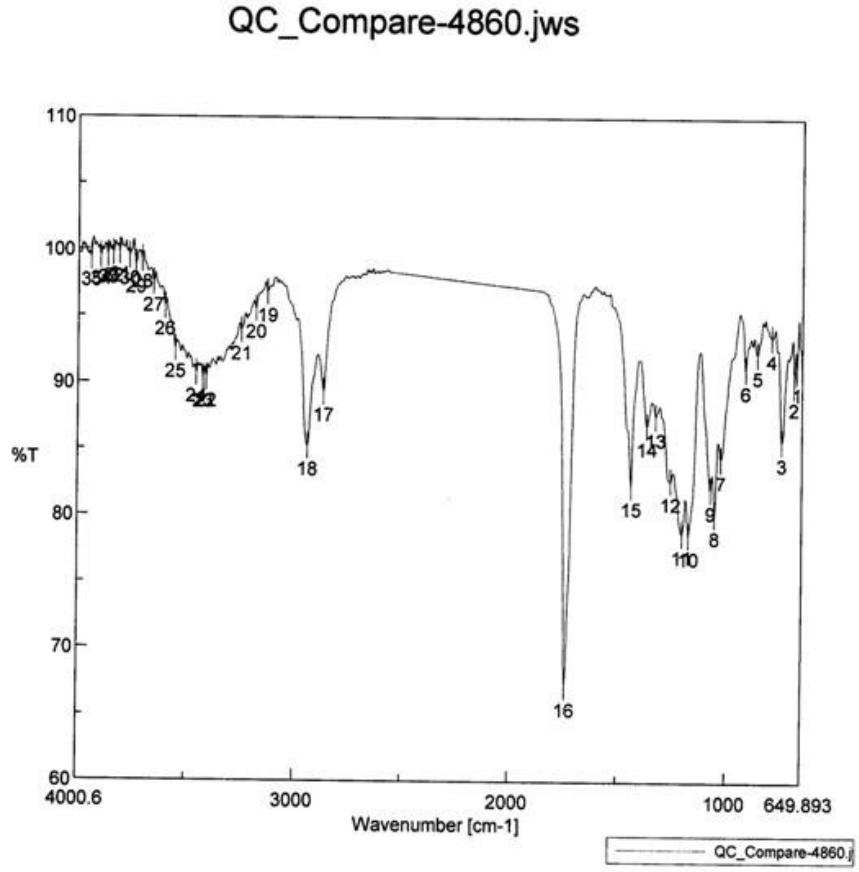

[Comment]	
Sample Name	
Comment	
User	
Division	
Company	wsu

[Data Information]	
Creation Date	4/5/2009 4:18 PM
Data array type	Linear data array
Horizontal	Wavenumber [cm-1]
Vertical	%T
Start	649.893 cm-1
End	4000.6 cm-1
Data pitch	0.964233 cm-1
Data points	3476

Result of Peak Picking

No.	Position	Intensity	No.	Position	Intensity	No.	Position	Intensity
1	673.999	91.0351	2	686.534	89.905	3	744.388	85.6748
4	791.636	93.5149	5	857.204	92.2656	6	912.165	91.108
7	1025.94	84.3461	8	1054.87	80.1357	9	1074.16	82.0291
10	1174.44	78.5907	11	1205.29	78.701	12	1257.36	82.7027
13	1324.86	87.5379	14	1365.35	86.8582	15	1437.67	82.3079
16	1737.55	67.2027	17	2865.7	89.3144	18	2939.95	85.199
19	3127.01	96.7679	20	3181.01	95.5156	21	3247.54	93.8683
22	3408.57	90.3437	23	3423.99	90.2941	24	3453.88	90.6642
25	3551.27	92.5011	26	3599.48	95.7016	27	3652.52	97.485
28	3706.51	99.2434	29	3734.48	98.8638	30	3763.4	99.463
31	3809.69	99.7949	32	3838.61	99.6812	33	3865.61	99.5846
34	3897.43	99.4758	35	3941.79	99.3579			

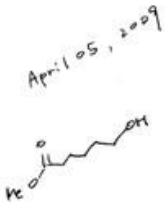

D.1.4 HRMS

Elemental Composition Report **Page 1**

Single Mass Analysis
Tolerance = 5.0 PPM / DBE: min = -1.5, max = 50.0
Element prediction: Off
Number of isotope peaks used for i-FIT = 3

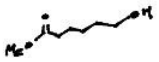

Monoisotopic Mass, Even Electron Ions
31 formula(e) evaluated with 1 results within limits (up to 50 best isotopic matches for each mass)
Elements Used:
C: 0-500 H: 0-1000 O: 0-6 23Na: 0-1
pflum- Sun Choi July2708-C6-alcohol-PG127 mw146 LCT0082 10pg/ul meoh 2ul 4cm stk RF150
Shsy 2008-07b.pro
2008_0818_0082_10 13 (0.300) Cm (10:18-28:45x2.000)

LCT Premier 18-Aug-2008 15:04:26
1: TOF MS ES+
7.98e+003

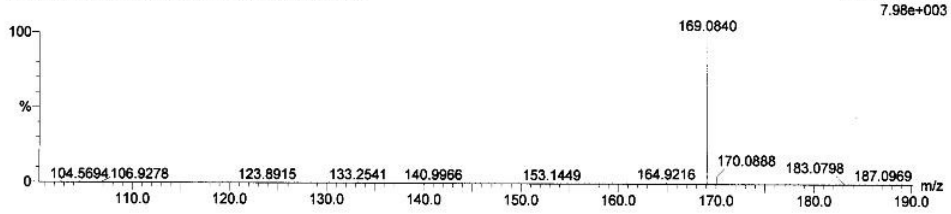

Minimum:				-1.5			
Maximum:		5.0	5.0	50.0			
Mass	Calc. Mass	mDa	PPM	DBE	i-FIT	i-FIT (Norm)	Formula
169.0840	169.0841	-0.1	-0.6	0.5	52.3	0.0	C7 H14 O3 23Na

D.2 1-Benzyl 8-methyl oct-2-enedioate (**11**)

D.2.1 ^{1}H NMR

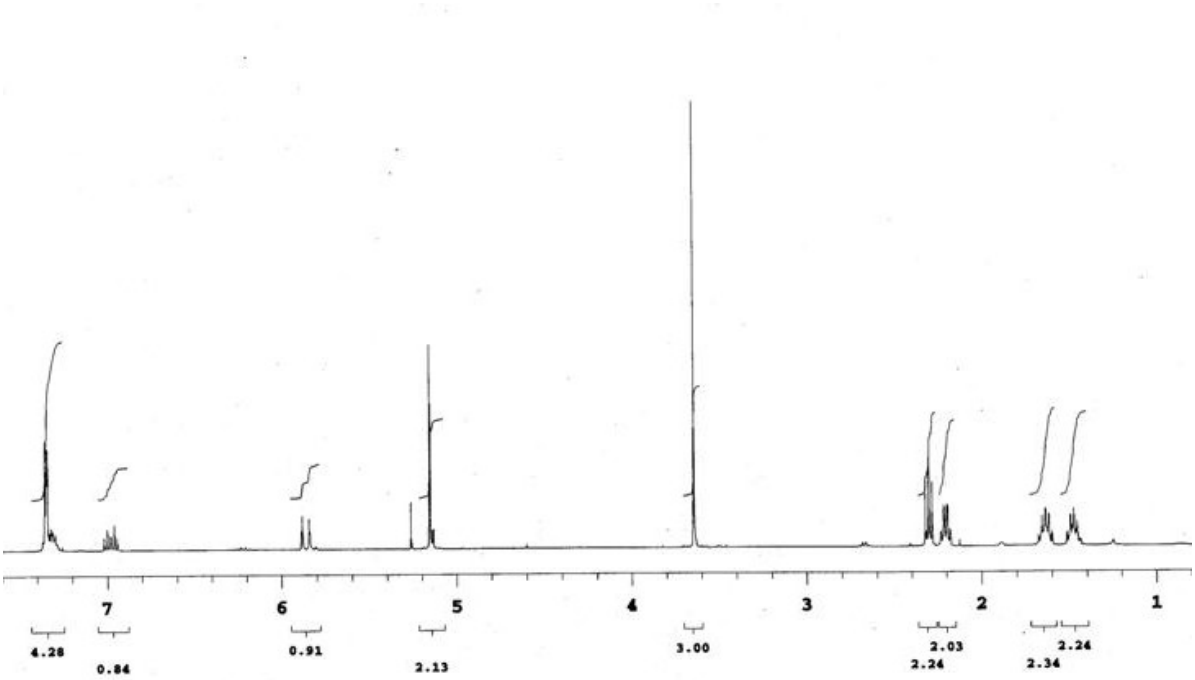

D.2.2 ^{13}C NMR

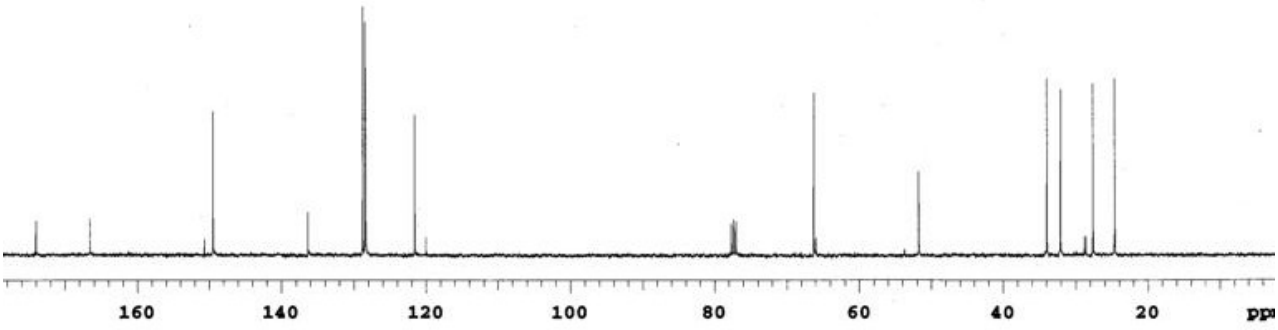

D.2.3 IR

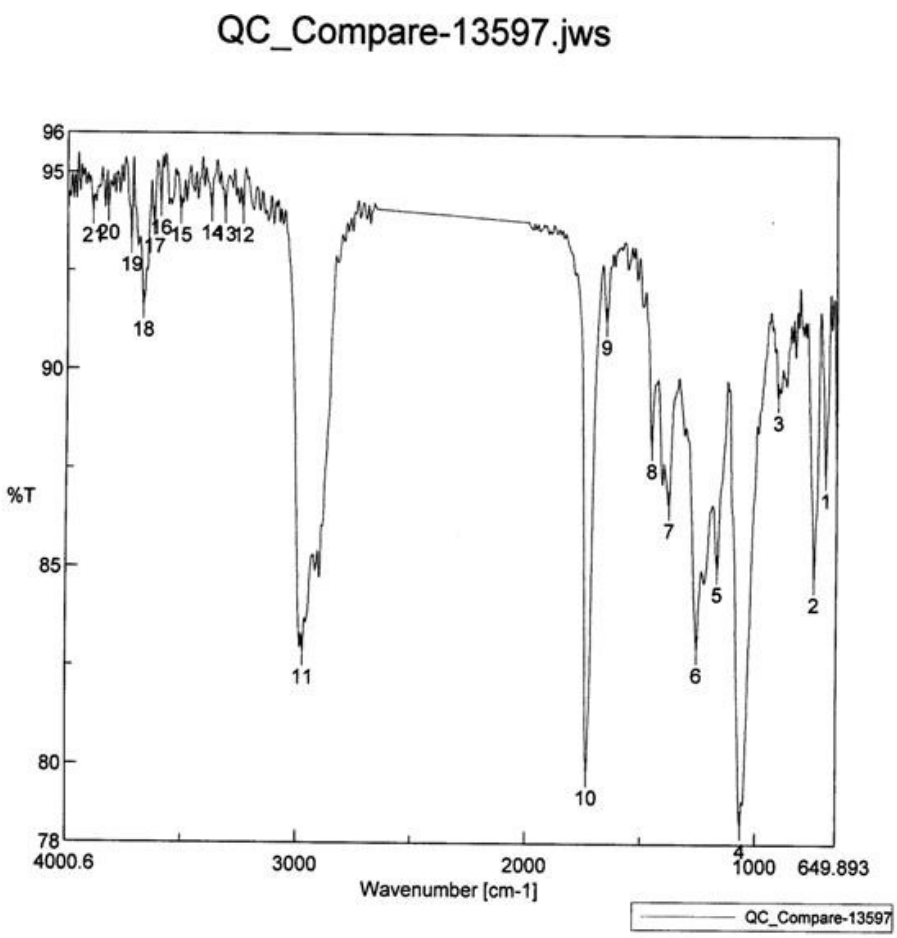

[Comment]		[Data Information]	
Sample Name		Creation Date	10/1/2011 4:48 PM
Comment		Data array type	Linear data array
User		Horizontal	Wavenumber [cm-1]
Division		Vertical	%T
Company	wsu	Start	649.893 cm-1
		End	4000.6 cm-1
		Data pitch	0.964233 cm-1
		Data points	3476

Result of Peak Picking

No.	Position	Intensity	No.	Position	Intensity	No.	Position	Intensity
1	698.105	87.3824	2	748.245	84.7388	3	907.344	89.3488
4	1066.44	78.4833	5	1169.62	84.977	6	1258.32	82.9455
7	1378.85	86.5885	8	1455.03	88.0995	9	1652.7	91.234
10	1734.66	79.812	11	2973.7	82.8371	12	3240.79	94.0265
13	3317.93	94.0414	14	3376.75	94.0754	15	3508.85	94.0252
16	3594.66	94.2108	17	3623.59	93.731	18	3670.84	91.5991
19	3722.91	93.2618	20	3823.19	94.0722	21	3889.72	93.989

D.2.4 HRMS

Elemental Composition Report **Page 1**

Single Mass Analysis
Tolerance = 5.0 PPM / DBE: min = -1.5, max = 50.0
Element prediction: Off
Number of isotope peaks used for i-FIT = 3

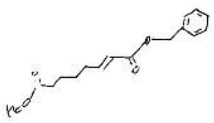

Monoisotopic Mass, Even Electron Ions
423 formula(e) evaluated with 3 results within limits (up to 50 best isotopic matches for each mass)
Elements Used:
C: 0-500 H: 0-1000 N: 0-5 O: 0-10 23Na: 0-1
pflum- Sun Choi Aug2008-C6-ester-PG143 mw276 LCT0102 10pg/ul meoh 1ul
Shay 2008-07b.pro
2008_0822_0102_17 14 (0.300) Cm (13:16-(1:6+36:42)x2.000)

LCT Premier 22-Aug-2008 15:13:23
1: TOF MS ES+
9.59e+003

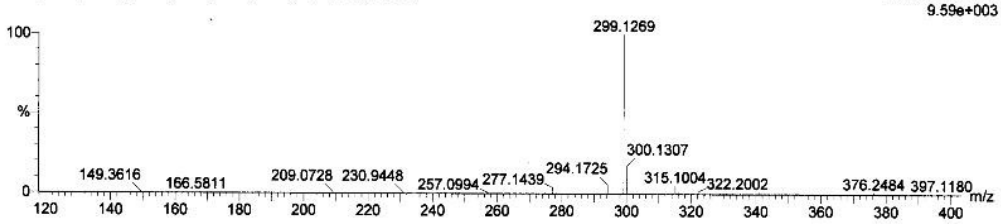

Minimum:				-1.5						
Maximum:		2.0	5.0	50.0						
Mass	Calc. Mass	mDa	PPM	DBE	i-FIT	i-FIT (Norm)	Formula			
299.1269	299.1273	-0.4	-1.3	11.5	44.7	0.5	C17	H16	N4	23Na
	299.1259	1.0	3.3	6.5	45.6	1.4	C16	H20	O4	23Na
	299.1283	-1.4	-4.7	9.5	46.2	2.0	C18	H19	O4	

D.3 1-Benzyl 8-methyl 3-methyloctanedioate (**12a**)

D.3.1 ^{1}H NMR

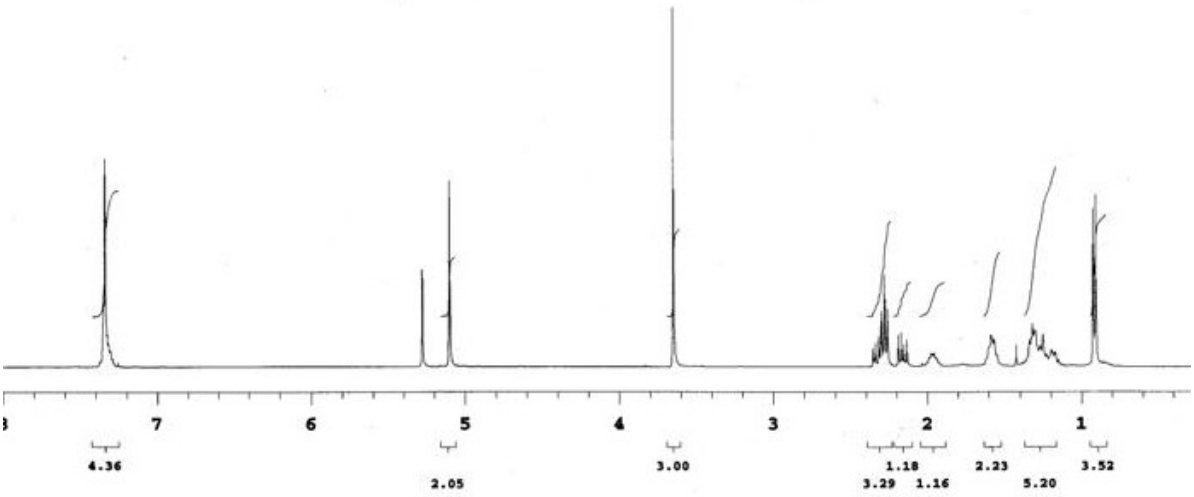

D.3.2 ^{13}C NMR

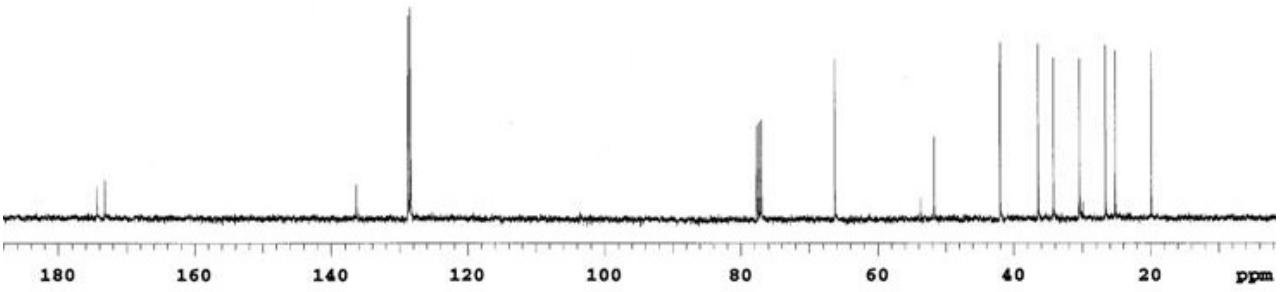

D.3.3 HRMS

Elemental Composition Report

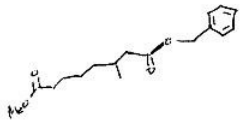

Page 1

Single Mass Analysis
Tolerance = 5.0 PPM / DBE: min = -1.5, max = 50.0
Element prediction: Off
Number of isotope peaks used for i-FIT = 3

Monoisotopic Mass, Even Electron Ions
269 formula(e) evaluated with 2 results within limits (up to 50 closest results for each mass)
Elements Used:
C: 0-50 H: 0-100 N: 0-4 O: 0-6 23Na: 0-1
Pflum- Sun Choi Aug2608-C6-Methylester Pg156 mw292 LCT0129 10pg/ul meoh 2ul 4cm stk
Shay 2008-07b.pro
2008_0827_0129_10 14 (0.300) Cm (12:18-(1:7+32:46)x2.000)

LCT Premier 27-Aug-2008 16:10:20
1: TOF MS ES+
4.12e+004

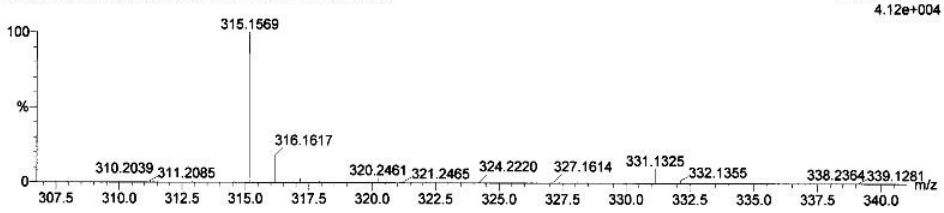

Minimum:				-1.5			
Maximum:		5.0	5.0	50.0			
Mass	Calc. Mass	mDa	PPM	DBE	i-FIT	i-FIT (Norm)	Formula
315.1569	315.1572	-0.3	-1.0	5.5	37.4	2.3	C17 H24 O4 23Na
	315.1556	1.3	4.1	4.5	35.1	0.1	C14 H23 N2 O6

D.4 1-Benzyl 8-methyl 3-(*tert*-butyl)octanedioate (**12c**)

D.4.1 ^{1}H NMR

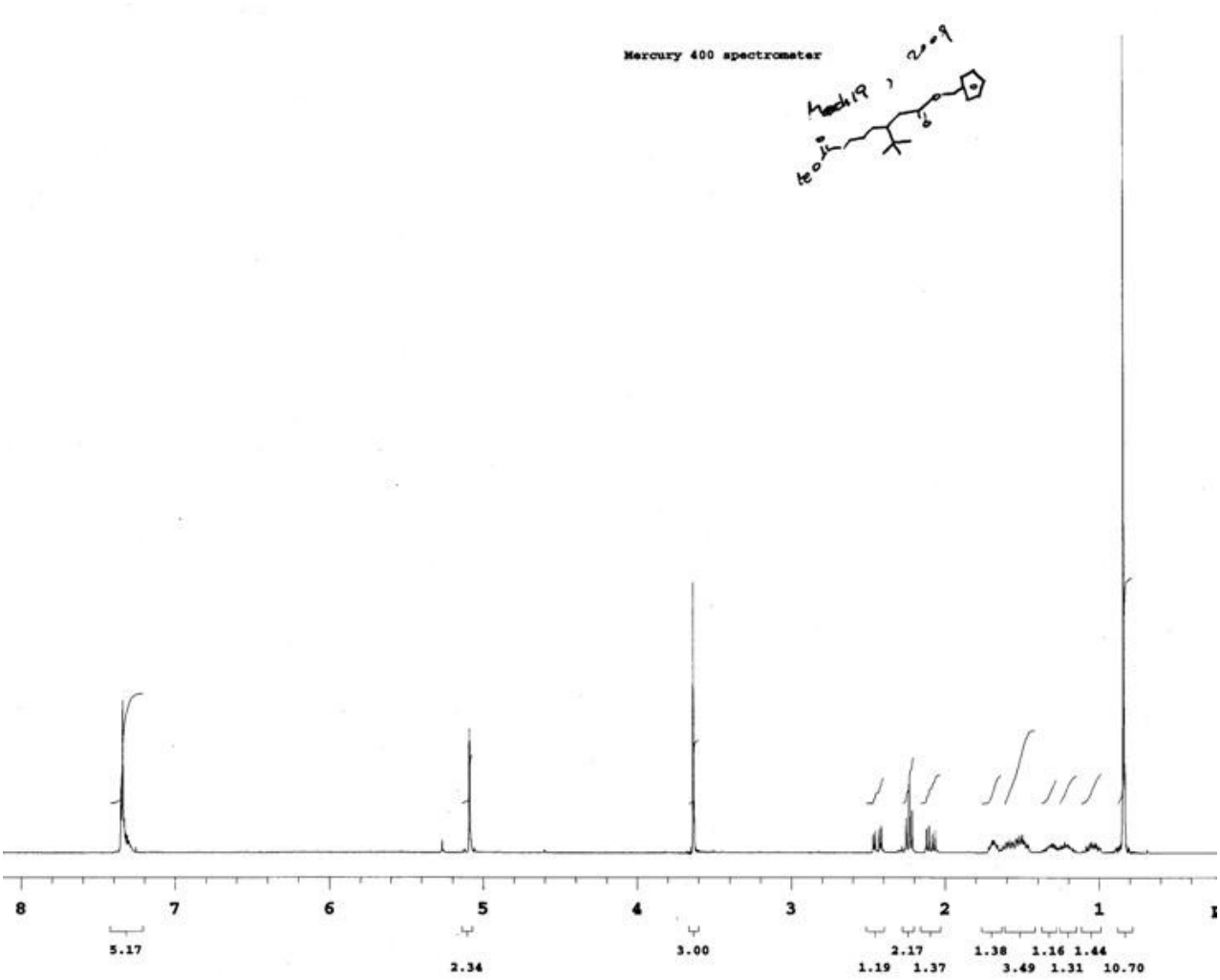

D.4.2 ^{13}C NMR

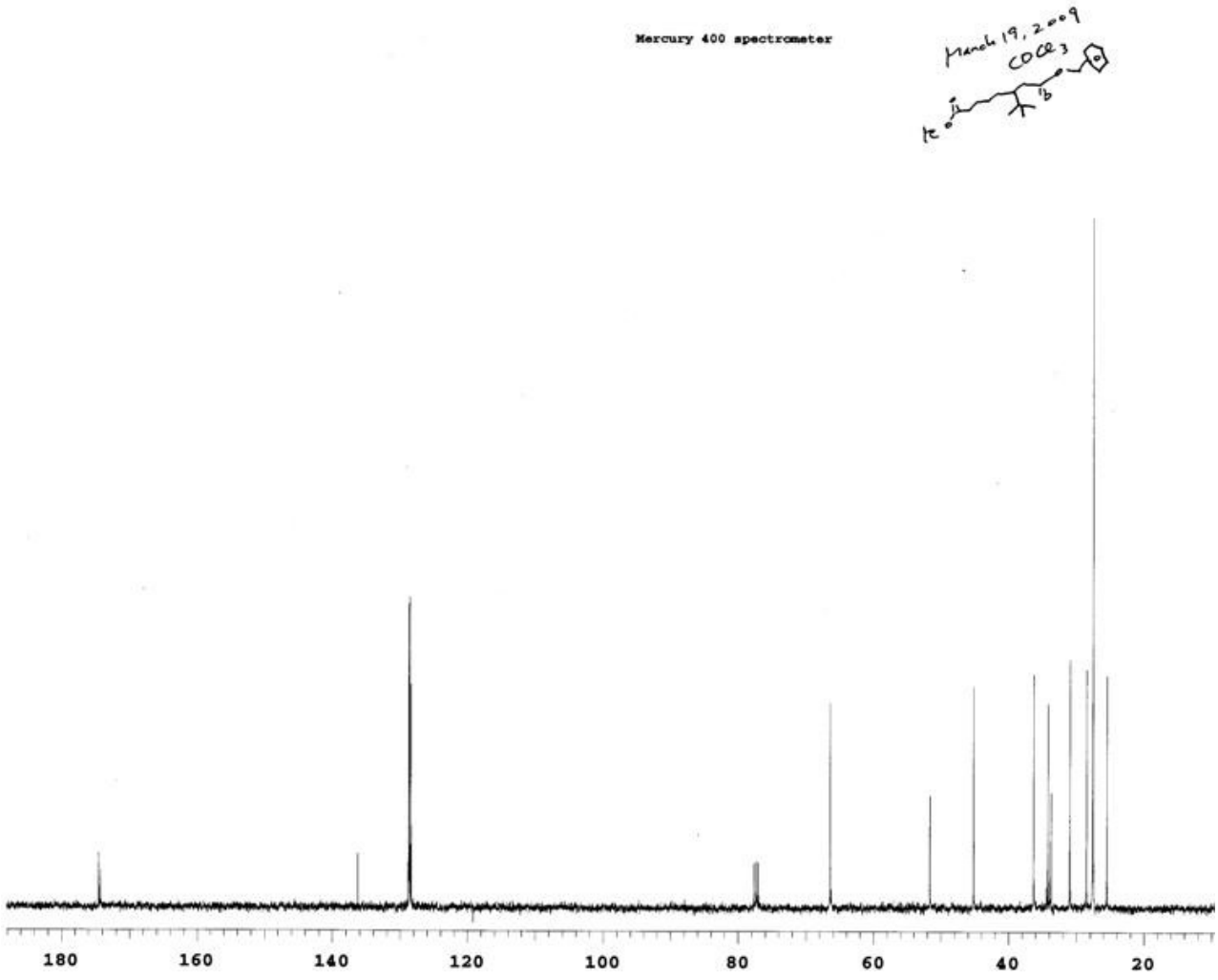

D.4.3 IR

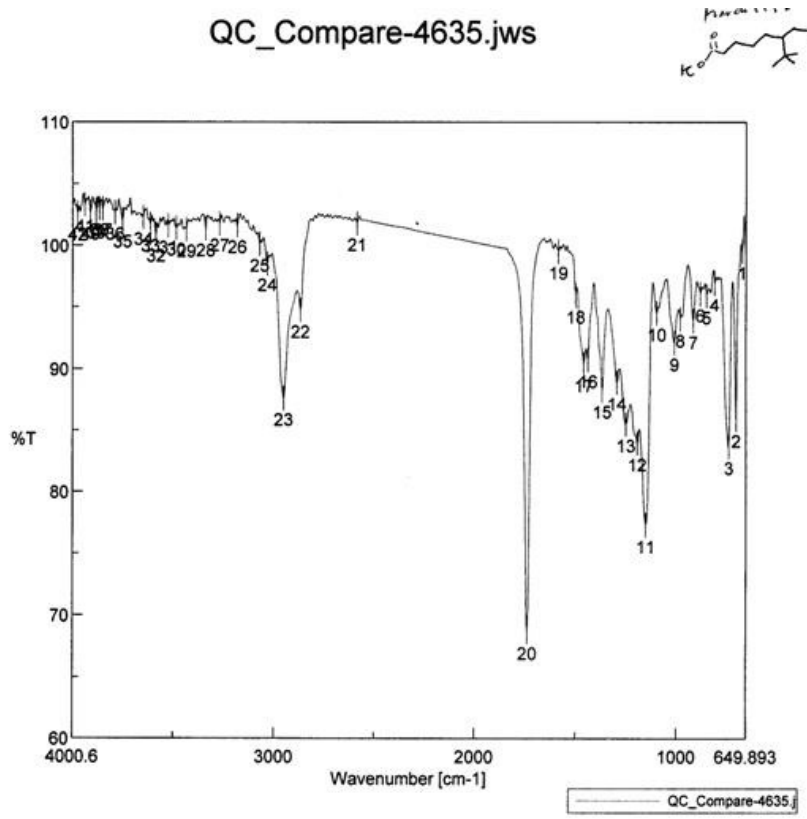

[Comment]
Sample Name
Comment
User
Division
Company wsu

[Data Information]

Creation Date	3/19/2009 5:00 PM
Data array type	Linear data array
Horizontal	Wavenumber [cm-1]
Vertical	%T
Start	649.893 cm-1
End	4000.6 cm-1
Data pitch	0.964233 cm-1
Data points	3476

Result of Peak Picking

No.	Position	Intensity	No.	Position	Intensity	No.	Position	Intensity
1	669.178	99.4871	2	699.069	85.8577	3	736.674	83.6462
4	806.099	96.8893	5	846.597	95.8718	6	877.452	96.0518
7	914.093	93.8752	8	978.697	94.0256	9	1008.59	92.0753
10	1096.33	94.4782	11	1151.29	77.2669	12	1193.72	83.9463
13	1250.61	85.4742	14	1294	88.8751	15	1367.28	88.219
16	1437.67	90.699	17	1456.96	90.3703	18	1497.45	95.8946
19	1582.31	99.4924	20	1736.58	68.6225	21	2586.07	101.761
22	2868.59	94.6945	23	2952.48	87.5955	24	3033.48	98.4804
25	3071.08	100.071	26	3182.93	101.59	27	3270.68	101.724
28	3340.1	101.305	29	3436.53	101.217	30	3485.7	101.363
31	3525.24	101.541	32	3586.95	100.855	33	3613.95	101.664
34	3649.62	102.214	35	3751.83	102.022	36	3789.44	102.634
37	3849.22	102.954	38	3866.58	102.952	39	3882.97	102.729
40	3911.9	102.652	41	3938.89	103.26	42	3975.53	102.557

D.4.4 LRMS [M+Li]

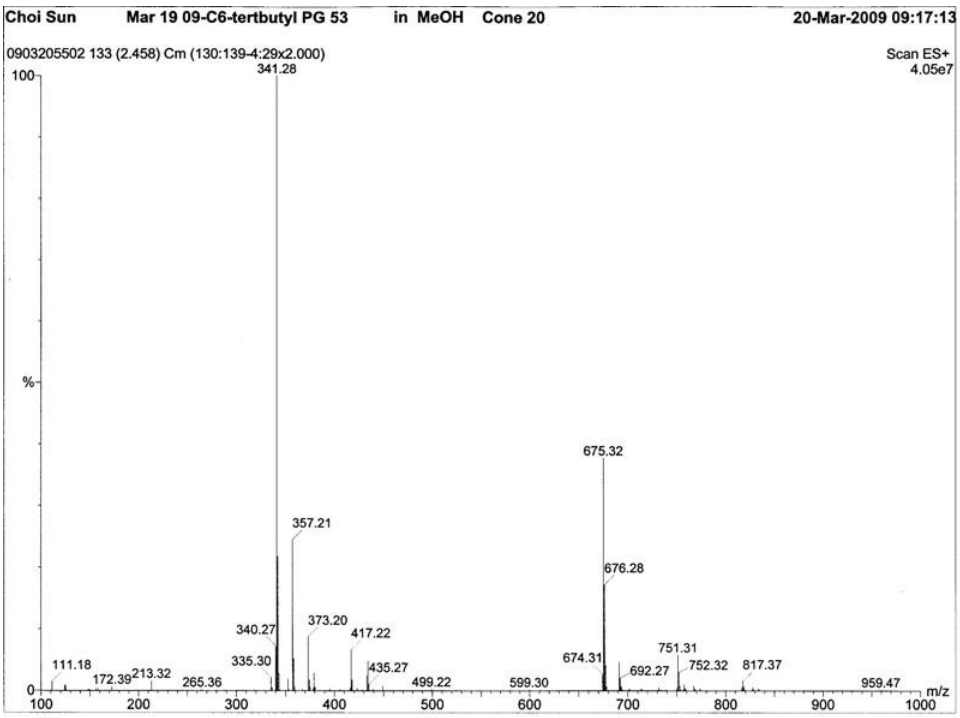

D.5 1-Benzyl 8-methyl 3-(2-ethylhexyl)octanedioate (**12d**)
D.5.1 ^{1}H NMR

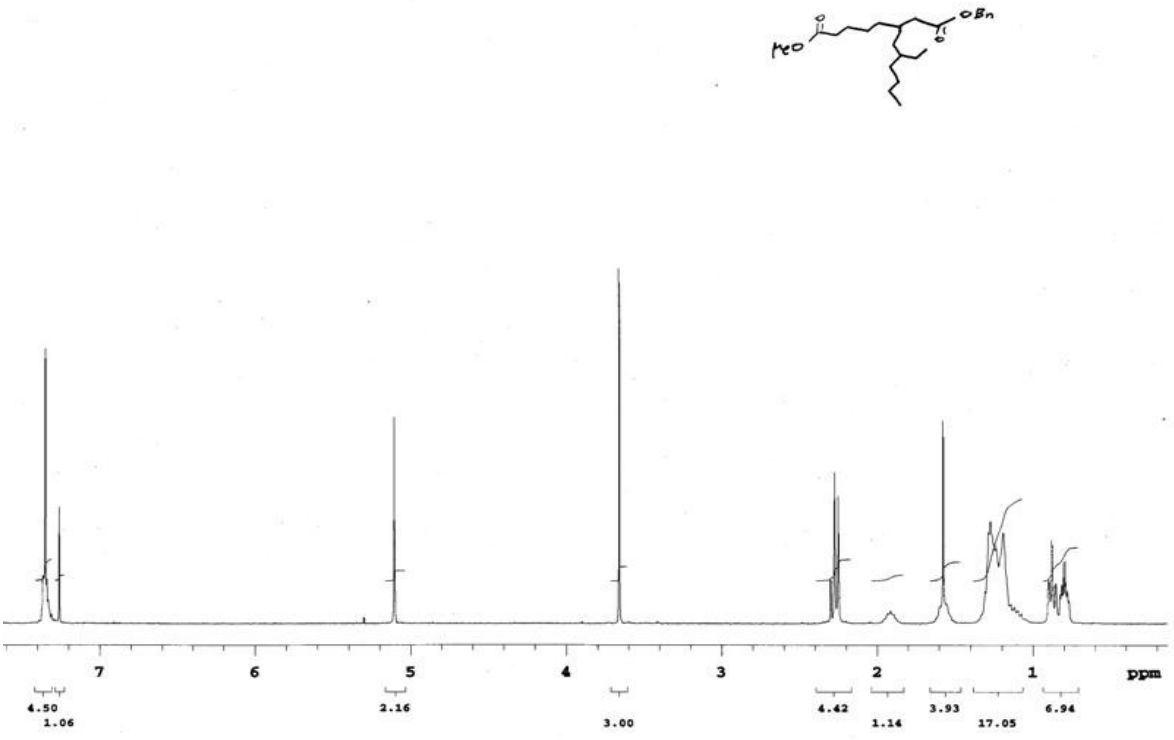

D.5.2 ^{13}C NMR

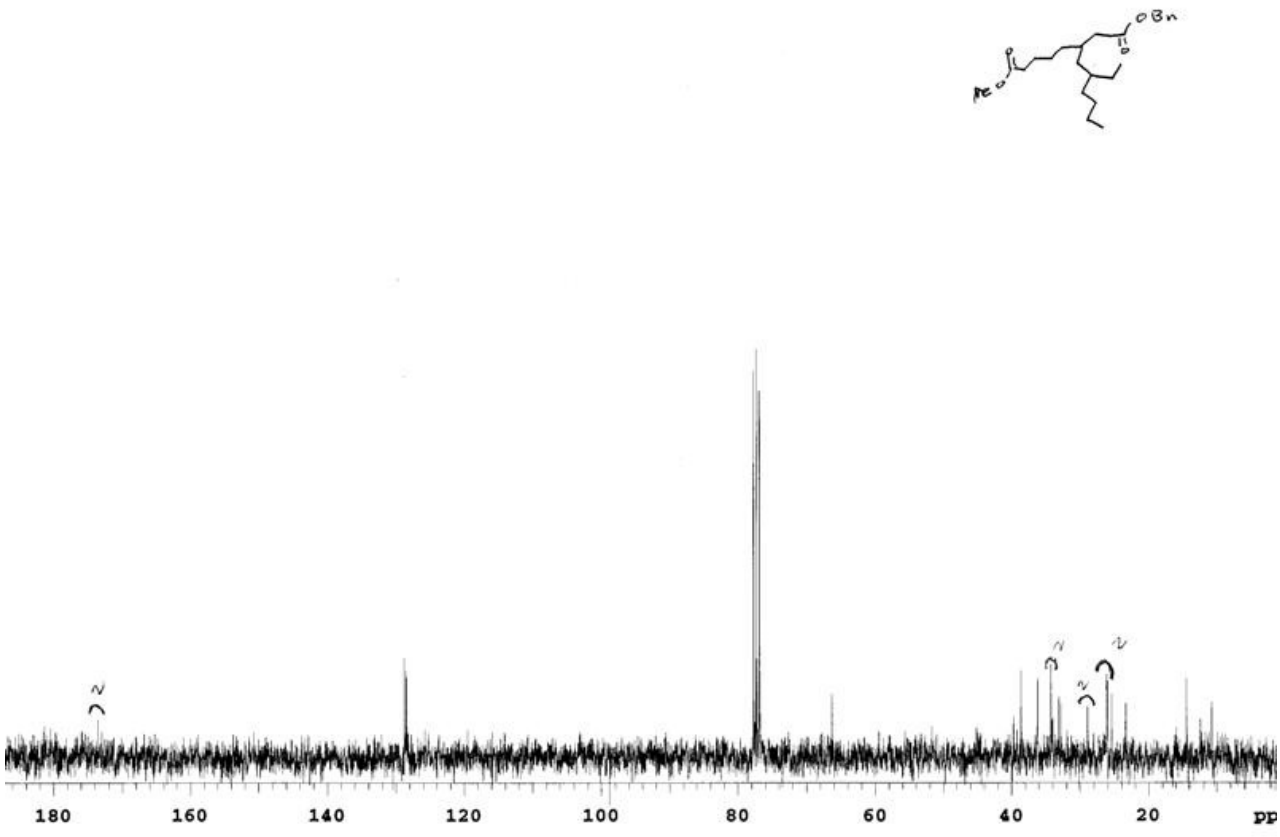

D.5.3 IR

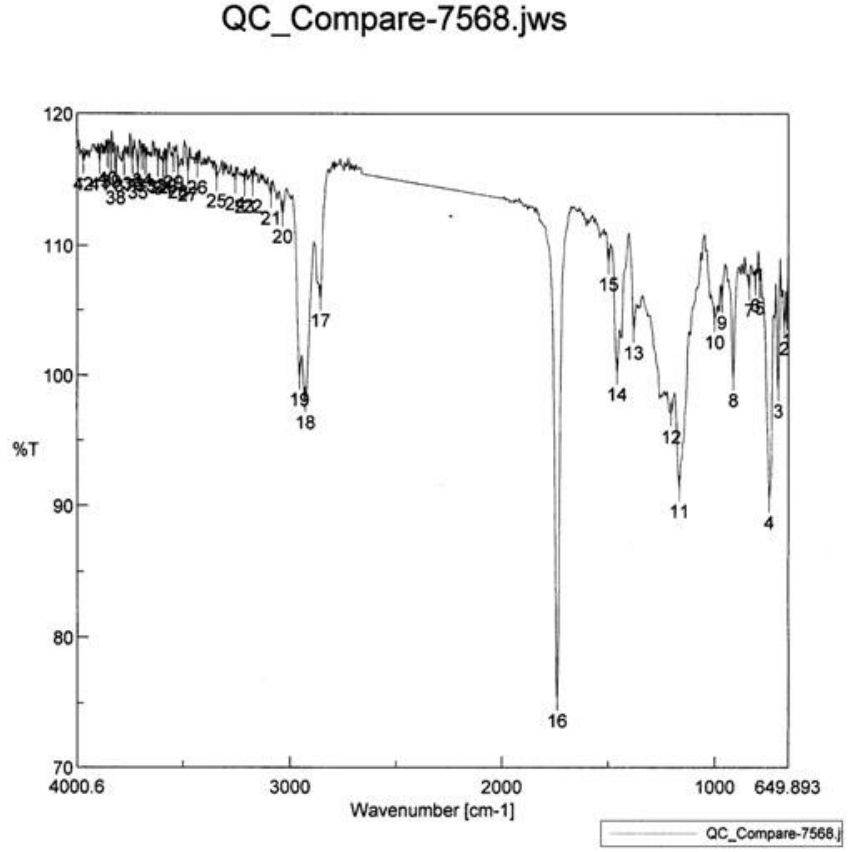

[Comment]
Sample Name
Comment
User
Division
Company wsu

[Data Information]

Creation Date	5/17/2010 4:16 PM
Data array type	Linear data array
Horizontal	Wavenumber [cm-1]
Vertical	%T
Start	649.893 cm-1
End	4000.6 cm-1
Data pitch	0.964233 cm-1
Data points	3476

Result of Peak Picking

No.	Position	Intensity	No.	Position	Intensity	No.	Position	Intensity
1	656.643	104.479	2	668.214	103.802	3	699.069	99.0019
4	741.496	90.4552	5	785.85	106.916	6	807.063	107.131
7	836.955	106.774	8	912.165	99.8285	9	966.162	105.812
10	1000.87	104.295	11	1166.72	91.32	12	1204.33	97.0088
13	1379.82	103.466	14	1456.96	100.25	15	1497.45	108.741
16	1738.51	75.3619	17	2857.99	105.93	18	2929.34	98.1008
19	2956.34	99.8614	20	3035.41	112.411	21	3090.37	113.821
22	3176.19	114.703	23	3213.79	114.713	24	3257.18	114.896
25	3344.93	115.133	26	3435.56	116.164	27	3479.92	115.608
28	3525.24	115.79	29	3547.41	116.525	30	3579.23	116.3
31	3593.7	116.121	32	3618.77	116.178	33	3677.59	116.319
34	3693.98	116.703	35	3713.26	115.775	36	3739.3	116.415
37	3779.8	116.288	38	3818.36	115.358	39	3841.51	116.604
40	3855.97	116.852	41	3893.57	116.403	42	3971.68	116.405

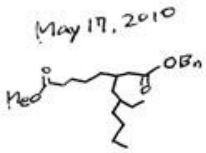

D.5.4 LRMS [M+K], [M+Li], and [M+Na]

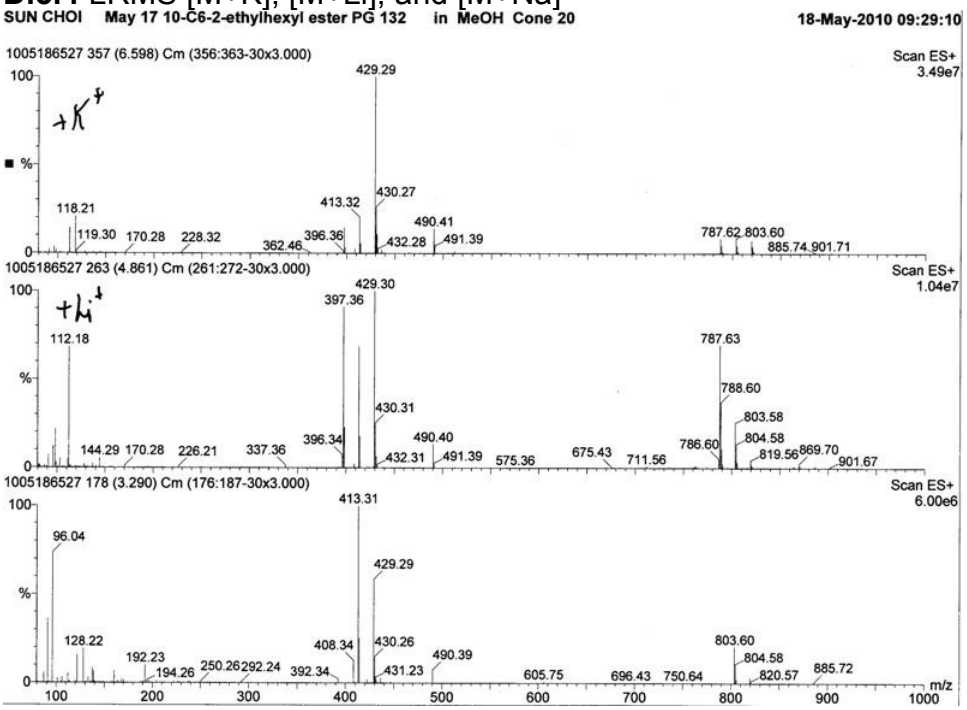

D.6.1 1-Benzyl 8-methyl 3-isopropyloctanedioate (**12e**)

D.6.1 ^{1}H NMR

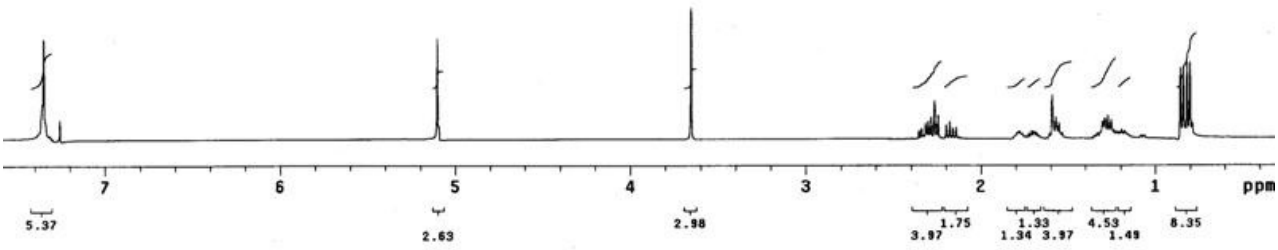

D.6.2 ^{13}C NMR

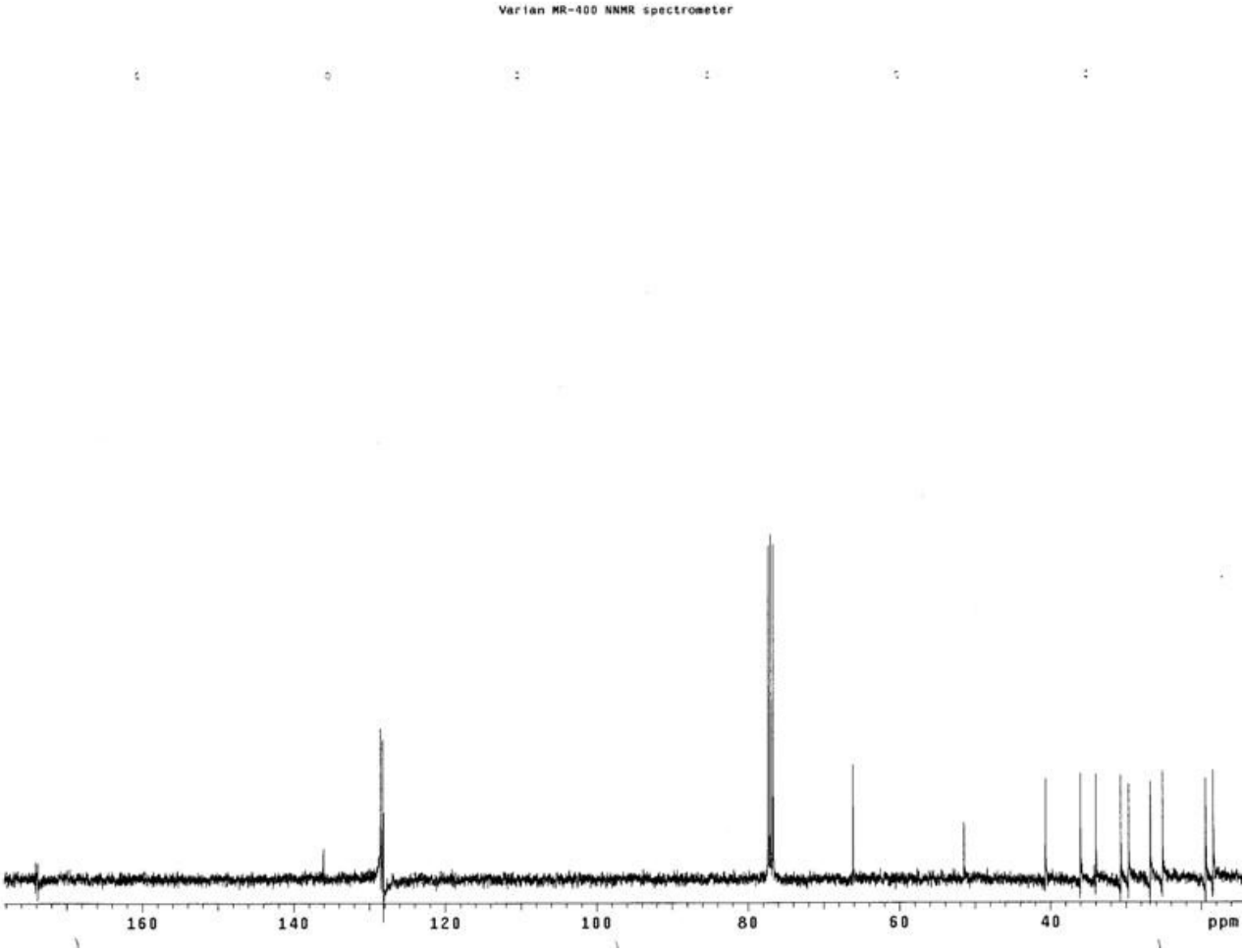

D.6.3 IR

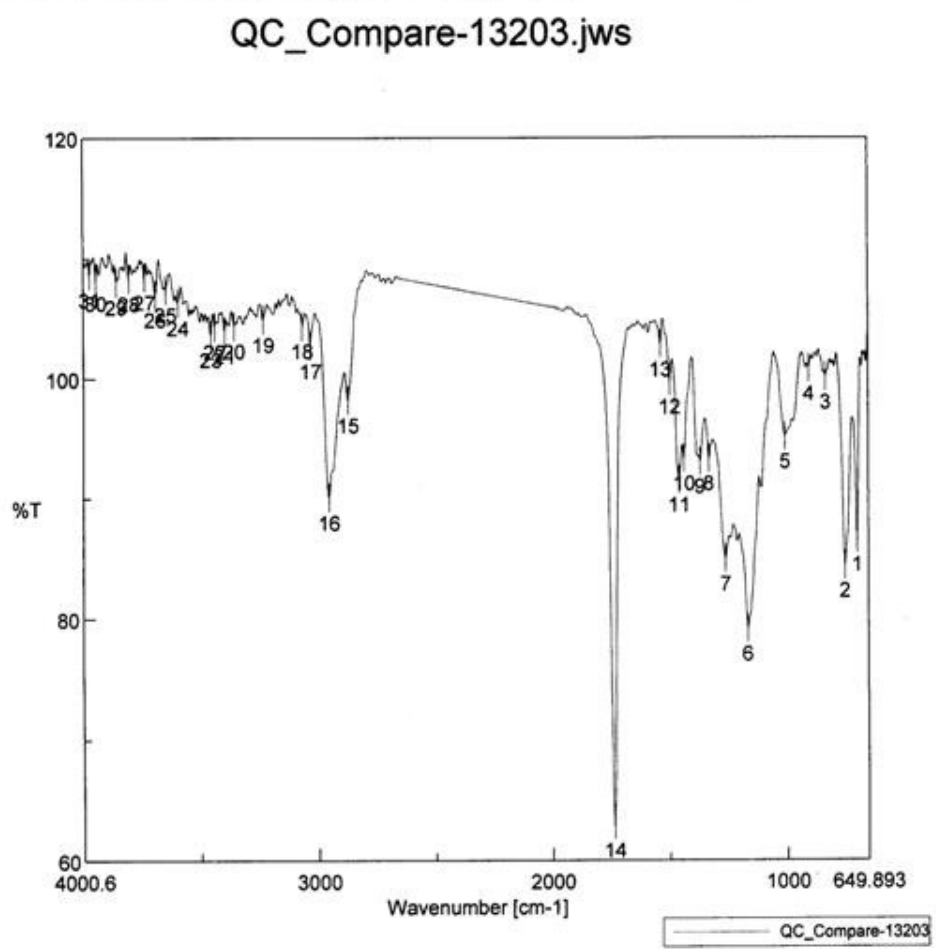

[Comment]	
Sample Name	
Comment	
User	
Division	
Company	wsu

[Data Information]	
Creation Date	8/30/2011 2:08 PM
Data array type	Linear data array
Horizontal	Wavenumber [cm-1]
Vertical	%T
Start	649.893 cm-1
End	4000.6 cm-1
Data pitch	0.964233 cm-1
Data points	3476

Result of Peak Picking

No.	Position	Intensity	No.	Position	Intensity	No.	Position	Intensity
1	698.105	86.5607	2	750.174	84.3826	3	833.098	100.086
4	905.415	100.779	5	1007.62	95.1192	6	1166.72	79.1288
7	1261.22	84.9644	8	1331.61	93.3073	9	1369.21	93.0366
10	1436.71	93.2952	11	1457.92	91.5472	12	1498.42	99.7057
13	1536.99	102.807	14	1736.58	62.9414	15	2873.42	98.1547
16	2954.41	90.0358	17	3032.51	102.67	18	3066.26	104.337
19	3233.07	104.837	20	3355.53	104.313	21	3396.03	103.939
22	3438.46	104.291	23	3454.85	103.619	24	3595.63	106.262
25	3646.73	107.379	26	3690.12	106.951	27	3737.37	108.42
28	3804.87	108.301	29	3857.9	107.98	30	3945.64	108.33
31	3972.64	108.599						

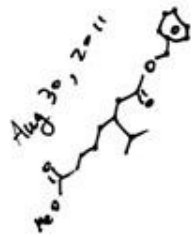

D.6.4 HRMS

Single Mass Analysis
Tolerance = 5.0 PPM / DBE: min = -1.5, max = 150.0
Element prediction: Off
Number of isotope peaks used for i-FIT = 6

Monoisotopic Mass, Even Electron Ions
845 formula(e) evaluated with 4 results within limits (up to 50 closest results for each mass)
Elements Used:
C: 0-100 H: 0-1000 N: 0-10 O: 0-10 23Na: 0-1

SUN CHOI Aug 20 11-C6-Isopropylester
LCT2008-07b.pro 2010-clf.spl

2011_0822_2184 14 (0.283) Cm (11:19-1:8x2.000)

22-Aug-2011LCT Premier10:11:10
1: TOF MS ES+
2.56e+004

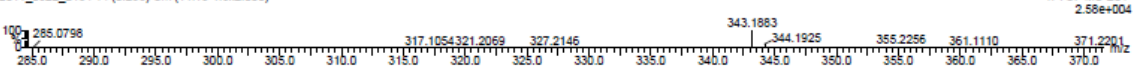

Minimum:				-1.5						
Maximum:		50.0	5.0	150.0						
Mass	Calc. Mass	mDa	PPM	DBE	i-FIT	i-FIT (Norm)	Formula			
343.1883	343.1882	0.1	0.3	9.5	60.4	2.1	C17	H23	N6	O2
	343.1885	-0.2	-0.6	5.5	60.4	2.2	C19	H28	O4	23Na
	343.1869	1.4	4.1	4.5	63.1	4.8	C16	H27	N2	O6
	343.1899	-1.6	-4.7	10.5	58.5	0.3	C20	H24	N4	23Na

D.7 Methyl 6-methyl-8-oxo-8-(phenylamino)octanoate (**13a**)

D.7.1 ^{1}H NMR

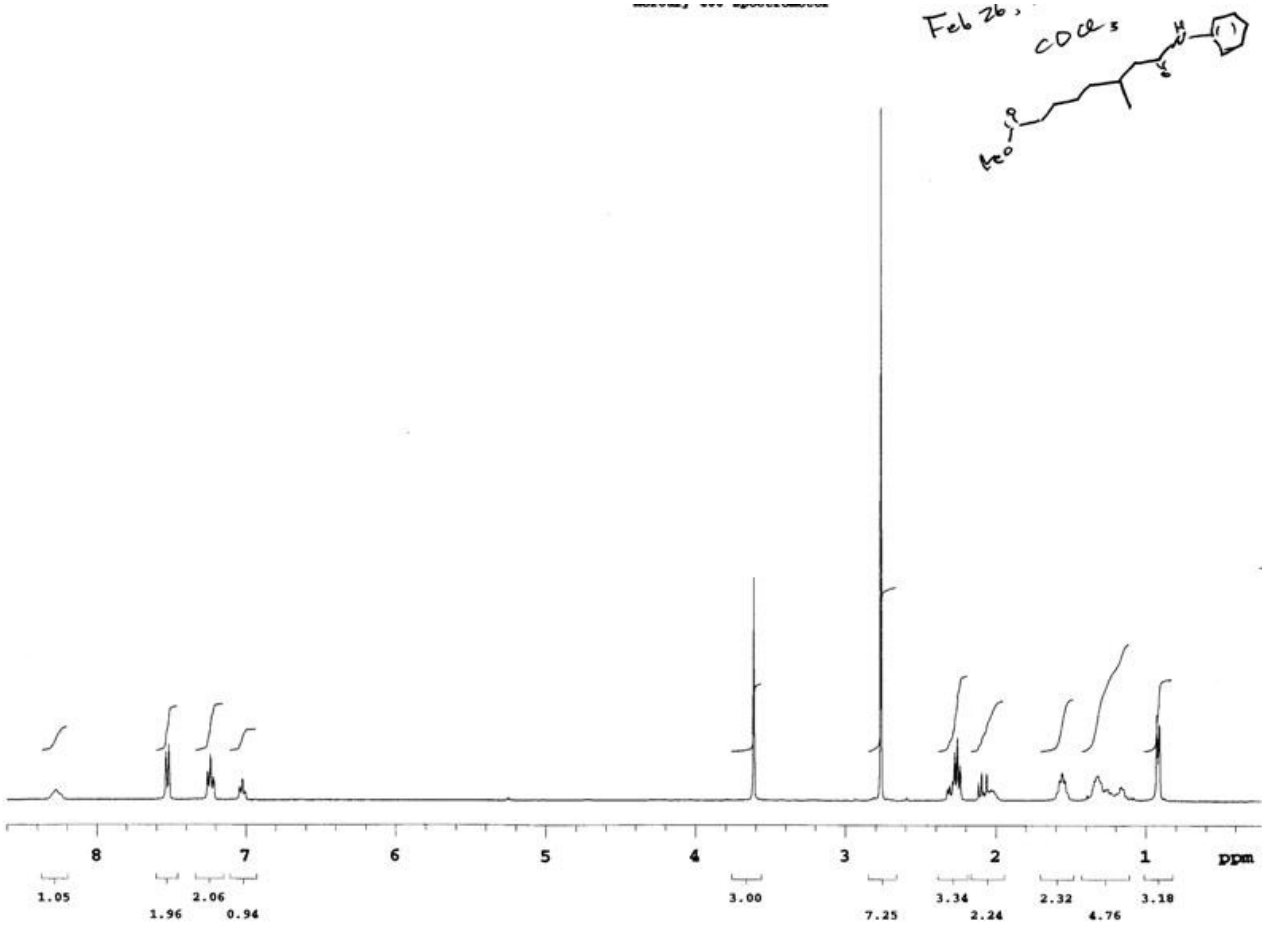

D.7.2 ^{13}C NMR

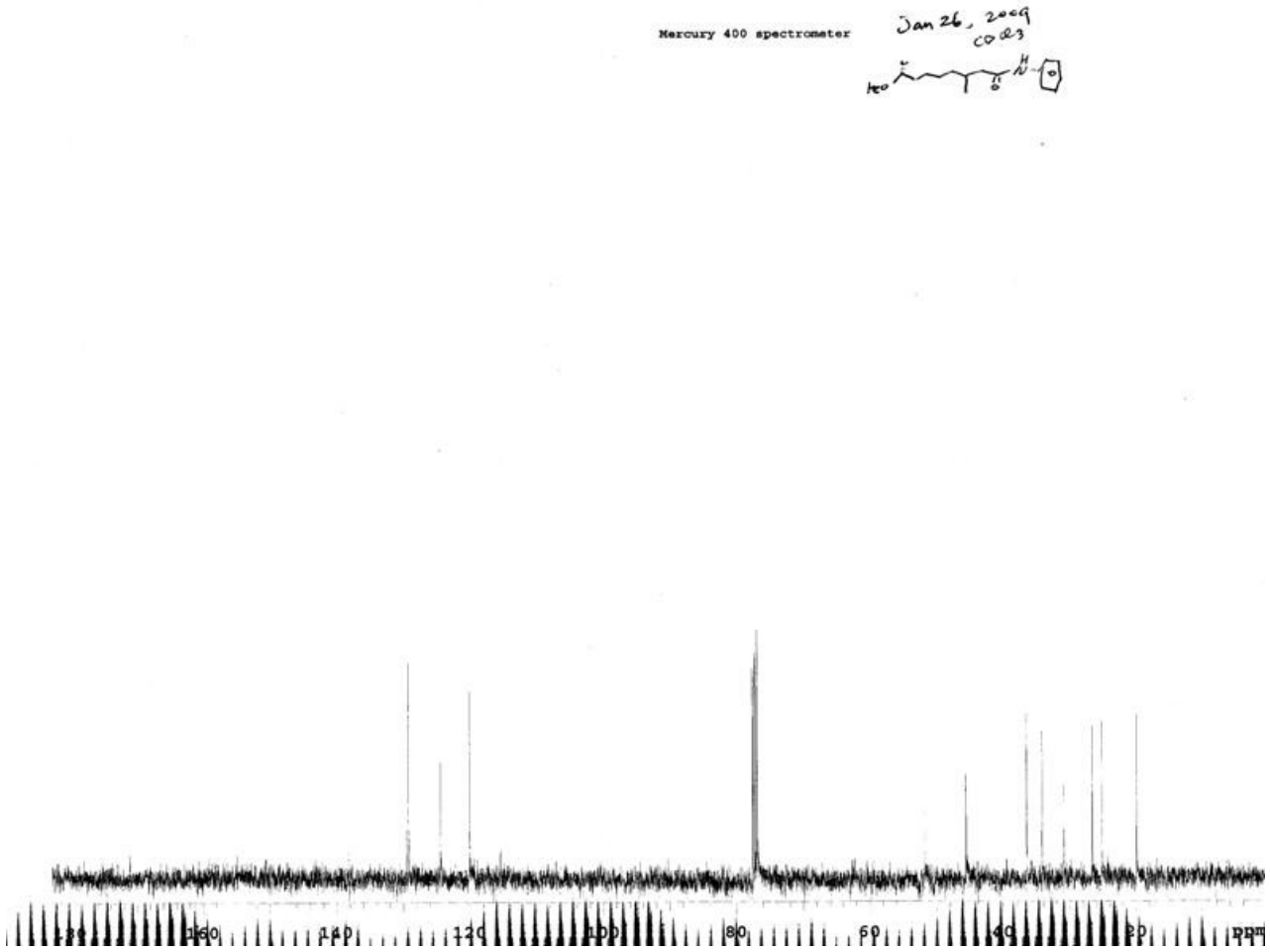

D.7.3 IR

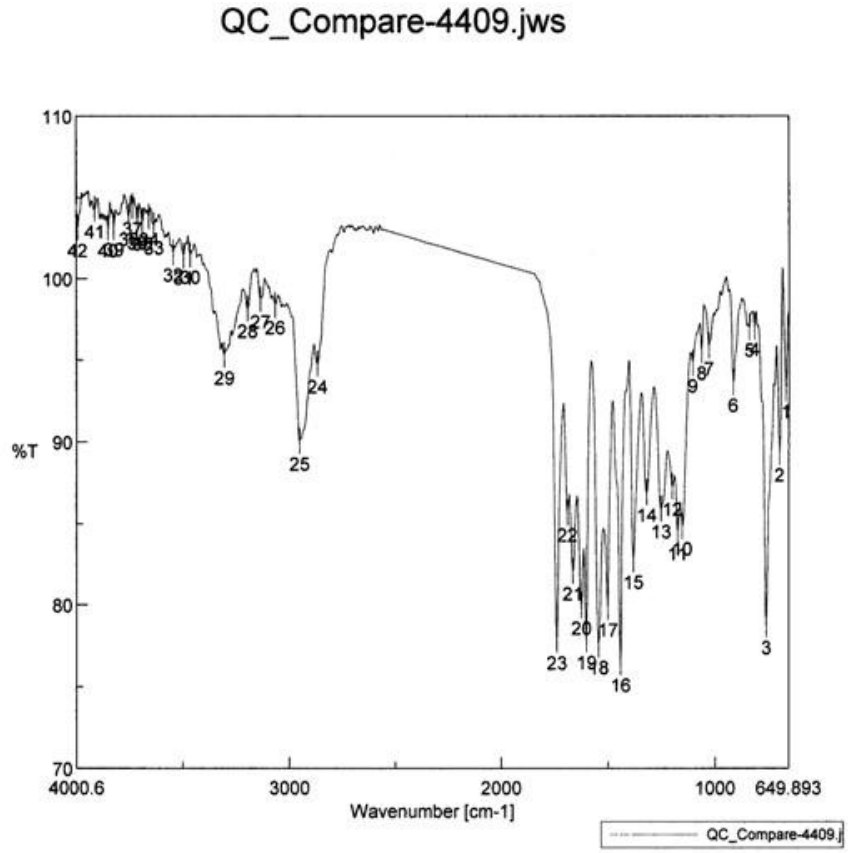

[Comment]
Sample Name
Comment
User
Division
Company wsu

[Data Information]

Creation Date	2/26/2009 12:25 PM
Data array type	Linear data array
Horizontal	Wavenumber [cm-1]
Vertical	%T
Start	649.893 cm-1
End	4000.6 cm-1
Data pitch	0.964233 cm-1
Data points	3476

Result of Peak Picking

No.	Position	Intensity	No.	Position	Intensity	No.	Position	Intensity
1	664.357	93.2486	2	693.284	89.3793	3	756.923	78.7849
4	813.813	97.0377	5	837.919	97.0001	6	913.129	93.6316
7	1028.84	95.8579	8	1062.59	95.5843	9	1105.01	94.8123
10	1151.29	84.8491	11	1173.47	84.5418	12	1198.54	87.2668
13	1250.61	85.8924	14	1318.11	86.9138	15	1379.82	82.7804
16	1441.53	76.481	17	1500.35	79.8401	18	1543.74	77.5712
19	1600.63	77.879	20	1623.77	79.9496	21	1662.34	82.0668
22	1688.37	85.694	23	1738.51	77.845	24	2867.63	94.7622
25	2952.48	90.0183	26	3066.26	98.3501	27	3135.69	98.727
28	3196.43	98.1515	29	3306.36	95.2862	30	3464.49	101.469
31	3495.35	101.413	32	3544.52	101.606	33	3634.2	103.291
34	3658.3	103.815	35	3688.19	103.531	36	3711.33	103.589
37	3734.48	104.472	38	3751.83	103.806	39	3822.22	103.174
40	3849.22	103.129	41	3912.86	104.278	42	3993.86	103.131

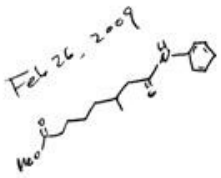

D.7.4 HRMS

Elemental Composition Report

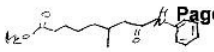

Page 1

Single Mass Analysis
Tolerance = 5.0 PPM / DBE: min = -1.5, max = 50.0
Element prediction: Off
Number of isotope peaks used for i-FIT = 3

Monoisotopic Mass, Even Electron Ions
768 formula(e) evaluated with 2 results within limits (up to 50 best isotopic matches for each mass)
Elements Used:
C: 2-70 H: 0-100 N: 0-13 O: 0-20 23Na: 0-1
Sun Choi Jan 29, 09-C6-methylaniline PG35
Lew 2008-07b.pro
2009_0130_0292 18 (0.388) Cm (18:23-(32:34+2:5)x2.000)

LCT Premier 30-Jan-2009 14:06:27
1: TOF MS ES+
5.13e+003

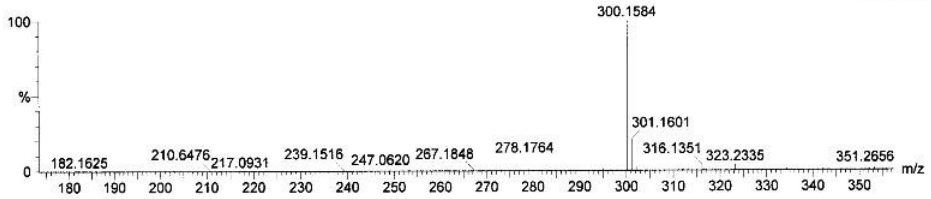

Minimum:				-1.5			
Maximum:		5.0	5.0	50.0			
Mass	Calc. Mass	mDa	PPM	DBE	i-FIT	i-FIT (Norm)	Formula
278.1764	278.1756	0.8	2.9	5.5	48.3	0.9	C16 H24 N O3
	278.1777	-1.3	-4.7	-0.5	48.0	0.5	C4 H21 N11 O2 23Na

D.8 Methyl 6-(*tert*-butyl)-8-oxo-8-(phenylamino)octanoate (**13c**)
D.8.1 ^{1}H NMR

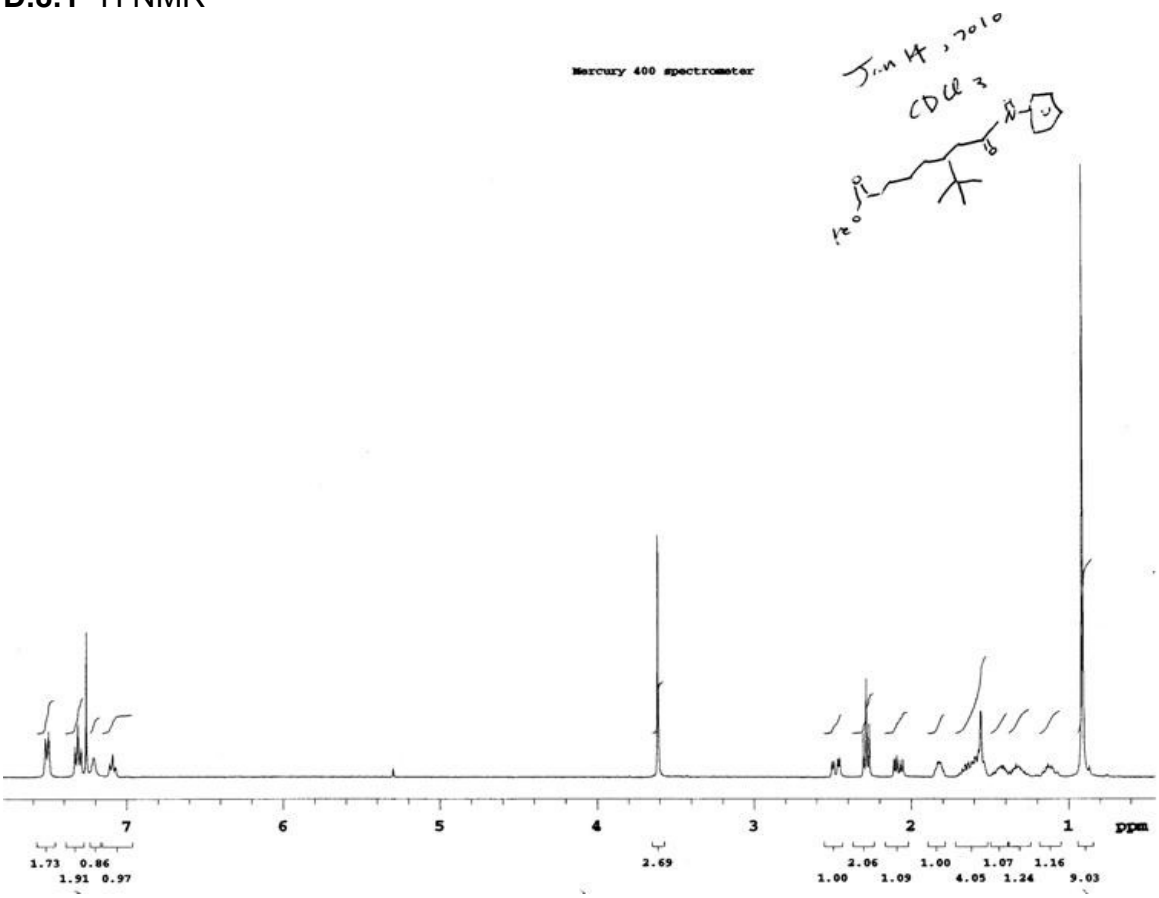

D.8.2 ^{13}C NMR

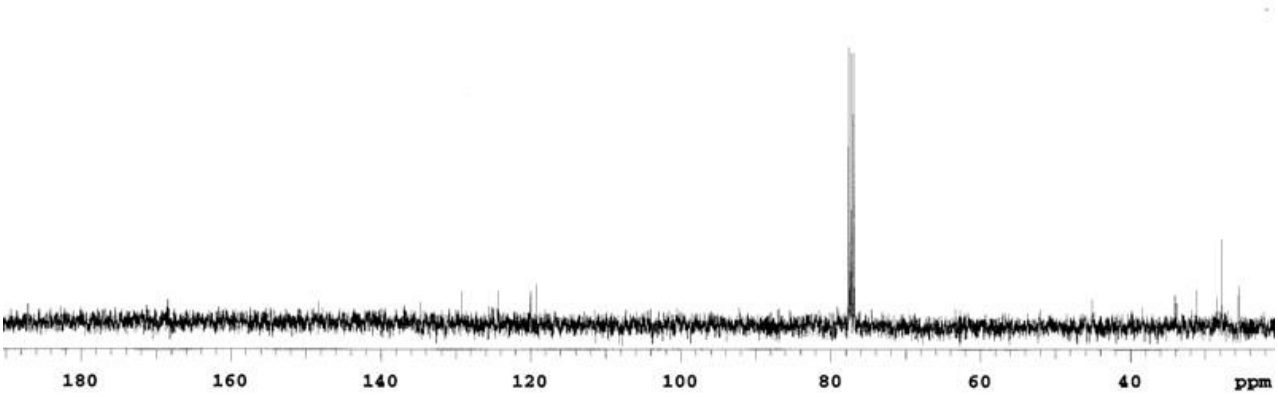

D.8.3 IR

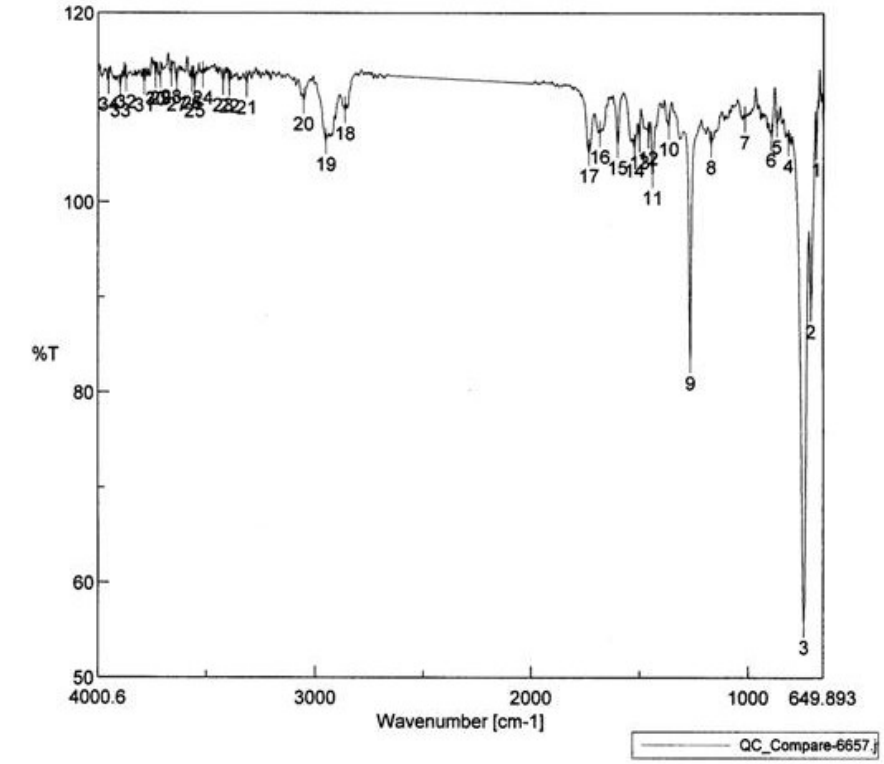

[Comment]
Sample Name
Comment
User
Division
Company wsu

[Data Information]

Creation Date	2/12/2010 5:28 PM
Data array type	Linear data array
Horizontal	Wavenumber [cm-1]
Vertical	%T
Start	649.893 cm-1
End	4000.6 cm-1
Data pitch	0.964233 cm-1
Data points	3476

Result of Peak Picking

No.	Position	Intensity	No.	Position	Intensity	No.	Position	Intensity
1	682.677	105.886	2	705.819	88.8522	3	740.531	55.6477
4	812.849	106.271	5	866.846	108.283	6	891.916	106.889
7	1016.3	108.771	8	1171.54	106.138	9	1265.07	83.4313
10	1366.32	108.067	11	1439.6	102.911	12	1458.89	107.077
13	1500.35	106.649	14	1522.52	105.774	15	1599.66	106.098
16	1680.66	107.264	17	1731.76	105.205	18	2864.74	109.708
19	2952.48	106.414	20	3054.69	110.697	21	3316	112.457
22	3396.03	112.588	23	3424.96	112.704	24	3517.52	113.469
25	3555.13	112.096	26	3566.7	112.93	27	3637.09	112.726
28	3662.16	113.556	29	3712.3	113.405	30	3734.48	113.351
31	3786.54	112.704	32	3871.4	113.011	33	3898.4	112.097

D.8.4 HRMS

Elemental Composition Report **Page 1**

Single Mass Analysis
Tolerance = 5.0 PPM / DBE: min = -1.5, max = 50.0
lement prediction: Off
Number of isotope peaks used for i-FIT = 3

Monoisotopic Mass, Even Electron Ions
1251 formula(e) evaluated with 4 results within limits (all results (up to 1000) for each mass)
Elements Used:
C: 0-70 H: 0-100 N: 0-20 O: 0-20 Na: 0-1
2010_0114_0759a 13 (0.283) Cm (11:16-(1:8+37:45)x2.000)
LCT Premier 15-Jan-2010 11:23:13 SUN, CHOI Jan 14 10 - C5-t-butylanilide
1: TOF MS ES+ 1.15e+004

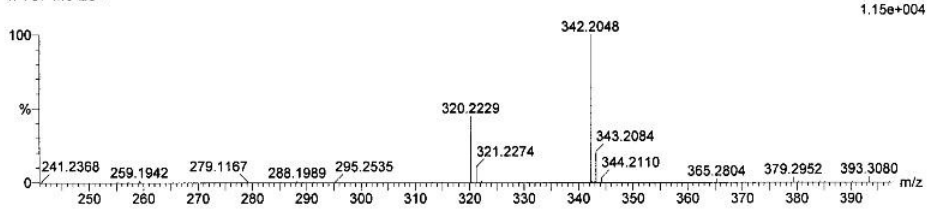

Minimum:				-1.5			
Maximum:		5.0	5.0	50.0			
Mass	Calc. Mass	mDa	PPM	DBE	i-FIT	i-FIT (Norm)	Formula
320.2229	320.2226	0.3	0.9	5.5	21.5	0.0	C19 H30 N O3 ←
	320.2244	-1.5	-4.7	3.5	31.6	10.1	C5 H22 N17
	320.2231	-0.2	-0.6	-1.5	31.9	10.4	C4 H26 N13 O4
	320.2220	0.9	2.8	0.5	33.5	12.0	C3 H23 N17 Na

D.9 Methyl 8-ethyl-6-(2-oxo-2-(phenylamino)ethyl)dodecanoate (**13d**)
D.9.1 ^{1}H NMR

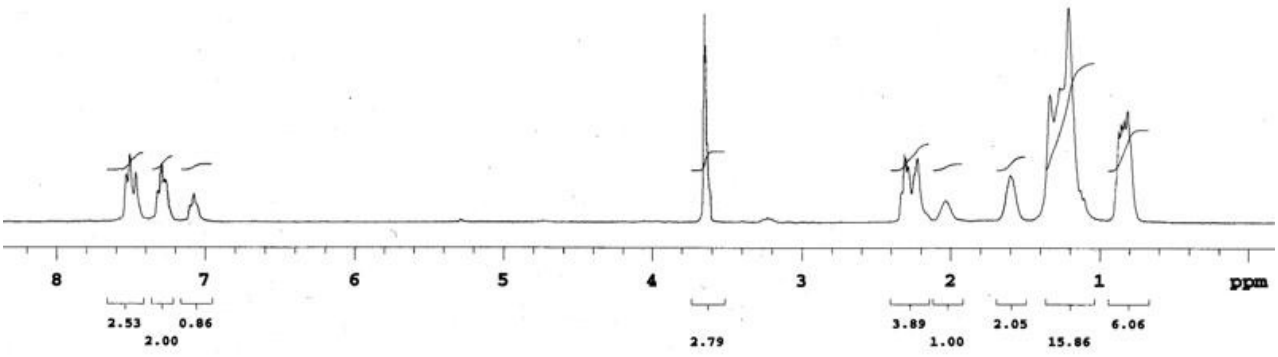

D.9.2 ^{13}C NMR

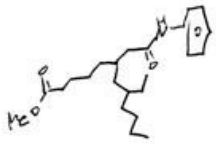

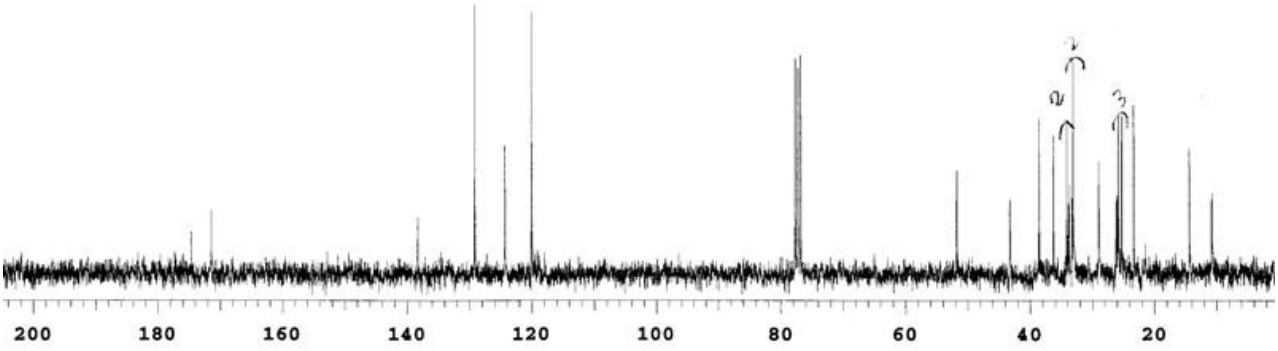

D.9.3 IR

QC_Compare-7572.jws

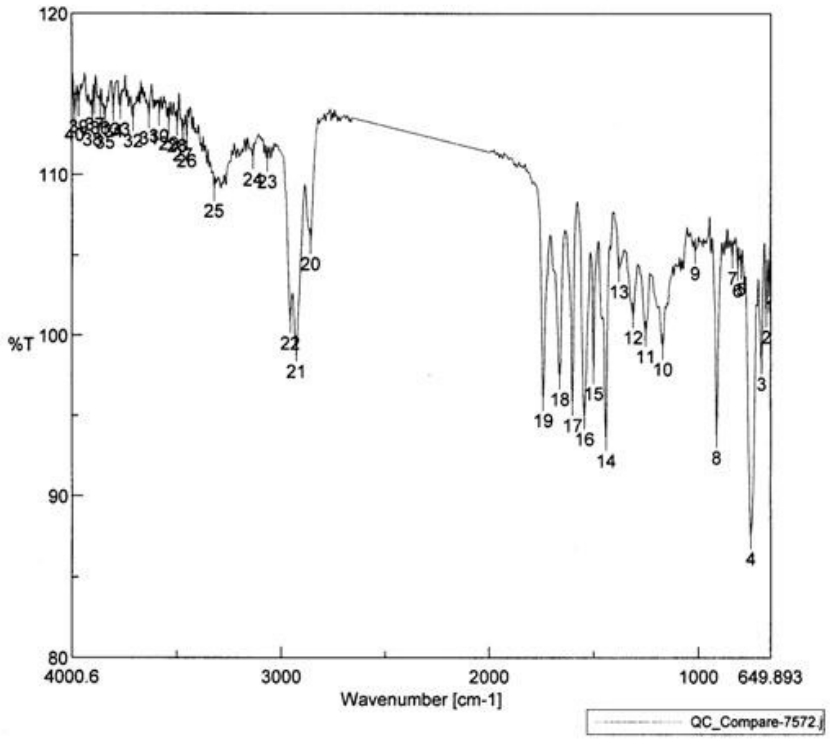

[Comment]	
Sample Name	
Comment	
User	
Division	
Company	wsu

[Data Information]	
Creation Date	5/21/2010 7:03 PM
Data array type	Linear data array
Horizontal	Wavenumber [cm-1]
Vertical	%T
Start	649.893 cm-1
End	4000.6 cm-1
Data pitch	0.964233 cm-1
Data points	3476

Result of Peak Picking

No.	Position	Intensity	No.	Position	Intensity	No.	Position	Intensity
1	657.607	103.227	2	670.142	101.272	3	694.248	98.3468
4	746.317	87.5088	5	794.528	104.286	6	810.92	104.221
7	836.955	104.978	8	912.165	93.7659	9	1016.3	105.295
10	1170.58	99.265	11	1252.54	100.06	12	1310.39	101.238
13	1377.89	104.116	14	1441.53	93.554	15	1499.38	97.7579
16	1543.74	94.9184	17	1600.63	95.7686	18	1661.37	97.3846
19	1740.44	96.0713	20	2858.95	105.87	21	2926.45	99.1291
22	2956.34	100.871	23	3066.26	110.939	24	3136.65	111.085
25	3321.78	109.13	26	3451.96	112.242	27	3471.24	112.615
28	3497.27	113.167	29	3537.77	113.316	30	3583.09	113.794
31	3631.3	113.638	32	3708.44	113.484	33	3768.22	114.208
34	3801.97	114.079	35	3842.47	113.398	36	3865.61	114.272
37	3892.61	114.503	38	3903.22	113.575	39	3969.75	114.37
40	3987.11	113.878						

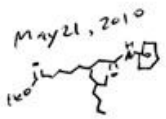

D.9.4 LRMS [M+Li], [M+Na], and [M+K]

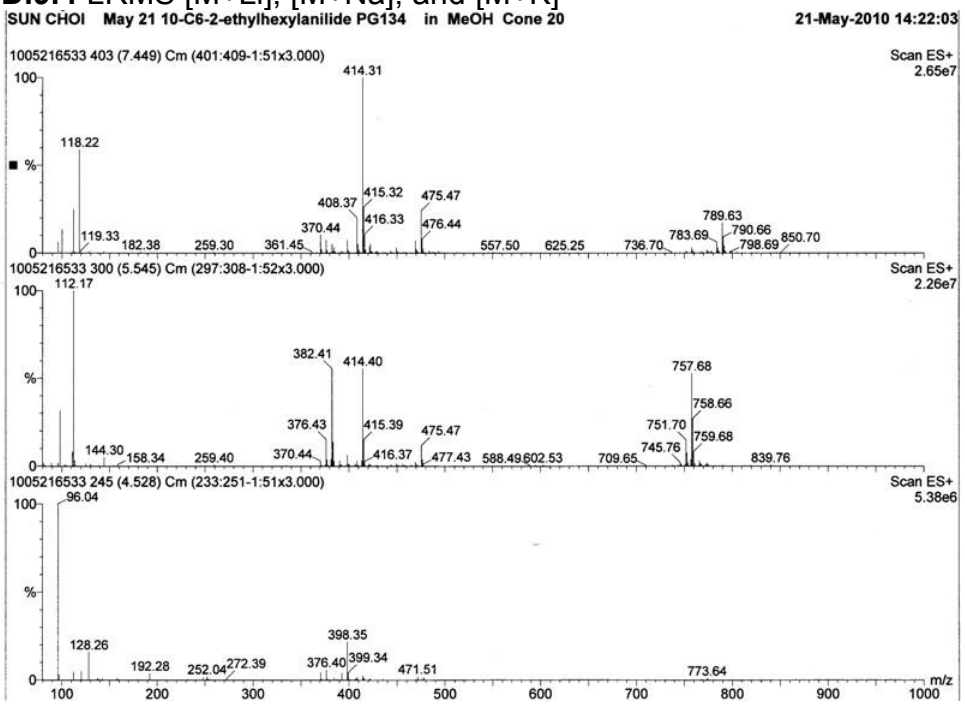

D.10 Methyl 6-isopropyl-8-oxo-8-(phenylamino)octanoate (**13e**)

D.10.1 ^{1}H NMR

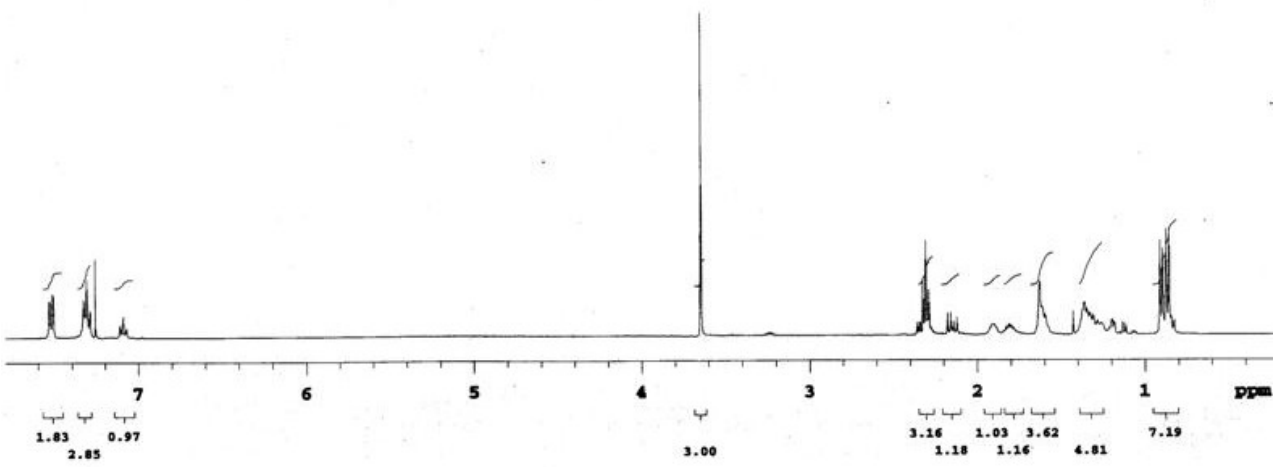

D.10.2 ^{13}C NMR

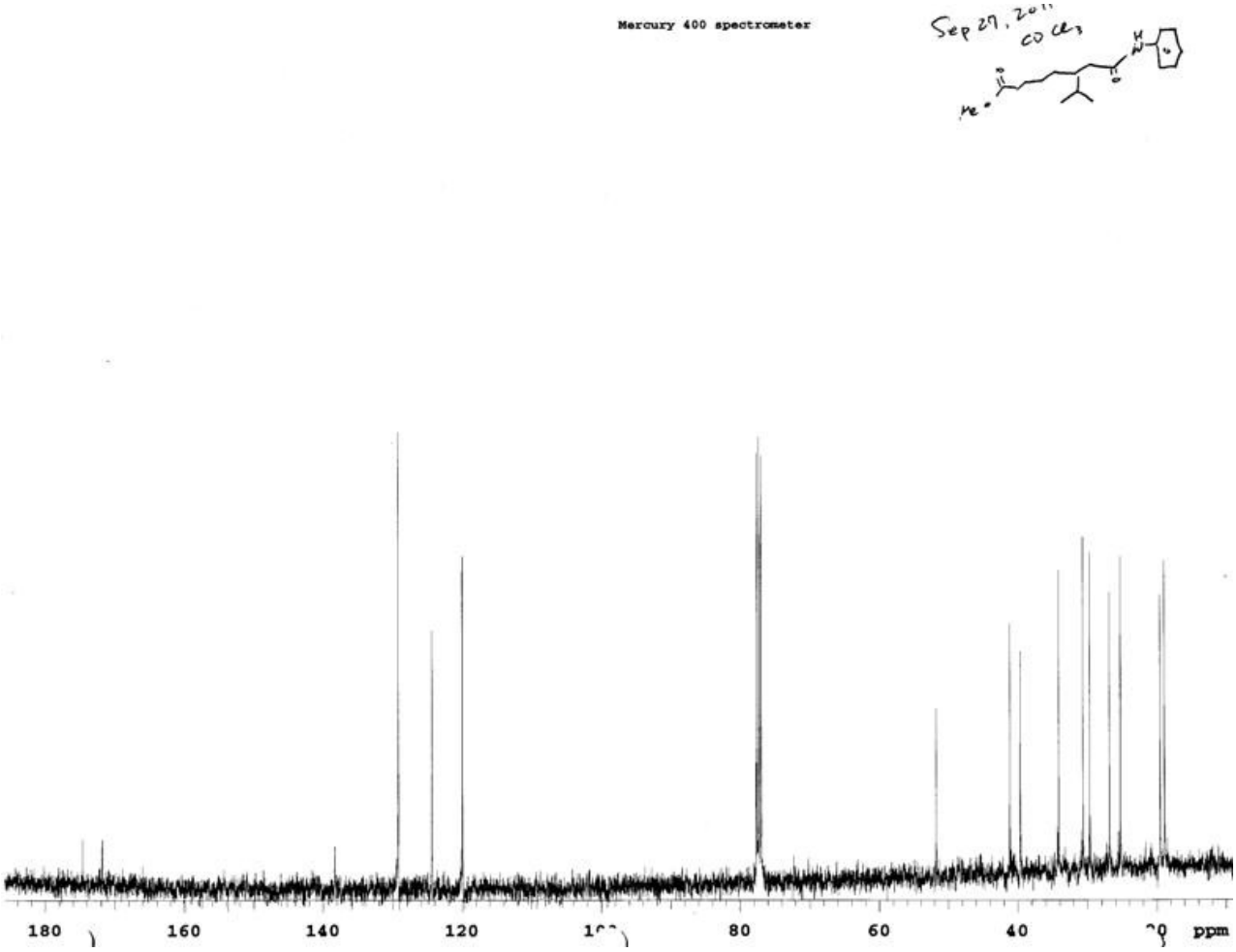

D.10.3 IR

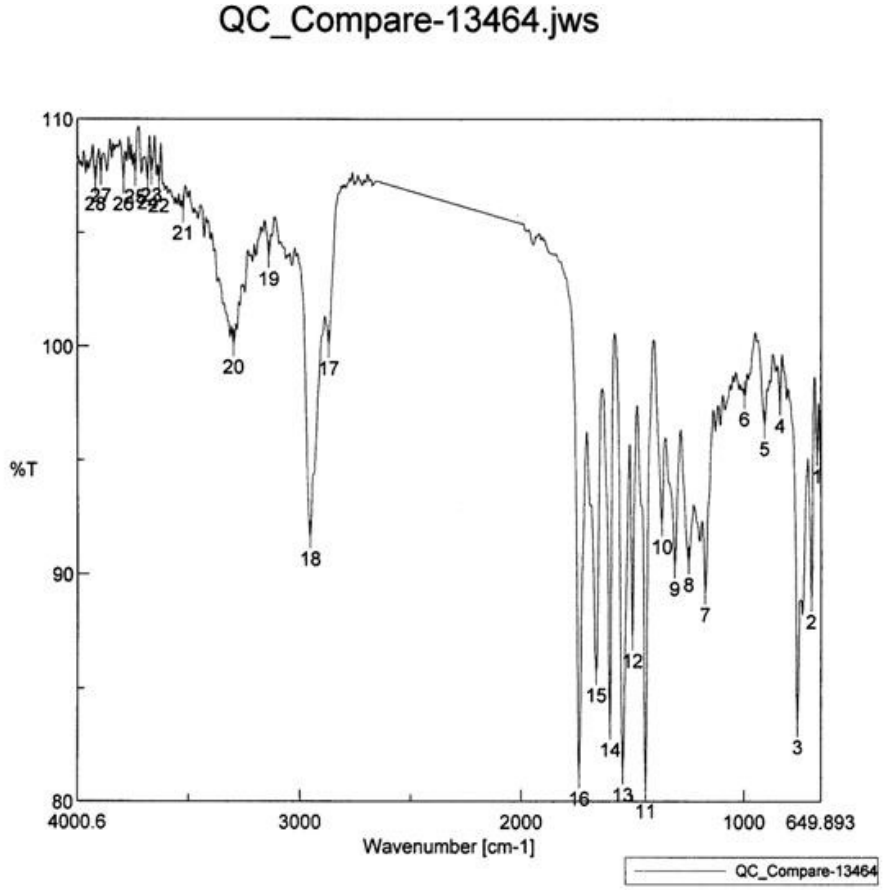

[Comment]	
Sample Name	
Comment	
User	
Division	
Company	wsu

[Data Information]	
Creation Date	9/28/2011 10:57 AM
Data array type	Linear data array
Horizontal	Wavenumber [cm-1]
Vertical	%T
Start	649.893 cm-1
End	4000.6 cm-1
Data pitch	0.964233 cm-1
Data points	3476

Result of Peak Picking

No.	Position	Intensity	No.	Position	Intensity	No.	Position	Intensity
1	668.214	95.3255	2	693.284	88.9571	3	756.923	83.4432
4	835.99	97.5496	5	906.379	96.5562	6	997.982	97.8382
7	1174.44	89.2625	8	1248.68	90.5758	9	1310.39	90.4028
10	1368.25	92.2447	11	1441.53	80.6307	12	1500.35	87.2391
13	1542.77	81.3368	14	1600.63	83.3133	15	1662.34	85.7399
16	1738.51	81.1697	17	2869.56	100.059	18	2954.41	91.6896
19	3139.54	103.989	20	3296.71	100.117	21	3524.27	106.023
22	3631.3	107.224	23	3666.02	107.692	24	3683.37	107.368
25	3738.33	107.627	26	3791.37	107.303	27	3893.57	107.673
28	3918.64	107.297						

D.10.4 HRMS

Single Mass Analysis
Tolerance = 5.0 PPM / DBE: min = -1.5, max = 150.0
Element prediction: Off
Number of isotope peaks used for i-FIT = 6

Monoisotopic Mass, Even Electron Ions
845 formula(e) evaluated with 1 results within limits (up to 50 closest results for each mass)
Elements Used:
C: 0-100 H: 0-1000 N: 0-10 O: 0-15 23Na: 0-1
SUN, CHOI Sept 27 11-C6-Isopropylanilide
LCT2008-07b.pro 2010-clf.spl

2011_0927_2246 260 (5.695) Cm (257:269-130:195x2.000)

27-Sep-2011LCT Premier14:56:56
1: TOF MS ES+
8.79e+003

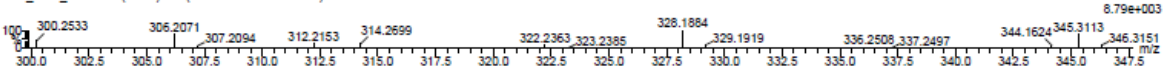

Minimum:				-1.5			
Maximum:		50.0	5.0	150.0			
Mass	Calc. Mass	mDa	PPM	DBE	i-FIT	i-FIT (Norm)	Formula
306.2071	306.2069	0.2	0.7	5.5	49.8	0.0	C18 H28 N O3

D.11 N^8-Hydroxyl-3-methyl-N^1-phenyloctanediamide (**14a**)

D.11.1 ^{1}H NMR

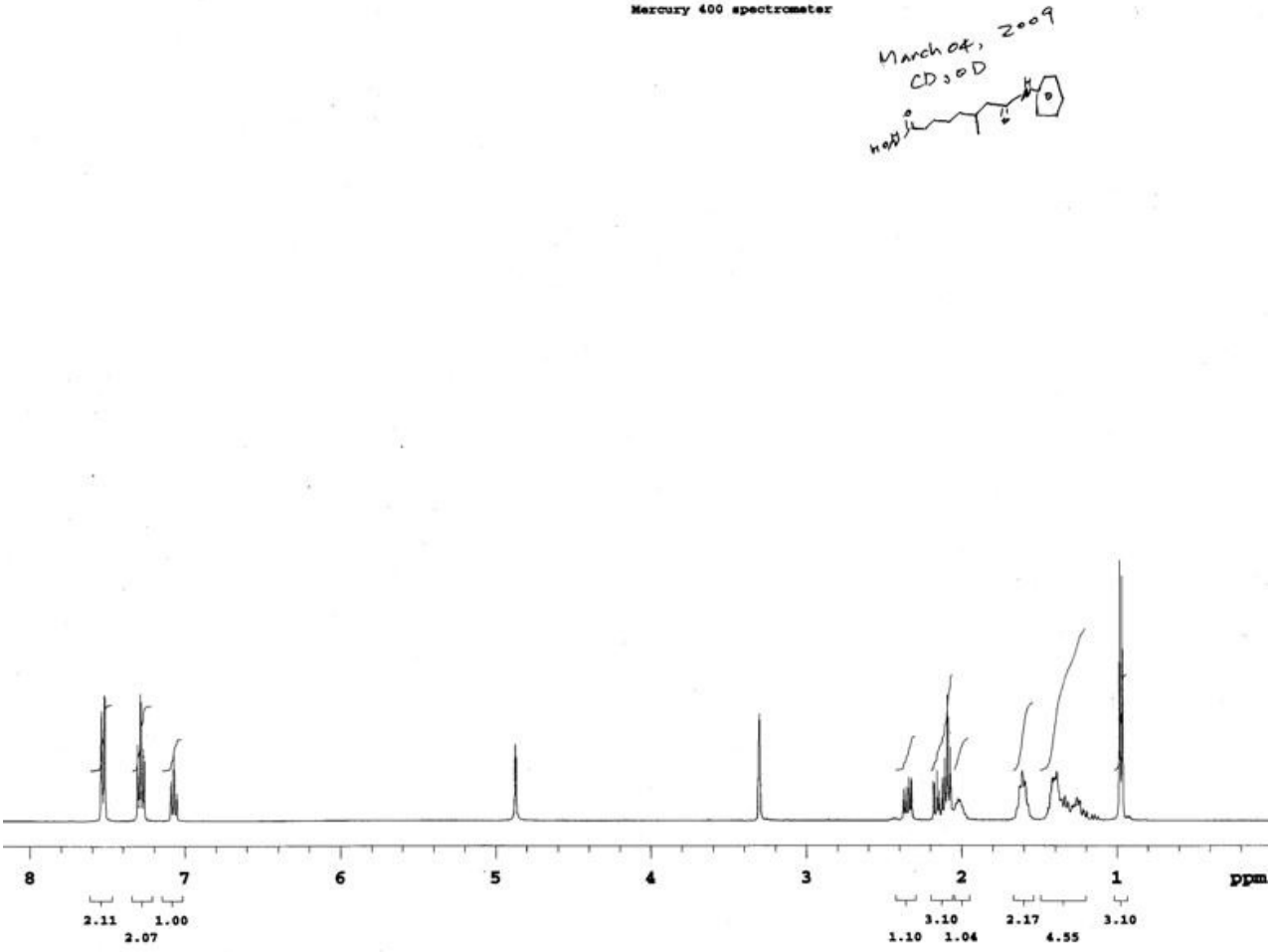

D.11.2 ^{13}C NMR

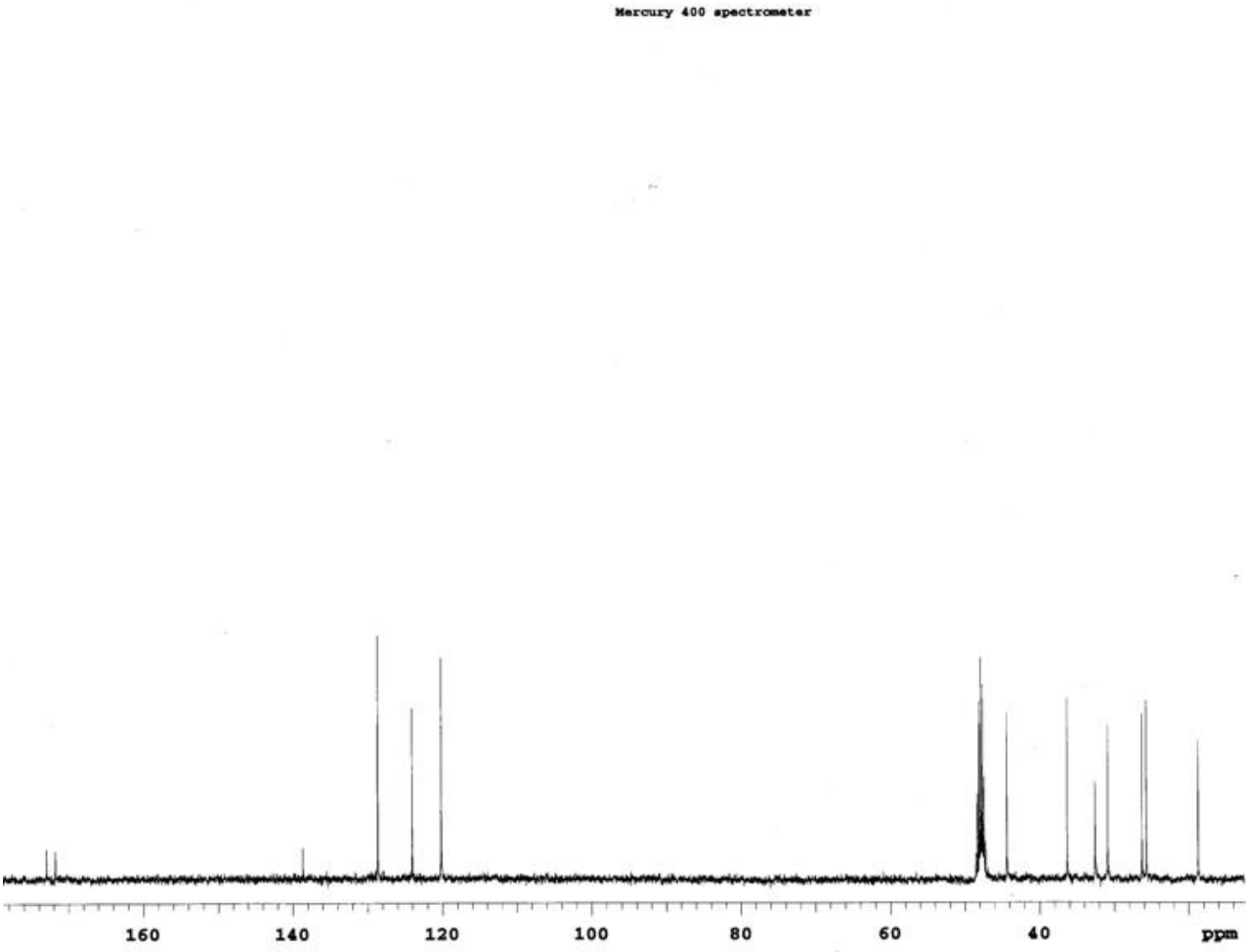

D.11.3 IR

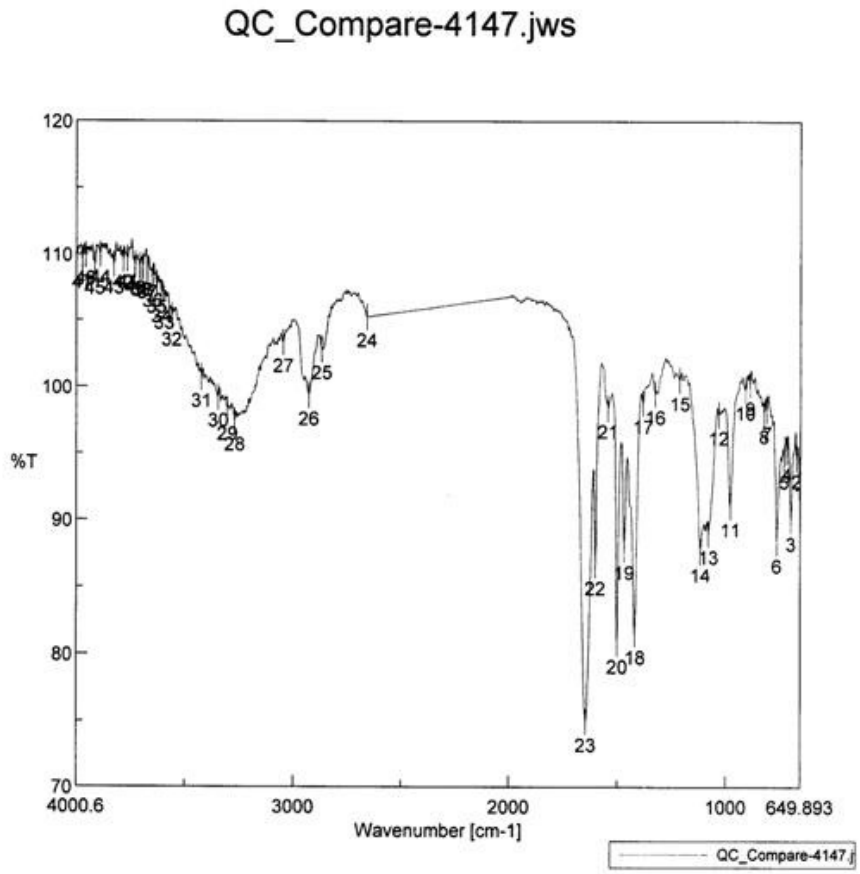

[Comment]
Sample Name
Comment
User
Division
Company wsu

[Data Information]

Creation Date	4/29/2009 10:53 AM
Data array type	Linear data array
Horizontal	Wavenumber [cm-1]
Vertical	%T
Start	649.893 cm-1
End	4000.6 cm-1
Data pitch	0.964233 cm-1
Data points	3476

Result of Peak Picking

No.	Position	Intensity	No.	Position	Intensity	No.	Position	Intensity
1	655.679	93.8041	2	667.25	94.6708	3	693.284	89.9711
4	712.569	95.1727	5	725.104	94.613	6	758.852	88.3224
7	806.099	98.2549	8	818.634	98.0289	9	885.166	100.111
10	908.308	99.7775	11	976.769	91.0572	12	1030.77	97.8745
13	1078.98	88.9712	14	1115.62	87.6483	15	1211.08	100.464
16	1323.89	99.4373	17	1379.82	98.7585	18	1418.39	81.5159
19	1467.56	87.8047	20	1500.35	80.8195	21	1540.85	98.3834
22	1599.66	86.6298	23	1643.05	74.9125	24	2658.39	105.222
25	2867.63	102.771	26	2928.38	99.2963	27	3046.98	103.277
28	3269.72	97.3753	29	3304.43	98.1533	30	3345.89	99.147
31	3422.06	100.63	32	3558.99	105.231	33	3593.7	106.522
34	3606.23	106.992	35	3627.45	107.714	36	3647.7	108.154
37	3671.8	108.83	38	3693.01	109.009	39	3706.51	109.03
40	3728.69	109.158	41	3763.4	109.622	42	3783.65	109.574
43	3827.04	109.151	44	3890.68	109.95	45	3914.79	109.119
46	3958.18	109.896	47	3973.61	109.571			

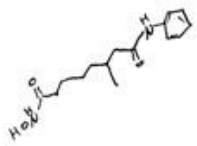

D.11.4 HRMS

Elemental Composition Report **Page 1**

Single Mass Analysis
Tolerance = 10.0 PPM / DBE: min = -1.5, max = 50.0
Element prediction: Off
Number of isotope peaks used for i-FIT = 3

Monoisotopic Mass, Even Electron Ions
231 formula(e) evaluated with 3 results within limits (up to 50 best isotopic matches for each mass)
Elements Used:
C: 0-27 H: 15-28 N: 0-2 O: 0-10 23Na: 0-1 S: 0-2

Sun Choi Mar 03 09-C6-methylH.A. PG48
Lew 2008-07b.pro
2009_0302_0327 14 (0.300) Cm (12:17-(2:8+29:36)x2.000)

LCT Premier 04-Mar-2009 11:16:21
1: TOF MS ES+
2.35e+004

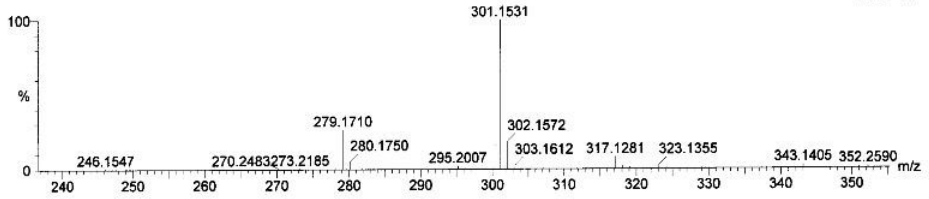

Minimum:				-1.5			
Maximum:		5.0	10.0	50.0			
Mass	Calc. Mass	mDa	PPM	DBE	i-FIT	i-FIT (Norm)	Formula
279.1710	279.1709	0.1	0.4	5.5	30.9	0.8	C15 H23 N2 O3
	279.1725	-1.5	-5.4	6.5	31.0	0.8	C18 H24 O 23Na
	279.1685	2.5	9.0	2.5	32.4	2.2	C13 H24 N2 O3 23Na

D. 12 N^8-Hydroxyl-N^8, 3-diphenyloctanediamide (**14b**)

D.12.1 ^{1}H NMR

Mercury 400 spectrometer

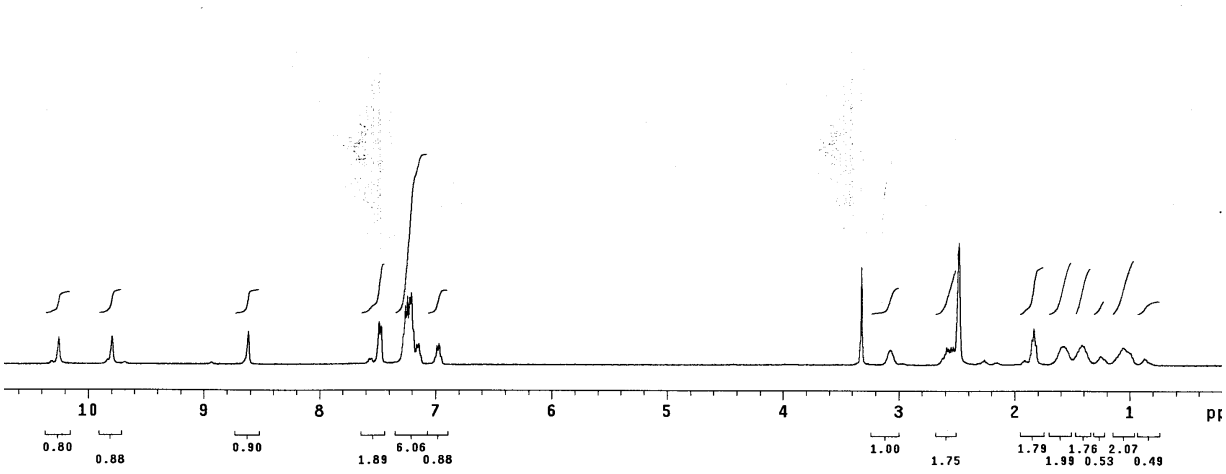

D.12.2 ^{13}C NMR

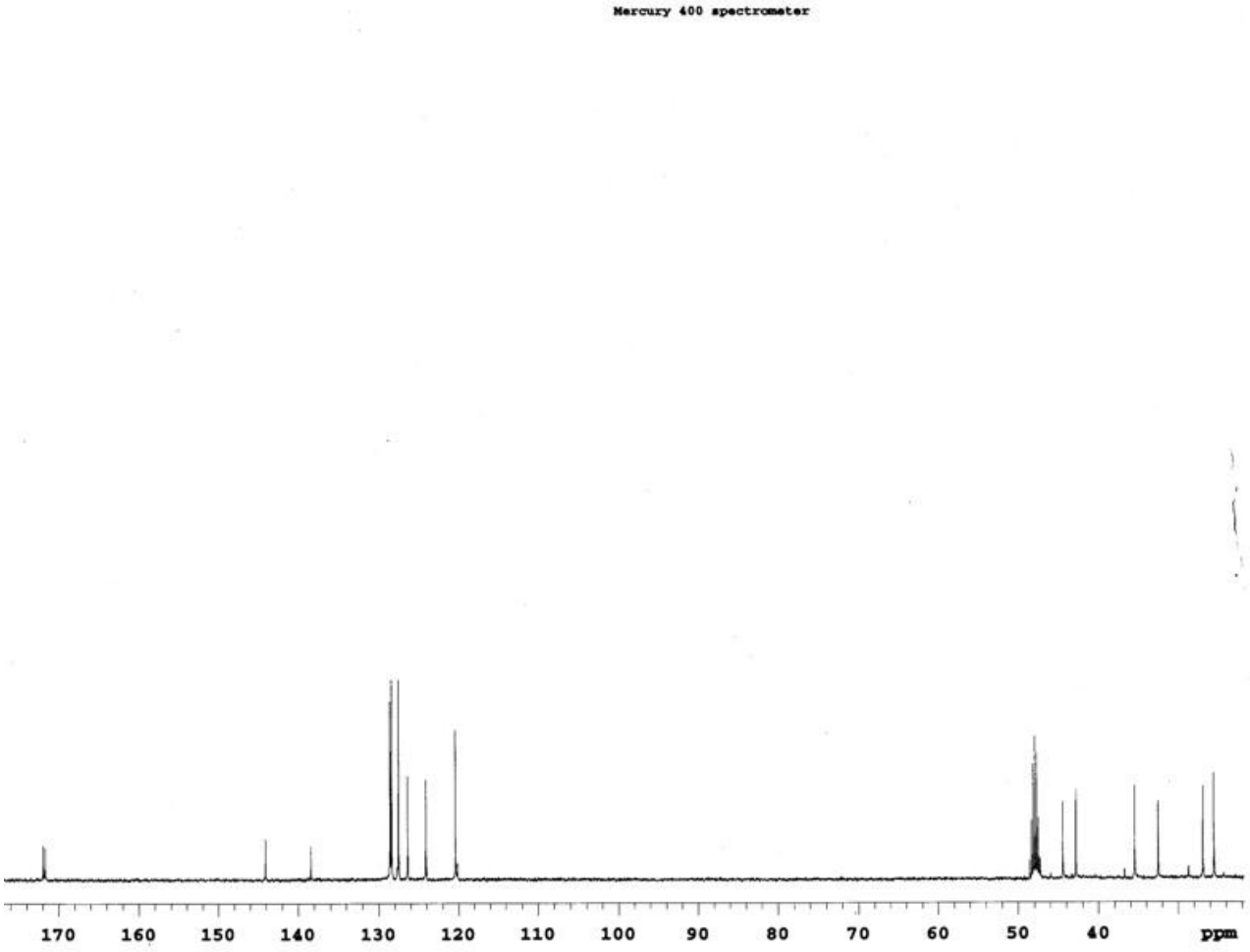

D.12.3 IR

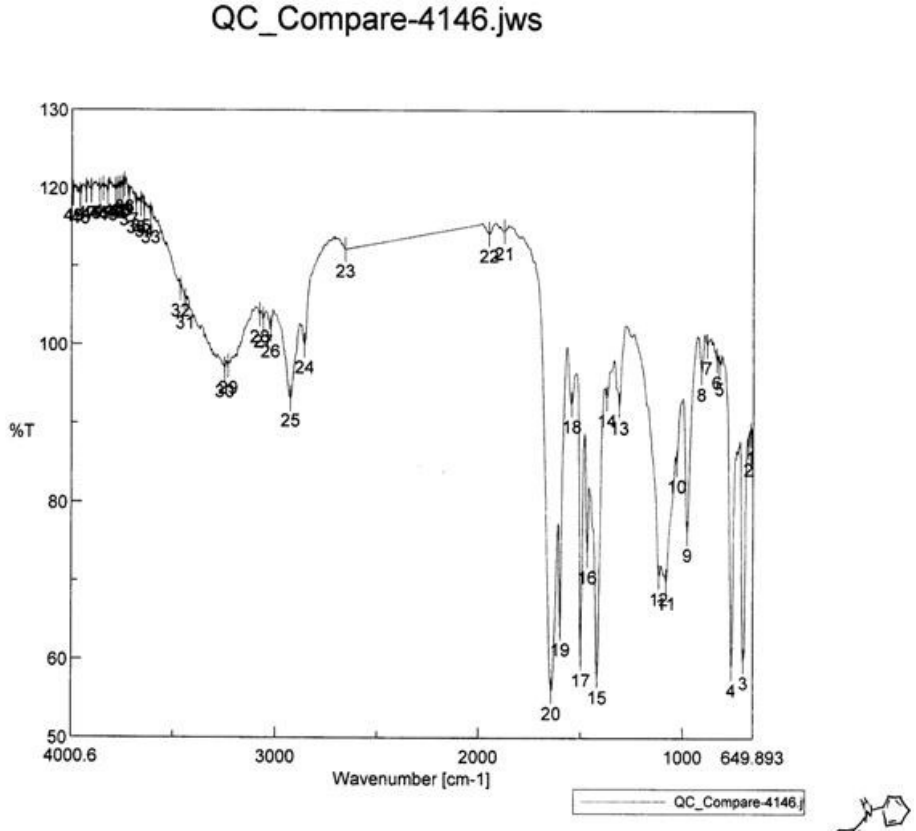

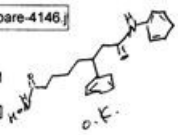

[Comment]
Sample Name
Comment
User
Division
Company wsu

[Data Information]
Creation Date 4/29/2009 10:46 AM
Data array type Linear data array
Horizontal Wavenumber [cm-1]
Vertical %T
Start 649.893 cm-1
End 4000.6 cm-1
Data pitch 0.964233 cm-1
Data points 3476

Result of Peak Picking

No.	Position	Intensity	No.	Position	Intensity	No.	Position	Intensity
1	662.428	88.5534	2	673.035	87.0451	3	699.069	59.8519
4	756.923	58.908	5	819.598	97.2237	6	832.133	98.0072
7	877.452	99.9279	8	906.379	96.4946	9	976.769	76.1605
10	1028.84	84.8868	11	1080.91	69.9513	12	1115.62	70.5389
13	1310.39	92.2177	14	1372.1	93.1551	15	1417.42	57.956
16	1466.6	73.2913	17	1498.42	60.1803	18	1543.74	92.363
19	1598.7	64.0633	20	1641.13	55.9554	21	1874.47	114.467
22	1948.72	114.166	23	2658.39	112.166	24	2858.95	99.8643
25	2928.38	93.0859	26	3026.73	101.895	27	3062.41	103.131
28	3080.73	103.741	29	3235	97.1994	30	3250.43	96.7722
31	3444.24	105.497	32	3467.38	107.039	33	3613.95	116.475
34	3645.77	117.245	35	3661.19	117.906	36	3685.3	117.715
37	3720.01	118.712	38	3740.26	120.395	39	3749.9	119.964
40	3761.47	119.828	41	3774.01	119.794	42	3784.62	119.681
43	3823.19	119.332	44	3845.36	119.848	45	3862.72	119.553
46	3904.18	119.573	47	3930.22	119.559	48	3958.18	118.95
49	3994.82	119.189						

D.12.4 HRMS

Elemental Composition Report **Page 1**

Single Mass Analysis
Tolerance = 5.0 PPM / DBE: min = -1.5, max = 200.0
Element prediction: Off
Number of isotope peaks used for i-FIT = 3

Monoisotopic Mass, Even Electron Ions
289 formula(e) evaluated with 2 results within limits (up to 50 best isotopic matches for each mass)
Elements Used:
C: 0-40 H: 0-60 N: 0-4 O: 0-6 23Na: 0-1
CHOI SUN April 28 09-C6-Phenyl H.A. PG 64
2008-07b.pro
2009_0429_0399 11 (0.229) Cm (9:12-(1:4+31:36)x2.000)

LCT Premier 29-Apr-2009 10:54:10
1: TOF MS ES+
2.35e+004

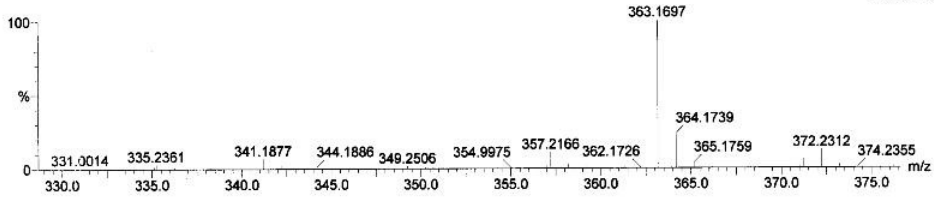

Minimum:				-1.5			
Maximum:		5.0	5.0	200.0			
Mass	Calc. Mass	mDa	PPM	DBE	i-FIT	i-FIT (Norm)	Formula
341.1877	341.1865	1.2	3.5	9.5	27.0	0.5	C20 H25 N2 O3
	341.1881	-0.4	-1.2	10.5	27.5	1.0	C23 H26 O 23Na

D.13 3-(*tert*-Butyl)-N^8-hydroxyl-N^1-phenyloctanediamide (**14c**)
D.13.1 ^{1}H NMR

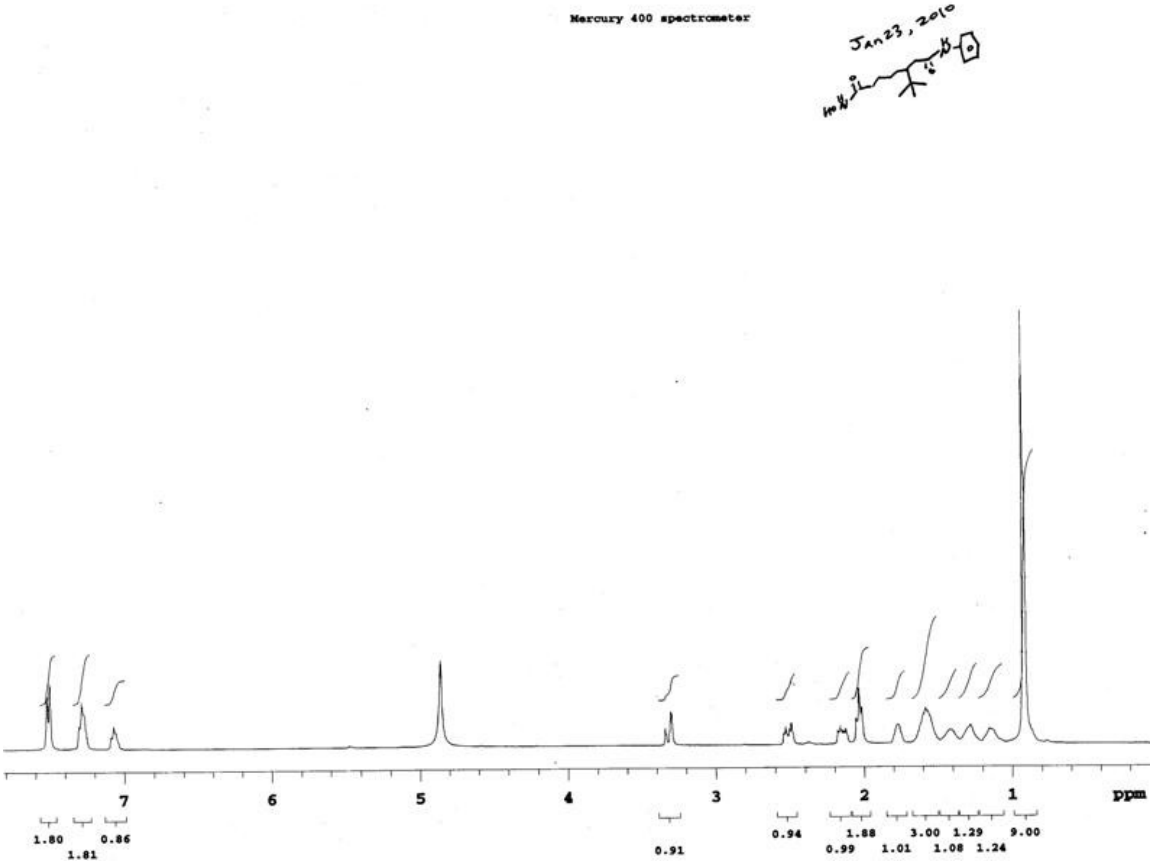

D.13.2 ^{13}C NMR

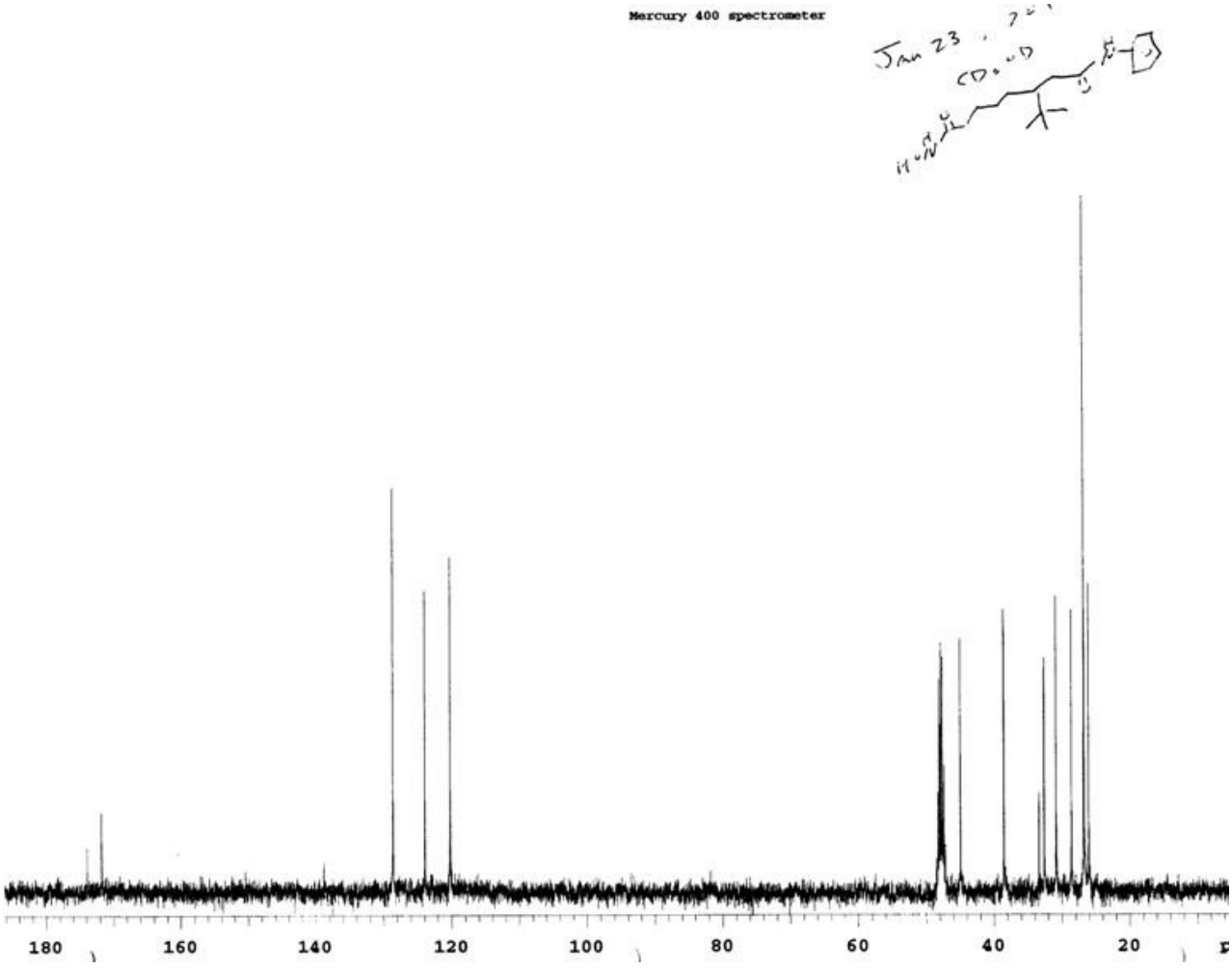

D.13.3 IR

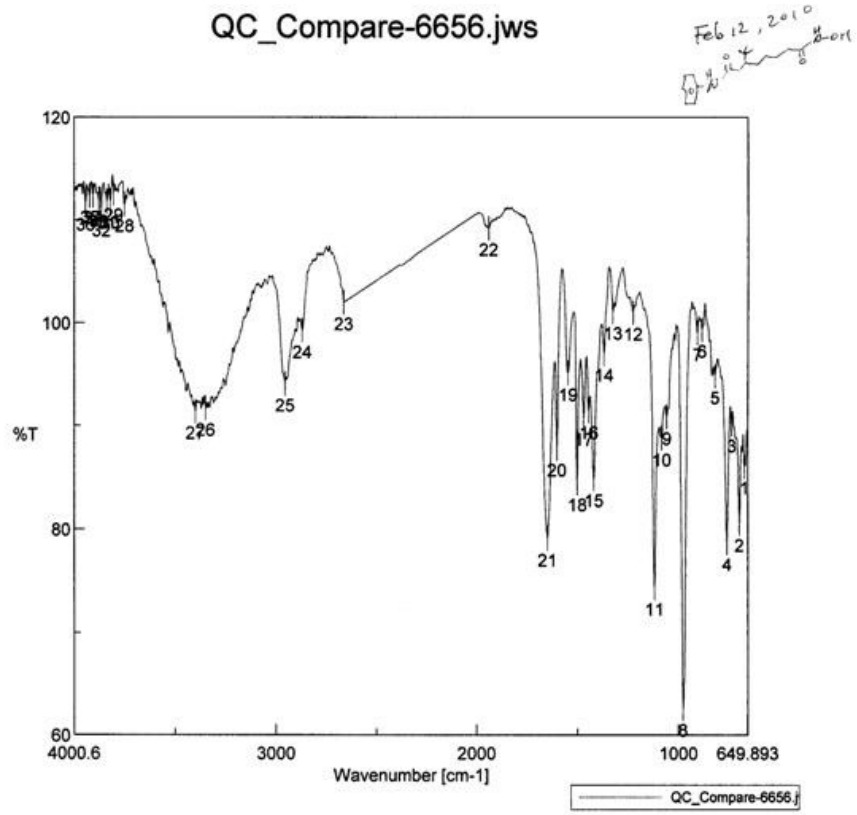

[Comment]	
Sample Name	
Comment	
User	
Division	
Company	wsu

[Data Information]	
Creation Date	2/12/2010 5:20 PM
Data array type	Linear data array
Horizontal	Wavenumber [cm-1]
Vertical	%T
Start	649.893 cm-1
End	4000.6 cm-1
Data pitch	0.964233 cm-1
Data points	3476

Result of Peak Picking

No.	Position	Intensity	No.	Position	Intensity	No.	Position	Intensity
1	667.25	86.0779	2	693.284	80.5017	3	731.853	90.1131
4	756.923	78.64	5	815.742	94.7932	6	880.345	99.2788
7	903.487	98.9418	8	975.804	62.5486	9	1057.76	90.8444
10	1083.8	88.7503	11	1119.48	74.3026	12	1223.61	100.948
13	1322.93	101.025	14	1367.28	96.9664	15	1417.42	84.8503
16	1443.46	91.4137	17	1467.56	90.7342	18	1500.35	84.4297
19	1546.63	95.0861	20	1599.66	87.763	21	1647.88	79.0675
22	1938.11	109.174	23	2662.25	101.933	24	2869.56	99.1823
25	2956.34	94.0468	26	3349.75	91.6398	27	3399.89	91.3507
28	3748.94	111.497	29	3802.94	112.575	30	3821.26	111.829
31	3836.68	111.803	32	3864.65	111.05	33	3878.15	111.945
34	3906.11	112.319	35	3923.47	112.337	36	3943.71	111.64

D.13.4 HRMS

Elemental Composition Report Page 1

Single Mass Analysis
Tolerance = 5.0 PPM / DBE: min = -1.5, max = 50.0
Element prediction: Off
Number of isotope peaks used for i-FIT = 3

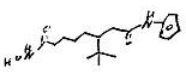

Monoisotopic Mass, Even Electron Ions
1165 formula(e) evaluated with 3 results within limits (all results (up to 1000) for each mass)
Elements Used:
C: 0-100 H: 0-200 N: 0-15 O: 0-19 Na: 0-1
2010_0121_0772 12 (0.246) Cm (12:16-(1:7+36:44)x2.000)
LCT Premier 22-Jan-2010 09:03:21 CHOI, SUN Jan 21 10 C6-t-butyl hydroxamic acid
1: TOF MS ES+ 1.46e+003

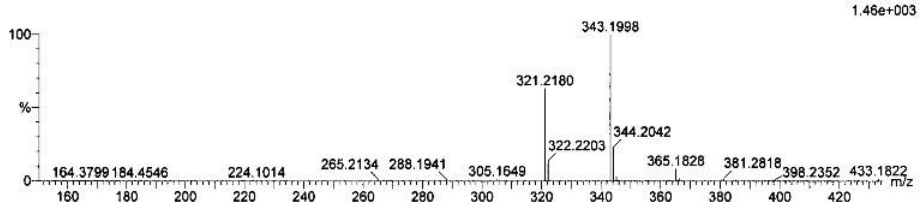

Minimum:				-1.5			
Maximum:		5.0	5.0	50.0			
Mass	Calc. Mass	mDa	PPM	DBE	i-FIT	i-FIT (Norm)	Formula
321.2180	321.2178	0.2	0.6	5.5	35.0	0.9	C18 H29 N2 O3
	321.2183	-0.3	-0.9	-1.5	34.8	0.6	C3 H25 N14 O4
	321.2194	-1.4	-4.4	6.5	37.2	3.0	C21 H30 O Na

D.14 3-(2-Ethylhexyl)-N^8-hydroxyl-N^1-phenyloctanediamide (**14d**)

D.14.1 ^{1}H NMR

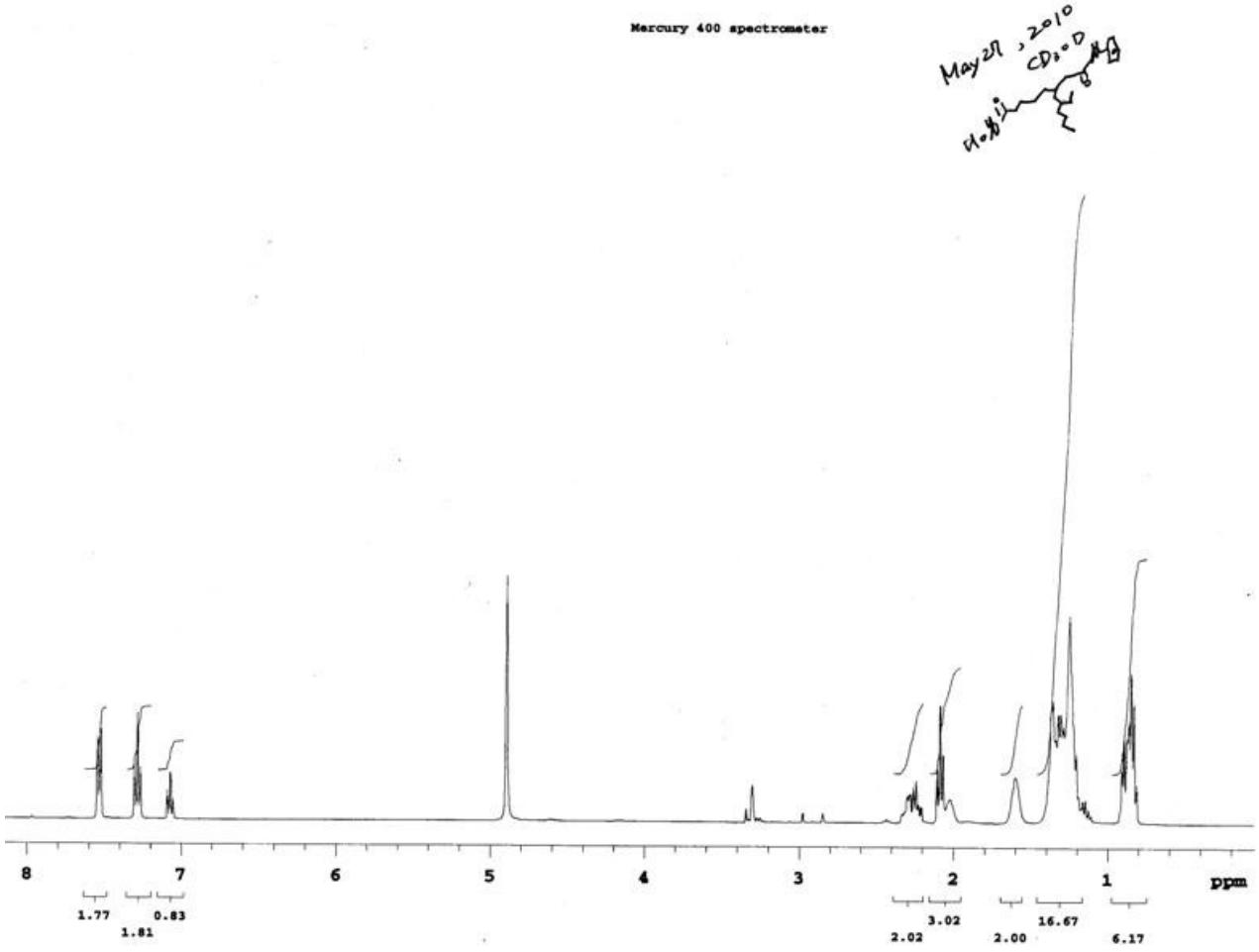

D.14.2 ^{13}C NMR

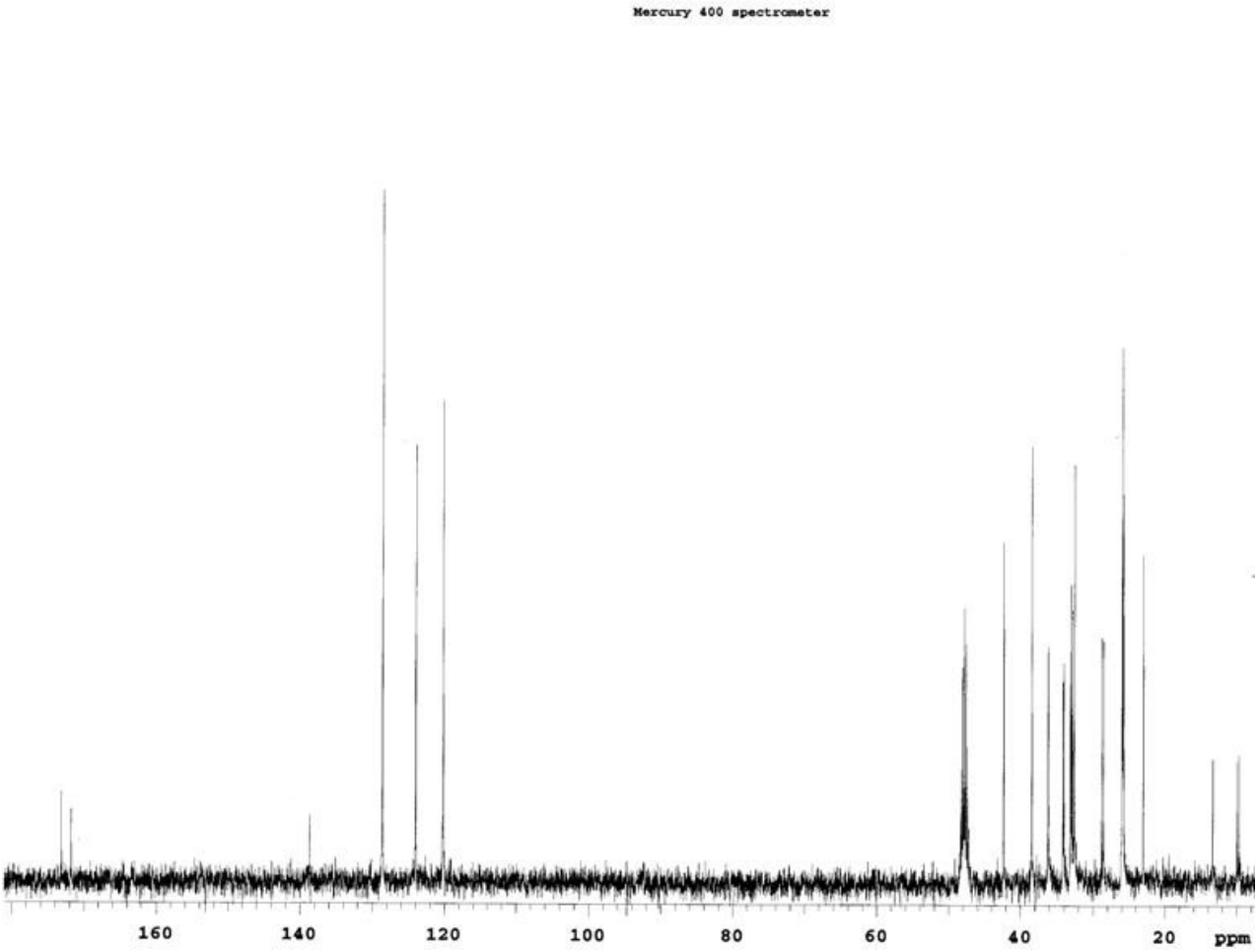

D.14.3 IR

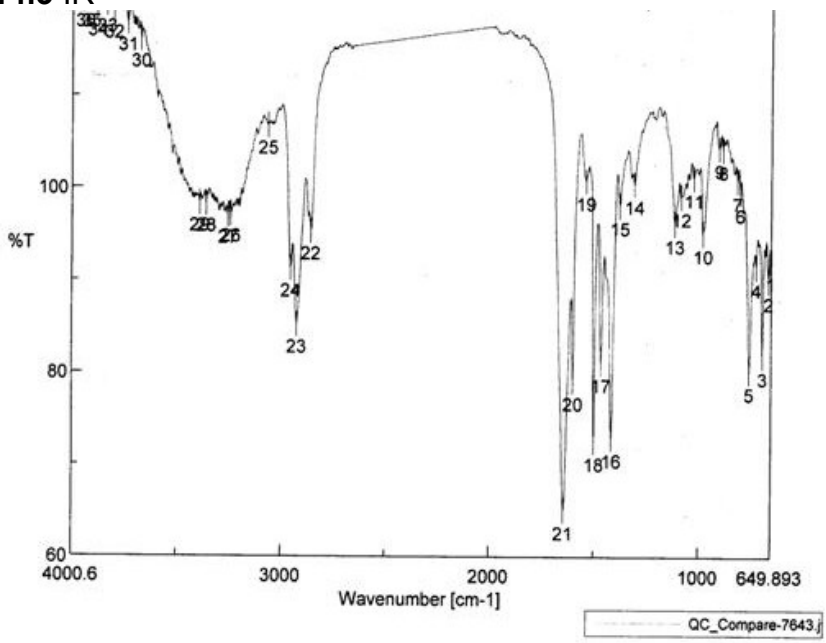

[Comment]	
Sample Name	
Comment	
User	
Division	
Company	wsu

[Data Information]	
Creation Date	5/27/2010 11:06 AM
Data array type	Linear data array
Horizontal	Wavenumber [cm-1]
Vertical	%T
Start	649.893 cm-1
End	4000.6 cm-1
Data pitch	0.964233 cm-1
Data points	3476

Result of Peak Picking

No.	Position	Intensity	No.	Position	Intensity	No.	Position	Intensity
1	653.75	92.1607	2	662.428	89.9245	3	692.32	81.8234
4	723.175	91.4144	5	755.959	80.1282	6	801.278	99.5807
7	814.777	100.824	8	885.166	104.267	9	903.487	104.373
10	981.59	95.0786	11	1024.98	101.138	12	1085.73	99.1041
13	1116.58	96.1331	14	1308.46	100.456	15	1377.89	98.1018
16	1416.46	72.8691	17	1466.6	81.034	18	1499.38	72.4784
19	1538.92	100.799	20	1599.66	79.0394	21	1643.05	64.993
22	2858.95	95.2775	23	2926.45	85.1781	24	2956.34	91.2262
25	3065.3	106.742	26	3242.72	97.1576	27	3256.22	97.046
28	3360.35	98.2909	29	3391.21	98.3378	30	3671.8	116.113
31	3735.44	117.913	32	3801.01	119.266	33	3835.72	119.961
34	3882	119.518	35	3911.9	120.49	36	3939.86	120.479

May 27, 2010

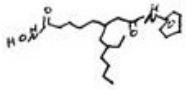

D.14.4 HRMS

Monoisotopic Mass, Even Electron Ions
1703 formula(e) evaluated with 3 results within limits (up to 700 best isotopic matches for each mass)
Elements Used:
C: 0-120 H: 0-1000 N: 0-16 O: 0-30 23Na: 0-1
SUN CHOI May 26 10-C6-2-ethylhexylhydroxamic acid
LCT2008-07b.pro 2010-cif.spl
2010_0526_989 13 (0.283) Cm (12:16-1:6x2.000)

LCT Premier 26-May-2010 13:36:06
1: TOF MS ES+
7.65e+003

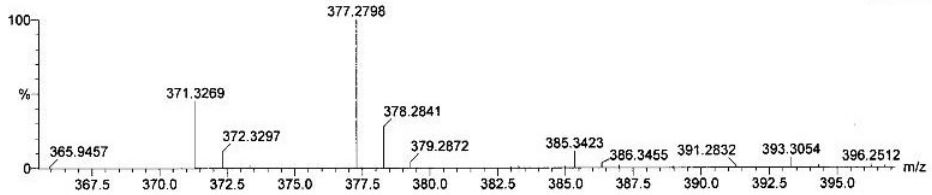

Minimum:				-1.5			
Maximum:		5.0	5.0	50.0			
Mass	Calc. Mass	mDa	PPM	DBE	i-FIT	i-FIT (Norm)	Formula
377.2798	377.2804	-0.6	-1.6	5.5	15.6	0.0	C22 H37 N2 O3
	377.2780	1.8	4.8	2.5	21.9	6.3	C20 H38 N2 O3

APPENDIX E. DOSE RESPONSE GRAPHS AND DATA FOR C7-SAHA LIBRARY

Table E.1. Percentage HDAC activity after incubation of SAHA with Hela Lysate

Concentration (M)	Trial 1	Trial 2	Trial 3	Mean	Standard Error (S.E.)
3.125×10^{-8}	75	75	76	75	0
6.25×10^{-8}	63	56	51	57	3
1.25×10^{-7}	44	35	40	40	3
2.5×10^{-7}	31	21	26	26	3
5.0×10^{-7}	20	16	15	17	2

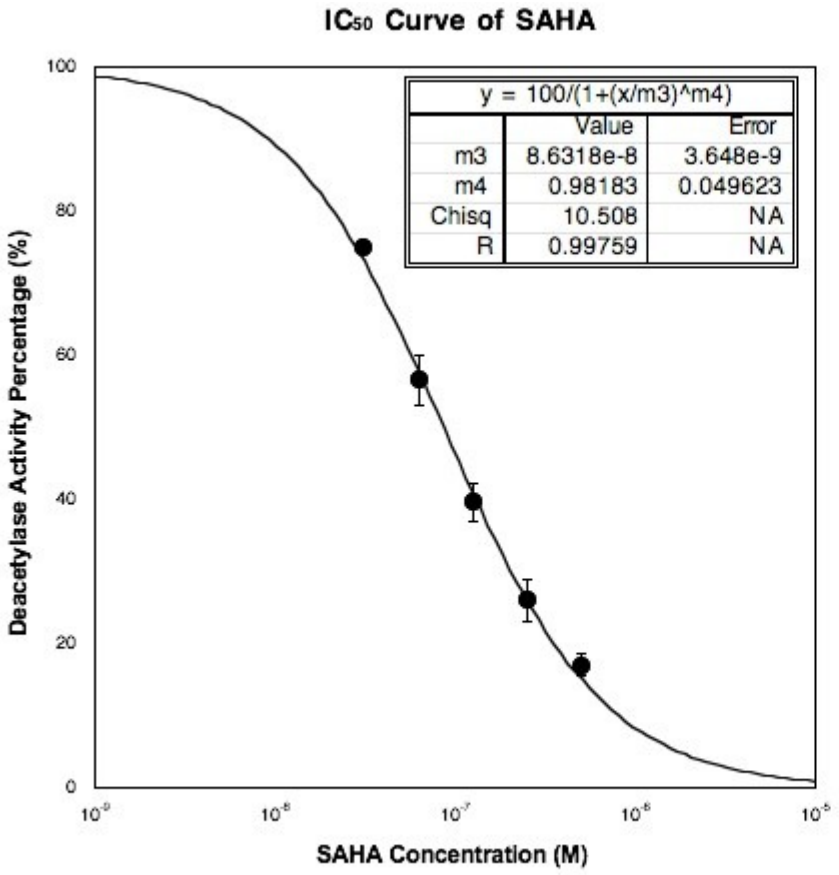

Figure E.1. Dose response curve of SAHA tested using the HDAC activity from HeLa cells lysates from three independent trials. In some case, the error bar is smaller than the marker size. Data were fit to the sigmoidal curve using Kaleidograph 4.0 (Synergy Software) to determine the IC_{50}. The insets were the results of the data analysis. The data are reported in Table 4.1.

Table E.2. Percentage HDAC activity after incubation of C7-SAHA pyridyl analogue **22d** with Hela Lysate

Concentration (M)	Trial 1	Trial 2	Trial 3	Mean	Standard Error (S.E.)
1.11×10^{-7}	70	70	86	75	5
3.33×10^{-7}	63	66	49	59	5
1.00×10^{-6}	45	24	31	33	6
3.00×10^{-6}	18	5	18	14	4
9.00×10^{-6}	8	-2	24	3	3

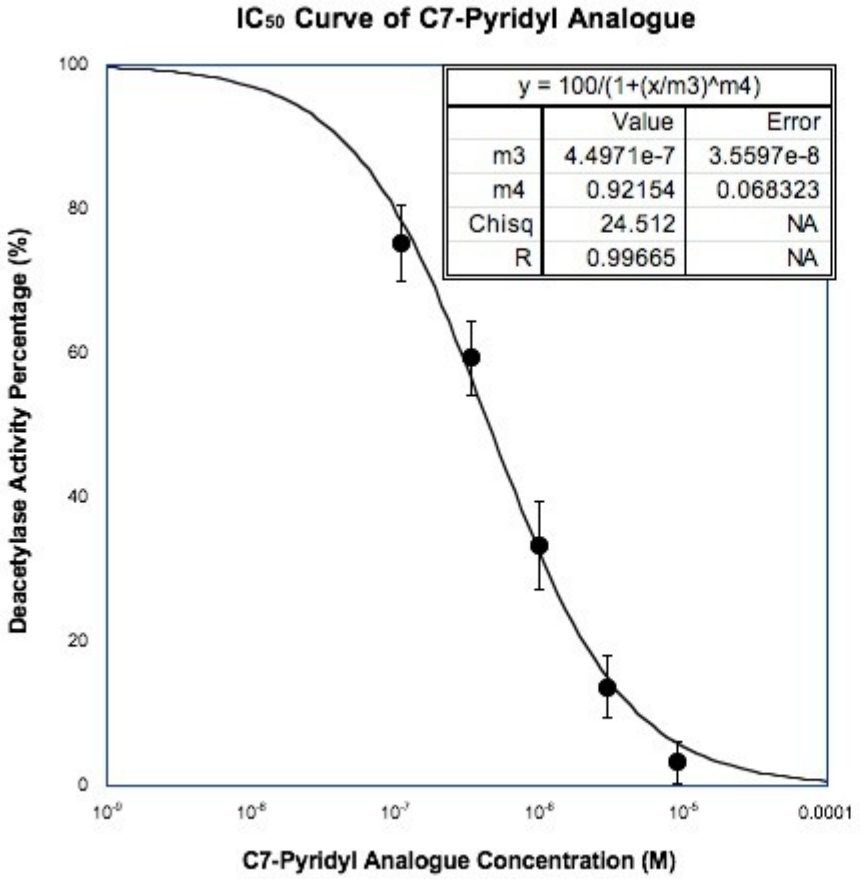

Figure E.2. Dose response curve of C7-SAHA pyridyl analogue **22d** tested using the HDAC activity from HeLa cells lysates from three independent trials. Data were fit to the sigmoidal curve using Kaleidograph 4.0 (Synergy Software) to determine the IC_{50}. The insets are the results of the data analysis. The data were reported in Table 4.2.

Table E.3. Percentage HDAC activity after incubation of C7-SAHA methylanthracene analogue **22f** with Hela Lysate.

Concentration (M)	Trial 1	Trial 2	Trial 3	Mean	S.E.
4.10×10^{-9}	81	76	75	77	2
1.23×10^{-8}	47	60	61	56	4
3.70×10^{-8}	33	38	49	40	4
1.11×10^{-7}	27	15	23	22	3
3.33×10^{-7}	10	12	13	12	1
1.00×10^{-6}	7	5	8	7	1

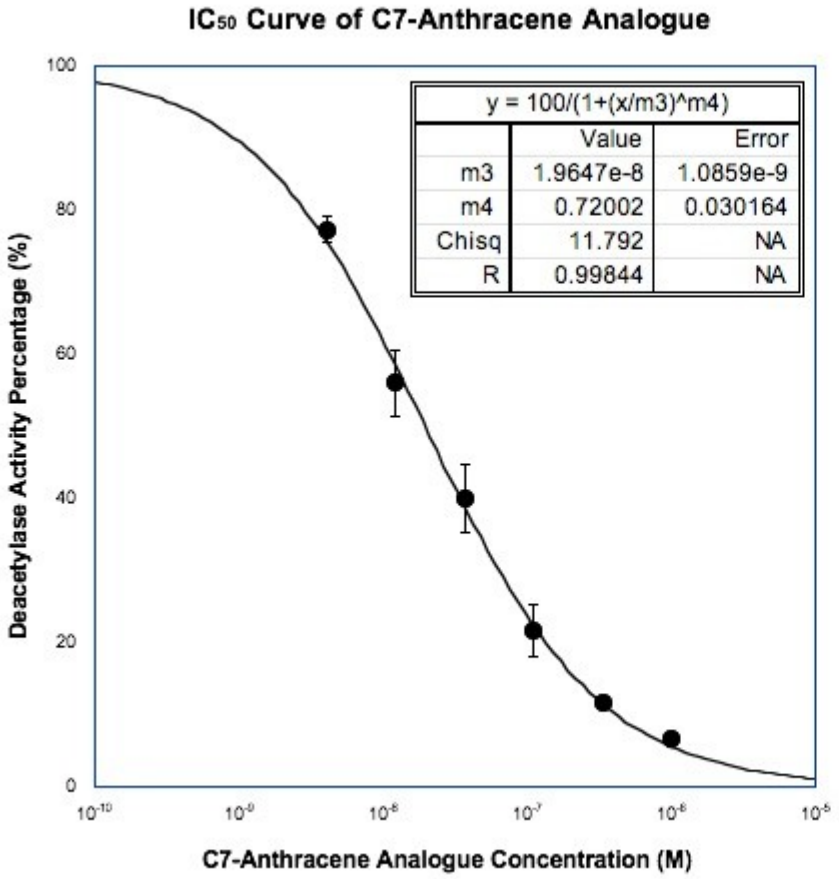

Figure E.3. Dose response curve of C7-SAHA anthracenylmethyl analogue **22f** tested using the HDAC activity from HeLa cells lysates from three independent trials. In some case, the error bars are smaller than the marker size. The insets were the results of the data analysis. The data are reported in Table 4.2.

Table E.4. Percentage HDAC activity after incubation of C7-SAHA methyltetrahydro-anthracene analogue **22g** with Hela Lysate.

Concentration (M)	Trial 1	Trial 2	Trial 3	Mean	S.E.
1.00×10^{-8}	92	124	92	102	10
5.00×10^{-8}	38	68	76	60	11
2.50×10^{-7}	27	27	30	28	1
1.25×10^{-6}	11	25	15	17	4
6.25×10^{-6}	-2	2	0.5	0	1

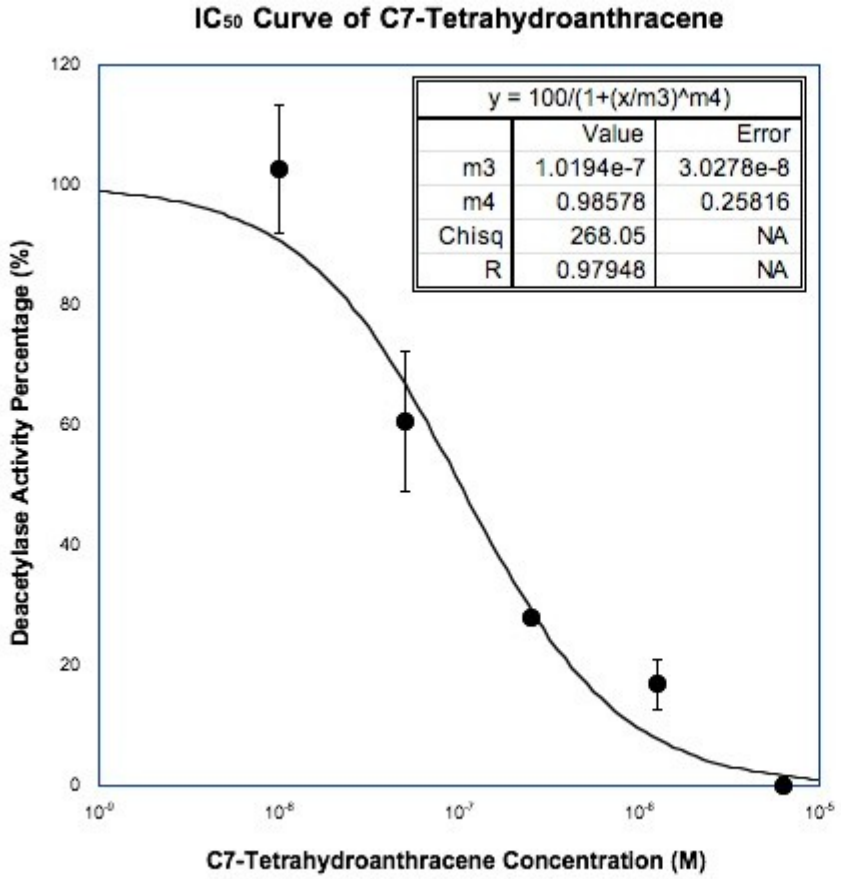

Figure E.4. Dose response curve of C7-SAHA tetrahydroanthracenylmethyl analogue **22g** tested using the HDAC activity from HeLa cells lysates from three independent trials with error bars indicating standard error. In some case, the error bars are smaller than the marker size. Data were fit to the sigmoidal curve using Kaleidograph 4.0 (Synergy Software) to determine the IC_{50}. The insets were the results of the data analysis. The data are reported in Table 4.2.

Table E.5. Deacetylase activity percentage remaining after incubation of HDAC1, HDAC3, or HDAC6 with SAHA and the C7-SAHA analogues **22a-g**.

Compound	HDAC Isoform	Trial 1	Trial 2	Mean	S.E.
SAHA (125 nM)	HDAC1	30	35	32	2
	HDAC3	44	45	44	1
	HDAC6	32	36	34	2
C7-Methyl (100 nM)	HDAC1	38	52	45	7
	HDAC3	27	57	42	10
	HDAC6	21	35	28	7
C7-Benzyl (100 nM)	HDAC1	66	87	76	10
	HDAC3	54	88	71	11
	HDAC6	55	66	60	5
C7-Pyridyl (500 nM)	HDAC1	44	68	56	10
	HDAC3	101	92	97	4
	HDAC6	62	55	59	3
C7-Tetrahydro-anthracene (100 nM)	HDAC1	64	66	65	1
	HDAC3	47	60	53	6
	HDAC6	76	84	80	4
C7-Biphenyl (100 nM)	HDAC1	91	114	102	10
	HDAC3	91	96	93	2
	HDAC6	71	82	76	5
C7-Naphthyl (10 nM)	HDAC1	103	121	112	9
	HDAC3	55	60	57	2
	HDAC6	82	104	93	10
C7-Anthracene (500 nM)	HDAC1	42	47	44	2
	HDAC3	89	90	89	0
	HDAC6	50	56	53	3

Deacetylase activity of HDAC1, HDAC3 and HDAC6 was determined with SAHA and with C7-SAHA analogues at given concentration using an in vitro fluorescence assay as described (Section 3.6). The fluorescence activity of background (No enzyme added) was subtracted from the no small molecule treated (positive control) and the percentage of the deacetylase activity was set

to 100%. Deacetylase activity percentage of each independent trial, mean percentage of deacetylase activity, and standard error (S.E.) are illustrated. The data are reported in the manuscript in Figure 4.2.

Table E.6. HDAC1 activity percentage after incubation of SAHA.

Concentration (M)	Trial 1	Trial 2	Trial 3	Mean	Standard Error (S.E.)
3.125×10^{-8}	68	91	82	80	7
6.25×10^{-8}	55	62	57	58	2
1.25×10^{-7}	48	27	37	37	6
2.50×10^{-7}	37	40	25	34	5

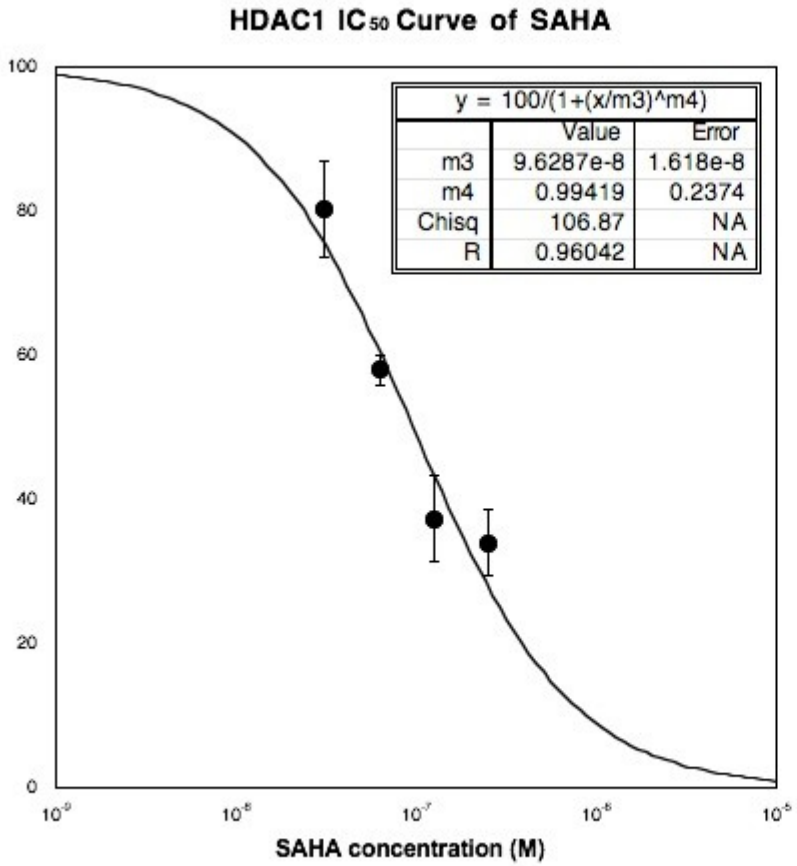

Figure E.5. Dose response curve of SAHA tested using the HDAC1 activity from three independent trials with error bars indicating standard error. In some case, the error bar is smaller than the marker size. Data were fit to the sigmoidal curve using Kaleidograph 4.0 (Synergy Software) to determine the IC_{50}. The insets were the results of the data analysis. The data are reported in Table 4.3.

Table E.7. HDAC3 activity percentage after incubation of SAHA.

Concentration (M)	Trial 1	Trial 2	Trial 3	Mean	Standard Error (S.E.)
3.125×10^{-8}	88	78	74	80	4
6.25×10^{-8}	76	74	70	73	2
1.25×10^{-7}	63	45	44	56	5
2.50×10^{-7}	27	39	37	34	4

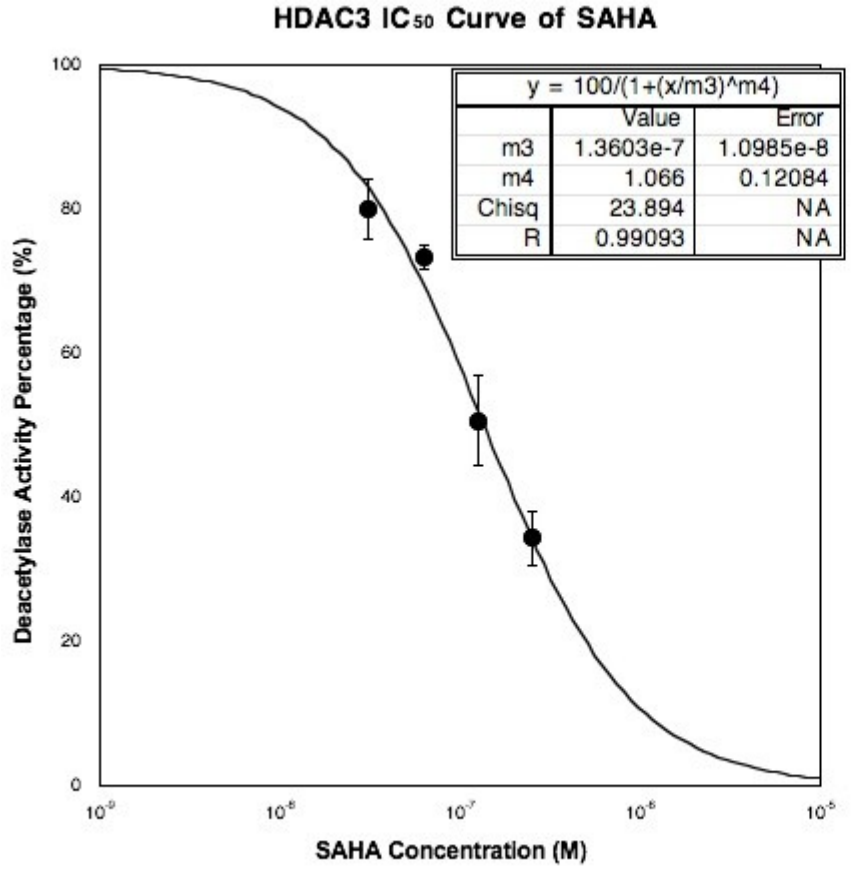

Figure E.6. Dose response curve of SAHA tested using the HDAC3 activity from three independent trials with error bars indicating standard error. In some case, the error bar is smaller than the marker size. Data were fit to the sigmoidal curve using Kaleidograph 4.0 (Synergy Software) to determine the IC_{50}. The insets were the results of the data analysis. The data are reported in Table 4.3.

Table E.8. HDAC6 activity percentage after incubation of SAHA.

Concentration (M)	Trial 1	Trial 2	Trial 3	Mean	Standard Error (S.E.)
3.125×10^{-8}	66	76	73	72	3
6.25×10^{-8}	64	62	60	62	1
1.25×10^{-7}	37	28	32	32	2
2.50×10^{-7}	13	12	9	11	1

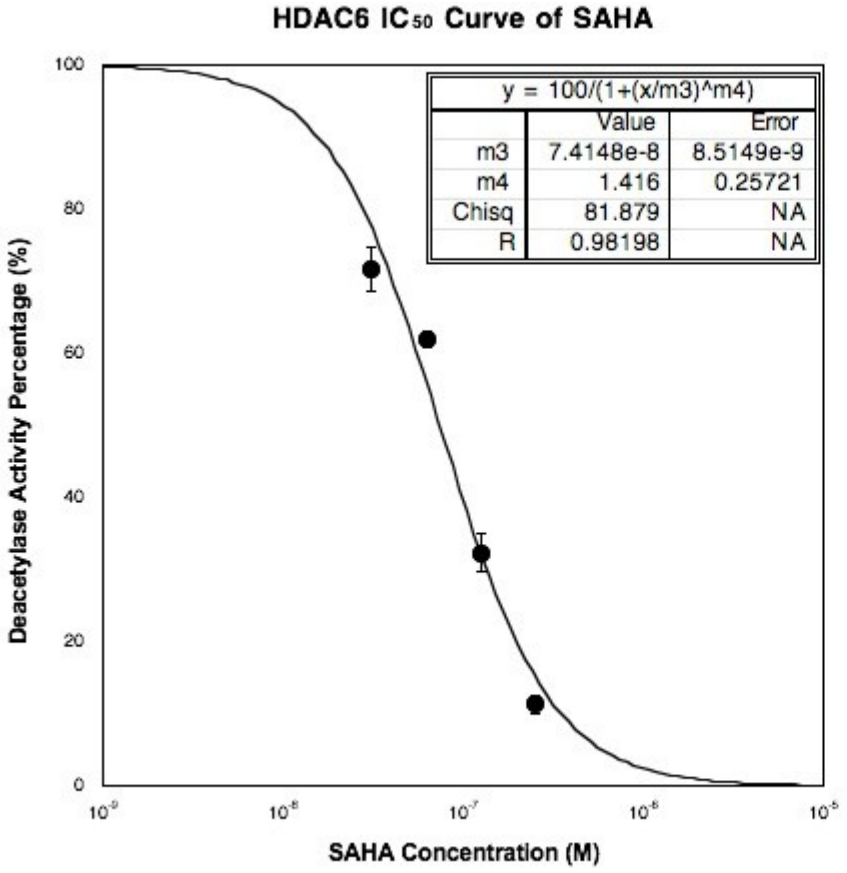

Figure E.7. Dose response curve of SAHA tested using the HDAC6 activity from three independent trials with error bars indicating standard error. In some case, the error bars are smaller than the marker size. Data were fit to the sigmoidal curve using Kaleidograph 4.0 (Synergy Software) to determine the IC_{50}. The insets were the results of the data analysis. The data are reported in Table 4.3.

Table E.9. HDAC1 activity percentage after incubation of C7-SAHA anthracenylmethyl **22f**.

Concentration (M)	Trial 1	Trial 2	Trial 3	Mean	Standard Error (S.E.)
1.11×10^{-7}	103	96	86	96	4
3.33×10^{-7}	33	42	43	39	3
1.00×10^{-6}	17	16	17	17	0

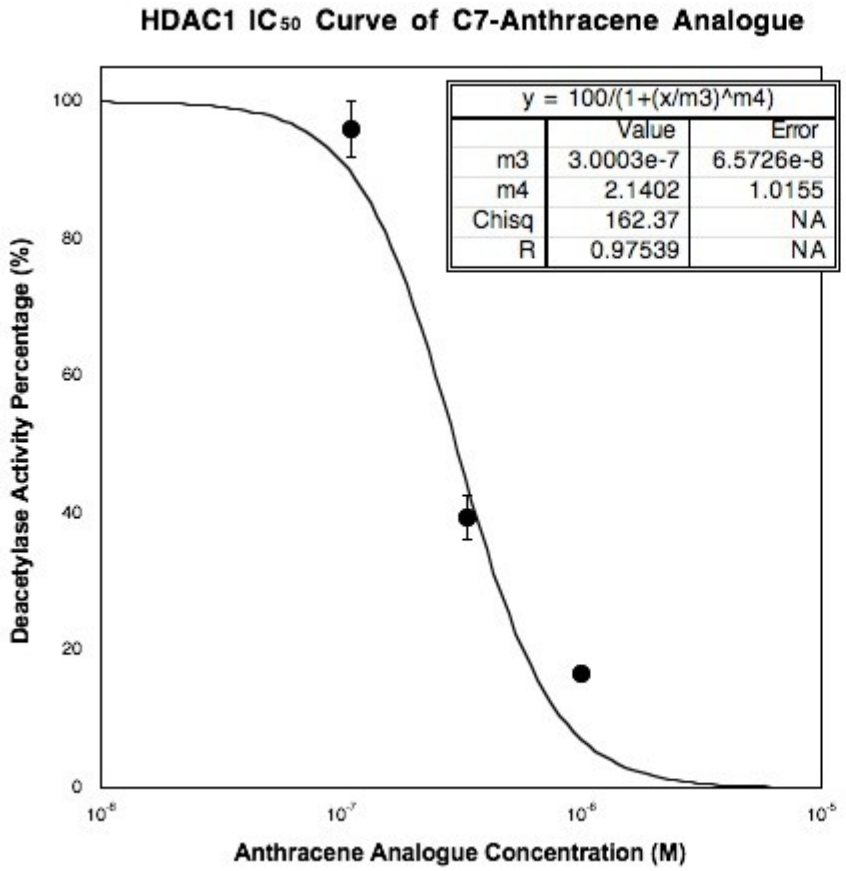

Figure E.8. Dose response curve of C7-SAHA anthracenylmethyl analogue **22f** tested using the HDAC1 activity from three independent trials with error bars indicating standard error. Data were fit to the sigmoidal curve using Kaleidograph 4.0 (Synergy Software) to determine the IC_{50}. The insets were the results of the data analysis. The data are reported in Table 4.3.

Table E.10. HDAC3 activity percentage after incubation of C7-SAHA anthracenylmethyl **22f**.

Concentration (M)	Trial 1	Trial 2	Trial 3	Mean	Standard Error (S.E.)
3.33×10^{-7}	84	87	86	86	1
1.00×10^{-6}	51	57	70	59	5
3.00×10^{-6}	13	23	27	21	4

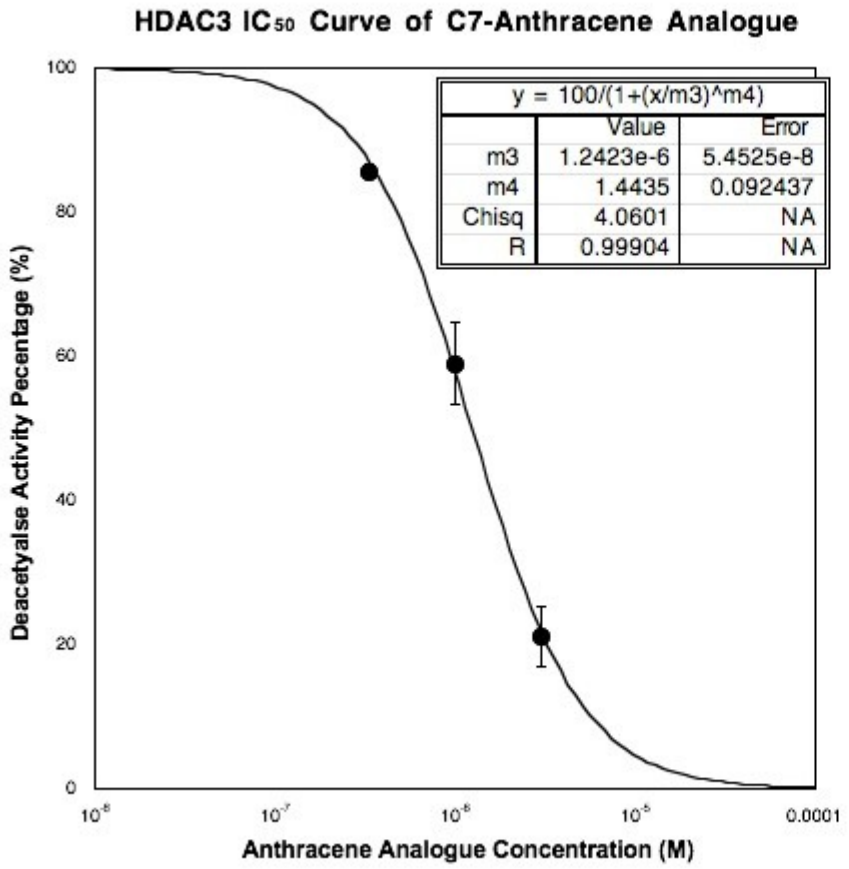

Figure E.9. Dose response curve of C7-SAHA anthracenylmethyl analogue **22f** tested using the HDAC3 activity from three independent trials with error bars indicating standard error. In some case, the error bar is smaller than the marker size. Data were fit to the sigmoidal curve using Kaleidograph 4.0 (Synergy Software) to determine the IC_{50}. The insets are the results of the data analysis. The data were reported in Table 4.3.

Table E.11. HDAC6 activity percentage after incubation of C7-SAHA anthracenylmethyl **22f**.

Concentration (M)	Trial 1	Trial 2	Trial 3	Mean	Standard Error (S.E.)
1.00×10^{-7}	85	84	63	77	7
3.00×10^{-7}	52	53	56	54	1
9.00×10^{-7}	37	36	44	39	2

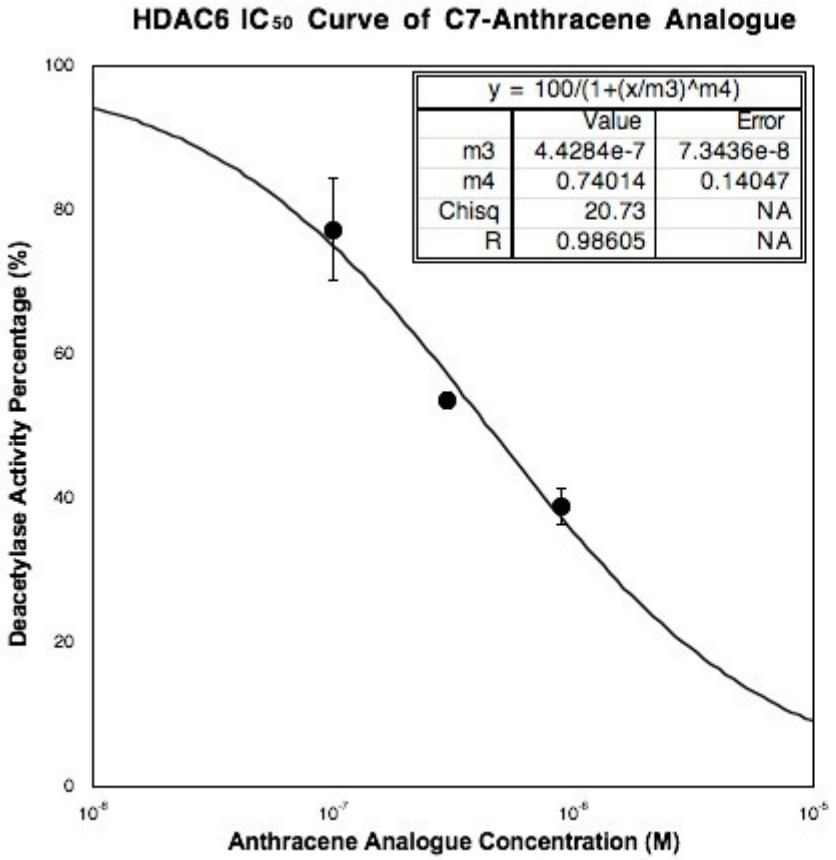

Figure E.10. Dose response curve of C7-SAHA anthracenylmethyl analogue **22f** tested using the HDAC6 activity from three independent trials with error bars indicating standard error. In some case, the error bar is smaller than the marker size. Data were fit to the sigmoidal curve using Kaleidograph 4.0 (Synergy Software) to determine the IC_{50}. The insets were the results of the data analysis. The data were reported in Table 4.3.

APPENDIX F. SUPPLEMENTARY INFORMATION FOR C7-SAHA LIBRARY

F.1. 1,1-Dibenzyl 6-methyl hexane-1, 1, 6-tricarboxylate (**24**).

F.1.1. ^{1}H NMR

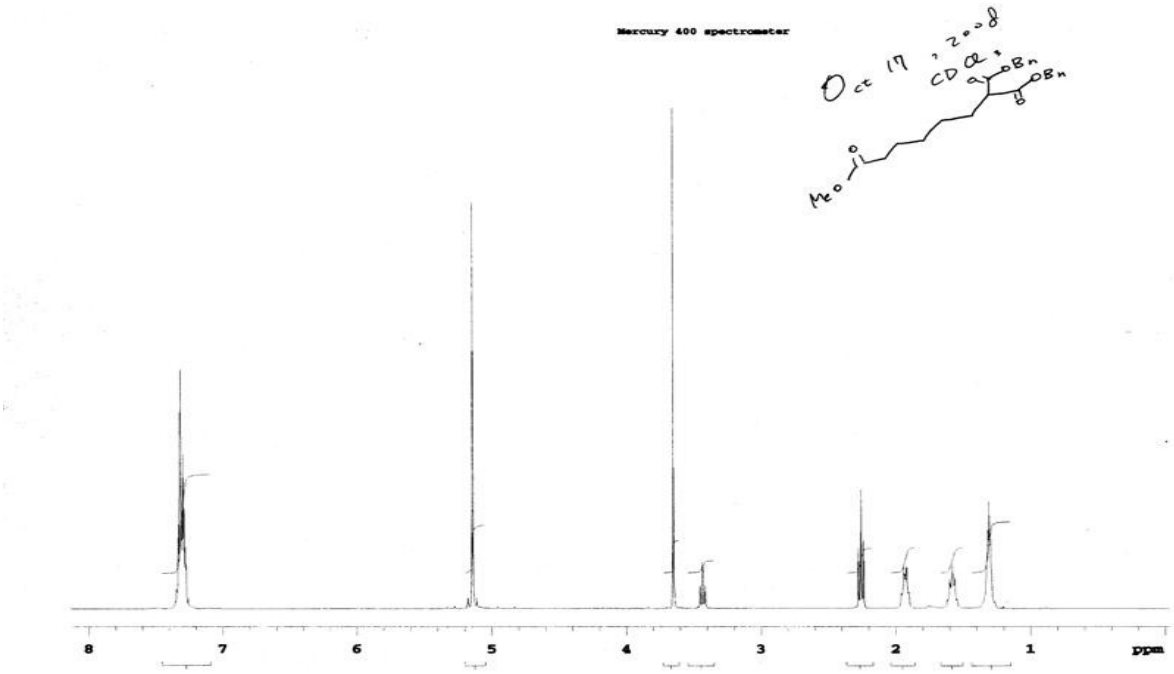

F.1.2. ^{13}C NMR

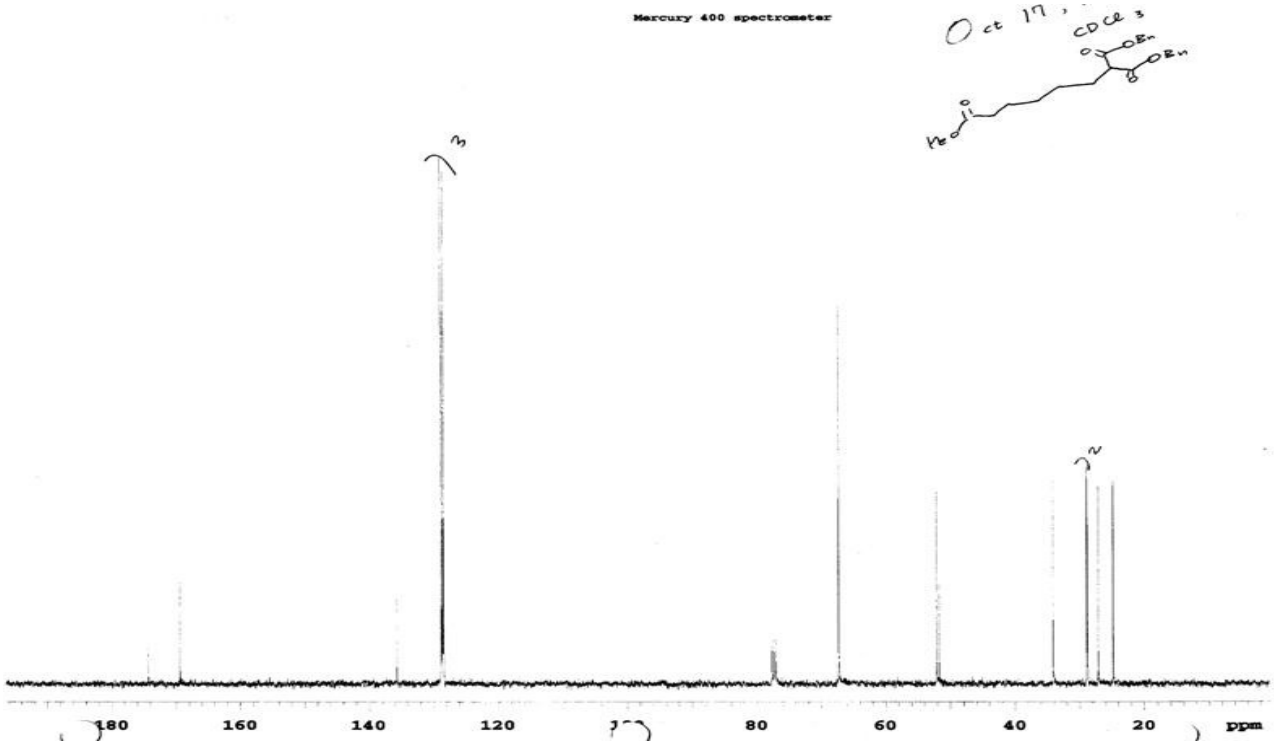

F.1.3. IR

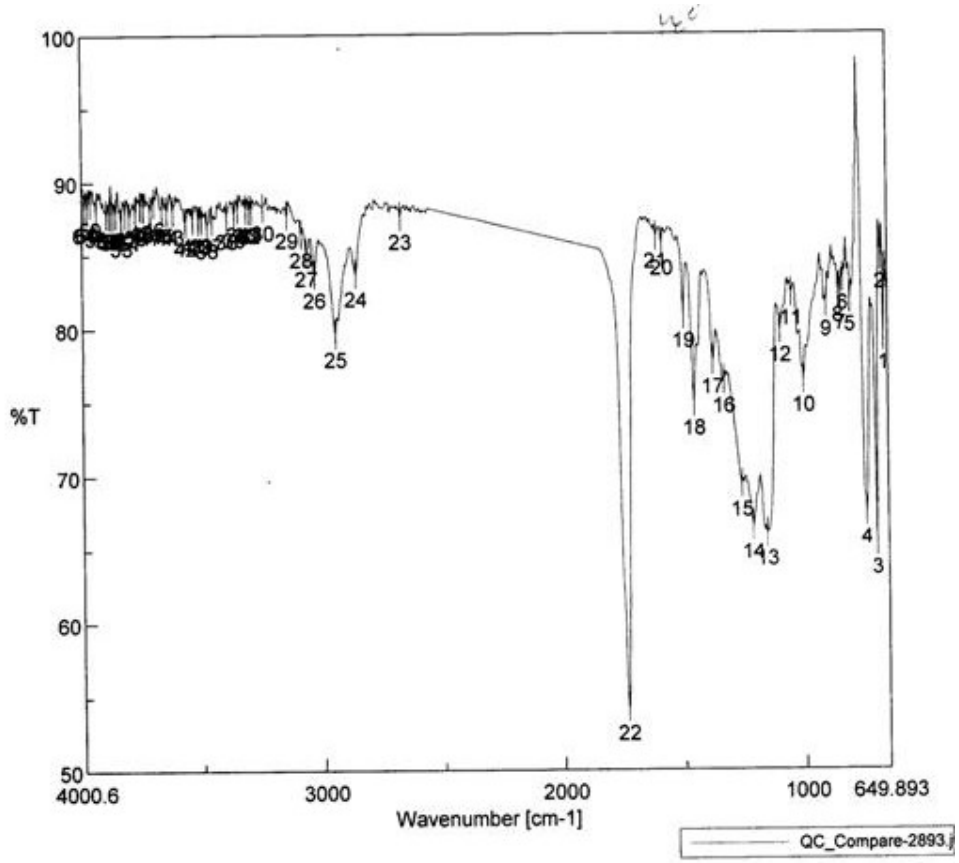

[Comment]
Sample Name
Comment
Result of Peak Picking

No.	Position	Intensity	No.	Position	Intensity	No.	Position	Intensity
1	Comment	39.2783	2	678.82	84.7458	3	698.16	65.3921
4	741.496	67.4622	5	806.099	81.8408	6	836.95	83.2872
7	846.597	81.9406	8	857.204	82.4557	9	907.34	81.5465
10	1062.6	76.46	11	1052.94	82.2899	12	1100.1	79.8154
13	1156.12	66.0605	14	1213.97	66.505	15	1261.22	69.3778
16	1332.57	76.4087	17	1377.89	77.7002	18	1455.99	74.9189
19	1498.42	80.8009	20	1586.16	85.7229	21	1610.27	86.2109
22	1733.69	54.2258	23	2673.82	87.5897	24	2861.84	83.6835
25	2948.63	79.6143	26	3033.48	83.6423	27	3066.26	85.1135
28	3087.48	86.3672	29	3147.26	87.7227	30	3245.61	88.2409
31	3292.86	88.0802	32	3304.43	88.0587	33	3316	88.1515
34	3348.78	88.162	35	3365.17	87.7866	36	3395.07	87.7035
37	3455.81	87.4194	38	3477.99	87.0564	39	3501.13	87.4002
40	3512.7	87.383	41	3536.81	87.4516	42	3565.74	87.2544
43	3617.8	88.039	44	3641.91	88.0199	45	3664.09	88.1246
46	3697.84	88.5384	47	3712.3	88.0316	48	3740.26	88.24
49	3752.8	88.348	50	3774.01	87.9889	51	3799.08	87.6495
52	3816.44	87.8602	53	3833.79	87.2302	54	3855.97	87.8314
55	3870.43	87.714	56	3883.93	87.7487	57	3896.47	87.8392
58	3939.86	87.9264	59	3965.89	88.5439	60	3978.43	88.2485
61	3990	88.1837						

[Data Information]
Creation Date 10/17/2008 3:15 PM
Data array type Linear data array
Horizontal Wavenumber [cm-1]
Vertical %T
Start 649.893 cm-1
End 4000.6 cm-1
Data pitch 0.964233 cm-1
Data points 3476

F.1.4. HRMS

Elemental Composition Report **Page 1**

Single Mass Analysis
Tolerance = 5.0 PPM / DBE: min = -1.5, max = 50.0
Element prediction: Off
Number of isotope peaks used for i-FIT = 3

Monoisotopic Mass, Even Electron Ions
369 formula(e) evaluated with 2 results within limits (up to 50 best isotopic matches for each mass)
Elements Used:
C: 0-500 H: 0-1000 N: 0-4 O: 0-6 23Na: 0-1
Pflum- Sun Choi oct1208-C7-MalonatePg16 mw412 LCT0171 1uL meoh
Shay 2008-07b.pro
2008_1020_0171_01 20 (0.439) Cm (17:20-1:6x4.000)

LCT Premier 20-Oct-2008 3::2::8
1: TOF MS ES+
2.88e+003

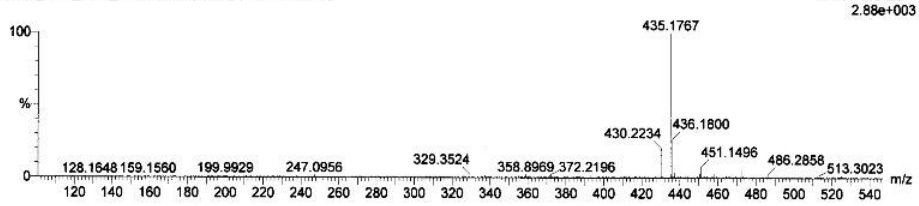

Minimum:				-1.5			
Maximum:		5.0	5.0	50.0			
Mass	Calc. Mass	mDa	PPM	DBE	i-FIT	i-FIT (Norm)	Formula
435.1767	435.1784	-1.7	-3.9	10.5	95.2	0.0	C24 H28 O6 23Na
	435.1749	1.8	4.1	22.5	99.6	4.4	C33 H23 O

F.2. 6, 6-Dibenzyl 1-methyl 7-(pyridine-4-yl)heptane-1, 6, 6-tricarboxylate (25).
F.2.1. ^{1}H NMR

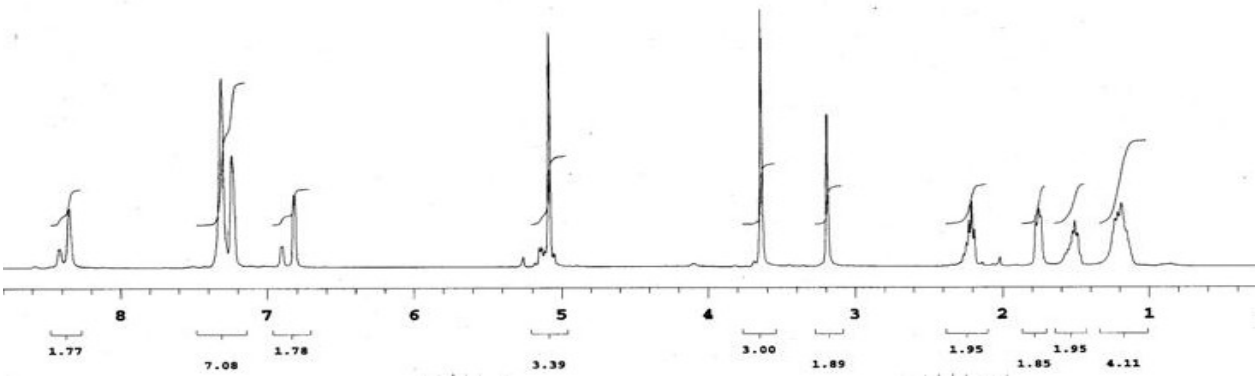

F.2.2. ^{13}C NMR

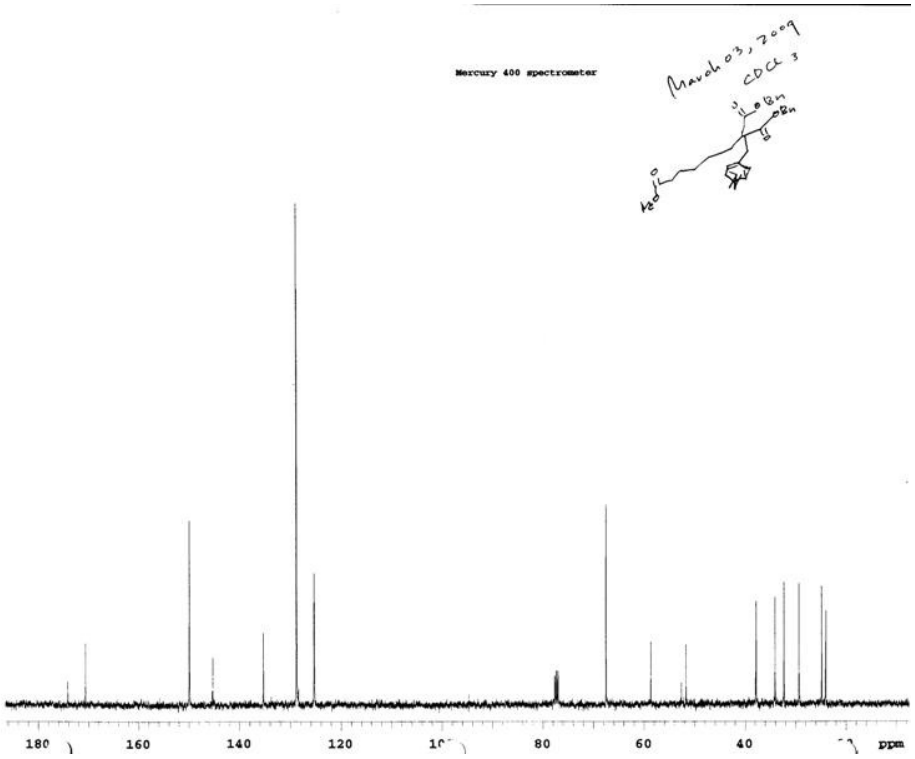

F.2.3. IR

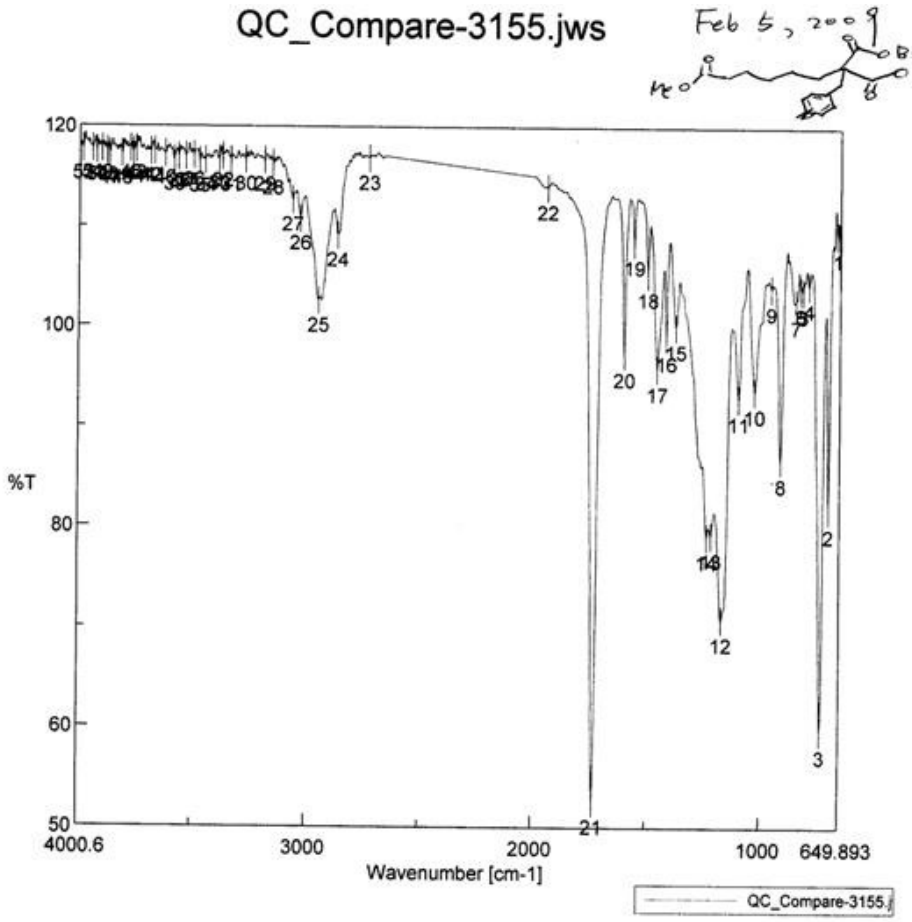

[Comment]
Sample Name
Comment
User
Division
Company wsu

[Data Information]
Creation Date 2/5/2009 3:26 PM
Data array type Linear data array
Horizontal Wavenumber [cm-1]
Vertical %T
Start 649.893 cm-1
End 4000.6 cm-1
Data pitch 0.964233 cm-1
Data points 3476

Result of Peak Picking

No.	Position	Intensity	No.	Position	Intensity	No.	Position	Intensity
1	663.393	109.215	2	698.105	81.5197	3	732.817	67.527
4	787.779	104.149	5	815.742	103.576	6	825.384	103.67
7	847.561	102.477	8	912.165	86.5883	9	954.591	103.832
10	1027.87	93.4998	11	1098.26	92.8216	12	1170.58	70.6822
13	1217.83	79.0602	14	1236.15	78.9271	15	1374.03	99.9891
16	1415.49	98.8035	17	1455.03	95.7541	18	1498.42	105.184
19	1558.2	108.416	20	1600.63	97.1595	21	1730.8	52.546
22	1939.07	113.935	23	2728.78	116.843	24	2865.7	109.085
25	2950.55	102.502	26	3031.55	110.746	27	3065.3	112.622
28	3152.08	116.272	29	3187.76	116.645	30	3271.64	116.682
31	3337.21	116.592	32	3372.89	117.013	33	3387.35	116.719
34	3449.06	116.562	35	3474.13	116.494	36	3498.24	117.066
37	3534.88	116.985	38	3564.77	116.911	39	3585.02	116.619
40	3623.59	117.249	41	3669.87	117.492	42	3687.23	117.439
43	3751.83	117.687	44	3764.37	117.352	45	3775.94	117.722
46	3813.54	117.203	47	3868.5	117.188	48	3880.08	117.518
49	3901.29	117.717	50	3925.39	117.565	51	3943.71	117.73
52	3986.14	117.71						

F.2.4. HRMS

Elemental Composition Report **Page 1**

Single Mass Analysis
Tolerance = 5.0 PPM / DBE: min = -1.5, max = 50.0
Element prediction: Off
Number of isotope peaks used for i-FIT = 3

Monoisotopic Mass, Even Electron Ions
426 formula(e) evaluated with 2 results within limits (up to 50 best isotopic matches for each mass)
Elements Used:
C: 0-500 H: 0-1000 N: 0-4 O: 0-6 23Na: 0-1
Ptlum-Sun Choi pct1808-C7-pyridinePg18 mw503 LCT0172 0.2uL meoh
Shay 2008-07b.pro
2008_1020_0172_03 13 (0.283) Cm (12:16-25:36x4.000)

LCT Premier 20-Oct-2008 3::0::8
1: TOF MS ES+
1.45e+004

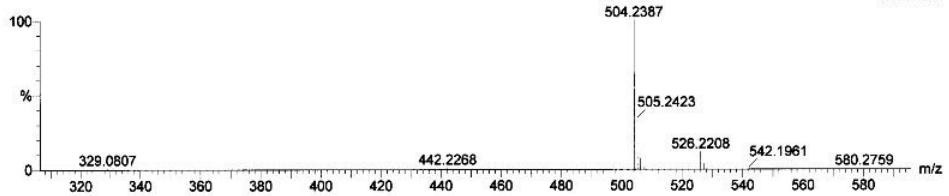

Minimum:				-1.5				
Maximum:		5.0	5.0	50.0				
Mass	Calc. Mass	mDa	PPM	DBE	i-FIT	i-FIT (Norm)	Formula	
504.2387	504.2386	0.1	0.2	14.5	28.1	0.0	C30 H34 N O6	
	504.2362	2.5	5.0	11.5	35.3	7.1	C28 H35 N O6	23Na

F.3. Benzyl 6-bromohexanoate (16).
F.3.1. ^{1}H NMR

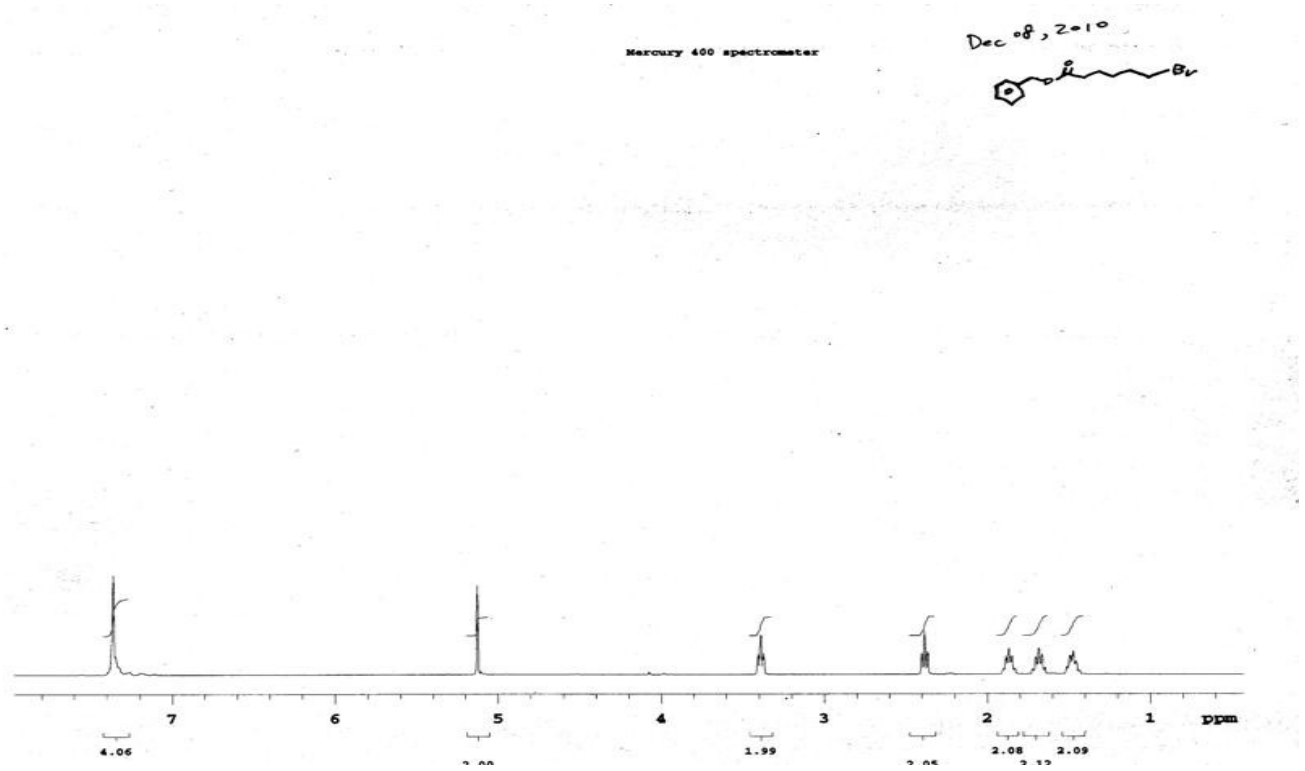

F.3.2. ^{13}C NMR

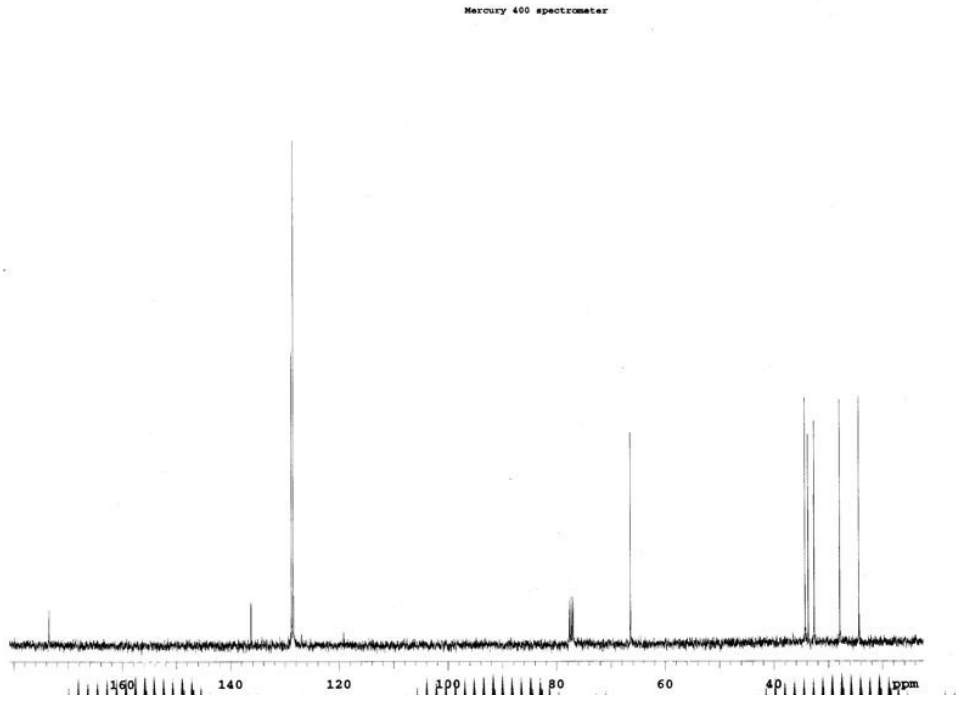

F.3.3. IR

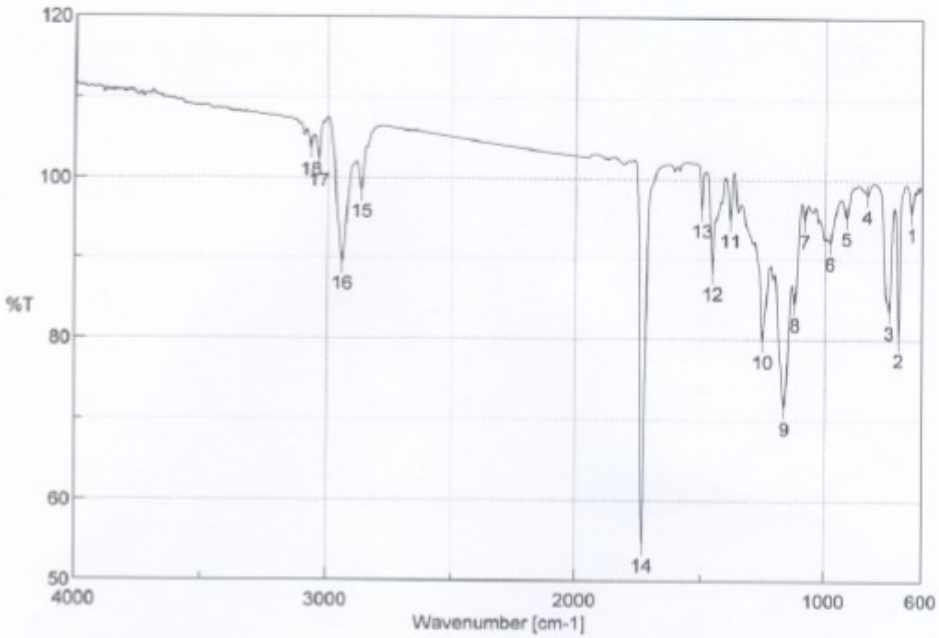

Result of Peak Picking

No.	Position	Intensity	No.	Position	Intensity
1	643.144	95.7992	2	697.141	80.0572
3	735.71	83.4347	4	825.384	98.0197
5	911.201	95.1909	6	978.697	92.0834
7	1080.91	94.8527	8	1123.33	84.3544
9	1164.79	71.5226	10	1253.5	79.7331
11	1384.64	94.8825	12	1455.03	88.2322
13	1497.45	96.0966	14	1732.73	54.5248
15	2863.77	98.4524	16	2938.98	89.3619
17	3033.48	102.248	18	3065.3	103.607

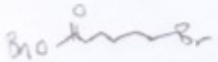

Book 4, pg. 77

[Comment]
Sample Name
Comment
User
Division
Company Wayne State

[Measurement Information]
Model Name FT/IR-4100typeA
Serial Number B071461016

Light Source Standard
Detector TGS
Accumulation Auto (63)
Resolution 4 cm-1
Zero Filling On
Apodization Cosine
Gain Auto (4)
Aperture Auto (7.1 mm)
Scanning Speed Auto (2 mm/sec)
Filter Auto (30000 Hz)

F.3.4. HRMS

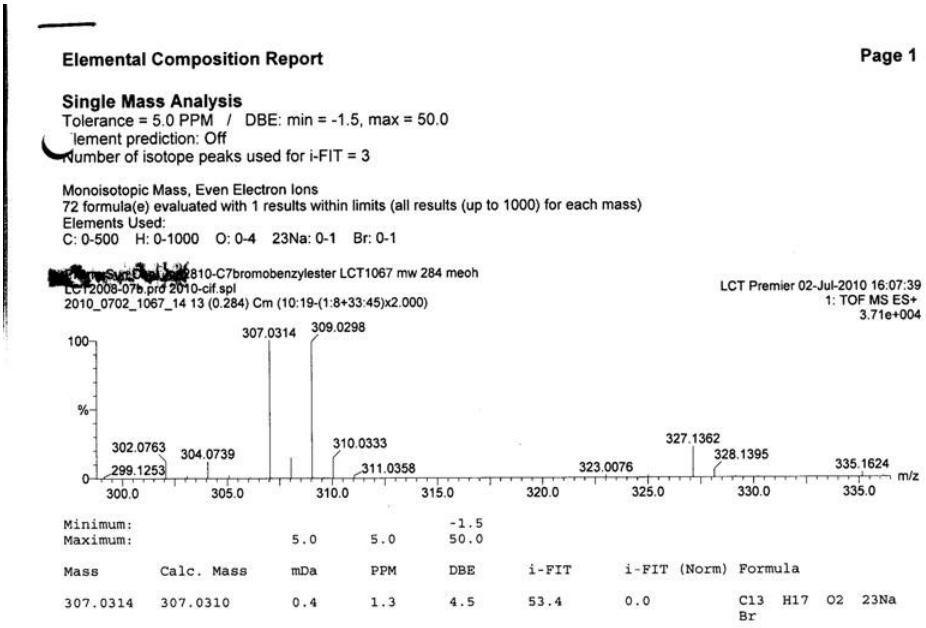

Elemental Composition Report Page 1

Single Mass Analysis
Tolerance = 5.0 PPM / DBE: min = -1.5, max = 50.0
Element prediction: Off
Number of isotope peaks used for i-FIT = 3

Monoisotopic Mass, Even Electron Ions
72 formula(e) evaluated with 1 results within limits (all results (up to 1000) for each mass)
Elements Used:
C: 0-500 H: 0-1000 O: 0-4 23Na: 0-1 Br: 0-1

[redacted]810-C7bromobenzylester LCT1067 mw 284 meoh
LCT2008-07b.prd 2010-cif.spl
2010_0702_1067_14 13 (0.284) Cm (10:19-(1:8+33:45)x2.000)

LCT Premier 02-Jul-2010 16:07:39
1: TOF MS ES+
3.71e+004

Minimum:				-1.5			
Maximum:		5.0	5.0	50.0			
Mass	Calc. Mass	mDa	PPM	DBE	i-FIT	i-FIT (Norm)	Formula
307.0314	307.0310	0.4	1.3	4.5	53.4	0.0	C13 H17 O2 23Na Br

F.4. 6-Benzyl 1,1-di-*tert*-butyl hexane-1,1,6-tricarboxylate (17).
F.4.1. ^{1}H NMR

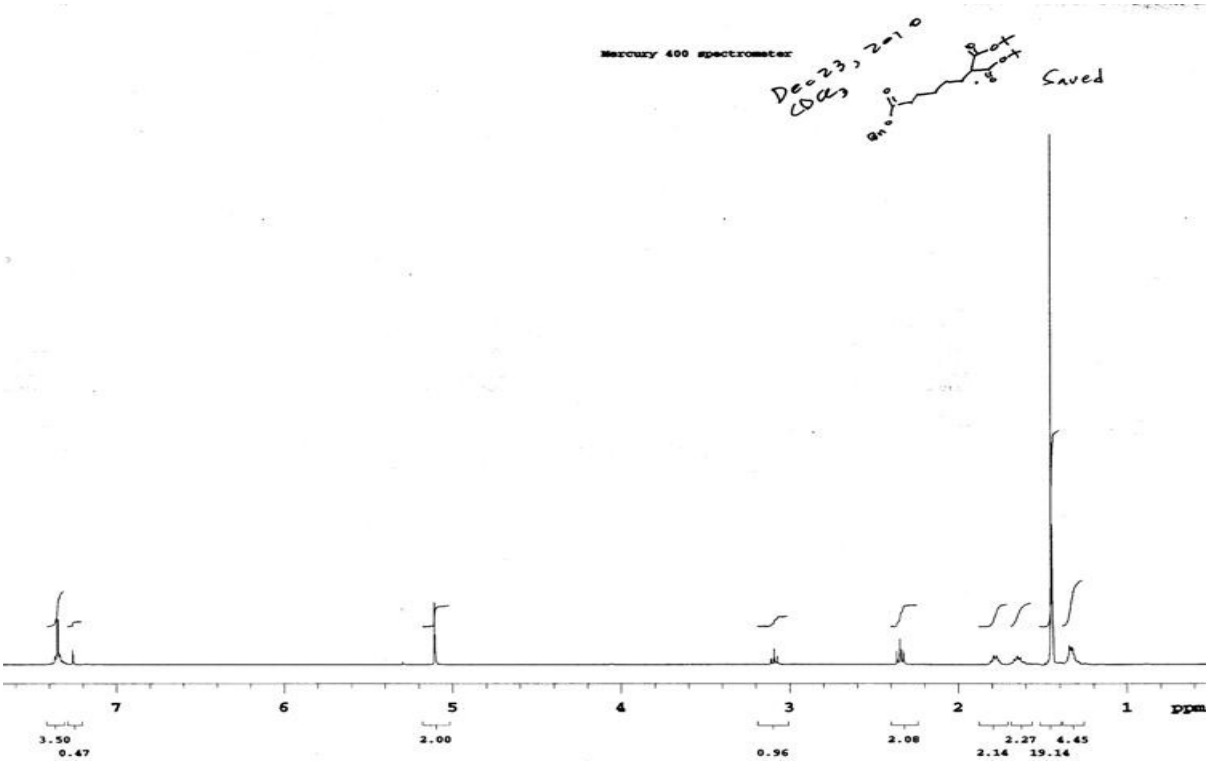

F.4.2. ^{13}C NMR

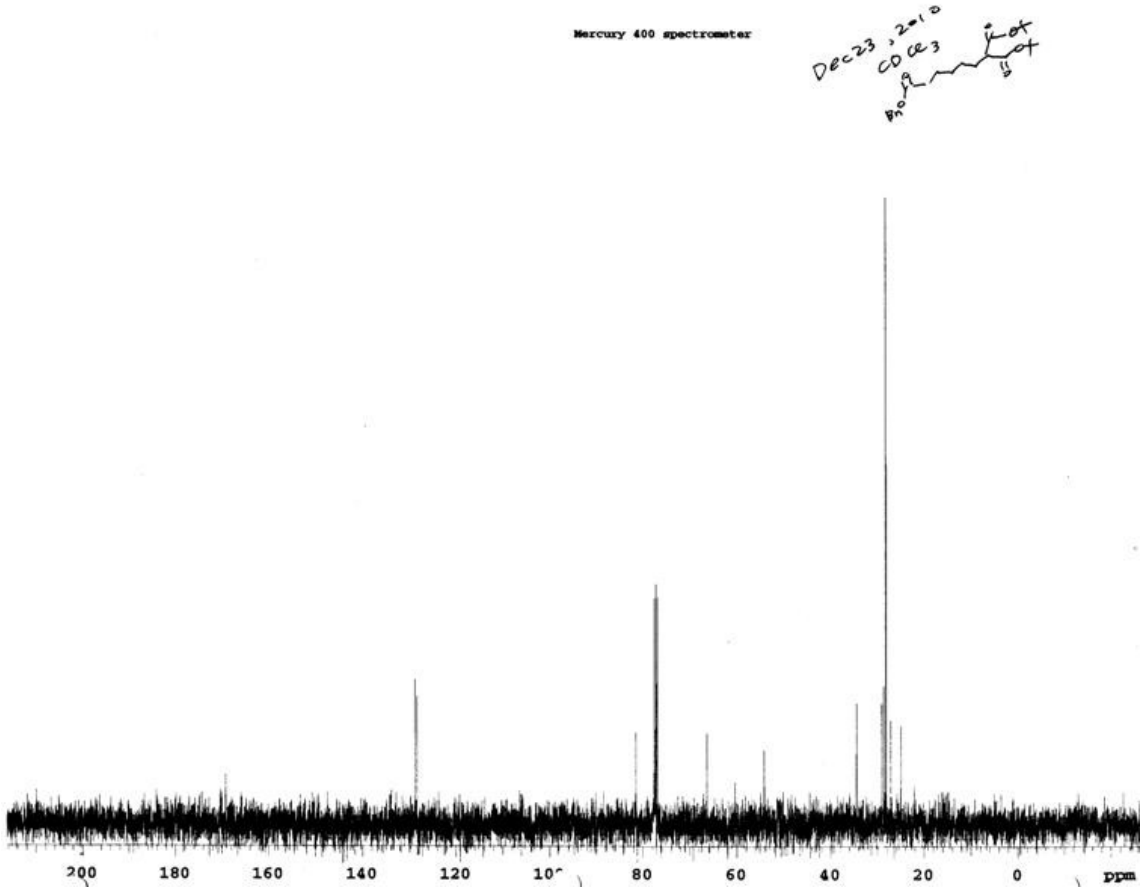

F.4.3. IR

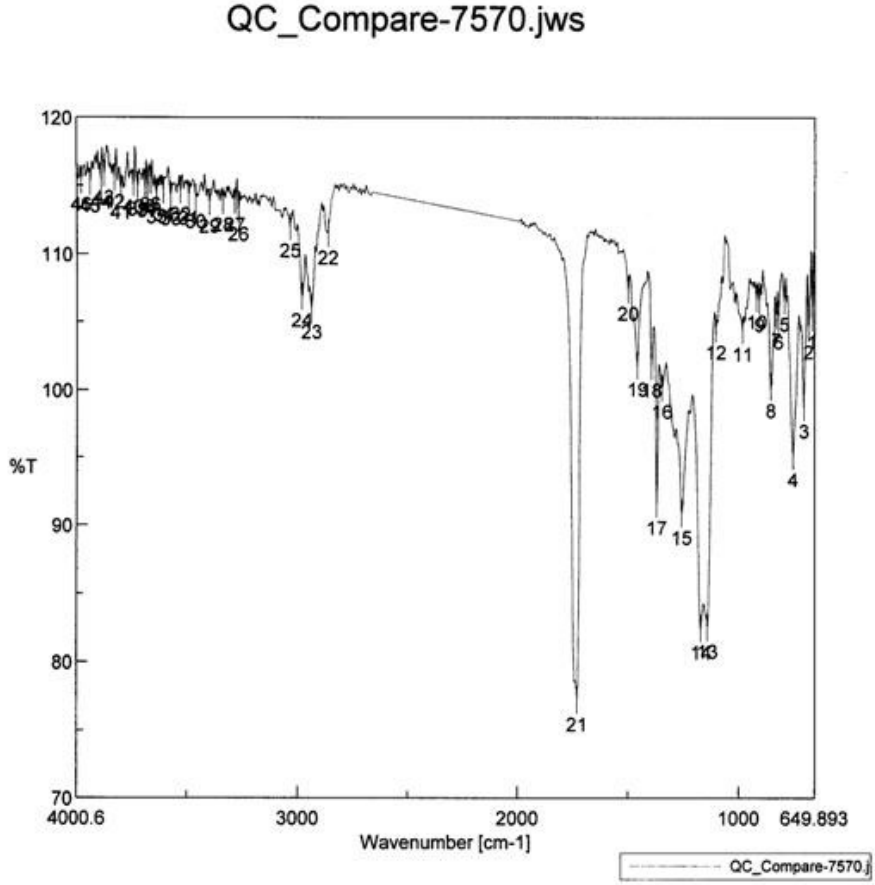

[Comment]
Sample Name
Comment
User
Division
Company wsu

[Data Information]

Creation Date	5/18/2010 3:06 PM
Data array type	Linear data array
Horizontal	Wavenumber [cm-1]
Vertical	%T
Start	649.893 cm-1
End	4000.6 cm-1
Data pitch	0.964233 cm-1
Data points	3476

Result of Peak Picking

No.	Position	Intensity	No.	Position	Intensity	No.	Position	Intensity
1	660.5	105.268	2	677.856	104.525	3	699.069	98.6691
4	748.245	95.0701	5	788.743	106.559	6	814.777	105.249
7	825.384	105.418	8	850.454	100.205	9	902.523	106.516
10	915.058	106.719	11	981.59	104.361	12	1102.12	104.479
13	1138.76	82.4753	14	1169.62	82.4066	15	1256.4	90.8133
16	1345.11	100.14	17	1369.21	91.5201	18	1392.35	101.704
19	1455.99	101.764	20	1498.42	107.354	21	1728.87	77.1507
22	2860.88	111.42	23	2935.13	105.966	24	2978.52	106.84
25	3032.51	111.969	26	3266.82	113.159	27	3283.21	113.849
28	3338.18	113.831	29	3397.96	113.735	30	3459.67	114.095
31	3491.49	114.341	32	3530.06	114.613	33	3574.41	114.28
34	3608.16	114.589	35	3639.02	114.43	36	3665.05	115.324
37	3679.51	114.863	38	3691.09	115.167	39	3723.87	114.982
40	3743.15	115.137	41	3800.04	114.745	42	3828.97	115.54
43	3876.22	115.831	44	3890.68	115.501	45	3938.89	115.231
46	3979.39	115.31						

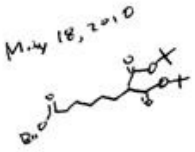

F.4.4. LRMS

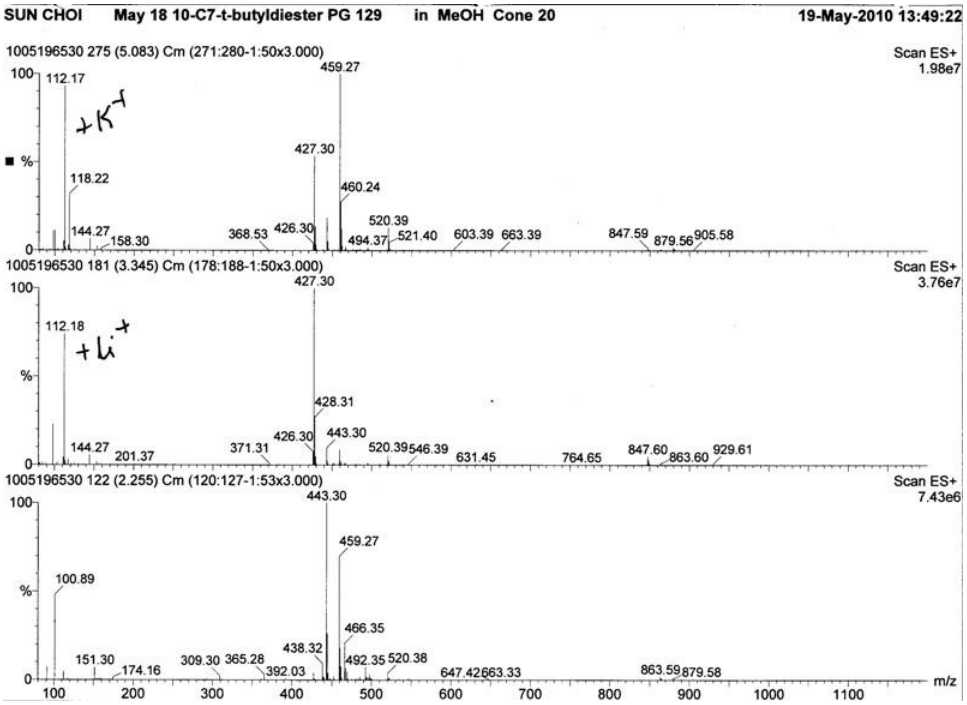

F.5. 1-Benzyl 6,6-di-tert-butyl 7-(pyridine-4-yl)heptane-1,6,6-tricaboxylate (18d).

F.5.1. ^{1}H NMR

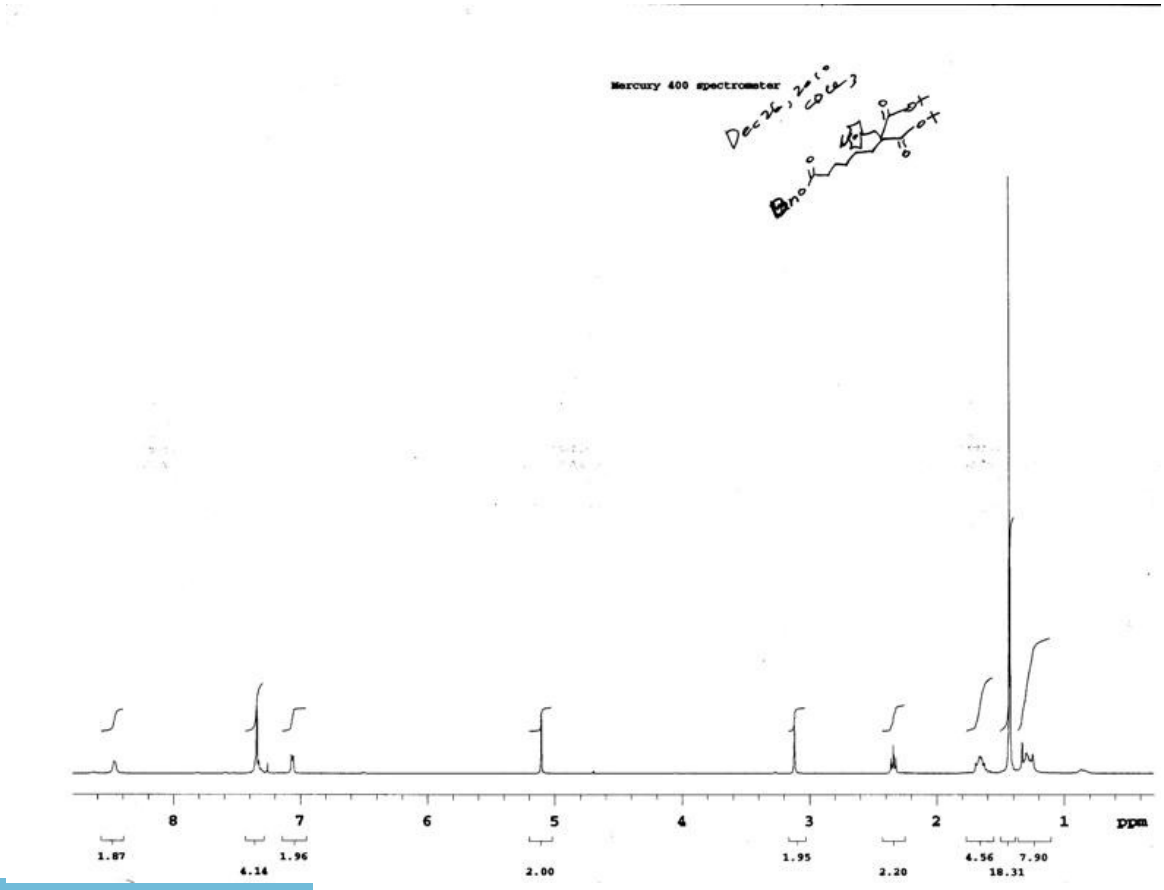

F.5.2. ^{13}C NMR

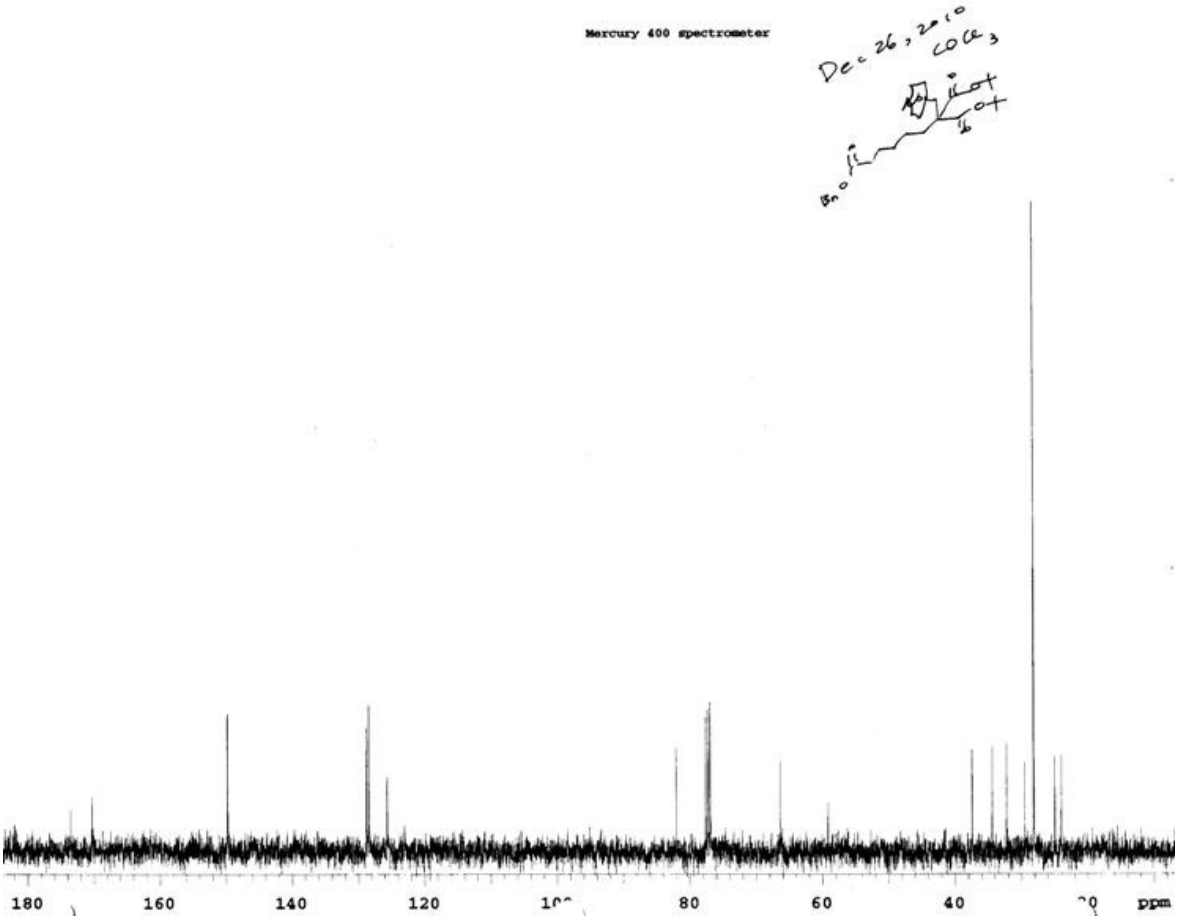

F.5.3. IR

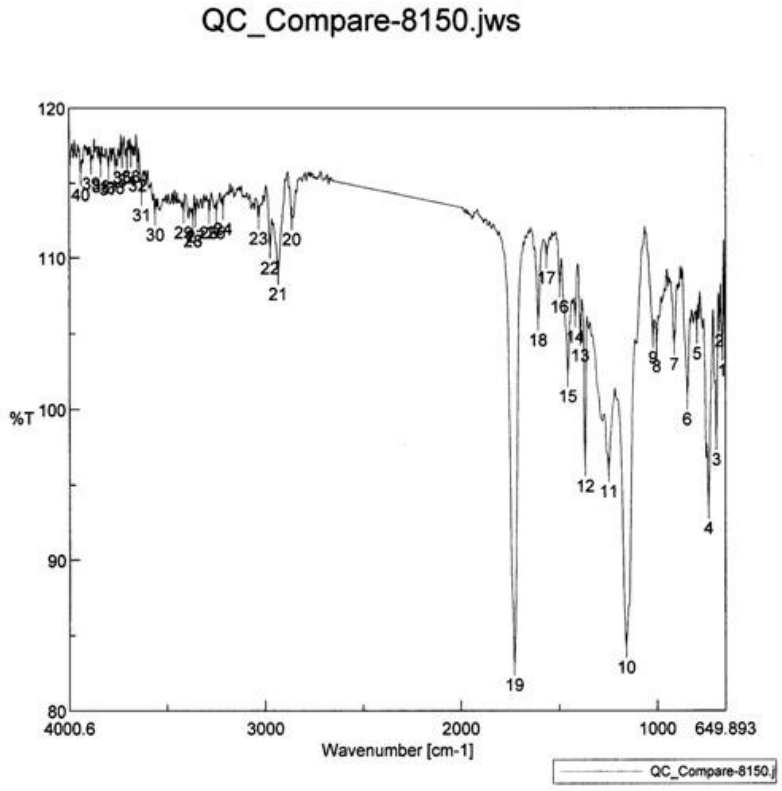

[Comment]
Sample Name
Comment
User
Division
Company wsu

[Data Information]

Creation Date	6/29/2010 11:19 AM
Data array type	Linear data array
Horizontal	Wavenumber [cm-1]
Vertical	%T
Start	649.893 cm-1
End	4000.6 cm-1
Data pitch	0.964233 cm-1
Data points	3476

Result of Peak Picking

No.	Position	Intensity	No.	Position	Intensity	No.	Position	Intensity
1	666.285	103.971	2	681.713	105.927	3	696.177	98.0724
4	736.674	93.5051	5	797.421	105.094	6	845.633	100.749
7	914.093	104.361	8	1003.77	104.232	9	1022.09	104.804
10	1159.01	84.2759	11	1248.68	95.9517	12	1368.25	96.3256
13	1392.35	104.946	14	1418.39	106.19	15	1455.03	102.266
16	1497.45	108.161	17	1563.99	110.064	18	1605.45	105.973
19	1726.94	83.115	20	2866.67	112.634	21	2935.13	109.009
22	2976.59	110.71	23	3036.37	112.682	24	3215.72	113.31
25	3250.43	113.074	26	3286.11	113.054	27	3355.53	112.814
28	3369.03	112.523	29	3416.28	113.075	30	3561.88	112.923
31	3629.37	114.245	32	3649.62	116.244	33	3683.37	116.807
34	3703.62	116.564	35	3728.69	116.759	36	3762.44	116.063
37	3797.15	115.985	38	3837.65	116.139	39	3886.83	116.353
40	3941.79	115.608						

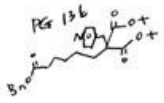

F.5.4. HRMS

Elemental Composition Report **Page 1**

Single Mass Analysis
Tolerance = 5.0 PPM / DBE: min = -1.5, max = 50.0
Element prediction: Off
Number of isotope peaks used for i-FIT = 3

Monoisotopic Mass, Even Electron Ions
71 formula(e) evaluated with 1 results within limits (all results (up to 1000) for each mass)
Elements Used:
C: 0-30 H: 0-1000 N: 0-2 O: 0-6 23Na: 0-1

[redacted]2910C7pyridylesterPG136 LCT1068 mw 511 meoh
LCT2008-075.pro 2010-cif.spl
2010_0702_1068_15 18 (0.389) Cm (18:23-1:6x2.000)

LCT Premier 02-Jul-2010 16:28:06
1: TOF MS ES+
2.12e+004

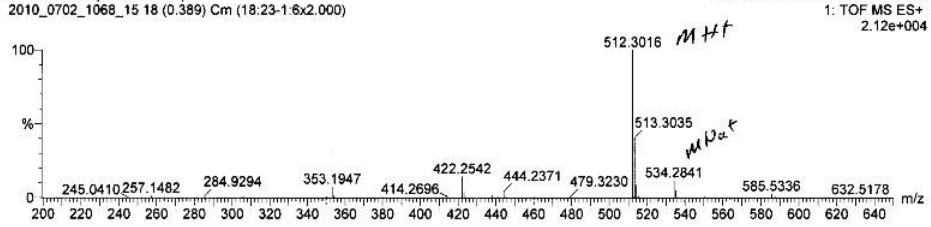

Minimum:				-1.5			
Maximum:		5.0	5.0	50.0			
Mass	Calc. Mass	mDa	PPM	DBE	i-FIT	i-FIT (Norm)	Formula
512.3016	512.3012	0.4	0.8	10.5	147.6	0.0	C30 H42 N O6

F.6. Benzyl 8-oxo-8-(phenylamino)-7-(pyridine-4-ylmethyl)octanoate (20d).
F.6.1. ^{1}H NMR

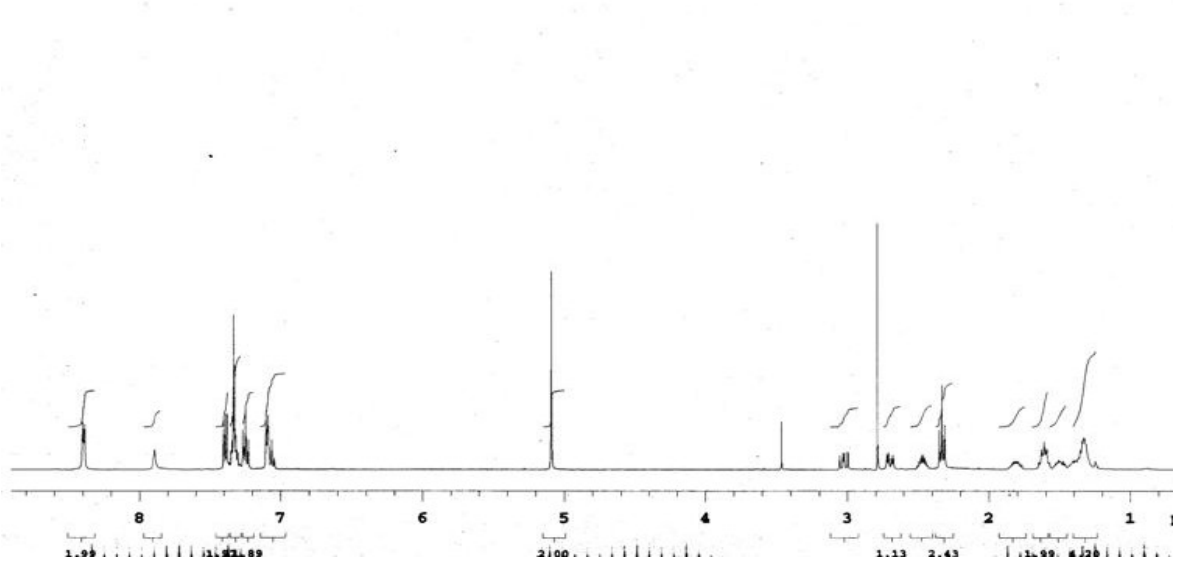

F.6.2. ^{13}C NMR

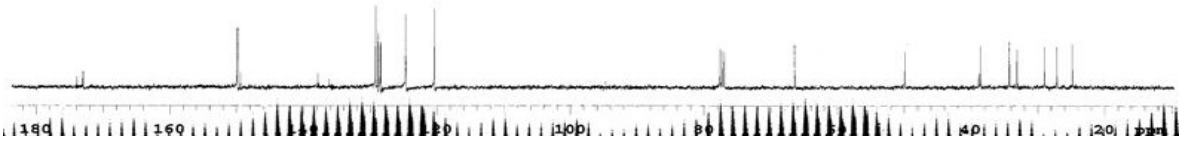

F.6.3. IR

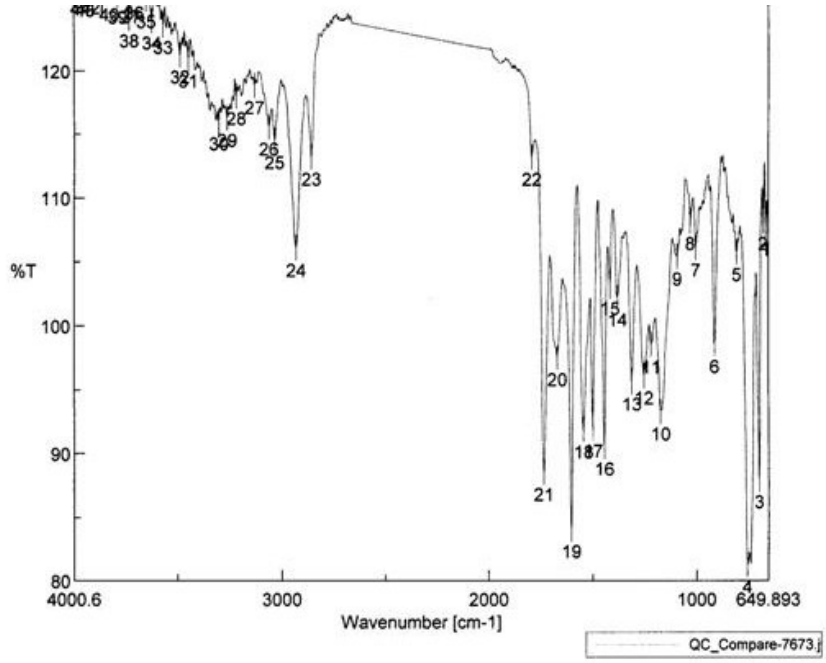

[Comment]
Sample Name
Comment
User
Division
Company wsu

[Data Information]

Creation Date	5/28/2010 12:07 PM
Data array type	Linear data array
Horizontal	Wavenumber [cm-1]
Vertical	%T
Start	649.893 cm-1
End	4000.6 cm-1
Data pitch	0.964233 cm-1
Data points	3476

Result of Peak Picking

No.	Position	Intensity	No.	Position	Intensity	No.	Position	Intensity
1	662.428	107.723	2	674.963	108.159	3	696.177	87.9459
4	752.102	81.2856	5	805.135	105.762	6	912.165	98.5639
7	1002.8	106.102	8	1029.8	108.17	9	1094.4	105.396
10	1172.51	93.267	11	1218.79	98.5468	12	1253.5	96.089
13	1311.36	95.6232	14	1379.82	102.228	15	1416.46	103.115
16	1443.46	90.5378	17	1498.42	91.946	18	1543.74	91.8761
19	1601.59	84.0694	20	1670.05	97.5435	21	1733.69	88.5415
22	1791.55	113.196	23	2857.99	113.186	24	2931.27	106.065
25	3035.41	114.497	26	3063.37	115.559	27	3131.83	118.84
28	3220.54	117.972	29	3263.93	116.23	30	3304.43	115.96
31	3450.03	120.916	32	3490.53	121.23	33	3570.56	123.573
34	3626.48	123.915	35	3653.48	125.601	36	3709.41	126.272
37	3723.87	125.963	38	3735.44	124.077	39	3788.47	125.953
40	3829.94	126.14	41	3894.54	126.733	42	3918.64	126.706
43	3945.64	126.507	44	3969.75	126.598			

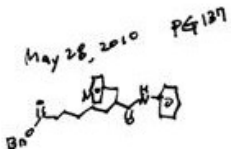

F.6.4. HRMS

Elemental Composition Report Page 1

Single Mass Analysis
Tolerance = 5.0 PPM / DBE: min = -1.5, max = 50.0
Element prediction: Off
Number of isotope peaks used for i-FIT = 3

Monoisotopic Mass, Even Electron Ions
2283 formula(e) evaluated with 7 results within limits (up to 700 best isotopic matches for each mass)
Elements Used:
C: 0-120 H: 0-1000 N: 0-16 O: 0-30 23Na: 0-1
SUN CHOI May 26 10-C7-Pyridylaniline
LCT2008-07b.pro 2010-cif.spl
2010_0526_990 13 (0.284) Cm (11:16-1:6x2.000)

LCT Premier 26-May-2010 14:05:49
1: TOF MS ES+
1.78e+003

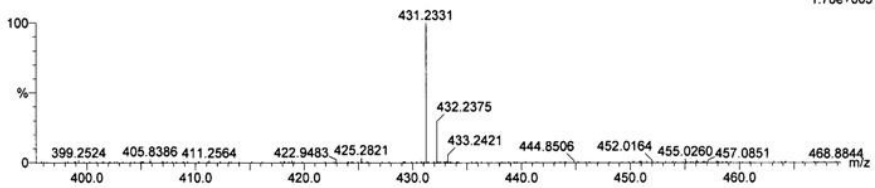

Minimum:		5.0	5.0	-1.5			
Maximum:				50.0			
Mass	Calc. Mass	mDa	PPM	DBE	i-FIT	i-FIT (Norm)	Formula
431.2331	431.2335	-0.4	-0.9	13.5	63.2	0.2	C27 H31 N2 O3
	431.2311	2.0	4.6	10.5	65.3	2.2	C25 H32 N2 O3 23Na
	431.2351	-2.0	-4.6	14.5	66.2	3.1	C30 H32 O 23Na
	431.2343	-1.2	-2.8	2.5	70.5	7.4	C14 H32 N8 O6 23Na
	431.2340	-0.9	-2.1	6.5	71.7	8.7	C12 H27 N14 O4
	431.2326	0.5	1.2	1.5	72.3	9.2	C11 H31 N10 O8
	431.2316	1.5	3.5	3.5	73.8	10.8	C10 H28 N14 O4 23Na

F.7. N^8-hydroxy-N^1-phenyl-2-(pyridin-4-ylmethyl)octanediamide (22d)
F.7.1. ^{1}H NMR

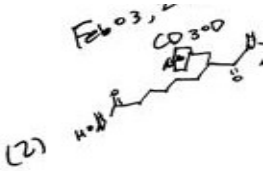

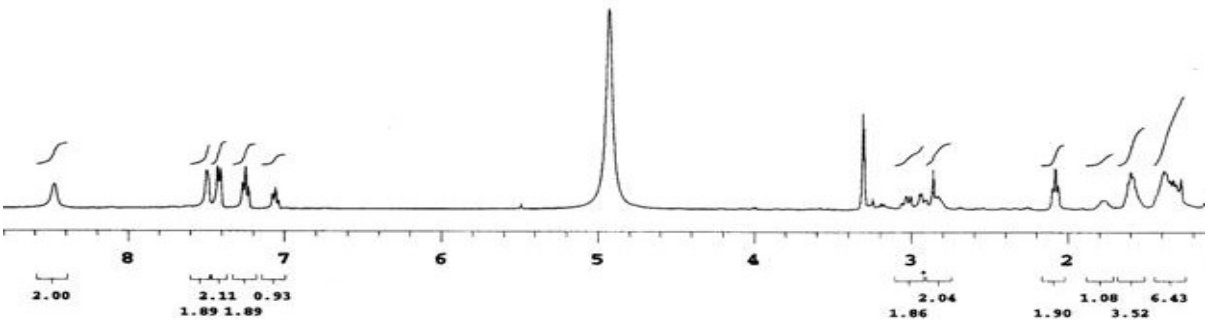

F.7.2. ^{13}C NMR

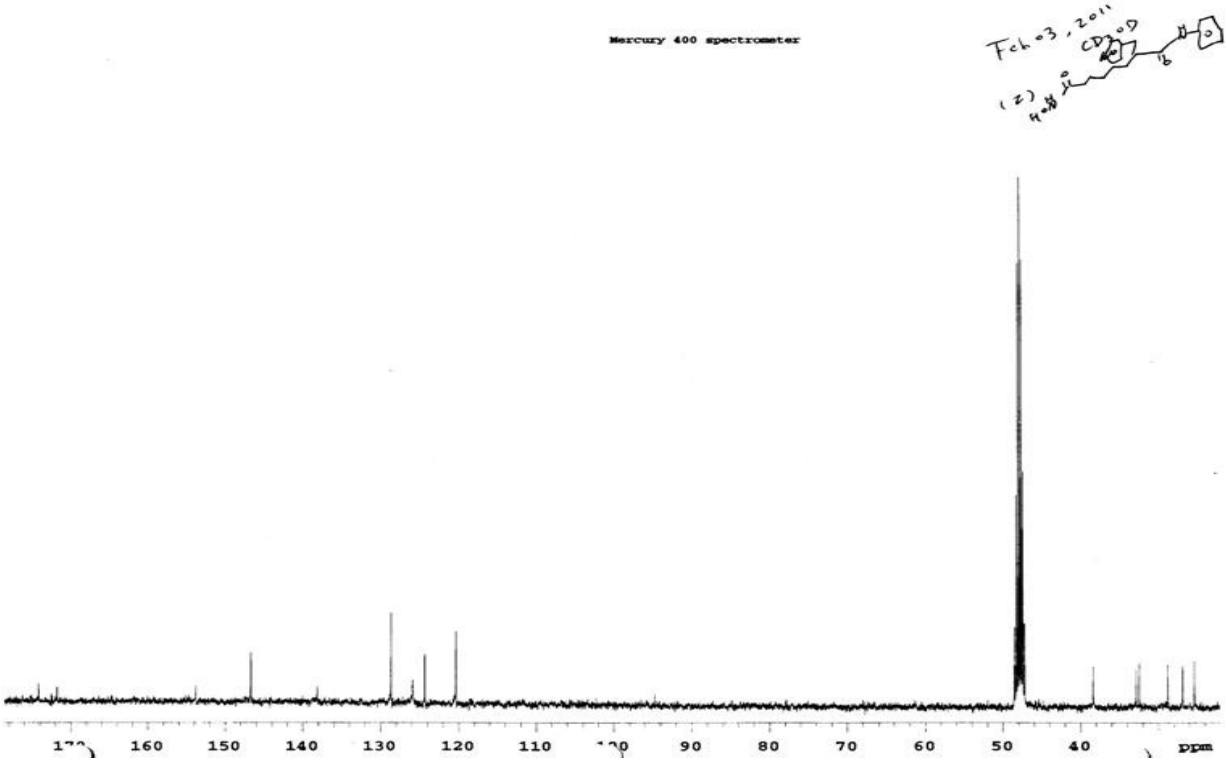

F.7.3. IR

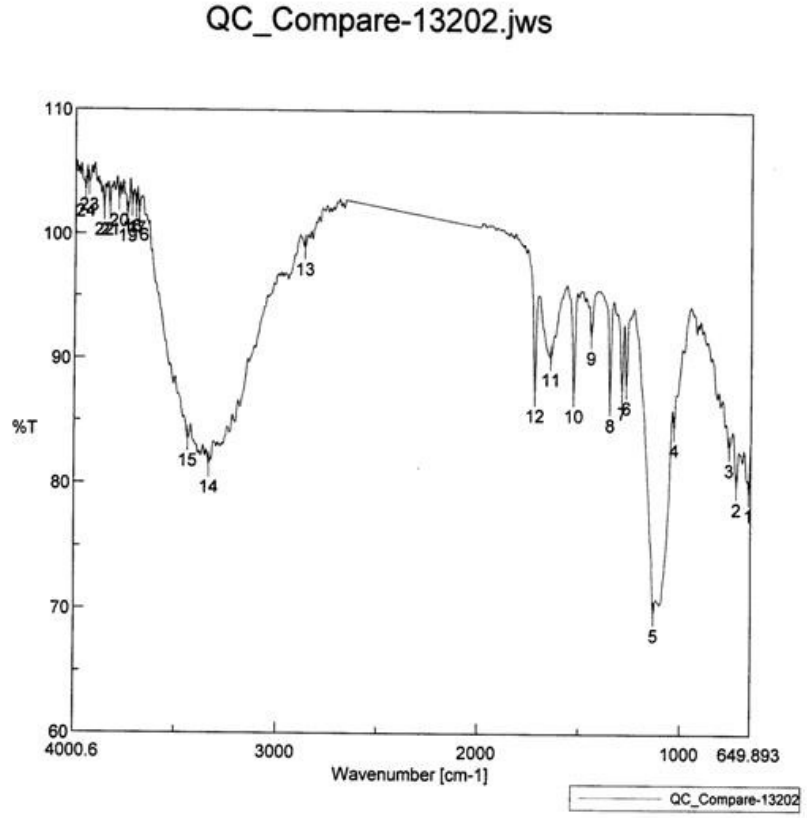

[Comment]
Sample Name
Comment
User
Division
Company wsu

[Data Information]

Creation Date	8/30/2011 2:03 PM
Data array type	Linear data array
Horizontal	Wavenumber [cm-1]
Vertical	%T
Start	649.893 cm-1
End	4000.6 cm-1
Data pitch	0.964233 cm-1
Data points	3476

Result of Peak Picking

No.	Position	Intensity	No.	Position	Intensity	No.	Position	Intensity
1	659.536	79.4143	2	721.247	79.8651	3	758.852	82.9898
4	1033.66	84.6034	5	1132.97	69.7215	6	1269.9	87.9266
7	1290.14	87.4945	8	1349.93	86.5345	9	1442.49	91.9062
10	1528.31	87.278	11	1641.13	90.1698	12	1720.19	87.2619
13	2865.7	98.9411	14	3335.28	81.4322	15	3440.39	83.513
16	3684.34	101.596	17	3699.76	102.18	18	3720.01	102.344
19	3743.15	101.552	20	3784.62	102.766	21	3829.94	102.038
22	3858.86	102.032	23	3934.07	104.023	24	3950.46	103.537

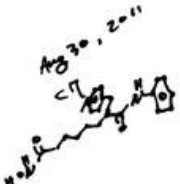

F.7.4. HRMS

Elemental Composition Report **Page 1**

Single Mass Analysis
Tolerance = 5.0 PPM / DBE: min = -1.5, max = 50.0
lement prediction: Off
Number of isotope peaks used for i-FIT = 3

Monoisotopic Mass, Even Electron Ions
930 formula(e) evaluated with 2 results within limits (up to 50 best isotopic matches for each mass)
Elements Used:
C: 0-100 H: 0-1000 N: 0-8 O: 0-15 23Na: 0-1
SUN CHOI Sep1501-07-Pyridyl hydrooxamic acid PG 152
LCT2008-07b.pro 2010-cif.spl
2010_0916_1296 14 (0.301) Cm (12:16-1:7x2.000)

LCT Premier 16-Sep-2010 15:06:40
1: TOF MS ES+
1.51e+004

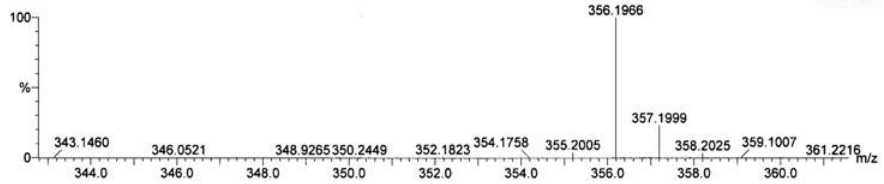

Minimum:		5.0	5.0	-1.5			
Maximum:				50.0			
Mass	Calc. Mass	mDa	PPM	DBE	i-FIT	i-FIT (Norm)	Formula
356.1966	356.1974	-0.8	-2.2	9.5	120.1	0.0	C20 H26 N3 O3
	356.1950	1.6	4.5	6.5	124.4	4.3	C18 H27 N3 O3 23Na

F.7.4. HPLC

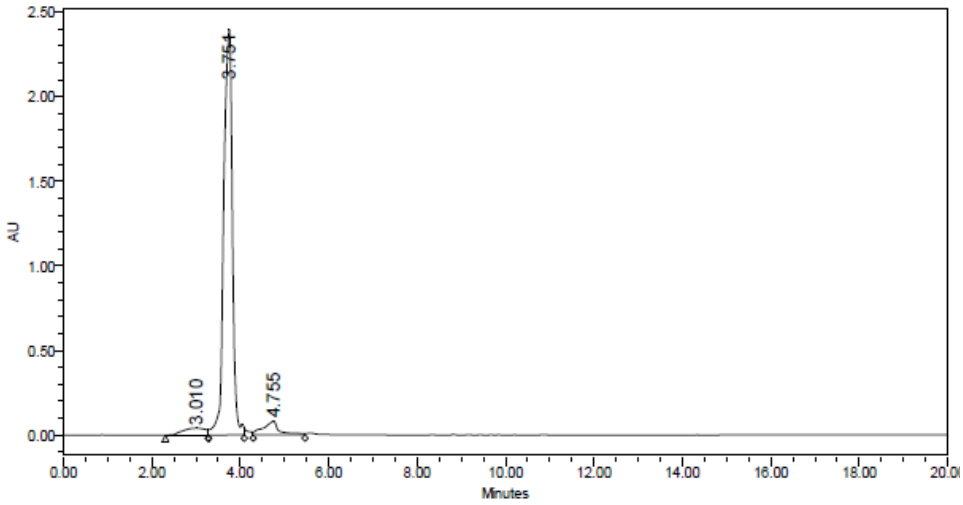

	RT	Area	% Area	Height
1	3.010	1425507	3.98	40391
2	3.751	32357117	90.35	2398048
3	4.755	2029952	5.67	82024

REFERENCES

1. Moving AHEAD with an international human epigenome project. *Nature* **2008,** *454* (7205), 711-5.

2. Yoo, C. B.; Jones, P. A., Epigenetic therapy of cancer: past, present and future. *Nat Rev Drug Discov* **2006,** *5* (1), 37-50.

3. Gregoretti, I. V.; Lee, Y. M.; Goodson, H. V., Molecular evolution of the histone deacetylase family: functional implications of phylogenetic analysis. *J Mol Biol* **2004,** *338* (1), 17-31.

4. Grozinger, C. M.; Schreiber, S. L., Deacetylase enzymes: biological functions and the use of small-molecule inhibitors. *Chem Biol* **2002,** *9* (1), 3-16.

5. Khabele, D.; Son, D. S.; Parl, A. K.; Goldberg, G. L.; Augenlicht, L. H.; Mariadason, J. M.; Rice, V. M., Drug-induced inactivation or gene silencing of class I histone deacetylases suppresses ovarian cancer cell growth: implications for therapy. *Cancer Biol Ther* **2007,** *6* (5), 795-801.

6. Song, J.; Noh, J. H.; Lee, J. H.; Eun, J. W.; Ahn, Y. M.; Kim, S. Y.; Lee, S. H.; Park, W. S.; Yoo, N. J.; Lee, J. Y.; Nam, S. W., Increased expression of histone deacetylase 2 is found in human gastric cancer. *APMIS* **2005,** *113* (4), 264-8.

7. Bartling, B.; Hofmann, H. S.; Boettger, T.; Hansen, G.; Burdach, S.; Silber, R. E.; Simm, A., Comparative application of antibody and gene array for expression profiling in human squamous cell lung carcinoma. *Lung Cancer* **2005,** *49* (2), 145-54.

8. Krennhrubec, K.; Marshall, B. L.; Hedglin, M.; Verdin, E.; Ulrich, S. M., Design and evaluation of 'Linkerless' hydroxamic acids as selective HDAC8 inhibitors. *Bioorg Med Chem Lett* **2007,** *17* (10), 2874-8.

9. Saji, S.; Kawakami, M.; Hayashi, S.; Yoshida, N.; Hirose, M.; Horiguchi, S. I.; Itoh, A.; Funata, N.; Schreiber, S. L.; Yoshida, M.; Toi, M., Significance of HDAC6 regulation via estrogen signaling for cell motility and prognosis in estrogen receptor-positive breast cancer. *Oncogene* **2005,** *24* (28), 4531-4539.

10. (a) de Ruijter, A. J.; van Gennip, A. H.; Caron, H. N.; Kemp, S.; van Kuilenburg, A. B., Histone deacetylases (HDACs): characterization of the classical HDAC family. *Biochem J* **2003,** *370* (Pt 3), 737-49; (b) Fischer, D. D.; Cai, R.; Bhatia, U.; Asselbergs, F. A.; Song, C.; Terry, R.; Trogani, N.; Widmer, R.; Atadja, P.; Cohen, D., Isolation and characterization of a novel class II histone deacetylase, HDAC10. *J Biol Chem* **2002,** *277* (8), 6656-66.

11. (a) Kramer, O. H.; Gottlicher, M.; Heinzel, T., Histone deacetylase as a therapeutic target. *Trends in endocrinology and metabolism: TEM* **2001,** *12* (7), 294-300; (b) Garber, K., HDAC inhibitors overcome first hurdle. *Nat Biotechnol* **2007,** *25* (1), 17-9.

12. Grant, S.; Easley, C.; Kirkpatrick, P., Vorinostat. *Nat Rev Drug Discov* **2007,** *6* (1), 21-2.

13. Robey, R. W.; Chakraborty, A. R.; Basseville, A.; Luchenko, V.; Bahr, J.; Zhan, Z.; Bates, S. E., Histone deacetylase inhibitors: emerging mechanisms of resistance. *Mol Pharm* **2011,** *8* (6), 2021-31.

14. Bressi, J. C.; Jennings, A. J.; Skene, R.; Wu, Y.; Melkus, R.; De Jong, R.; O'Connell, S.; Grimshaw, C. E.; Navre, M.; Gangloff, A. R., Exploration of the HDAC2 foot pocket: Synthesis and SAR of substituted N-(2-aminophenyl)benzamides. *Bioorg Med Chem Lett* **2010,** *20* (10), 3142-5.

15. Watson, P. J.; Fairall, L.; Santos, G. M.; Schwabe, J. W., Structure of HDAC3 bound to co-repressor and inositol tetraphosphate. *Nature* **2012,** *481* (7381), 335-40.

16. Bottomley, M. J.; Lo Surdo, P.; Di Giovine, P.; Cirillo, A.; Scarpelli, R.; Ferrigno, F.; Jones, P.; Neddermann, P.; De Francesco, R.; Steinkuhler, C.; Gallinari, P.; Carfi, A., Structural and functional analysis of the human HDAC4 catalytic domain reveals a regulatory structural zinc-binding domain. *J Biol Chem* **2008,** *283* (39), 26694-704.

17. (a) Somoza, J. R.; Skene, R. J.; Katz, B. A.; Mol, C.; Ho, J. D.; Jennings, A. J.; Luong, C.; Arvai, A.; Buggy, J. J.; Chi, E.; Tang, J.; Sang, B. C.; Verner, E.; Wynands, R.; Leahy, E. M.; Dougan, D. R.; Snell, G.; Navre, M.; Knuth, M. W.; Swanson, R. V.; McRee, D. E.; Tari, L. W., Structural snapshots of human HDAC8 provide insights into the class I histone deacetylases. *Structure* **2004,** *12* (7), 1325-34; (b) Vannini, A.; Volpari, C.; Filocamo, G.; Casavola, E. C.; Brunetti, M.; Renzoni, D.; Chakravarty, P.; Paolini, C.; De Francesco, R.; Gallinari, P.; Steinkuhler, C.; Di Marco, S., Crystal structure of a eukaryotic zinc-dependent histone deacetylase, human HDAC8, complexed with a hydroxamic acid inhibitor. *Proceedings of the National Academy of Sciences of the United States of America* **2004,** *101* (42), 15064-9.

18. Marks, P.; Rifkind, R. A.; Richon, V. M.; Breslow, R.; Miller, T.; Kelly, W. K., Histone deacetylases and cancer: causes and therapies. *Nat Rev Cancer* **2001,** *1* (3), 194-202.

19. O'Connor, O. A.; Heaney, M. L.; Schwartz, L.; Richardson, S.; Willim, R.; MacGregor-Cortelli, B.; Curly, T.; Moskowitz, C.; Portlock, C.; Horwitz, S.; Zelenetz, A. D.; Frankel, S.; Richon, V.; Marks, P.; Kelly, W. K., Clinical experience with intravenous and oral formulations of the novel histone deacetylase inhibitor suberoylanilide

hydroxamic acid in patients with advanced hematologic malignancies. *J Clin Oncol* **2006,** *24* (1), 166-73.

20. Bieliauskas, A. V.; Pflum, M. K. H., Isoform-selective histone deacetylase inhibitors. *Chemical Society Reviews* **2008,** *37* (7), 1402-1413.

21. (a) Suzuki, T.; Ando, T.; Tsuchiya, K.; Fukazawa, N.; Saito, A.; Mariko, Y.; Yamashita, T.; Nakanishi, O., Synthesis and histone deacetylase inhibitory activity of new benzamide derivatives. *J Med Chem* **1999,** *42* (15), 3001-3; (b) Dai, Y.; Guo, Y.; Guo, J.; Pease, L. J.; Li, J.; Marcotte, P. A.; Glaser, K. B.; Tapang, P.; Albert, D. H.; Richardson, P. L.; Davidsen, S. K.; Michaelides, M. R., Indole amide hydroxamic acids as potent inhibitors of histone deacetylases. *Bioorg Med Chem Lett* **2003,** *13* (11), 1897-901; (c) Mai, A.; Massa, S.; Pezzi, R.; Rotili, D.; Loidl, P.; Brosch, G., Discovery of (aryloxopropenyl)pyrrolyl hydroxyamides as selective inhibitors of class IIa histone deacetylase homologue HD1-A. *J Med Chem* **2003,** *46* (23), 4826-9.

22. (a) Bouchain, G.; Delorme, D., Novel hydroxamate and anilide derivatives as potent histone deacetylase inhibitors: synthesis and antiproliferative evaluation. *Curr Med Chem* **2003,** *10* (22), 2359-72; (b) Nagaoka, Y.; Maeda, T.; Kawai, Y.; Nakashima, D.; Oikawa, T.; Shimoke, K.; Ikeuchi, T.; Kuwajima, H.; Uesato, S., Synthesis and cancer antiproliferative activity of new histone deacetylase inhibitors: hydrophilic hydroxamates and 2-aminobenzamide-containing derivatives. *Eur J Med Chem* **2006,** *41* (6), 697-708; (c) Uesato, S.; Kitagawa, M.; Nagaoka, Y.; Maeda, T.; Kuwajima, H.; Yamori, T., Novel histone deacetylase inhibitors: N-hydroxycarboxamides possessing a terminal bicyclic aryl group. *Bioorg Med Chem Lett* **2002,** *12* (10), 1347-9; (d) Jung, M.; Brosch, G.; Kolle, D.; Scherf, H.; Gerhauser, C.; Loidl, P., Amide analogues of

trichostatin A as inhibitors of histone deacetylase and inducers of terminal cell differentiation. *J Med Chem* **1999,** *42* (22), 4669-79.

23. (a) Hu, E.; Dul, E.; Sung, C. M.; Chen, Z.; Kirkpatrick, R.; Zhang, G. F.; Johanson, K.; Liu, R.; Lago, A.; Hofmann, G.; Macarron, R.; de los Frailes, M.; Perez, P.; Krawiec, J.; Winkler, J.; Jaye, M., Identification of novel isoform-selective inhibitors within class I histone deacetylases. *J Pharmacol Exp Ther* **2003,** *307* (2), 720-8; (b) Beckers, T.; Burkhardt, C.; Wieland, H.; Gimmnich, P.; Ciossek, T.; Maier, T.; Sanders, K., Distinct pharmacological properties of second generation HDAC inhibitors with the benzamide or hydroxamate head group. *Int J Cancer* **2007,** *121* (5), 1138-48.

24. (a) Hanessian, S.; Auzzas, L.; Giannini, G.; Marzi, M.; Cabri, W.; Barbarino, M.; Vesci, L.; Pisano, C., Omega-alkoxy analogues of SAHA (vorinostat) as inhibitors of HDAC: a study of chain-length and stereochemical dependence. *Bioorg Med Chem Lett* **2007,** *17* (22), 6261-5; (b) Belvedere, S.; Witter, D. J.; Yan, J.; Secrist, J. P.; Richon, V.; Miller, T. A., Aminosuberoyl hydroxamic acids (ASHAs): a potent new class of HDAC inhibitors. *Bioorg Med Chem Lett* **2007,** *17* (14), 3969-71.

25. (a) Lavoie, R.; Bouchain, G.; Frechette, S.; Woo, S. H.; Abou-Khalil, E.; Leit, S.; Fournel, M.; Yan, P. T.; Trachy-Bourget, M. C.; Beaulieu, C.; Li, Z.; Besterman, J.; Delorme, D., Design and synthesis of a novel class of histone deacetylase inhibitors. *Bioorg Med Chem Lett* **2001,** *11* (21), 2847-50; (b) Varghese, S.; Senanayake, T.; Murray-Stewart, T.; Doering, K.; Fraser, A.; Casero, R. A., Jr.; Woster, P. M., Polyaminohydroxamic acids and polyaminobenzamides as isoform selective histone deacetylase inhibitors. *J Med Chem* **2008,** *51* (8), 2447-56.

26. Bieliauskas, A. V.; Weerasinghe, S. V.; Pflum, M. K., Structural requirements of HDAC inhibitors: SAHA analogs functionalized adjacent to the hydroxamic acid. *Bioorg Med Chem Lett* **2007,** *17* (8), 2216-9.

27. (a) Vinodhkumar, R.; Song, Y. S.; Ravikumar, V.; Ramakrishnan, G.; Devaki, T., Depsipeptide a histone deacetlyase inhibitor down regulates levels of matrix metalloproteinases 2 and 9 mRNA and protein expressions in lung cancer cells (A549). *Chem Biol Interact* **2007,** *165* (3), 220-9; (b) You, J. S.; Kang, J. K.; Lee, E. K.; Lee, J. C.; Lee, S. H.; Jeon, Y. J.; Koh, D. H.; Ahn, S. H.; Seo, D. W.; Lee, H. Y.; Cho, E. J.; Han, J. W., Histone deacetylase inhibitor apicidin downregulates DNA methyltransferase 1 expression and induces repressive histone modifications via recruitment of corepressor complex to promoter region in human cervix cancer cells. *Oncogene* **2008,** *27* (10), 1376-86; (c) Furumai, R.; Komatsu, Y.; Nishino, N.; Khochbin, S.; Yoshida, M.; Horinouchi, S., Potent histone deacetylase inhibitors built from trichostatin A and cyclic tetrapeptide antibiotics including trapoxin. *Proceedings of the National Academy of Sciences of the United States of America* **2001,** *98* (1), 87-92.

28. Woo, S.; Gardner, E. R.; Chen, X.; Ockers, S. B.; Baum, C. E.; Sissung, T. M.; Price, D. K.; Frye, R.; Piekarz, R. L.; Bates, S. E.; Figg, W. D., Population pharmacokinetics of romidepsin in patients with cutaneous T-cell lymphoma and relapsed peripheral T-cell lymphoma. *Clin Cancer Res* **2009,** *15* (4), 1496-503.

29. Furumai, R.; Matsuyama, A.; Kobashi, N.; Lee, K. H.; Nishiyama, M.; Nakajima, H.; Tanaka, A.; Komatsu, Y.; Nishino, N.; Yoshida, M.; Horinouchi, S., FK228 (depsipeptide) as a natural prodrug that inhibits class I histone deacetylases. *Cancer Res* **2002,** *62* (17), 4916-21.

30. Khan, N.; Jeffers, M.; Kumar, S.; Hackett, C.; Boldog, F.; Khramtsov, N.; Qian, X.; Mills, E.; Berghs, S. C.; Carey, N.; Finn, P. W.; Collins, L. S.; Tumber, A.; Ritchie, J. W.; Jensen, P. B.; Lichenstein, H. S.; Sehested, M., Determination of the class and isoform selectivity of small-molecule histone deacetylase inhibitors. *Biochem J* **2008,** *409* (2), 581-9.

31. Jones, P.; Altamura, S.; Chakravarty, P. K.; Cecchetti, O.; De Francesco, R.; Gallinari, P.; Ingenito, R.; Meinke, P. T.; Petrocchi, A.; Rowley, M.; Scarpelli, R.; Serafini, S.; Steinkuhler, C., A series of novel, potent, and selective histone deacetylase inhibitors. *Bioorg Med Chem Lett* **2006,** *16* (23), 5948-52.

32. Hanessian, S., Vorinostat-Like Molecules as Structural, Stereochemical, and Pharmacological Tools. *ACS Medicinal Chemistry Letters* **2010,** *1*, 70-74.

33. Spencer, J., Synthesis and Biological Evaluation of JAHAs: Ferrocene-Based Histone Deacetylase Inhibitors. *ACS Medicinal Chemistry Letters* **2011,** *2*, 358-362.

34. (a) Schuetz, A.; Min, J.; Allali-Hassani, A.; Schapira, M.; Shuen, M.; Loppnau, P.; Mazitschek, R.; Kwiatkowski, N. P.; Lewis, T. A.; Maglathin, R. L.; McLean, T. H.; Bochkarev, A.; Plotnikov, A. N.; Vedadi, M.; Arrowsmith, C. H., Human HDAC7 harbors a class IIa histone deacetylase-specific zinc binding motif and cryptic deacetylase activity. *J Biol Chem* **2008,** *283* (17), 11355-63; (b) Vannini, A.; Volpari, C.; Gallinari, P.; Jones, P.; Mattu, M.; Carfi, A.; De Francesco, R.; Steinkuhler, C.; Di Marco, S., Substrate binding to histone deacetylases as shown by the crystal structure of the HDAC8-substrate complex. *EMBO Rep* **2007,** *8* (9), 879-84.

35. Lemon, D. D.; Horn, T. R.; Cavasin, M. A.; Jeong, M. Y.; Haubold, K. W.; Long, C. S.; Irwin, D. C.; McCune, S. A.; Chung, E.; Leinwand, L. A.; McKinsey, T. A., Cardiac

HDAC6 catalytic activity is induced in response to chronic hypertension. *J Mol Cell Cardiol* **2011,** *51* (1), 41-50.

36. Mai, A.; Massa, S.; Pezzi, R.; Simeoni, S.; Rotili, D.; Nebbioso, A.; Scognamiglio, A.; Altucci, L.; Loidl, P.; Brosch, G., Class II (IIa)-selective histone deacetylase inhibitors. 1. Synthesis and biological evaluation of novel (aryloxopropenyl)pyrrolyl hydroxyamides. *J Med Chem* **2005,** *48* (9), 3344-53.

37. Butler, K. V.; Kalin, J.; Brochier, C.; Vistoli, G.; Langley, B.; Kozikowski, A. P., Rational design and simple chemistry yield a superior, neuroprotective HDAC6 inhibitor, tubastatin A. *J Am Chem Soc* **2010,** *132* (31), 10842-6.

38. (a) Dai, Y.; Guo, Y.; Curtin, M. L.; Li, J.; Pease, L. J.; Guo, J.; Marcotte, P. A.; Glaser, K. B.; Davidsen, S. K.; Michaelides, M. R., A novel series of histone deacetylase inhibitors incorporating hetero aromatic ring systems as connection units. *Bioorg Med Chem Lett* **2003,** *13* (21), 3817-20; (b) Remiszewski, S. W.; Sambucetti, L. C.; Bair, K. W.; Bontempo, J.; Cesarz, D.; Chandramouli, N.; Chen, R.; Cheung, M.; Cornell-Kennon, S.; Dean, K.; Diamantidis, G.; France, D.; Green, M. A.; Howell, K. L.; Kashi, R.; Kwon, P.; Lassota, P.; Martin, M. S.; Mou, Y.; Perez, L. B.; Sharma, S.; Smith, T.; Sorensen, E.; Taplin, F.; Trogani, N.; Versace, R.; Walker, H.; Weltchek-Engler, S.; Wood, A.; Wu, A.; Atadja, P., N-hydroxy-3-phenyl-2-propenamides as novel inhibitors of human histone deacetylase with in vivo antitumor activity: discovery of (2E)-N-hydroxy-3-[4-[[(2-hydroxyethyl)[2-(1H-indol-3-yl)ethyl]amino]methyl]phenyl]-2-propenamide (NVP-LAQ824). *J Med Chem* **2003,** *46* (21), 4609-24.

39. Gupta, S. P., Quantitative structure-activity relationship studies on zinc-containing metalloproteinase inhibitors. *Chem Rev* **2007,** *107* (7), 3042-87.

40. Leung, D.; Abbenante, G.; Fairlie, D. P., Protease inhibitors: current status and future prospects. *J Med Chem* **2000,** *43* (3), 305-41.

41. Hanessian, S.; Moitessier, N.; Gauchet, C.; Viau, M., N-Aryl sulfonyl homocysteine hydroxamate inhibitors of matrix metalloproteinases: further probing of the S(1), S(1)', and S(2)' pockets. *J Med Chem* **2001,** *44* (19), 3066-73.

42. Bhansali, P.; Hanigan, C. L.; Casero, R. A.; Tillekeratne, L. M., Largazole and analogues with modified metal-binding motifs targeting histone deacetylases: synthesis and biological evaluation. *J Med Chem* **2011,** *54* (21), 7453-63.

43. Taori, K.; Paul, V. J.; Luesch, H., Structure and activity of largazole, a potent antiproliferative agent from the Floridian marine cyanobacterium Symploca sp. *J Am Chem Soc* **2008,** *130* (6), 1806-7.

44. Karagiannis, T. C.; El-Osta, A., Will broad-spectrum histone deacetylase inhibitors be superseded by more specific compounds? *Leukemia* **2007,** *21* (1), 61-5.

45. (a) Krusche, C. A.; Wulfing, P.; Kersting, C.; Vloet, A.; Bocker, W.; Kiesel, L.; Beier, H. M.; Alfer, J., Histone deacetylase-1 and -3 protein expression in human breast cancer: a tissue microarray analysis. *Breast Cancer Res Treat* **2005,** *90* (1), 15-23; (b) Hirokawa, Y.; Arnold, M.; Nakajima, H.; Zalcberg, J.; Maruta, H., Signal therapy of breast cancers by the HDAC inhibitor FK228 that blocks the activation of PAK1 and abrogates the tamoxifen-resistance. *Cancer Biol Ther* **2005,** *4* (9), 956-60; (c) Fritsche, P.; Seidler, B.; Schuler, S.; Schnieke, A.; Gottlicher, M.; Schmid, R. M.; Saur, D.; Schneider, G., HDAC2 mediates therapeutic resistance of pancreatic cancer cells via the BH3-only protein NOXA. *Gut* **2009,** *58* (10), 1399-409; (d) Marshall, G. M.; Gherardi, S.; Xu, N.; Neiron, Z.; Trahair, T.; Scarlett, C. J.; Chang, D. K.; Liu, P. Y.; Jankowski, K.;

Iraci, N.; Haber, M.; Norris, M. D.; Keating, J.; Sekyere, E.; Jonquieres, G.; Stossi, F.; Katzenellenbogen, B. S.; Biankin, A. V.; Perini, G.; Liu, T., Transcriptional upregulation of histone deacetylase 2 promotes Myc-induced oncogenic effects. *Oncogene* **2010,** *29* (44), 5957-68; (e) Xu, X.; Xie, C.; Edwards, H.; Zhou, H.; Buck, S. A.; Ge, Y., Inhibition of histone deacetylases 1 and 6 enhances cytarabine-induced apoptosis in pediatric acute myeloid leukemia cells. *PLoS One* **2011,** *6* (2), e17138.

46. Liu, T.; Kapustin, G.; Etzkorn, F. A., Design and synthesis of a potent histone deacetylase inhibitor. *J Med Chem* **2007,** *50* (9), 2003-6.

47. Choi, S. E.; Weerasinghe, S. V.; Pflum, M. K., The structural requirements of histone deacetylase inhibitors: Suberoylanilide hydroxamic acid analogs modified at the C3 position display isoform selectivity. *Bioorg Med Chem Lett* **2011,** *21* (12), 6139-42.

48. Hanessian, S.; Chahal, N.; Giroux, S., Iterative synthesis of deoxypropionate units: the inductor effect in acyclic conformation design. *J Org Chem* **2006,** *71* (19), 7403-11.

49. Estiu, G.; Greenberg, E.; Harrison, C. B.; Kwiatkowski, N. P.; Mazitschek, R.; Bradner, J. E.; Wiest, O., Structural origin of selectivity in class II-selective histone deacetylase inhibitors. *J Med Chem* **2008,** *51* (10), 2898-906.

50. (a) Hideshima, T.; Bradner, J. E.; Wong, J.; Chauhan, D.; Richardson, P.; Schreiber, S. L.; Anderson, K. C., Small-molecule inhibition of proteasome and aggresome function induces synergistic antitumor activity in multiple myeloma. *Proceedings of the National Academy of Sciences of the United States of America* **2005,** *102* (24), 8567-72; (b) Namdar, M.; Perez, G.; Ngo, L.; Marks, P. A., Selective inhibition of histone deacetylase 6 (HDAC6) induces DNA damage and sensitizes

transformed cells to anticancer agents. *Proceedings of the National Academy of Sciences of the United States of America* **2010,** *107* (46), 20003-8.

51. http://www.enzolifesciences.com/BML-AK500/fluor-de-lys-hdac-fluorometric-activity-assay-kit/.

52. Choi, S. E.; Weerasinghe, S. V.; Pflum, M. K., The structural requirements of histone deacetylase inhibitors: Suberoylanilide hydroxamic acid analogs modified at the C3 position display isoform selectivity. *Bioorg Med Chem Lett* **2011**.

53. Sun Ea Choi, S. V. W. W., and Mary Kay Pflum, The Structural Requirements of Histone Deacetylase Inhibitors: Suberoylanilide Hydroxamic Acid Analogues Modified at the C3 Position Display Isoform Selectivity. **2011**.

54. Finnin, M. S.; Donigian, J. R.; Cohen, A.; Richon, V. M.; Rifkind, R. A.; Marks, P. A.; Breslow, R.; Pavletich, N. P., Structures of a histone deacetylase homologue bound to the TSA and SAHA inhibitors. *Nature* **1999,** *401* (6749), 188-93.

55. Hanessian, S., Design and synthesis of MMP inhibitors using N-arylsulfonylaziridine hydroxamic acids as constrained scaffolds. *Tetrahedron* **2001,** *57*, 6885-6900.

56. Zacharie, B.; Moreau, N.; Dockendorff, C., A mild procedure for the reduction of pyridine N-oxides to piperidines using ammonium formate. *J Org Chem* **2001,** *66* (15), 5264-5.

57. Moradei, O. M.; Mallais, T. C.; Frechette, S.; Paquin, I.; Tessier, P. E.; Leit, S. M.; Fournel, M.; Bonfils, C.; Trachy-Bourget, M. C.; Liu, J.; Yan, T. P.; Lu, A. H.; Rahil, J.; Wang, J.; Lefebvre, S.; Li, Z.; Vaisburg, A. F.; Besterman, J. M., Novel aminophenyl

benzamide-type histone deacetylase inhibitors with enhanced potency and selectivity. *J Med Chem* **2007,** *50* (23), 5543-6.

58. Nielsen, T. K.; Hildmann, C.; Dickmanns, A.; Schwienhorst, A.; Ficner, R., Crystal structure of a bacterial class 2 histone deacetylase homologue. *J Mol Biol* **2005,** *354* (1), 107-20.

ABSTRACT

THE STRUCTURAL REQUIREMENTS OF HISTONE DEACETYLASE INHIBITORS: SUBEROYLANILIDE HYDROXAMIC ACID (SAHA) ANALOGUES MODIFIED AT C3, C6, AND C7 POSITIONS ENHANCE SELECTIVITY

by

SUN EA CHOI

May 2012

Advisor: Dr. Mary Kay H. Pflum

Major: Chemistry (Organic)

Degree: Doctor of Philosophy

Histone deacetylase (HDAC) proteins are targets for drug design towards the treatment of cancers since overexpression of HDAC proteins is linked to cancer. Several HDAC inhibitors, including the FDA approved drug suberoyl-anilide hydroxamic acid (SAHA, Vorinostat), have cleared clinical trials and emerged as anti-cancer drugs. However, SAHA inhibits all of the 11 metal ion-dependent HDAC proteins. Therefore, we synthesized several libraries of small molecule HDAC inhibitors based on SAHA to help understand the structural requirements of inhibitory potency and isoform selectivity.

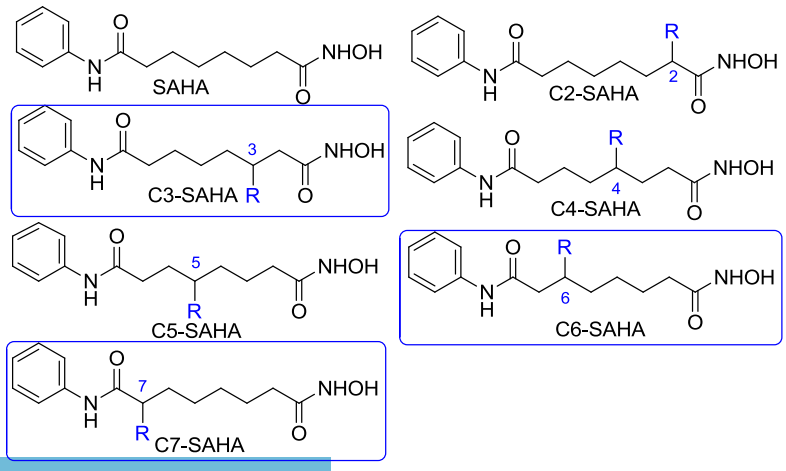

In previous work, SAHA analogues functionalized at the C2 position (C2-SAHA analogues) near the metal binding hydroxamic

acid displayed decreased inhibitory activity compared to the parent compound, SAHA. The lack of potency of the C2 library indicated that limited flexibility exists in the HDAC active site near the hydroxamic acid. Therefore, we theorized the substituents on the C3, C4, C5, C6, and C7 positions would display more potent inhibition compared to the C2-SAHA library due to the more solvent exposed location. Interestingly, while the C2-SAHA analogues containing any substituents were poor potent, the C3-SAHA analogue with a methyl substituent displayed potency. The potency of the remaining analogues decreased with increasing size of the C3 substituents. Moreover, the C6-SAHA phenyl analogue even displayed potency in the submicromolar range. Finally, most of the C7-SAHA analogues displayed equal or greater potency compared to SAHA. The results indicate that more flexibility in the HDAC active site exists closer to the capping group region near the C6 and C7 positions, while only modest flexibility exists in the bottom of the active site near the C2 and C3 positions.

After analyzing the potency of SAHA analogues, isoform selective inhibition of the individual compounds was evaluated. Seven of the SAHA analogues demonstrated selectivity. The C3-SAHA ethyl-substituted analogue showed preference for HDAC6 over HDAC1 and HDAC3 even though it displayed decreased potency.

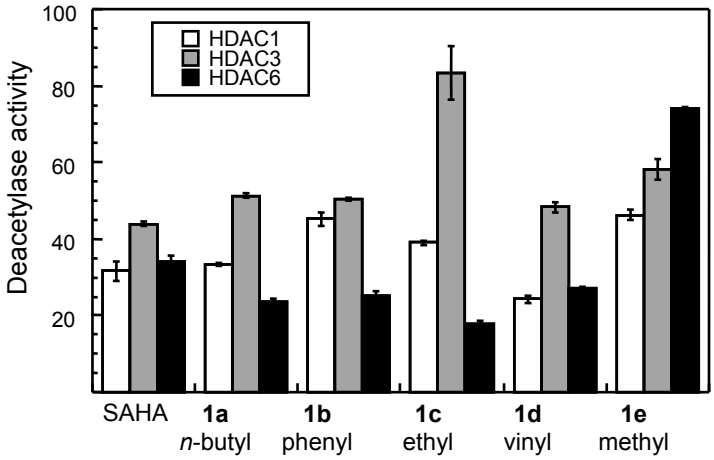

The C6-SAHA analogues displayed diverse selectivity; the C6-SAHA methyl variant displayed preference for class I, *t*-butyl variant showed a dual-HDAC1 and HDAC6 selectivity, and 2-ethylhexyl variant showed HDAC3-selectivity. The C7-SAHA analogues displayed selective inhibition as well; the C7-SAHA pyridylmethyl and anthracenylmethyl variants displayed a dual-HDAC1 and HDAC6 selectivity, and naphthylmethyl variant showed HDAC3-selectivity. The interesting potency and selectivity of linker-modified SAHA analogues suggest that linker region substituents can be exploited in the design of new anti-cancer drugs.

AUTOBIOGRAPHICAL STATEMENT

SUN EA CHOI

Education

Wayne State University, Detroit, MI. (2006-2012) Ph.D., 2012

Cincinnati State College, Sung Kyun Kwan University, Tokyo Institute University A.D., B.A., R.A.

Research Experience

Graduate Student Studies September 2007-2012

Advisor: Prof. Mary Kay H. Pflum, Ph.D
Dissertation Title: 'Structural Requirements of Histone Deacetylase (HDAC) Inhibitors: Suberoylanilide Hydroxamic Acid (SAHA) Analogues Modified at the C3, C6, and C7 Positions Enhance Selectivity
Synthesis of SAHA analogues to elucidate the structural requirements of HDAC inhibitors
Determination IC_{50} values of HDAC inhibitors using Fluor de Lys *in vitro* fluorescence activity assay kit (Enzo) using HeLa cell lysates as the source of HDAC activity

Research Student Studies August 2004-2006
Advisor: Prof. Martha Brosz
Research title: Synthesis of Vitamin D Analogues

Affiliations/Honors

Member of American Chemical Society (**2010** to **present**)
Member of Golden Key International Honor Society (**2007** to **present**)
Member of Phi Lamda Upsilon-Honorary Chemical Society (**2007** to **present**)
Honor Students Scholarship (**2005** to **2006**)

Publications

Sun Ea Choi, Sujith V. W. Weerasinghe and Mary Kay H. Pflum. "The Structural Requirement of Histone Deacetylase (HDAC) Inhibitors: Suberoyl Anilide Hydroxamic Acid (SAHA) analogues at the C3 position display Class II Selectivity", *Bioorganic and Medicinal Chemistry Letter* **2011**, 21, 6139-6142.

Sun Ea Choi, and Mary Kay Pflum, "The Structural Requirement of Histone Deacetylase (HDAC) Inhibitors: Suberoyl Anilide Hydroxamic Acid (SAHA) analogues at the C6 position Enhance Selectivity" in preparation.

Sun Ea Choi, Anton V. Bieliauskas, V. W. Weerashinghe, Geetha Padige, Satish Garre V. R. and Mary Kay Pflum, "The Structural Requirement of Histone Deacetylase (HDAC) Inhibitors: Suberoyl Anilide Hydroxamic Acid (SAHA) analogues at the C7 position display Dual-Selectivity" in preparation.